

Diss. ETH Nr. 13917

# **Influence of Organic Ligands on the Adsorption of Copper, Cadmium, and Nickel on Goethite**

A dissertation submitted to the  
SWISS FEDERAL INSTITUTE OF TECHNOLOGY ZÜRICH

for the degree of  
DOCTOR OF NATURAL SCIENCES

presented by  
DIANE ANNEMARIE WEIRICH  
Dipl. Chem. Ing. ETH  
born March 13, 1970  
citizen of Luxembourg

accepted on the recommendation of  
Prof. Laura Sigg, examiner  
Prof. Philippe Behra, co-examiner  
Prof. Bernhard Wehrli, co-examiner

Zürich 2000

### **De aqua.**

Übrigens füllt sich das Meer und die Ströme und Quellen durch Zufluss  
Frischen Wassers beständig, und dauerend rinnen die Bäche,  
Was bedarf es der Worte? Beweis sind die Ströme, die talwärts  
Überall fließen. Doch dampfen die obersten Schichten des Wassers  
Wieder empor, und das Nass läuft niemals über als Ganzes.  
Denn teils fegen die Winde gewaltig die Flächen des Meeres;  
Dadurch nehmen sie weg, was die himmlische Sonne dann aufsaugt,  
Teils verläuft sich das Wasser auch weiterhin unter die Erde,  
Wie durch ein Sieb, und der Stoff der Flüchtigkeit fließet nun rückwärts  
Wieder zur Quelle der Flüsse. Da kommet dann alles zusammen  
Und ergießet sich von da im munteren Lauf, wo die Welle  
Einmal ihr Bett sich geschnitten und flüchtigen Fusses hinabhüpft.

Lukrez. De rerum natura.

# Dank

An erster Stelle möchte ich meiner Doktormutter Laura Sigg danken, die eine sehr gute Betreuerin für mich war. Mit ihrem grossen Fachwissen und ihrem Gespür für chemische Reaktivitäten hat sie die Arbeit ausgezeichnet geleitet und mir auch immer genügend Freiheit gelassen meinen eigenen Interessen nachzugehen. In zahlreichen gemeinsamen Kaffeepausen, Konferenzen oder Gartenfesten habe ich sie auch als Mensch sehr schätzen gelernt.

J'aimerais remercier mon coréférent Philippe Behra pour les nombreuses discussions qui ont amené de nouvelles idées à ce travail. Sa grande expérience en modélisation m'a donné du courage pour aborder cette partie de ma thèse. Les visites à Strasbourg resteront un bon souvenir, non seulement pour des raisons scientifiques mais aussi parce que Philippe a été un hôte exceptionnel et généreux. Les restaurants dans lesquelles il m'a invitée ont toujours été de succulents choix!

Bernhard Wehrli möchte ich danken, dass er sich noch zu einem späten Zeitpunkt bereit erklärt hat, das Koreferat zu übernehmen. Seine fachliche Kompetenz und seine Fähigkeit, die Daten kritisch anzuschauen haben mich sehr motiviert.

Ein grosses Dankeschön geht an den wichtigsten Mann in unserer Gruppe: David Kistler. Er hat mich in die Geheimnisse der Spurenanalytik eingeweiht, und mir auch bei anderen Schwierigkeiten (technischer und anderer Art) beigestanden. An dieser Stelle möchte ich auch René Schönenberger danken, der mir unter anderem bei Probenahmen und AAS-Messungen zur Hand ging. Seine Begeisterung und stets gute Laune haben mich immer wieder angesteckt.

Renat Hari und Hanbin Xue haben ganz wesentlich zu dieser Arbeit beigetragen. Mit grossem Elan gingen sie an die Speziierungsmessungen von Kupfer, Cadmium und Nickel in Gegenwart organischer Liganden. Mich hat die unkomplizierte Zusammenarbeit sehr beeindruckt. In diesem Zusammenhang sollen auch die zwei Diplomanden Andreas Prash und Stefan Janssen erwähnt werden, die über Nickelspeziierungen gearbeitet haben.

Adi Ammann, Thomas Rüttimann, Niksa Odzak, Sébastien Meylan, Felix Bürgi, Annemarie Mezzanotte, Laura Canonica, Elio Larcán, Denise Balluch und Stephan Walker möchte ich danken für ihre Hilfe bei analytischen Messungen, beim

Experimentieren und bei den Probenahmen im Felde (teils bei kräftigem Schneegestöber!).

Auch das Bibliotheksteam soll nicht vergessen werden. Monika Zemp war immer bereit mir Zeitschriften aus dem Keller hervorzusuchen und hatte stets einen lustigen Spruch parat. Lilo Schwarz ging mir beim Zusammenstellen der Referenzliste zur Hand.

Ursi Schönenberger, Raoul Schaffner und Bouziane Outiti waren zur Stelle bei Computerfragen. Ursi hat meinen Computer immer auf dem neuesten Stand gehalten und Raoul ging mir oft bei Softwareproblemen zur Hand.

Daniel Kobler und Yvo Weidmann haben mir BET-Messungen und REM Aufnahmen vom Goethit gemacht.

Nun kann eine Arbeit nur gelingen wenn das Arbeitsklima stimmt. Laura hat es verstanden, eine Gruppe zusammenzusetzen in der ich mich sehr wohlfühlt habe. Anfangs waren dort Lukas Emmenegger, Aria Amirbahman, Suzanne Mettler, Andrea Ulrich, Sabine Hilger (jetzt Suter), Renat Hari, Hanbin Xue, David Kistler und Ursula Lindauer. Später kamen noch Niksa Odzak, Annette Aldrich, Liu Shanjun und Sébastien Meylan hinzu. Stets herrschte eine angenehme, konkurrenzfreie Atmosphäre in unserer Gruppe. Lukas, Sébastien und Renat haben mit mir das Labor geteilt und grosse Toleranz gezeigt, wenn ich wieder mal klassische Musik gehört habe. Sowohl Freude über erfolgreiche, wie Kummer über weniger gute Experimente haben wir miteinander geteilt. Annette Aldrich war immer fröhlich und mit ihr konnte ich über alles reden. Sie hat auch einige Kapitel aus dem Manuskript kritisch durchgelesen.

Aber auch Leute aus anderen Gruppen haben dazu beigetragen, dass ich mich an der EAWAG wohlfühlt habe. Vor allem werden mir Juan Acero, Diana Aga, Hans-Ruedi Aerni, Alfredo Alder, Marianne Balmer, Isabel Baur, Renata Behra, Silvio Canonica, You Chunhui, Mike Elovitz, Mireille Faist, Edi Hoehn, Stephan Hug, Annette Johnson, Edith Kaiser, Hans-Ueli Laubscher, Olivier Leupin, Christa McArdeLL, Eva Molnar, Hermann Mönch, Beat Müller, Max Reutlinger, Sonja Riediker, Lisa Sahli, Ursi und René Schönenberger, Michele Steiner, Barbara Sulzberger, Marc Suter und Jürg Zobrist in Erinnerung bleiben.

Mengen Elteren soen ech Merci, dass sie mëch während dem Studium finanziell ënnerstëtzt hunn an mier déi ganz Ausbildung esou erméiglécht hunn.

Zuletzt möchte ich meinem Freund Ignaz danken für seine vielen aufmunternden Worte und seine Geduld während dieser Zeit.



# *Table of Contents*

## *Zusammenfassung*

### *Abstract*

<b>1</b>	<b><i>Introduction</i></b>	<b>1</b>
1.1	Motivation	1
1.2	System Definition	3
1.3	Objectives and Overview	4
1.4	Short Description of the Adsorbates	5
	1.4.1 Copper	5
	1.4.2 Cadmium	6
	1.4.3 Nickel	7
	1.4.4 Organic ligands in freshwater systems	9
1.5	<b>Interactions of Ligands and Major Cations with Heavy Metal Adsorption</b>	<b>12</b>
<b>2</b>	<b><i>Modelling of Adsorption Reactions at Mineral Surfaces</i></b>	<b>15</b>
2.1	Introduction	15
2.2	Adsorption isotherms	16
2.3	Classical Surface Complexation Models	18
	2.3.1 Adsorption Reactions of Metal Cations and Organic Ligand Anions	18
	2.3.2 Formation of the Electric Double Layer (EDL)	23
	2.3.3 Definition of Surface charges	23
	2.3.4 Definition of Intrinsic Constants	24
	2.3.5 Description of the Most Important Electrostatic Models	24
2.4	<b>Basic Stern Model (BSM)</b>	<b>28</b>
2.5	<b>CD-MUSIC (Charge Distribution Multi Site Complexation)</b>	<b>29</b>
	2.5.1 Concept of Charge Distribution	29
	2.5.2 Multi Site Complexation	32
2.6	<b>Common points and differences between Surface Complexation Models</b>	<b>33</b>
2.7	<b>Applicability of Models</b>	<b>34</b>

---

<b>2.8</b>	<b>Modelling of copper, cadmium, nickel, and oxalate on goethite</b>	<b>34</b>
2.8.1	Copper-Goethite System	35
2.8.2	Cadmium-Goethite System	37
2.8.3	Nickel-Goethite System	39
2.8.4	Variations of the Adsorption Constant with Metal Concentration	41
<b>2.9</b>	<b>Modelling of Oxalate, Salicylate, and Pyromellitate on Goethite</b>	<b>41</b>
2.9.1	Oxalate-Goethite System	41
2.9.2	Salicylate-Goethite System	43
2.9.3	Pyromellitate-Goethite System	44
<b>3</b>	<b><i>Characterisation of Goethite</i></b>	<b>47</b>
<b>3.1</b>	<b>Introduction</b>	<b>47</b>
<b>3.2</b>	<b>Description of Goethite</b>	<b>47</b>
<b>3.3</b>	<b>Determination of Acidity Constants</b>	<b>49</b>
<b>3.4</b>	<b>Treatment of Goethite</b>	<b>49</b>
<b>4</b>	<b><i>Adsorption of Cu, Cd, and Ni on Goethite in the Presence of Simple Organic Ligands</i></b>	<b>52</b>
<b>4.1</b>	<b>Introduction</b>	<b>52</b>
<b>4.2</b>	<b>Experimental Conditions</b>	<b>53</b>
4.2.1	Chemicals	53
4.2.2	Treatment of Goethite	53
4.2.3	General Experimental Setup	54
4.2.4	Analytical Methods	55
<b>4.3</b>	<b>Modelling</b>	<b>56</b>
<b>4.4</b>	<b>Influence of Oxalate on the Adsorption of Copper, Cadmium, and Nickel on Goethite</b>	<b>60</b>
4.4.1	Copper-Oxalate-Goethite System	60
4.4.2	Cadmium-Oxalate-Goethite System	62
4.4.3	Nickel-Oxalate-Goethite System	64
4.4.4	Summary of the Oxalate System	68
<b>4.5</b>	<b>Influence of Salicylate on the Adsorption of Copper, Cadmium, and Nickel on Goethite</b>	<b>69</b>
4.5.1	Copper-Salicylate-Goethite System	69
4.5.2	Cadmium-Salicylate-Goethite System	70

---

4.5.3	Nickel-Salicylate-Goethite System	72
4.5.4	Summary of the Salicylate System	73
<b>4.6</b>	<b>Influence of Pyromellitate on the Adsorption of Copper, Cadmium, and Nickel on Goethite</b>	<b>74</b>
4.6.1	Copper-Pyromellitate-Goethite System	74
4.6.2	Cadmium-Pyromellitate-Goethite System	75
4.6.3	Nickel-Pyromellitate-Goethite System	77
4.6.4	Summary of the Pyromellitate System	78
<b>4.7</b>	<b>General Discussion of Adsorption Experiments in the Presence of Simple Organic Ligands</b>	<b>79</b>
4.7.1	Summary of the Main Results	79
4.7.2	Formation of ternary complexes	82
4.7.3	Discussion	91
4.7.4	Kinetic effects	92
4.7.5	Influence of the structure of the ligands	93
<b>5</b>	<b><i>Adsorption of Cu, Cd, and Ni on Goethite in the Presence of Natural Groundwater Organic Ligands</i></b>	<b>95</b>
<b>5.1</b>	<b>Introduction</b>	<b>95</b>
<b>5.2</b>	<b>Sampling site and methods</b>	<b>96</b>
<b>5.3</b>	<b>Experimental Conditions</b>	<b>101</b>
5.3.1	Chemicals	101
5.3.2	Pretreatment of Groundwater	101
5.3.3	Treatment of Goethite	102
5.3.4	General Experimental Setup	102
5.3.5	Analytical Methods	107
<b>5.4</b>	<b>Modelling description</b>	<b>108</b>
5.4.1	Metal Complexation by Infiltration Groundwater Organic Ligands	108
5.4.2	Metal Adsorption on Goethite in the Presence of Groundwater Organic Ligands	109
5.4.3	Influence of Phosphate on Metal Adsorption on Goethite	111
5.4.4	Influence of Calcium and Magnesium on Metal Adsorption on Goethite	112
<b>5.5</b>	<b>Influence of a Groundwater Matrix on the Adsorption of Copper on Goethite</b>	<b>113</b>

---

5.5.1	pH Adsorption Edge of Copper on Goethite in an Infiltration Groundwater Matrix	113
5.5.2	Adsorption of Copper on Goethite in an Infiltration Groundwater Matrix at pH 3.5	114
5.5.3	Adsorption of Copper on Goethite in an Infiltration Groundwater Matrix at pH 7.35	116
5.5.4	Adsorption of Copper on Goethite in a Deep Groundwater Matrix at pH 7.6	117
<b>5.6</b>	<b>Modelling of Copper Experiments</b>	<b>118</b>
5.6.1	Adsorption of Copper in the Presence of Infiltration Groundwater Organic Ligands	118
5.6.2	Adsorption of Copper in the Presence of Deep Groundwater Organic Ligands	123
<b>5.7</b>	<b>Influence of a Groundwater Matrix on the Adsorption of Cadmium on Goethite</b>	<b>126</b>
5.7.1	pH Adsorption Edge of Cadmium on Goethite in an Infiltration Groundwater Matrix	126
5.7.2	Adsorption of Cadmium on Goethite in an Infiltration Groundwater Matrix at pH 7.6	127
5.7.3	Adsorption of Cadmium in a Deep Groundwater Matrix at pH 7.6	127
<b>5.8</b>	<b>Modelling of Cadmium Experiments</b>	<b>129</b>
5.8.1	Adsorption of Cadmium in the Presence of Infiltration Groundwater Organic Ligands	129
<b>5.9</b>	<b>Influence of a Groundwater Matrix on the Adsorption of Nickel on Goethite</b>	<b>131</b>
5.9.1	pH Adsorption Edge of Nickel on Goethite in an Infiltration Groundwater Matrix	131
5.9.2	Adsorption of Nickel on Goethite in an Infiltration Groundwater Matrix at pH 7.35	132
<b>5.10</b>	<b>Modelling of Nickel Experiments</b>	<b>133</b>
5.10.1	Adsorption of Nickel in the Presence of Infiltration Groundwater Organic Ligands	133
<b>5.11</b>	<b>Competitive Adsorption of Cu and Ni on Goethite in the Presence of Natural Organic Ligands</b>	<b>134</b>

---

<b>5.12</b>	<b>Adsorption of Several Metals on Goethite in the Groundwater Matrix</b>	<b>140</b>
<b>5.13</b>	<b>Discussion of Metal Complexation with Natural Groundwater Organic Ligands</b>	<b>144</b>
5.13.1	Total Ligand Concentration in Natural Groundwater	144
5.13.2	WHAM model calculations	145
<b>5.14</b>	<b>Discussion of Metal Adsorption Modelling</b>	<b>149</b>
5.14.1	Formation of Ternary Complexes	149
5.14.2	Influence of Phosphate on Metal Adsorption on Goethite	150
5.14.3	Influence of Calcium and Magnesium on Metal Adsorption on Goethite	152
5.14.4	Effect of $\log K_1$ and $[L_1]$ on Metal Adsorption	154
<b>5.15</b>	<b>Conclusions</b>	<b>161</b>
<b>6</b>	<b><i>Summary and Outlook</i></b>	<b>161</b>
<b>6.1</b>	<b>Main Results</b>	<b>164</b>
<b>6.2</b>	<b>Environmental Significance</b>	<b>165</b>
<b>6.3</b>	<b>Limitations and Outlook</b>	<b>165</b>
	<b><i>References</i></b>	<b>167</b>

Seite Leer /  
Blank leaf

# *List of Abbreviations*

[Cu] <sub>tot</sub>	total copper concentration [M]
[Cu <sup>2+</sup> ]	free copper concentration [M]
ATR	Attenuated Total Reflection
BSM	Basic Stern Model
C	Capacitance [F]
CCM	Constant Capacitance Model
CD-MUSIC	Charge Distribution - Multi Site Complexation Model
CIR	Cylindrical Internal Reflection
Cu-ISE	Copper – Ion Selective Electrode
deepGW	deep groundwater
DLM	Double Layer Model
DOC	Dissolved Organic Carbon
DP-ASV	Differential Pulse – Anodic Stripping Voltammetry
DP-CSV	Differential Pulse – Cathodic Stripping Voltammetry
DTPA	Diethylenetriaminepentaacetate
EAWAG	Swiss Federal Institute for Environmental Science and Technology
E-CC	Extended Constant Capacitance Model
EDL	Electric Double Layer
EDTA	Ethylenediaminetetraacetate
EM	Electron Microscopy
EPA	Environmental Protection Agency
EXAFS	Extended X – ray Absorption Fine Structure
FA	Fulvic Acid
FTIR	Fourier Transform Infrared Spectroscopy
GF-AAS	Graphite Furnace – Atomic Absorption Spectroscopy
G-TLM	Generalised Two Layer Model
GW	Groundwater
HA	Humic Acid
HFO	Hydrous Ferric Oxide
HS	Humic Substance

---

I	Ionic strength [M]
ICP-MS	Inductively Coupled Plasma – Mass Spectroscopy
ICP-OES	Inductively Coupled Plasma - Optical Emission Spectroscopy
ISE	Ion Selective Electrode
$K_{\text{int}}$	intrinsic equilibrium constant
$\log K_{\text{ads}}$	logarithm of adsorption constant
$\log K_{\text{ter,A}}$	logarithm of adsorption constant of ternary complex of type A
$\log K_{\text{ter,B}}$	logarithm of adsorption constant of ternary complex of type B
MUSIC	Multi Site Complexation
NICA	Non Ideal Competitive Adsorption
NOM	Natural Organic Matter
NTA	nitrilotriacetate
Ox	Oxalate
$\text{p}K_{\text{a}}$	negative logarithm of the acidity constant
Pyr	Pyromellitate
pzc	Point of Zero Charge
Sal	Salicylate
SCM	Surface Complexation Model
SEM	Scanning microscopy
TLM	Triple Layer Model
TOC	Total Organic Carbon
TPM	Three Plane Model
WHAM	Windermere Humic Aqueous Model
WSOS/DF	Weighted sum of square of residuals divided by the degrees of freedom
XPS	X – ray Photo Electron Spectroscopy
$\alpha\text{-FeOOH}$	Goethite
$\lambda$	wavelength [nm]
$\sigma_{\text{x}}$	Surface charge on the plane x [C]
$\psi_{\text{x}}$	Surface potential on the plane x [V]



# Summary

Metal contaminations in groundwater systems may present a major environmental problem. If mobilised, metals may reach the groundwater, which represents an important source for drinking water, or they may become bioavailable and thus possibly toxic for plants and groundwater fauna. Therefore it is very important to understand under which conditions they are mobilised or immobilised.

In this work, the influence of organic ligands on heavy metal adsorption (copper, cadmium, and nickel) was studied in batch laboratory experiments using goethite as a solid phase. On the one hand, simple organic ligands (oxalate, pyromellitate (1,2,4,5-benzenetetracarboxylate), and salicylate), and on the other hand a natural unfractionated DOC from an infiltration groundwater of the river Glatt (Switzerland) were used.

Experiments were performed using untreated groundwater with DOC in its natural concentrations (1.5 – 2.3 mg/L), and metal concentrations close to environmental conditions. Complexation of the metals by natural ligands was determined by voltammetric methods and by an ion selective electrode and was described by a model defining the minimum necessary number of discrete ligands. Complexation of copper and cadmium was described by assuming the presence of a strong ligand with a low concentration and additional weaker ligands with higher concentrations, whereas complexation of nickel within a limited concentration range was described with only one strong ligand with low concentration. In the presence of the natural ligands, copper, cadmium, and nickel adsorption was decreased at high pH values. Metal adsorption at low total metal concentrations was suppressed, as could be shown by adsorption isotherms at pH 7.35.

The three synthetic ligands showed quite different results. Salicylate had no major effect on the adsorption of copper, and nickel, and only a slight enhancement of cadmium adsorption at  $\text{pH} > 6$  could be observed. In the presence of oxalate, the pH adsorption edge of copper was shifted to higher pH, and nickel adsorption was decreased at pH values above 7. Cadmium adsorption in the oxalate system was weakly increased between pH 6 and 7. In the presence of pyromellitate, adsorption of copper, cadmium, and nickel was stronger than expected according to the complexation capacity of pyromellitate in solution.

Modelling of the metal-ligand-goethite systems was performed by a surface complexation model for metal adsorption, with a double layer model for the

electrostatic interactions, to which three modules were applied step by step. These modules take into account competition reactions between the surface functional groups and the aqueous ligands, electrostatic attraction of the metal by the adsorbed ligand, and formation of ternary surface complexes of type A (surface-metal-ligand) or B (surface-ligand-metal).

In the case of salicylate, a model including competition between surface and solution complexation was sufficient to describe the experimental data for cadmium and nickel, whereas ternary surface complexes of type A had to be defined for copper. In the case of oxalate, competition between surface and solution complexation was able to describe the cadmium data, but gave unsatisfactory results for copper and nickel. Ternary surface complexes of type B were assumed for the nickel-oxalate-goethite system. In the case of pyromellitate, formation of ternary surface complexes of type B had to be included to describe the copper and cadmium data, which is in agreement with the favourable pyromellitate structure.

Adsorption of copper, cadmium, and nickel in presence of the natural groundwater ligands was satisfactorily described by a model considering competition between surface adsorption and complexation by the ligands in solution and using independently determined adsorption and complexation parameters. No formation of ternary surface complexes with the natural ligands had to be invoked to explain the data. Inhibition of metal adsorption appeared to be mostly due to the presence of strong ligands at low concentrations.

# Zusammenfassung

Metallkontaminationen im Grundwasser können ein grosses Umweltproblem darstellen. Werden die Metalle mobilisiert, so können sie ins tiefe Grundwasser gelangen, welches eine wichtige Trinkwasserressource ist, oder sie können bioverfügbar werden, und somit toxisch für die im Grundwasser lebende Organismen. Aus diesem Grund ist es sehr wichtig zu verstehen, unter welchen Bedingungen sie mobilisiert oder immobilisiert werden.

In dieser Arbeit wurde der Einfluss von organischen Liganden auf die Adsorption von Schwermetallen (Kupfer, Cadmium und Nickel) in Laborexperimenten untersucht. Als Festphase wurde Goethit eingesetzt. Die Experimente wurden sowohl in Gegenwart von einfachen organischen Liganden (Oxalat, Pyromellitat (1,2,4,5-Benzentetracarboxylat) und Salicylat), als auch in Gegenwart von unfraktioniertem organischem Material aus dem Infiltrationsgrundwasser des Flusses Glatt (Schweiz) durchgeführt.

Die Adsorptionsexperimente wurden beim natürlichen DOC-Gehalt (1.5 – 2.3 mg/L) im unbehandelten Grundwasser durchgeführt. Die Metallkonzentrationen waren ebenfalls im natürlichen Bereich. Die Komplexeigenschaften der organischen Liganden wurden mit voltammetrischen Methoden und ionenselektiven Elektroden untersucht und können durch ein Modell mit einer minimalen Anzahl einzelner Liganden beschrieben werden. Die Komplexierung von Kupfer und Cadmium durch DOC kann durch einen starken Liganden mit tiefer Konzentration und weiteren schwächeren Liganden dargestellt werden. Die Komplexierung von Nickel wurde in einem engen Konzentrationsbereich durch einen starken Liganden mit tiefer Konzentration beschrieben. In Gegenwart organischer Liganden wurde die Adsorption von Kupfer, Cadmium und Nickel erniedrigt. Bei niedrigen totalen Metallkonzentrationen wurde die Metalladsorption vollständig unterdrückt, wie anhand von Adsorptionsisothermen bei pH 7.35 gezeigt wurde.

Salicylat zeigt keinen grösseren Einfluss auf die Adsorptionen von Kupfer und Nickel, nur die Cadmiumadsorption war bei pH-Werten oberhalb 6 leicht erhöht. In Gegenwart von Oxalat wurde die Kupferadsorptionskante zu höheren pH-Werten verschoben; die Nickeladsorption bei pH-Werten oberhalb 7 wurde erniedrigt. Die Cadmiumadsorption in Gegenwart von Oxalat hingegen wurde schwach zwischen pH 6 und 7 erhöht. Die Adsorptionen von Kupfer, Cadmium und

Nickel in Gegenwart von Pyromellitat waren höher als aufgrund der Komplexierungseigenschaften von Pyromellitat in Lösung zu erwarten war.

Die Modellierung der Metall-Ligand-Goethit Reaktionen erfolgte mit dem Oberflächenkomplexierungsmodell, zusammen mit dem Doppelschichtmodell zur Berücksichtigung der elektrostatischen Wechselwirkungen, dem schrittweise verschiedene Module zugefügt wurden. Die 3 Module beinhalten die Konkurrenzreaktionen zwischen Oberflächenliganden und gelösten Liganden, die elektrostatische Anziehung von Metallen durch adsorbierte organische Liganden und die Bildung ternärer Oberflächenkomplexe des Typus A (Oberfläche-Metall-Ligand) oder Typus B (Oberfläche-Ligand-Metall).

Im Salicylatsystem genügte zur Beschreibung der Cadmium- und Nickeladsorption ein Modell, das die Konkurrenzreaktionen zwischen Oberflächen- und Lösungskomplexierung berücksichtigt, während ternäre Komplexe des Typus A nötig waren, um die Kupferadsorption zu berechnen. Im Oxalatsystem, reichte es für die Darstellung der Cadmiumadsorption aus, Konkurrenzreaktionen zwischen Oberflächen- und Lösungskomplexierung zu definieren. Dies ergab aber unbefriedigende Resultate im Kupfer- und Nickelsystem. Ternäre Komplexe des Typus B für das Nickel-Oxalat-Goethit-System wurden angenommen. In Gegenwart von Pyromellitat, das eine günstige Struktur zur Bildung von ternären Komplexen aufweist, musste die Bildung dieser Komplexe berücksichtigt werden, um die Kupfer- und Cadmiumadsorption beschreiben zu können.

Die Adsorption von Kupfer, Cadmium, und Nickel in Gegenwart natürlicher Grundwasserliganden wurde anhand eines Modells, das die Konkurrenzreaktionen zwischen Oberflächenliganden und gelösten Liganden berücksichtigt, zufriedenstellend beschrieben. Für die Berechnung wurden voneinander unabhängig geschätzte Parameter benutzt. Die Bildung von ternären Komplexen musste für die natürlichen Liganden nicht berücksichtigt werden. Die Metalladsorption wurde hauptsächlich durch die Gegenwart starker gelöster Liganden mit tiefen Konzentrationen unterdrückt.

# *Introduction*

## **1.1 Motivation**

Metal contaminations still present a major environmental problem, as they are per se not biodegradable. Major sources of metal pollution on the global scale are coal and oil combustion, mining and smelting. Furthermore high concentrations of metals enter the aquatic system by release of industrial cooling water into rivers, by dumping sewage sludge and by wet and dry deposition. In groundwater systems, heavy metals are of concern, as, depending on their concentration and speciation, they may be toxic for certain plants and groundwater fauna. Furthermore they are undesired in groundwater, as it represents an important source for our drinking water.

Heavy metals enter groundwater systems through different pathways, such as infiltration of landfill leachates, river water or urban stormwater. Urban stormwater includes roof as well as street runoff waters. Runoff waters from highways and roofs have been shown to contain high concentrations of heavy metals (Herrmann et al., 1994; Zobrist et al., 2000).

In addition, groundwater may be polluted by heavy metals that have been disposed off in landfills. Organic matter leaching from the landfill waste may mobilise heavy metals (Christensen et al., 1996), which may thus become a potential risk for the groundwater quality.

Decontamination of nuclear equipment with strong chelating ligands, like EDTA, NTA or DTPA, is another important source for a variety of heavy metals and radionuclides in some aquifer systems (Jardine et al., 1993). These organic metal complexes were disposed off in shallow land burial sites and it has been shown that

e.g., the transport of cobalt was enhanced in the presence of EDTA (Jardine et al., 1993).

The transport of metals in groundwater and soil is governed by a number of chemical and physical factors such as complexation by organic and inorganic ligands, pH and redox conditions. Metals may be retained by adsorption on the surface of soil minerals or particulate organic material and by precipitation. On the other hand, metals may be mobilised as a result of complexation with dissolved organic ligands. In measurements performed at different depths at an infiltration site of roof runoff water, changes in the concentration of some heavy metals such as copper or cadmium were mostly due to the dynamics of inflowing water (Mason et al., 1999). By means of voltammetric methods, these metals in roof runoff were shown to be very labile (free aqua ions or weak inorganic complexes) (Ochs and Sigg, 1995), and they could thus react easily with either organic dissolved ligands or surface ligands during their infiltration way. The retention of the metals in the unsaturated zone was essentially negligible, therefore the metals were probably mobilised by complexation with dissolved organic ligands.

It has been shown by several authors that in natural systems heavy metals are highly complexed by organic ligands (Achterberg and van den Berg, 1997; Christensen et al., 1999; Christensen and Christensen, 1999; Nowack et al., 1997; Turner et al., 1998; Xue et al., 2000; Xue and Sigg, 1994 and 1998). Complexation of heavy metals with organic ligands may account to a large extent for the mobilisation of heavy metals (Davis and Leckie, 1978; Jacobs et al., 1988; Plavsic et al., 1980; Turner et al., 1998). If metals are mobilised, they may become bioavailable and thus become toxic to some organisms, or reach the deep groundwater, which is often used as drinking water.

In contrast to the above mentioned studies, other authors have observed immobilisation of heavy metals in the presence of organic ligands due to formation of ternary complexes (Ali and Dzombak, 1996; Bourg et al., 1979; Bourg and Schindler, 1979; Ludwig and Schindler, 1995; Nowack and Sigg, 1996; Schindler, 1990; Tipping et al., 1983).

Despite these studies, the conditions necessary for either mobilisation or immobilisation of heavy metals in an infiltration groundwater system are still poorly understood. Most studies have been performed in laboratory systems at elevated metal concentrations in the presence of treated natural ligands which can explain reactions in natural systems only in an unsatisfactory way. The aim of this study was to analyse how natural and simple organic ligands could influence heavy metal

adsorption under different pH conditions. Of special interest was the effect of natural groundwater organic ligands at ambient conditions, i.e., unfractionated organic material at its natural concentrations was used. For comparison, similar experiments have been performed with simple organic ligands. By combination different models, possible interactions of organic ligands and heavy metal cations in a natural system could be evaluated. Of special interest were competition reactions between the ligands in solution and the surface groups to complex the metal and whether the formation of ternary complexes was possible.

## 1.2 System Definition

The investigated system contained a metal cation, a simple organic ligand or a natural groundwater mixture, and a solid phase surface.

- Metal cations: cadmium, copper, and nickel were chosen. Their strong complexation by both surface and solution ligands make them well suitable for the study of competition reactions between surface and solution complexation.
- Organic ligands: either natural unfractionated groundwater DOC from Glattfelden, Switzerland, or simple organic molecules representing the complexation properties of natural organic ligands (oxalate, salicylate, or pyromellitate) were used.
- Surface: goethite ( $\alpha$ -FeOOH), a crystalline iron oxide, was selected to study adsorption reactions, as it occurs widespread in natural soils and groundwater systems. It has been shown that iron oxides represent an important part of the sorbents in natural soils (Schwertmann and Cornell, 1991).

## 1.3 Objectives and Overview

The goal of the work is to quantify adsorption of copper, cadmium, and nickel on goethite in the presence of natural organic ligands by simple models. In order to understand reactions in natural systems, experiments have to be performed as close as possible to natural conditions. This means in our situation that it was very important to use the organic ligands exactly as they were present in the natural groundwater, i.e., unfractionated and at the same concentrations. This implied that metal concentrations were also close to environmental conditions in order not to

saturate the organic ligands. Altogether simplifications have to be made to such complicated systems in order to get results that can be interpreted. This implied working in well defined batch laboratory system using a well-characterized solid surface. Further on little is still known about exact structure and behaviour of natural organic ligands, therefore similar metal adsorption experiments have been performed in the presence of simple organic ligands. In these systems, metal adsorption could be modelled in more detail and by comparison of these results with those in the natural system, it was possible to understand certain interactions in the natural system. Therefore the thesis is divided into two parts:

- studies with simple organic ligands (oxalate, salicylate, and pyromellitate (1,2,4,5-benzenetetracarboxylate))
- investigation with natural unfractionated groundwater DOC at environmental concentrations

In chapter 2, the most common adsorption models are described and compared. It is shown how these models have been used in literature. Adsorption modelling of the metal cations (copper, cadmium, and nickel) and of the simple organic ligands on goethite, as used in this study, are described.

In chapter 3, a brief description of the solid phase will be given. Goethite, a crystalline iron oxide, was used in our adsorption experiments.

In chapter 4, metal adsorption experiments in the presence of simple organic ligands are described. Modelling of metal adsorption was performed by starting with a simple model, which was refined by adding step by step possible interactions of organic ligand with metal adsorption till the calculated curve could describe the experimental one. With this method, the different possible influences of the ligands on metal adsorption could be distinguished separately and could mostly be explained by their properties, such as acidity, complexation capacity and adsorption behaviour.

In chapter 5, metal adsorption in the presence of an unfractionated natural infiltration groundwater DOC in the original matrix was analysed. The concentrations used of DOC and of the metals were close to environmental conditions. All adsorption experiments could be described by the combination of a surface complexation model and a complexation model in solution. To achieve this task, the complexation of copper, cadmium, and nickel by the natural infiltration groundwater was determined by voltammetric methods and ion selective electrodes.



Chapter 6 contains the conclusions of the whole work. The influence of the natural ligands and the simple ligands will be compared. Furtheron the influence of organic ligands on the adsorption of heavy metals in different groundwater systems will be discussed.

## 1.4 Short Description of the Adsorbates

### 1.4.1 Copper

Copper is used in numerous industrial applications (Nriagu, 1989), e.g., for windings of generators. Due to its high chemical resistance and its high thermal conductivity, copper has become a useful metal for condensers in chemical plants and for car radiators. Copper tubing is widely employed in plumbing. Furthermore copper is a very important material in certain countries in the construction of roofs. Copper(II)sulphate is used for the preparation of fungicides, in textil dyeing, as timber preservative, and in electroplating solutions. Copper has contraceptive effects, when present in the uterus (Irwin et al., 1997).

Copper is listed by the Environmental Protection Agency (EPA) and the European Union (Amtsblatt der Europäischen Gemeinschaften, 1999; Internationale Kommission zum Schutze des Rheins (IKSR), 1992) as one of 129 priority pollutants. The main anthropogenic sources for atmospheric pollution include emissions from mines, smelters, and municipal waste incinerators as well as burning of coal. About  $35 \cdot 10^3$  t/year copper were emitted from man-made sources to the atmosphere (Nriagu and Pacyna, 1988). Natural sources amount to  $28 \cdot 10^3$  t/year and include mainly soil dust, forest fires, and volcanoe emissions (Nriagu, 1989). Introduction of copper into the hydrosphere and the pedosphere occurs through waste waters of mines, its use as an antifouling agent in paints and its application in agriculture as fertilizer, algicide or fungicide. Another important input are human and animal excreta (World Health Organization, 1998), as well as roof runoffs, which originated from copper used in roofs and in drain gutters. Concentrations in roof runoffs ranged from 20-324  $\mu\text{g/l}$  copper (Mottier et al., 1995). Besides these direct inputs by man, atmospheric deposition plays a major role in the contamination of these compartments. The total anthropogenic input into aquatic ecosystem amounts to  $112 \cdot 10^3$  t/year and into soils to about  $10^6$  t/year (Nriagu and Pacyna, 1988).

The electronic configuration of copper is  $[\text{Ar}]3d^{10}4s$ .  $\text{Cu}^{2+}$  belongs therefore to the transition metal cations and can bind to ligand sites containing oxygen, sulfur, or nitrogen atoms (Stumm and Morgan, 1996). In fresh waters, copper is normally present in the oxidation state +II.  $\text{Cu(I)}$  is only stable if stabilised by ligands such as chloride (Libes, 1992) or under reducing conditions.

In a groundwater system, the distribution of copper is influenced by a number of factors, such as pH, type and distribution of organic matter, redox potential, and presence of mineral oxides. In natural systems, copper is mainly bound to organic ligands (Xue and Sigg, 1993, 1999) or adsorbed on mineral oxide surfaces. Acidic conditions and strong non-adsorbing ligands favour the transport of copper into groundwater.

Minute amounts of copper in the diet are needed for human, plant, and animal enzymes. Copper is the prosthetic element of more than a dozen specific copper proteins (National Research Council, 1977). Toxicosis due to copper is avoided at low to moderate concentrations in genetically normal individuals as most of the copper only acts through specific copper proteins. Such a metal-protein complex reduces the concentration of free copper ions throughout the body and thus avoids the toxicity that is inherent in free copper ions (Nriagu, 1979a). In patients with Wilson's disease, copper steadily accumulates, first in the liver and then in other parts of the body. Damage, particularly evident in the liver and central nervous system, is ultimately fatal (National Research Council, 1977).

## 1.4.2 Cadmium

Cadmium is used in metal plating, in batteries (Ni-Cd-battery), television tubes, solar cells, fungicides, as a stabilizer in PVC, and as pigments in plastic and glasses.

Cadmium acts as a cumulative poison and is listed among the 129 priority pollutants by the Environmental Protection Agency (EPA) and the European Union (Amtsblatt der Europäischen Gemeinschaften, 1999; Internationale Kommission zum Schutze des Rheins (IKSR), 1992).

Volcanic emanations can account for 40-50% (Nriagu, 1989) of the cadmium emitted annually (totally 0.96 t/year) (Nriagu, 1979b). The main anthropogenic sources ( $\sim 7$  t/year) are due to combustion of fossil fuel and coal, and liberation during smelting and refining of various ores. Non-ferrous metal mines represent a major source of cadmium released to the aquatic environment (Nriagu and Pacyna,

1988). Contaminations can arise from mine drainage water, waste water from ore processing, overflow from the tailings pond and rain water runoff from the mine area. Atmospheric fallout represent 20-40% of the input of cadmium into fresh water and marine systems (Nriagu and Pacyna, 1988). Solid wastes disposed off in landfill sites result in large input of cadmium into soils. Other important inputs are the application of phosphate fertilizer and municipal sewage sludge.

Much of the cadmium entering fresh waters is rapidly adsorbed by particulate matter, where it may settle. This can result in low concentrations of dissolved cadmium even in fresh waters that receive high concentration of cadmium. In other conditions, cadmium may remain suspended. In this case, it can be transported considerable distances from the source, e.g., in Japan, in several areas, soils have been contaminated with irrigation waters up to 50 km from the source (World Health Organisation, 1992 a).

The electronic configuration of cadmium is  $[\text{Kr}]4d^{10}5s^2$ . Therefore  $\text{Cd}^{2+}$  belongs to the B-type metal cations, the soft cations, i.e., it prefers to bind to ligands containing sulfur and nitrogen atoms (Stumm and Morgan, 1996). Its place in the periodic table is between zinc and mercury (group IIB), and it has many properties in common with these elements (Greenwood and Earnshaw, 1985).

In the absence of precipitating anions like phosphate, sulphate, or carbonate,  $\text{Cd(II)}$  is available for sorption onto suspended material and complexation with organic matter. It forms moderately stable complexes with a variety of organic compounds. Binding of cadmium to humic substances from sea, river, and lake waters follow in general the Irving-Williams series of stabilities of chelates (Moore and Ramamoorthy, 1984).

Cadmium toxicity became famous with the Itai-Itai disease in Japan. This is a bone disease with marked decalcification accompanied by severe pain. Cadmium toxicity was shown to have occurred by eating cadmium polluted rice (Nriagu, 1981). The main symptoms of acute occupational cadmium poisoning are related to the respiratory system. It causes problems for the kidneys (Nriagu, 1981).

### 1.4.3 Nickel

The main uses of nickel lie in alloys such as stainless steel, copper-nickel-zinc alloys known as German silver or nickel silver, and other corrosion resistant alloys. A nickel alloy used in more than 140 countries in coinage contains about

25% nickel and 75% copper. The first pure nickel coin was issued in Switzerland in 1881 and since then more than 100 countries have used this metal in their coins (Nriagu, 1980). Pure nickel is used in electron tubes and in the galvanic industry, where many objects must be coated with nickel before they can be chromium plated. Furthermore, it is an important catalyst for hydrogenation of organic substances, e.g., vegetable oils.

Nickel is listed by the Environmental Protection Agency (EPA) and by the European Union (Amtsblatt der Europäischen Gemeinschaften, 1999; Internationale Kommission zum Schutze des Rheins (IKSR), 1992) as one of 129 priority pollutants. In most urban settings, nickel concentrations are usually elevated at least 4 times above background levels (National Research Council, 1975).

About  $43 \cdot 10^6$  kg/year nickel are emitted from man-made sources into the atmosphere (World Health Organisation, 1991). The main anthropogenic sources for emission into the atmosphere are oil combustion, municipal incinerators, and nickel mining and refining. The main natural sources to the atmosphere are soil dust and volcano emissions ( $26 \cdot 10^6$  kg/year) (Nriagu, 1980). Nickel is found as a constituent in most meteorites and often serves as one of the criteria for distinguishing a meteorite from other minerals (Nriagu, 1980). Nickel is introduced into the hydrosphere by wet and dry atmospheric deposition, by surface runoff in urban areas, by discharge of industrial and municipal waste, and as a result of natural erosion of soils and rocks (World Health Organisation, 1991). The anthropogenic input of nickel into the aquatic environment amounts to about  $113 \cdot 10^6$  kg/year (Nriagu and Pacyna, 1988).

The electronic configuration of nickel is  $[\text{Ar}]3d^84s^2$ . The cation  $\text{Ni}^{2+}$  belongs to the transition metal cations and can therefore bind to ligand sites containing oxygen, sulfur, or nitrogen atoms. According to the Irving-Williams series, nickel complexes are less stable than copper complexes (Stumm and Morgan, 1996). It can also form quite stable complexes with inorganic ligands such as halides, sulphates, phosphates, carbonates, and carbonyls (Moore and Ramamoorthy, 1984).

In freshwaters, nickel is mainly transported in the form precipitated coatings on particles and in association with organic matter. It may be adsorbed onto clay particles and other minerals and may be taken up by biota.

Nickel is an essential trace element for the nutrition of man and animals. Man normally ingest nickel in food and water at an estimated 300-600  $\mu\text{g}/\text{day}$ . There is evidence that nickel is associated with proteins, amino acids, and possibly nucleic acids (National Research Council, 1975). Nickel deprivation has an effect on body

weight, reproductive capability, viability of offspring, and induction of anemia through reduced absorption of iron. Inhalation of nickel carbonyl,  $\text{Ni}(\text{CO})_4$ , has shown to be carcinogenic (National Research Council, 1975). Nickel present in asbestos may possibly contribute to the carcinogenicity associated with asbestos inhalation in man (National Research Council, 1975). Nickel was a common source of chronic dermatitis in man, as a result of industrial and other exposures such as jewelry (National Research Council, 1975).

#### 1.4.4 Organic ligands in freshwater systems

Besides the natural organic matter (NOM), also anthropogenic ligands like EDTA, NTA, or residues from pesticides can be found in a freshwater system.

The production of NOM is very complex and not yet well understood. Generally it can be said that NOM originates from degradation of higher plants by bacteria and fungi (mainly pedogenic NOM) or by decomposition of plankton and aquatic bacteria (aquagenic NOM) (Buffle, 1988; Stevenson, 1982).

Usually, NOM is separated into different fractions to work with. The most common method is shown in Fig. 1.1 (Leenheer and Huffman, 1976; Thurman, 1985). A XAD resin is used for the fractionation: organic substances that adsorb onto the resin at pH 2 are termed hydrophobic or humic substances (HS), those that do not adsorb are hydrophilic. Humic acids are humic substances that are precipitated at pH 1, whereas fulvic acids stay in solution at this pH value.

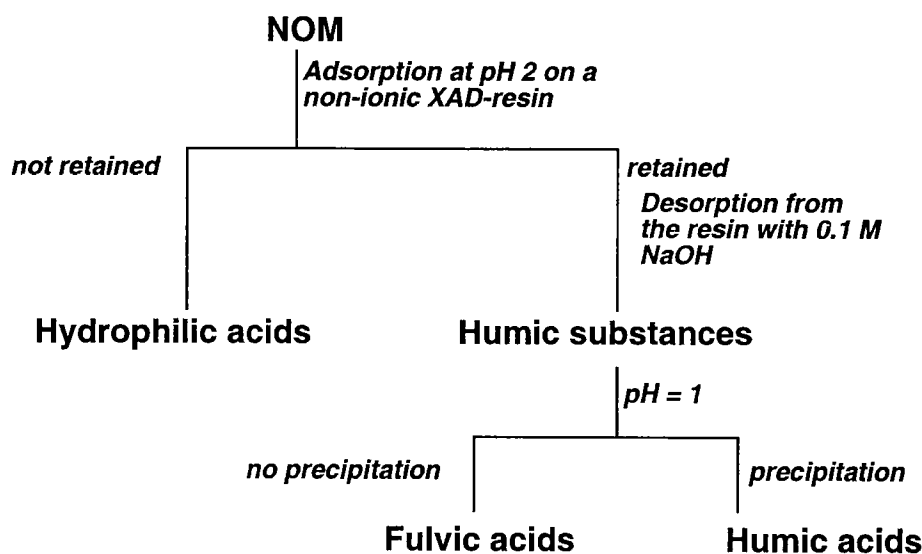


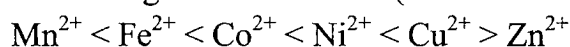
Fig. 1.1: Fractionation of NOM

It is essentially impossible to determine a unified structure for HS or hydrophilic acids. They present a complex mixture of (macro)molecules with a composition that changes over time and space. For example, it has been shown that dissolved organic carbon in groundwaters is more hydrophilic than in surface waters. The longer residence time of organic matter in groundwater results in hydrophobic substances being either sorbed onto the aquifer solids or degraded into simpler organic acids by bacteria present in the aquifer (Aiken et al., 1985). In general, ground water HS contain less oxygen than fresh surface water HS (Aiken et al., 1985). As the carboxyl content is about the same for both groups, oxygen depletion must occur in other functional groups such as carbonyls or hydroxyls. Groundwater HS are less coloured than surface water HS, i.e., they contain fewer chromophores such as aromatic rings and phenolic functional groups. This is consistent with the fact that they are more aliphatic (Aiken et al., 1985).

In general, the following statements for the structure of humic and fulvic acids can be made: humic acids have a molecular weight of 2000-5000, whereas fulvic acids are of smaller molecular weight (about 500-2000) (Aiken et al., 1985). The relative amount of aromatic carbon is larger in humic acids compared to fulvic acids. Fulvic acids have in general a larger amount of total acidity and a higher ratio of carboxyl to phenolic groups. In connection with this, a higher O/C ratio for fulvic acids is usually found than for humic acids. Leenheer and co-workers have shown that a major part of the strong acidic groups in fulvic acids ( $pK_a$  values around 2) can be represented by aliphatic carboxylic groups (Leenheer et al., 1995 a and b). In addition fulvic acids have a smaller total C-, and a larger N- and S-content.

Only few studies have dealt with hydrophilic acids. They are thought to be similar to humic substances with lower molecular weights, and a more carboxylic and hydroxylic character (Aiken et al., 1985; Thurman, 1985).

Generally it is assumed that metal ions form complexes with the functional groups of humic substances. The most important complexing moieties are the carboxylic and phenolic groups, but also nitrogen and sulphur containing functional groups have been identified (Buffle, 1984; Stevenson, 1982). Complexation constants of transition metals correlate rather well with hydroxide and carbonate stability constants of the metals (Turner et al., 1998). For example, Cu(II) forms readily complexes with hydroxides and carbonates and is therefore most likely to form complexes with fulvic and humic acids. The sorption affinity follows in general the Irving-Williams series (Stumm and Morgan, 1996):



At very low metal concentrations, binding mainly occurs at sites which have a high and specific affinity. With increasing metal concentrations, the complexation sites get occupied according to their complexation strength. In many natural waters the complexation groups with the weakest affinity represent the highest fraction.

To represent the complicated complexation behaviour of humic substances, different models have been developed:

- Discrete site modes: Typically 2 to 5 different ligands are defined, each with its own concentration, complexation and acidity constants (Cabaniss and Shuman, 1988 a and b; Tipping, 1994; Tipping and Hurley, 1992). To describe the dependence of the complexation behaviour on the ionic strength, electrostatic effects have to be considered. Examples for this are given in the WHAM (Windermere Humic Aqueous Model) model of Tipping (Tipping, 1994; Tipping and Hurley, 1992) and in the oligoelectric model of Bartschat et al. (1992).

These models have the advantage that they can be easily used in common speciation programmes, as ChemEQL (Müller, 1996) or FITEQL (Herbelin and Westall, 1994) to describe the complexation of heavy metals by humic and fulvic acids.

- Continuum models: A continual distribution of binding sites having varying pK values and different complexation constants is assumed. The probability that the complexation constants are in a certain range is estimated (Buffle and Altmann, 1987). An example is the NICA model (Non Ideal Competitive Adsorption model) (Benedetti et al., 1995). In this model, two types of functional groups, representative of carboxylic and phenolic groups, are defined. For both groups, a mean complexation constant with a distribution of constants around this value is assumed. To describe the complexation behaviour of the different cations, it is taken into account that the different metal ions do not experience the same interactions with the ligand (Koopal et al., 1994). This model was improved by considering electrostatic effects (Benedetti et al., 1996). A detailed description of other continuum models can be found elsewhere (Allison and Perdue, 1994; Dobbs et al., 1989; Susetyo et al., 1991).

The advantage of this kind of model is that they can better represent the physical reality of the complex natural structures as they represent a distribution of complexation constants.

## 1.5 Interactions of Ligands and Major Cations with Heavy Metal Adsorption

In the absence of competing ligands and cations, metal adsorption onto (hydr)oxide surfaces is described by the typical pH adsorption edge which means that adsorption is strongly increased in a very narrow pH range. The adsorption in a system without ligands and competing cations is considered as the reference system.

However, the presence of cations and anions can affect the adsorption of heavy metals onto goethite in different ways.

### *Increased Heavy Metal Adsorption compared to the reference system*

This would be expected mainly at low pH values and may be due to:

- *Electrostatic interactions* (Fig. 1.2)

At pH values below  $\text{pH}_{\text{pzc}}$ , the surface is positively charged. For example, if a negatively charged ligand is adsorbed on the surface, it may induce a charge reversal on the surface and thus may electrostatically attract positively charged copper cations.

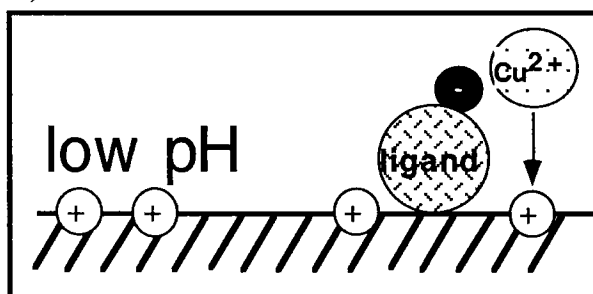


*Fig. 1.2: Electrostatic interactions on the surface.*

Above described mechanism may also work with anionic organic ligands (Tipping and Cooke, 1982).

- *Formation of ternary complexes*

Ternary complexes are defined as coadsorption of a metal cation and a ligand anion on the same surface site. Two types of ternary complexes can be distinguished (for more details see chapter 2).

In Fig. 1.3, the adsorption of a ternary complex type B is represented schematically. Organic ligands preferentially adsorb at low pH values. If these organic ligands have more than one complexing functional group, they can react with surface ligands with one group and can complex a metal cation on the solution side with the other group. This complexation capacity can be estimated by



considering the complexation behaviour in solution. However, some authors have argued that the complexation by an adsorbed ligand is smaller than that in solution because of steric effects on the surface. Other authors have reported that an electron transfer of the adsorbed ligand to the surface can enhance its complexation properties.

At pH values, where metal cations preferentially adsorb, formation of ternary complexes of type A is possible (Fig. 1.3).

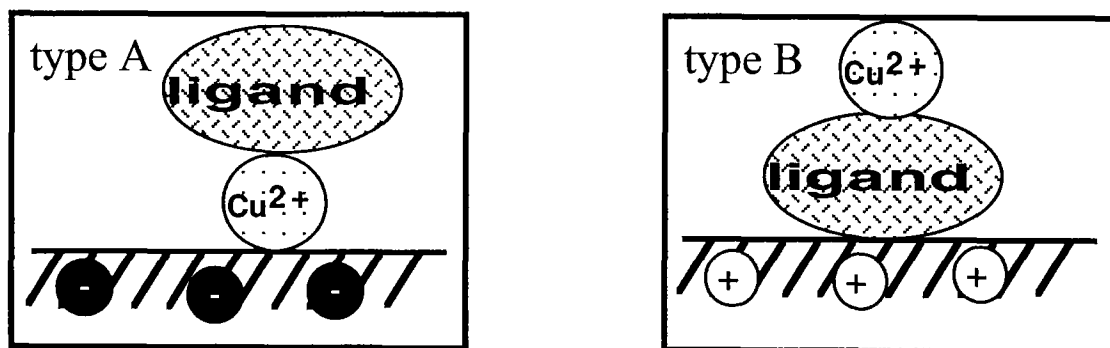


Fig. 1.3: Formation of ternary complexes of type A and type B

### ***Decreased heavy metal adsorption compared to the reference system***

This would be expected at higher pH values where almost 100% of the heavy metal are adsorbed in reference experiments. Again, two possibilities for decreasing adsorption can be distinguished.

- *Competition reactions with other cations*

In a groundwater matrix, competition of heavy metals with e.g., Ca or Mg may occur. The concentration of calcium, for instance, is usually several orders of magnitude higher than that of heavy metals like copper, cadmium, zinc, lead, or nickel. The adsorption of calcium, although weaker than that of heavy metals, may block surface sites and thus decrease because of its high concentrations heavy metal adsorption (Fig. 1.4).

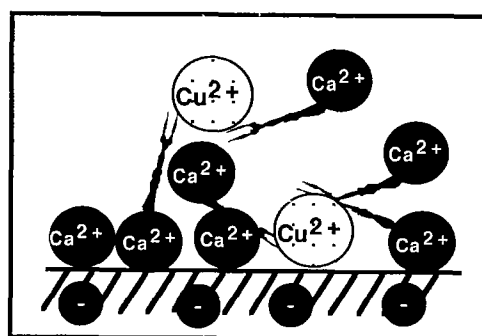
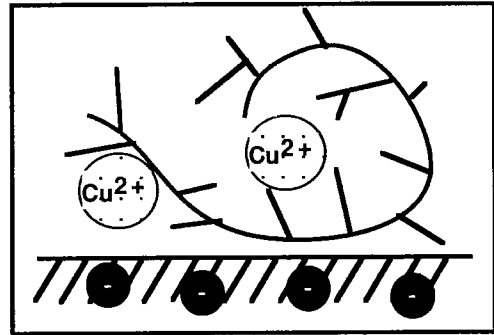


Fig. 1.4: Competition reactions of copper with calcium adsorption

- *Complexation of heavy metals in solution*

Various ligands can complex heavy metals in solution. If this complex is unable to adsorb, i.e., formation of ternary complexes is not likely to occur, heavy metals are mobilised. For example, such mobilisation was observed for mercury with chloride (Behra, 1986) or for copper with humic acids (Tipping et al., 1983) (Fig. 1.5).



*Fig. 1.5: Complexation reactions in solution by a chelating agent*

A combination of these different mechanisms is often observed. For instance, Nowack and Stone (1999) found reduced adsorption of copper and zinc on goethite in the presence of phosphonates. However, according to the surface complexation model developed, the reduction in metal adsorption should have been more pronounced. Simultaneous formation of ternary complexes may account for this difference in adsorption.

# *Modelling of Adsorption Reactions at Mineral Surfaces*

## **2.1 Introduction**

Different kinds of models have been developed to quantify the key parameters of adsorption reactions.

- Physical models

These purely physical models only take into account physisorption and chemisorption. They have a foundation in statistical thermodynamics. The best known are the Langmuir type isotherm, BET type isotherm, and the Freundlich type isotherm (Morel and Hering, 1993; Stumm and Morgan, 1996). The advantage of these models is that they are easy to use and that an adsorption constant and the number of surface sites of the solid can be estimated. The disadvantage is that they give no chemical mechanistic information and that the determined coefficients are only applicable to the conditions at which they were determined.

Electrostatic interactions can be taken into account by the Gouy-Chapman relationship or by the Stern models (Davis and Kent, 1990; Stumm and Morgan, 1996; Westall and Hohl, 1980).

- Classical Surface Complexation Models (SCM)

Their origin is the inorganic complexation theory. In these models, adsorbing cations and anions are supposed to form surface complexes with the reactive >OH groups of (hydr)oxides (Stumm, 1987). In order to calculate the intrinsic adsorption constants, the electrostatic effects caused by these surface reactions have to be estimated by models. These differ in how the solid-water interface is described by

planes within the double layer in order to simulate the distribution of the surface charges and then the surface potential. The most common electrostatic models are the Constant Capacitance Model (CCM), the Double Layer Model (DLM), and the Triple Layer Model (TLM) (Brown, 1990; Stumm, 1987; Stumm, 1996; Stumm and Morgan, 1996)

- Multi Site Complexation Models

In above models surface sites have been considered to be independent on the structure of the crystal. But recent spectroscopic studies have rejected this simplification (Nagashima and Blum, 1999; Weidler et al., 1996), which has led to the definition of the MUSIC model. In addition all ions were classically represented as point charges, which did not allow to account for all electrostatic effects. That is why the concept of charge distribution was developed with the MUSIC model (Hiemstra, 1996). The recently developed model, the charge distribution-multi site complexation model (CD-MUSIC), takes into account this additional information (Hiemstra et al., 1989 a, b).

The aim of this chapter is to describe the most used models for adsorption reactions on mineral surfaces, and to show how these models have been used in literature to describe the adsorption reactions of copper, cadmium, nickel, oxalate, salicylate, and pyromellitate on goethite. The adsorption constants of metal or ligand adsorption on goethite in the reference systems as needed in chapters 4 and 5 will be determined by parameter estimation with the SCM using the DLM model for electrostatic interactions. Furtheron it will be discussed on the basis of the pH adsorption edge of copper on goethite, how the use of different models affects the intrinsic adsorption constant. It will be shown that constants defined with one model cannot be used for calculations with another model.

## 2.2 Adsorption Isotherms

The discussion will be restricted to the Langmuir type isotherm. The typical shape of such an adsorption isotherm is given in Fig. 2.1. Three assumptions are made in this model. First, the adsorbed molecules are forming a monolayer on the surface, which means that once a certain concentration of metal has adsorbed on the surface, a saturation is reached. This concentration corresponds to  $c_{\max}$ , the number of surface sites available. Secondly, equal energy for all surface sites is assumed,

which means concretely that all surface sites are assumed to react equally. Thirdly, adsorption is considered to be independent of surface coverage, which means that no interactions between the sorbed molecules are taken into account.

The expression for the Langmuir type isotherm is derived from the mass balance for surface sites and the mass action law (Eq 2.1) (Stumm and Morgan, 1996):

$$c_s = c_{\max} \cdot \frac{K_L \cdot c_w}{1 + K_L \cdot c_w} \quad [2.1]$$

where:  $c_s$ : adsorbed metal concentration on the surface [mol/g]  
 $c_w$ : concentration of metal in solution [M]  
 $K_L$ : Langmuir type adsorption constant [M<sup>-1</sup>]  
 $c_{\max}$ : maximum metal concentration that can be adsorbed on the surface [mol/g]

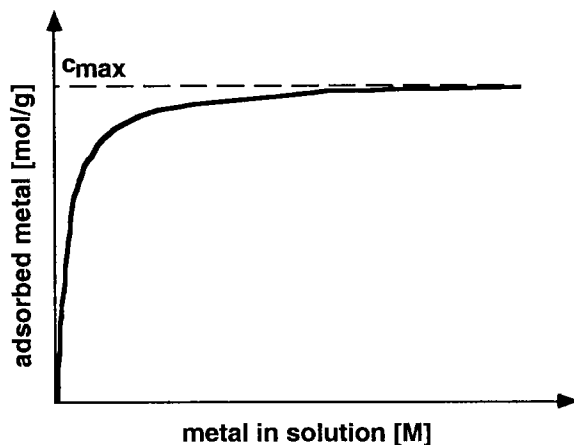


*Fig. 2.1: Langmuir type adsorption isotherm*

The most common linearisation is the following (Eq 2.2):

$$\frac{1}{c_s} = \frac{1}{c_{\max} \cdot K_L} \cdot \frac{1}{c_w} + \frac{1}{c_{\max}} \quad [2.2]$$

From intercept and slope,  $c_{\max}$  and  $K_L$  can be estimated.

There is no difference between a Langmuir constant and an apparent surface complexation constant at constant pH. A Langmuir constant defined at a certain pH value can be used as conditional constant in the surface complexation models.

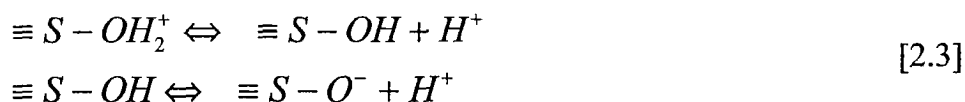
The advantage of such models is that they are easy to use and that they allow an estimation for the conditional adsorption constants and the number of surface sites. The Langmuir type isotherm can describe surface complexation mechanisms, but the disadvantage is that no detailed chemical reactions can be included in these

models. The Surface Complexation models, presented next, try to take into account chemical reactions.

## 2.3 Classical Surface Complexation Models

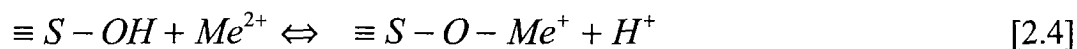
### 2.3.1 Adsorption Reactions of Metal Cations and Organic Ligand Anions

The surface ligands responsible for adsorption reactions are supposed to be amphoteric groups, mainly >OH surface groups, i.e., in acidic conditions, there is formation of >OH<sub>2</sub><sup>+</sup> and at high pH-values formation of >O<sup>-</sup> groups on the surface (Stumm, 1996) (Eq 2.3):



Anions and cations can adsorb by forming either innersphere or outersphere complexes with these amphoteric surface groups. Innersphere complexes form a direct coordination bond with a surface functional group. This means that the ion that binds coordinatively to the surface will only be partially affected by electrostatics, and will be minimally susceptible to small differences in surface site density and distribution of surface charge. In contrary to this, outersphere complexes form ion pairs with the surface and thus their binding is coulombic and more susceptible to differences in site density and distribution of surface charge. The biggest difference between inner- and outersphere complexes lies in the fact that innersphere coordination affects the orbital of the coordinated metal ions and is therefore more sensitive to be detected with spectroscopic methods (Schindler, 1990).

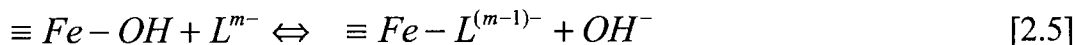
Spectroscopic measurements gave ample evidence that most heavy metal ions adsorb innerspherically (Brown, 1990; Schindler, 1990). Metal cation adsorption in the surface complexation modelling approach is often defined to be monodentate according to Eq 2.4:



The metal adsorption is strongly pH dependent presenting typically a steep pH adsorption edge (Stumm, 1987; Stumm and Morgan, 1996): at low pH values small concentration of metals are adsorbed, and at high pH values a high amount of

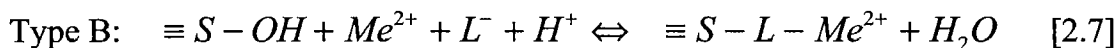
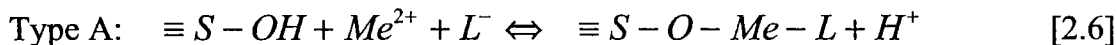
metal is adsorbed. At low pH values, there is no adsorption because of the competition of metal cations with protons for surface sites. Typical adsorption constants, as they were defined in the literature, are reported in Tab. 2.1.

The general equation for the organic ligand anion adsorption is given in Eq 2.5:



Organic ligands adsorb more extensively at low pH values with decreasing adsorption at increasing pH. Modelling results for adsorption of oxalate, salicylate, and pyromellitate on mineral surfaces, as described in the literature are given in Tab. 2.2.

In a system containing both organic ligands and metal cations, competition reactions between them may occur, or formation of ternary complexes is possible. Ternary complex formation can be seen as coadsorption of metal cations and organic molecules onto the same mineral surface site. Two types of ternary complexes can be distinguished: type A (surface-metal-ligand) (Eq 2.6) and type B (surface-ligand-metal) (Eq 2.7).



The pH dependence for the formation of type A ternary complexes is metal-like. Their formation occurs mainly at higher pH values and it enhances the adsorption of organic ligands. Type A ternary surface complexes can as well enhance metal adsorption, especially in the presence of  $\pi$ -acceptor ligands. These ligands draw the electron density from the d-orbitals of the metal ion, and the positive charge on the metal ion is enhanced. Bourg et al. (1979) and Bourg and Schindler (1979) could explain an elevated copper adsorption on silica in the presence of 2,2'-bipyridine by assuming 2 ternary complexes of type A.

Formation of type B ternary complexes enhances the adsorption of metal cations at low pH values. Adsorption of multi functional organic anions onto positively charged surfaces creates additional sites for metal cation adsorption on the surface. This adsorption of metal organic complexes is ligand-like.

**Table 2.1:** Literature values of adsorption constants as calculated with surface complexation models of copper, cadmium, and nickel on goethite. The models used for the electrostatic interactions are precised in the table.

Metal	Reference	Surface equations	Model	log $K_{ads}$
Copper	Coughlin and Stone, 1995	$\equiv Fe-OH + Cu^{2+} \Leftrightarrow \equiv Fe-O-Cu^+ + H^+$	TLM <sup>[1]</sup>	2.5
	Ali and Dzombak, 1996	$\equiv Fe-OH + Cu^{2+} \Leftrightarrow \equiv Fe-O-Cu^+ + H^+$	G-TLM <sup>[2]</sup>	2.21
	Robertson, 1998	$\equiv Fe-OH + Cu^{2+} \Leftrightarrow \equiv Fe-O-Cu^+ + H^+$ $\equiv Fe-OH + Cu^{2+} + H_2O \Leftrightarrow \equiv FeO-CuOH + 2H^+$ $2 \equiv Fe-OH + Cu^{2+} \Leftrightarrow \equiv (Fe-O)_2 - Cu^+ + 2H^+$	DLM <sup>[3]</sup>	3.08 -5.15 -2.31
Cadmium	Cowan et al., 1991	$\equiv Fe-OH + Cd^{2+} \Leftrightarrow \equiv Fe-O-Cd^+ + H^+$	TLM <sup>[1]</sup>	-1.9
	Gunneriusson, 1993	$\equiv Fe-OH + Cd^{2+} \Leftrightarrow \equiv FeOHCd^{2+}$	CCM <sup>[4]</sup>	6.43±0.05
		$\equiv Fe-OH + Cd^{2+} \Leftrightarrow \equiv FeOCd^+ + H^+$		-2.22±0.05
		$\equiv Fe-OH + Cd^{2+} \Leftrightarrow \equiv FeOCdOH + 2H^+$		-12.01±0.08
Nickel	Bryce et al., 1994	$\equiv Fe-OH + Ni^{2+} \Leftrightarrow \equiv FeO-Ni^{2+} + H^+$ (mineral = HFO)	DLM <sup>[3]</sup>	0.87

<sup>[1]</sup>: Triple Layer Model

<sup>[2]</sup>: Generalized Two Layer Model

<sup>[3]</sup>: Double Layer Model

<sup>[4]</sup>: Constant Capacitance Model



**Table 2.2:** Literature values of adsorption constants as calculated by surface complexation models of oxalate, salicylate, and pyromellitate on goethite. The models used to correct for the electrostatic interactions are listed in the table.

Ligand	Literature	Surface equations	Model	log $K_{ads}$
Oxalate	Mesuere and Fish, 1992	$\equiv Fe-OH + Ox^{2-} + 2H^+ \Leftrightarrow \equiv Fe-Ox-H + H_2O$	DLM <sup>[1]</sup>	15.7
		$\equiv Fe-OH + Ox^{2-} + H^+ \Leftrightarrow \equiv Fe-Ox^- + H_2O$		9.1
		$\equiv Fe-OH + Ox^{2-} \Leftrightarrow \equiv Fe-O-Ox^{3-} + H^+$		-5.9±0.1
	Mesuere and Fish, 1992	$\equiv Fe-OH + Ox^{2-} + H^+ \Leftrightarrow \equiv FeOH_2^+ \dots Ox^{2-}$ <sup>[4]</sup>	TLM <sup>[2]</sup>	11.5±0.1
$\equiv Fe-OH + Ox^{2-} + 2H^+ \Leftrightarrow \equiv FeOH_2^+ \dots HOx^-$ <sup>[4]</sup>	17.7±0.2			
Salicylate	Nilsson, 1995	$\equiv Fe-OH + HSal^- \Leftrightarrow \equiv Fe-Sal^- + H_2O$	E-CC <sup>[3]</sup>	6.34
		$\equiv Fe-OH + HSal^- + H^+ \Leftrightarrow \equiv Fe-OH_2^+ \dots HSal^-$ <sup>[4]</sup>		0.69
Pyromellitate	Boily et al., 2000	$2[\equiv FeOH^{0.5-}]_{\{110\}} + Pyr^{4-} + 2H^+ \Leftrightarrow [(\equiv FeOH_2^{0.5+})_2 - Pyr^{4-}]_{\{110\}}$	TPM <sup>[5]</sup>	20.88±0.06
		$[\equiv FeOH^{0.5-}]_{\{110\}} + Pyr^{4-} + 3H^+ \Leftrightarrow [\equiv FeOH_2^{0.5+} - H_2Pyr^{2-}]_{\{110\}}$		19.91±0.08
		$2[\equiv FeOH^{0.5-}]_{\{001\}} + Pyr^{4-} + 2H^+ \Leftrightarrow [(\equiv Fe_2)Pyr^-]_{\{001\}} + H_2O$		13.86±0.2

<sup>[1]</sup>: Double Layer Model

<sup>[2]</sup>: Triple Layer Model

<sup>[3]</sup>: Extended Constant Capacitance Model

<sup>[4]</sup>: Outer Sphere Complex

<sup>[5]</sup>: Three Plane Model. The surface complexation model used with this model was the multisite complexation model (MUSIC).

**Tab. 2.3:** *Examples of ternary complex formation in different system*

Reference	Type	Mineral	Metal	Ligand
Davis and Leckie, 1978	B	amorphous	copper	glutamic acid
	B	iron oxide	copper	pyrazinedi-carboxylic acid
	B		silver	thiosulphate
Bourg et al., 1979a	A	silica	copper	2,2'-Bipyridyl
Benjamin and Leckie, 1982	A	different oxide	cadmium	chloride
	A	surfaces	cadmium	sulphate
	B		cadmium	thiosulphate
Dalang et al., 1984	B	kaolinite	copper	fulvic acids
Lövgren, 1991	A	goethite	aluminum	phthalic acid
Zachara et al., 1994	B	subsurface mineral	cobalt	leonardite humic acid
Tiffreau et al., 1995	A	HFO	mercury	chloride
Boily and Fein, 1996	B	$\alpha$ -Al <sub>2</sub> O <sub>3</sub>	cadmium	citric acid
			cadmium	
Ali and Dzombak, 1996	B	$\alpha$ -FeOOH	copper	chelidamic acid
			copper	phthalic acid
Nowack et al., 1996b	B	goethite	different	EDTA
	B	hydrous ferric	metals e.g.,	
	B	oxide	Fe(III), Ni	
	B	lepidocrocite	Zn, Cu, Pb, Pd, Ca, Co	
Angove et al., 1999	B	goethite and	cadmium	phthalic acid
	B	kaolinite	cadmium	hemimellitic acid
	B		cadmium	trimellitic acid
	B		cadmium	trimesic acid
	B		cadmium	pyromellitic acid
	B		cadmium	mellitic acid
Bonnissel-Gissinger et al., 1999	A	goethite amorphous silica	mercury	chloride

For simple organic molecules, there is a preference for formation of ternary complexes of type A (Schindler, 1990). However, in natural waters there seems to be a preference for the formation of type B ternary complexes, as the polyfunctional groups of humic and fulvic acids are ubiquitous in this system. The thermodynamic stability of ternary complexes is in general low (Schindler, 1990).

Tab. 2.3 shows different systems, in which ternary complexes have been defined in literature.

### 2.1.2 Formation of the Electric Double Layer (EDL)

The surface charge is defined by the formation of charged innersphere complexes. This leads to the formation of charged groups at the surface such as  $>\text{OH}_2^+$ ,  $>\text{O}^-$ ,  $>\text{O}-\text{M}^{n+}$ , and  $>\text{O}-\text{L}^{m-}$ . Because of the condition of electroneutrality, this surface charge is compensated by outersphere complexes and by counterions in solution, which form a diffuse plane at closest distance of the surface.

### 2.1.3 Definition of Surface Charges

The following charges at the solid-liquid interface can be distinguished (Sposito, 1984; Stumm, 1996):

- A permanent structural charge  $\sigma_s$ , due to isomorphous substitutions in the crystal lattice. For example, if a Si atom in silica is substituted by an Al atom, a negatively charged framework is established, because Al is trivalent and Si is tetravalent.
- A net surface charge  $\sigma_o$ , due to specific adsorption of ions on the surface. It can be distinguished between the charge resulting from adsorption of protons and hydroxides,  $\sigma_H$ , and the charge resulting from adsorption of other ions,  $\sigma_{CC}$ . The sum of  $\sigma_s$  and  $\sigma_o$  defines the charge on the surface,  $\sigma_p$ .
- A charge of the outersphere complexes,  $\sigma_\beta$ .
- A counter charge resulting from the counterions,  $\sigma_d$ .

Because of the condition of electroneutrality, the sum of these charges must be zero (Eq 2.8):

$$\sigma_s + \sigma_H + \sigma_{CC} + \sigma_d + \sigma_\beta = 0 \quad [2.8]$$

Relying on these charges, different points of zero charge can be defined (Sposito, 1984).

- $\text{pH}_{\text{pzc}}$ : point of zero charge ( $\sigma_{\text{p}} = 0$ ) ( $\sigma_{\text{p}} = \sigma_{\text{s}} + \sigma_{\text{o}}$ ).
- $\text{pH}_{\text{pznc}}$ : point of zero net charge ( $\sigma_{\text{s}} + \sigma_{\text{H}} = 0$ )
- $\text{pH}_{\text{pznpc}}$ : point of zero net proton charge ( $\sigma_{\text{H}} = 0$ ). The point of zero charge is solely established due to binding of  $\text{H}^+$  and  $\text{OH}^-$ .
- $\text{pH}_{\text{iep}}$ : isoelectric point ( $\sigma_{\text{d}} = 0$ ). The electrophoretic mobility of a particle is zero.
- $\text{pH}_{\text{pzse}}$ : point of zero salt effect ( $\partial\sigma_{\text{H}}/\partial I = 0$ , where  $I$  is the ionic strength). At this point the surface charge is not effected by a change in concentration of a background electrolyte.

## 2.1.4 Definition of Intrinsic Constants

The apparent constants calculated directly from experimental data include chemical and electrostatic interactions. For calculations, however, intrinsic constants, i.e., the constants which define only the chemical reactions on the surface, are of interest. Therefore a relationship between intrinsic and apparent constants has been defined (Eq 2.9) (Stumm, 1996; Stumm and Morgan, 1996):

$$K_{\text{int}} = K_{\text{app}} \cdot \exp\left(\frac{\Delta z \cdot F \cdot \Psi}{R \cdot T}\right) \quad [2.9]$$

where  $\Delta z$ : change of the surface charge

$\Psi$ : surface potential [V]

$F$ : Faraday constant ( $F = 96\,485 \text{ C/mol}$ )

The surface potential  $\Psi$ , which cannot be directly measured, is function of the surface charge. Different models have been proposed to estimate the surface potential as seen in the next paragraph.

## 2.1.5 Description of the Most Important Electrostatic Models

**Constant Capacitance Model (CCM)** (Schindler and Kamber, 1968; Schindler and Gamsjäger, 1972)

In this model, two planes are defined (Fig. 2.3)

- A plane 0 where innersphere complexes are formed

- A plane 1 where the surface potential equals zero

Only innersphere complexes are taken into account. Ions like  $K^+$ ,  $Na^+$ ,  $Cl^-$ ... are assumed not to interact with the surface.

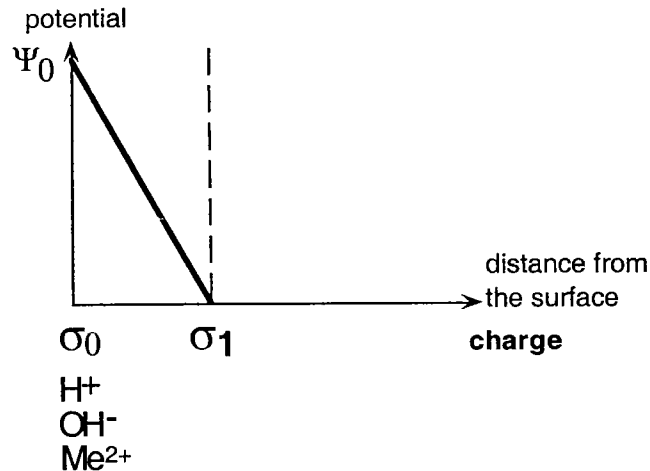


*Fig. 2.2: Scheme of Constant Capacitance Model (CCM)*

The relationship between the charge and the surface potential is given by the equation of a parallel plate condenser:

$$\sigma_o = C \cdot \psi_o \quad [2.10]$$

where:  $\sigma_o$ : surface charge [C]

C: capacitance [F]

The condition for electroneutrality gives:

$$\sigma_o + \sigma_1 = 0 \quad [2.11]$$

To estimate the adsorption constant and the concentration of the surface sites, at the most 5 parameters are needed:

- The capacitance can be estimated by linearisation of potentiometric titrations (Stumm and Morgan, 1996). The model is optimised with the capacitance.
- The site density on the surface can be calculated from potentiometric titrations of the solid phase.
- The specific surface area is measured with the BET method (Cornell and Schwertmann, 1996; Schwertmann and Cornell, 1991).
- Acid-base equilibrium constants of the surface ligands can be estimated from potentiometric titration data with surface complexation models.

The constant capacitance model is a special case of the double layer model. For a small surface potential, the sinus hyperbolicus expression in the Gouy-Chapman relationship (Eq. 2.12) is reduced to the expression  $\frac{z\psi_0 F}{2RT}$  and thus the surface charge is simply proportional to the surface potential. The coefficient of proportionality is the capacitance defined in Eq. 2.10.

The Constant Capacitance Model can only be used for high ionic strengths ( $I > 0.1$  M). Explanations are given in the paragraph Basic Stern Model in this chapter. More details on the CCM are given in Lützenkirchen (1996, 1999).

**Double Layer Model (DLM)** (Davis and Kent, 1990; Dzombak and Morel, 1990; Stumm, 1996; Stumm and Morgan, 1996)

Three planes are defined (Fig. 2.3):

- A plane 0 where ions adsorb specifically to form innersphere complexes
- A plane d with accumulation of the counterions
- A plane where the surface potential gets zero

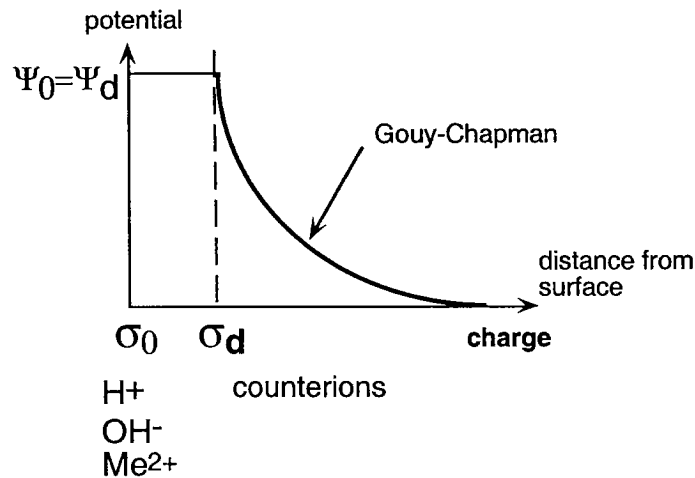


*Fig. 2.3: Scheme of Double Layer Model (DLM)*

Only innersphere complexes are taken into account to define the surface charge. The surface potential is related to the surface charge via the Gouy-Chapman theory (Eq 2.12). This relationship was derived from the one-dimensional Poisson-Boltzmann equation (Morel and Hering, 1993).

$$\sigma_o = (8RT\epsilon\epsilon_o c \times 10^3)^{1/2} \sinh(Z\Psi_o F / 2RT) \quad [2.12]$$

where: R: gas constant ( $R = 8.314$  J/(mol·K))

$\epsilon$ : dielectric constant of water ( $\epsilon = 78.5$  at  $25^\circ\text{C}$ )

$\epsilon_0$ : permittivity of free space ( $\epsilon_0 = 8.854 \cdot 10^{-12} \text{ C} \cdot (\text{V} \cdot \text{m})^{-1}$ )

$c$ : concentration of the electrolyte [M]

$Z$ : charge for a symmetrical electrolyte

The condition for electroneutrality gives:

$$\sigma_o + \sigma_d = 0 \quad [2.13]$$

To estimate the adsorption constant and the concentration of surface sites, at the most four parameters are needed:

- site density (calculated from potentiometric titrations of the solid phase)
- specific surface area (measured with the BET method)
- two acid-base equilibrium constants for the surface ligands (estimated from potentiometric titration data)

The double layer model is only applicable for low ionic strengths. In the Gouy Chapman theory, all ions are assumed to be point charges. Therefore, at high ionic strength, the number of counter ions accumulated on the plane d, and as a consequence, the surface charge, would be easily overestimated.

**Triple Layer Model (TLM)** (Brown, 1990; Stumm, 1987 and 1996; Stumm and Morgan, 1996)

In this model, four different planes are defined (Fig. 2.4):

- A plane 0 where ions form innersphere complexes
- A plane  $\beta$  where outer sphere complexes are bound electrostatically
- A plane d where the counterions accumulate
- A plane where the surface potential gets zero

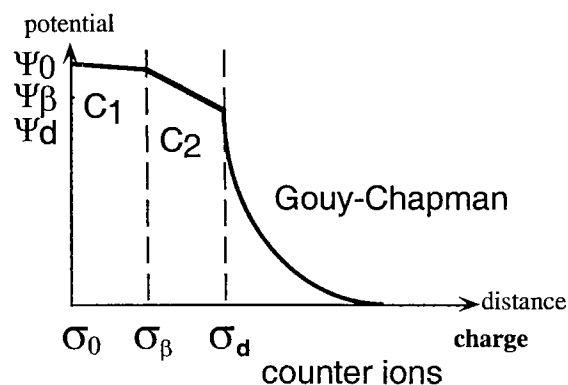


**Fig. 2.4:** Scheme of Triple Layer Model (TLM)

The  $\beta$ - and d-plane are assumed to be Helmholtz planes and are treated like 2 parallel condensers in series. The surface charge is related to the surface potential via the condenser equations and the Gouy-Chapman theory:

$$\sigma_d = -(8RT\epsilon\epsilon_0 c \times 10^3)^{1/2} \sinh(Z\Psi_d F / 2RT) \quad [2.14]$$

$$\sigma_d = C_2(\Psi_d - \Psi_\beta) \quad [2.15]$$

$$\sigma_o = C_1(\Psi_o - \Psi_\beta) \quad [2.16]$$

The condition for electroneutrality gives:

$$\sigma_o + \sigma_\beta + \sigma_d = 0 \quad [2.17]$$

In this model, innersphere as well as outersphere complexes are taken into account. Several authors define ions like  $\text{NO}_3^-$ ,  $\text{SO}_4^{2-}$  to form outersphere complexes (Collins et al., 1999; Hoins, 1993).

To estimate the adsorption constant and the concentration of the surface sites at the most seven parameters are needed:

- The capacitances  $C_1$  and  $C_2$  (fitting parameter, whereas  $C_1$  is mostly defined to be  $0.2 \text{ F/m}^2$ )
- Site density (calculated from potentiometric titration data)
- Specific surface area (measured with the BET method)
- Two acid-base equilibrium constants for the surface ligands (estimated from potentiometric titration data)
- Adsorption constants for outersphere complexes (fitting parameter)

## 2.4 Basic Stern Model (BSM)

The basis of the BSM is the principle of the electric double layer and the fact that the charge of the diffuse layer is described by the Gouy-Chapman theory (Bockris and Reddy, 1976; Dzombak and Morel, 1990). As the Gouy-Chapman relationship does not limit the surface charge to reasonable values at high ionic strength, the surface charge that can be developed on an oxide surface is limited by the number of binding sites. Their number is obtained from adsorption isotherms. Consideration of surface complexation reactions is quite similar to this approach to limit the surface charge. The Stern model is described in more details by Westall and Hohl (1980).



The following relationships in the electrostatic description can be observed between the Basic Stern Model, the CCM, and the DLM. The total capacitance is defined in the following way:

$$\frac{1}{C_{total}} = \frac{1}{C_{Helmholtz}} + \frac{1}{C_{diffuse}} \quad [2.18]$$

where:  $C_{Helmholtz}$  is the capacitance between the surface and the outer Helmholtz layer (= boundary to the diffuse layer);  
 $C_{diffuse}$  is an operationally defined capacitance in the diffuse layer.

A high concentration of ions in the diffuse layer, i.e., a high ionic strength, increases the capacitance of the diffuse plane. Hence at high ionic strength,  $C_{diffuse} \gg C_{Helmholtz}$ , and due to this simplification, the BSM is reduced to the Constant Capacitance Model (Fig. 2.5). Similar considerations can be made for low ionic strength, where the BSM is reduced to the double layer model.

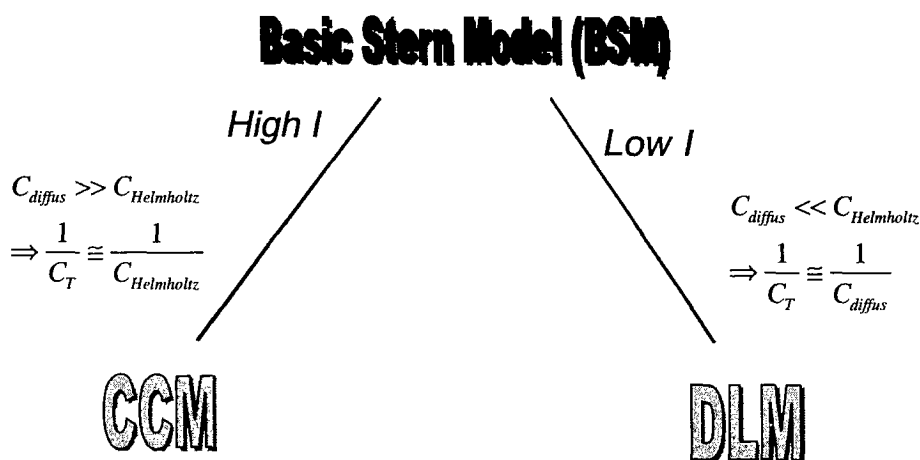


Fig. 2.5: Relationship between BSM, CCM, and DLM

## 2.5 CD-MUSIC (Charge Distribution Multi Site Complexation)

### 2.5.1 Concept of Charge Distribution

In the previous models, the charge of inner sphere complexes was assumed to be centered in one point. In the concept of charge distribution, the size of the molecule is taken into account. Only part of the adsorbed molecule is incorporated

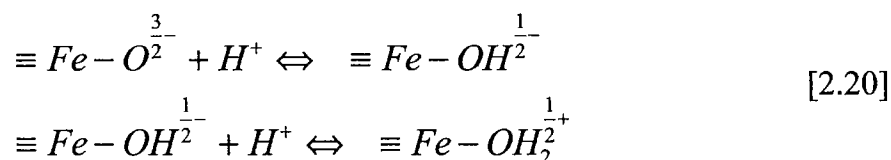
with its charge in the surface structure, while the other part is located in the so-called Stern layer. This phenomenon is taken into account by the concept of charge distribution.

The positive charge of a cation is distributed over several ligands and in the same way the charge of a ligand is distributed over several cations of the surface. The basis of this concept is the Pauling's rule (Pauling, 1929). A formal bond valence is defined as the quotient of the charge ( $z$ ) of a cation and its coordination number (CN):

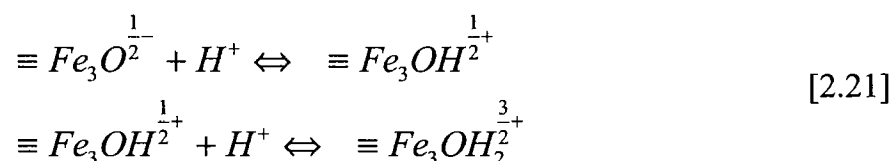
$$v = \frac{z}{CN} \quad [2.19]$$

For example, for the crystal structure of goethite, the formal bond valence  $v = 1/2$ , which means that half a charge can be neutralized per bond. This implies that  $Fe^{3+}$  needs six OH<sup>-</sup> to neutralize its charge and OH<sup>-</sup> needs two  $Fe^{3+}$  for neutralising its own charge.

Thus, for a singly coordinated oxygen (goethite planes {110} and {021}, see chapter 3) on a goethite surface, the following acid base equilibria can be written:



and for a triply coordinated oxygen (goethite plane {110}, see chapter 3), following reactions are defined:



Depending on the pH, the surface is positively or negatively charged. The surface charge is compensated by counterions, which leads to the formation of a double plane. The electrostatic interactions are taken into account by the three plane model (TPM) (Fig. 2.6).

It is known that some electrolyte ions form ion pairs with the surface, these are referred to as outersphere complexes (Hoins, 1993; Nilsson, 1995) and are located in the electrostatic plane d. These ions are treated as point charges - exactly as in the TLM model. The concentrations of the counterions increase towards the surface, but have a distance of closest approach to the surface, which is the plane d. They are as well treated as point charges and they are described by the Gouy-Chapman relationship.

Innersphere complexes are closer than the outersphere complexes to the surface. The ligands of adsorbed metal complexes or adsorbed oxoanions are partly incorporated in the surface plane (0-layer), and partly located in a plane within the Stern layer region, called 1-plane. The planes are treated as in TLM as two parallel condensers with capacitances  $C_1$  and  $C_2$ . For differences between the TLM and TPM, see the publication of Venema et al. (1996)

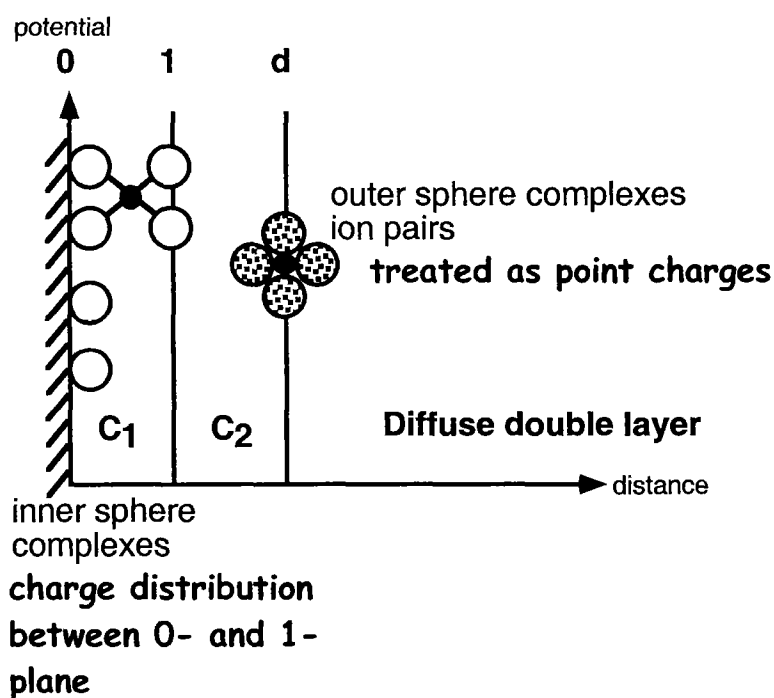


Fig. 2.6: Three plane model (TPM)

The charge distribution of the ligand is calculated with the Pauling bond valence concept. The charge of innersphere ligands is shared between the metal of the surface and the central atom of the adsorbed ligand, which means that it is shared between the 0-plane and the 1-plane. In order to calculate the charge distribution among the planes, a charge distribution factor  $f$  is defined as:

$$f = n \cdot v \quad [2.22]$$

where:  $n$ : number of common ligands  
 $v$ : valence bond of the adsorbing cation as previously defined (Eq. 2.19)

In case of equal charge distribution ( $f = 0.5$ ) within the adsorbing complex, half of the charge of the cation is attributed to the surface and the remaining to the solution orientated ligands. However, an equal distribution of charge may be in

conflict with the Pauling concept of local neutralization of charge. As a result of the adsorption reaction, the surface ligands may become “buried” and therefore they may be more part of the solid. As a result they will have a larger neutralization than the solution ligands, which leads to a larger value of  $f$ . As it is very difficult to predict  $f$ , it is treated as an adjustable parameter in the CD-model. More detailed information is given in the publication of Hiemstra (1996).

## 2.1.2 Multi Site Complexation

The MUSIC model is a surface complexation model that was developed to account for the diversity of surfaces in natural soils. Information on the structure of surfaces can be incorporated (Hiemstra et al., 1989 a,b, 1996) and thus give insight into mechanisms of adsorption reactions (Boily, 1999). Adsorption of cations as well as anions can be modelled (Hiemstra, 1996). In Fig. 2.7 all the information needed for this model is summarised. For classical surface complexation models, only the information on the right side of the figure was needed: adsorption experiments and information on how ions are distributed between the planes in order to calculate the surface potential. For the MUSIC model, additional data on the structure of the surface, given by crystallographic methods (spectroscopic and microscopic analysis), and information on surface binding, given by spectroscopic methods, are needed.

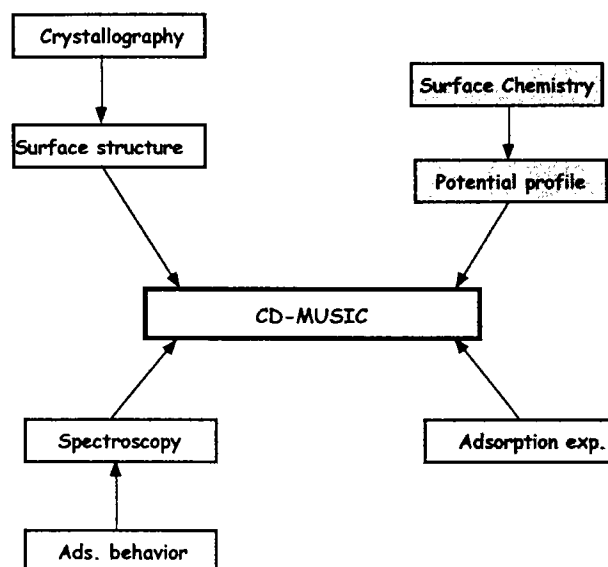


Fig. 2.7: Information needed to use the CD-MUSIC model

### ***Definition of an intrinsic constant***

The intrinsic constant is defined as in the classical surface complexation models over the Gibbs energy:

$$\Delta G_{app} = \Delta G_{int}^o + \Delta G_{el} \quad [2.23]$$

$\Delta G_{el}$  is the electric work done/released when a charge at a position  $i$  with a certain potential  $\Psi_i$  is changed by  $\Delta z_i$ :

$$\Delta G_{el} = \sum \frac{\Delta z_i \cdot F}{RT} \cdot \Psi_i \quad [2.24]$$

where:  $\Delta z_i$ : change in the charge at the position  $i$  due to adsorption.

Detailed calculations can be found elsewhere (Hiemstra, 1996).

The following parameters are needed to work with the CD-MUSIC model:

- Capacitances  $C_1$  and  $C_2$  (fitting parameter)
- charge distribution factor  $f$  (fitting parameter)
- intrinsic constants for the different binding sites of the goethite layers (estimated from potentiometric titration of the solid phase)
- surface site density (estimated from potentiometric titration of the solid phase)

## **2.6 Common points and differences between Surface Complexation Models**

The models presented in this chapter have the following points in common (see also (Sigg et al., 2000), chapter 9):

- Surface >OH-groups are assumed to be the main ligands on the surface. They react similarly to hydroxyl ions in solution.
- Adsorption reactions are independent on the structure of the solid phase, with exception of the MUSIC model.
- All charges are treated as point charges.
- The surface charge results from adsorption reactions.
- Equilibria can be described by law of mass action.
- The effect of the surface charge on sorption is taken into account by applying a correction factor derived from the EDL theory to the law of mass action.

The differences lie in the description of the electric double layer:

- The ions are differently distributed between the planes.

- The electrostatic relationships between the surface potential and the surface charge are different.

## 2.7 Applicability of Models

Models are often used in a somewhat unfortunate manner. In the following, some points are listed to illustrate how models should not be used:

- The DLM cannot be used to model data points at high ionic strength.
- The CCM is not applicable to low ionic strengths.
- The TLM should not be used when only data points at one ionic strength were measured. 7 parameters have to be estimated in this model, so the system gets too many degrees of freedom if not enough independent data points can be used.
- Information which you can obtain corresponds to the used model. For example, it is impossible to characterise the electric double layer by using the CCM and doing experiments at only one ionic strength.
- Constants fitted with different models should not be compared. They depend on the model and on the fitting parameters used. Hence, when defining a constant, it is necessary to give the values of all parameters.
- Models are never a proof for correctness of a mechanism.

## 2.8 Modelling of copper, cadmium, nickel, and oxalate on goethite

In this section, adsorption constants for heavy metal and ligand adsorption will be determined with the DLM model for the systems used in chapters 4 and 5. Parameter estimation was performed with the software FitEQL (Herbelin and Westall, 1994). Only experimental data below 90 % copper adsorption was used for parameter estimation. For these high adsorption values, only low concentrations of the sorbate were measured in the filtrate. As for all measurements, the same relative error for the total copper concentration (10 %) was assumed, this error became very low for low concentrations measured in the filtrate, i.e., for high copper adsorption.

The goodness of fit was mainly checked with the so called WSOS/DF factor (weighted sum of square of residuals divided by the degree of freedom). For an ideal fit, this value should equal 1, but generally values between 0.1 and 20 indicate a

reasonably good fit (Herbelin and Westall, 1994). This value directly depends on the relative and absolute error for the total defined concentration. The relative error was always chosen to be 10 % and the total absolute error was set to 10% of the total initial copper concentration. Further, it was checked that the actual error in the copper material balance was approximately equal to the defined experimental error, and that the quotient of both was randomly varying around 1 for all data points, to make sure that the model was appropriate.

For all the following models, properties of the goethite were defined as follows. The site density was defined to be 2.3 sites/nm<sup>2</sup> and the specific surface area was measured by the BET method to be 21.4 m<sup>2</sup>/g. The pK<sub>a</sub> values of the surface were set to 7.9 and 10.5. More details to goethite characterization are given in chapter 3.

### 2.8.1 Copper-Goethite System

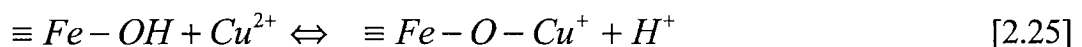
The intrinsic equilibrium constant for the pH dependence of the adsorption of copper onto goethite was determined by two surface complexation models: the constant capacitance (only for adsorption edge recorded with [Cu]<sub>tot</sub> = 5 μM) and the diffuse layer model. The results given by these two models will be compared.

The experimental setup for the pH adsorption edge of copper on goethite is explained in detail in chapter 4 respectively in chapter 5, but the most important parameters are summarized in Tab. 2.4.

**Table 2.4:** Parameters for copper adsorption experiments onto goethite

Parameter	Concentration (chapter 4)	Concentration (chapter 5)
Cu [M]	5·10 <sup>-6</sup>	3.03·10 <sup>-7</sup>
goethite [g/L]	0.5	0.5
Ionic strength (KNO <sub>3</sub> ) [M]	0.01	0.01

To describe copper adsorption on goethite, one surface complexation reaction was found to be able to describe the data sufficiently well (Eq. 2.25):



Copper speciation in solution was calculated with the constants reported in Tab. 2.5.

**Table 2.5:** Constants used to calculate copper speciation in solution

Species	log K
CuOH <sup>+</sup>	6.1 <sup>[1]</sup>
Cu(OH) <sub>2</sub>	11.6 <sup>[1]</sup>
Cu(OH) <sub>3</sub> <sup>-</sup>	14.5 <sup>[1]</sup>
Cu(OH) <sub>4</sub> <sup>2-</sup>	16.4 <sup>[1]</sup>

<sup>[1]</sup>: stability constants as defined in Smith and Martell (1976 and 1982), corrected with Davies equation (b=0.2) (Stumm and Morgan, 1996) for I = 0.01M. The components needed to describe the reactions are Cu<sup>2+</sup> and OH<sup>-</sup>.

The results obtained are listed in Tab. 2.6. Parameter estimation with the constant capacitance model was optimized with the value defined for the capacitance. The best results were obtained by taking into account a capacitance of  $3.7 \cdot 10^{-2} \text{ F/m}^2$ . The total capacitance depends on the ionic strength and can be estimated by Eq. 2.26 (Lützenkirchen, 1999). This equation was derived for small potentials from the Gouy-Chapman relationship (Eq. 2.12).

$$C_{tot} < 2.28 \cdot \sqrt{I} \quad [2.26]$$

This means that in our system, the total capacitance should be smaller than  $0.228 \text{ F/m}^2$ , and the capacitance of the diffuse layer is per definition much larger than the capacitance in the Helmholtz layer (see chapter 2.4). However, it has to be taken into account that the CCM can normally only be used for  $I > 0.1 \text{ M}$ . The low ionic strengths used in our study are the reason that the defined value for the capacitance is so unusually low.

**Table 2.6.:** Copper adsorption constants obtained by parameter estimation with CCM and DLM

[Cu] [M]	log K	WSOS/DF
	<b>DLM</b>	
$5 \cdot 10^{-6}$	1.9	0.18
$3.03 \cdot 10^{-7}$	2.93	0.3
$6.9 \cdot 10^{-8}$	3.09	1.06
	<b>CCM</b>	
$5 \cdot 10^{-6}$	2.95	0.17

The experimental data and the fitted adsorption curves are shown in Fig. 2.8. Both models can adequately represent the data. Further, as could be expected, with



both models the same adsorption behaviour of copper onto goethite could be calculated.

The fact that the constant estimated by parameter estimation for the constant capacitance is larger than for the double layer model results from the electrostatic definition of the layers. In the constant capacitance model, it is assumed that the diffuse layer is approximated as a plane of charge parallel to the surface. This has as a consequence that the potential of the surface is overestimated and thus the value of the constant increases in order to fit the data.

This example shows clearly that constants defined with one model cannot be used in another model, i.e., intrinsic constants are dependent on the model used (Westall and Hohl, 1980). Furtheron it shows how constants can be determined apparently adequately with a model that makes physically no sense under the conditions used.

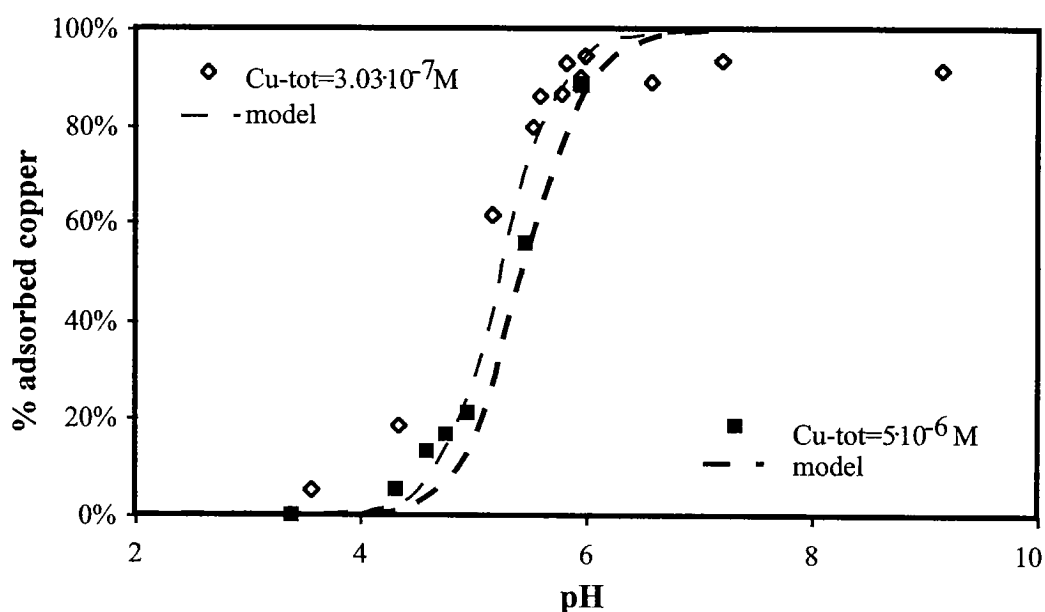


*Fig. 2.8: pH dependence of copper calculated with a surface complexation model using the constant capacitance model and the double layer model for electrostatic interactions. ( $[Cu]_{tot} = 5 \mu M$ )*

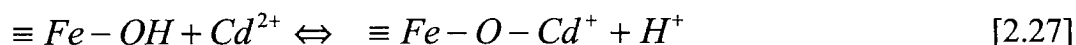
## 2.8.2 Cadmium-Goethite System

The experimental procedure to calculate the pH cadmium adsorption edge on goethite is explained in detail in sections 4.2 and 5.3. The most important parameters, however, are summarized in Tab. 2.7.

**Table 2.7:** Parameters used for calculation of cadmium adsorption on goethite

Parameter	concentration (chapter 4)	concentration (chapter 5)
cadmium [M]	$5 \cdot 10^{-6}$	$1.3 \cdot 10^{-9}$
goethite [g/L]	0.5	0.1
ionic strength (KNO <sub>3</sub> ) [M]	0.01	0.01

To model cadmium adsorption on goethite, one surface species,  $\equiv\text{Fe-O-Cd}^+$ , was postulated (Eq. 2.27)



Formation of the cadmium hydroxo complexes was calculated with the constants reported in Tab. 2.8.

**Table 2.8:** Constants used to calculate cadmium speciation in solution

Species	log K <sup>[1]</sup>
CdOH <sup>+</sup>	3.8
Cd(OH) <sub>2</sub>	7.5
Cd(OH) <sub>3</sub> <sup>-</sup>	10.2

<sup>[1]</sup>: stability constants as defined in Smith and Martell (1976 and 1982), corrected with Davies equation (b=0.2) (Stumm and Morgan, 1996) for I = 0.01 M. The components needed to describe the reactions are Cd<sup>2+</sup> and OH<sup>-</sup>.

The obtained results are reported in Tab. 2.9 and shown in Fig. 2.9. The slope of the experimental adsorption was lower than the slope of the fitted curve. In our model, we assumed that one proton was released per cadmium adsorbed. The steepness of the experimental curve, however, showed that less than one proton must be released per cadmium adsorbed. Different authors tried to solve this problem by defining an additional surface cadmium species, where less protons are liberated, or where the surface is not charged. (Gunneriusson, 1994) (Eq. 2.28).

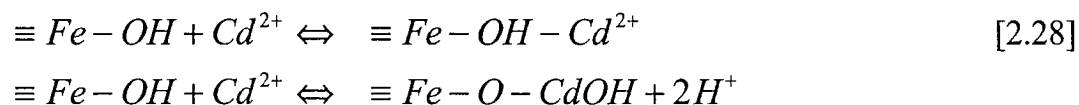


**Table 2.9:** Adsorption constant of cadmium on goethite as calculated by parameter estimation

[Cd] [M]	log K	WSOS/DF
$5 \cdot 10^{-6}$	-0.81	20.8
$1.3 \cdot 10^{-9}$	-0.18	5.99

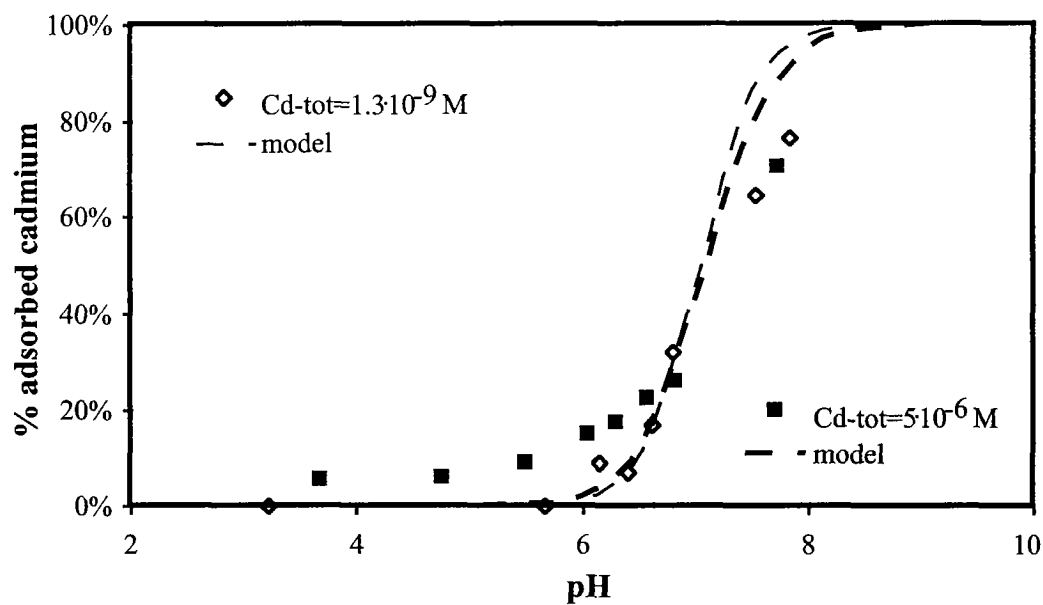
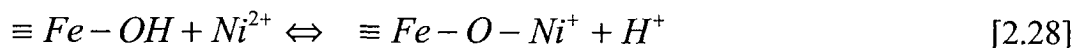


**Fig. 2.9:** pH dependence of cadmium adsorption on goethite calculated with a surface complexation model using the double layer model for electrostatic interactions. ( $[Cd]_{tot} = 5 \mu M$ ).

### 2.8.3 Nickel-Goethite System

The experimental procedure to determine the pH dependence of nickel adsorption on goethite is explained in detail in section 4.2 and 5.1. The most important parameters, however, are summarized in Tab. 2.10.

One surface species,  $\equiv Fe-O-Ni^+$ , was assumed for estimating the constant for the nickel adsorption on goethite:



Speciation of the aqueous nickel was calculated by the constants reported in Tab. 2.11. The results obtained are listed in Tab. 2.12, and shown in Fig. 2.10.

**Table 2.10:** Parameters used for calculation of nickel adsorption on goethite

Parameter	concentration (chapter 4)	concentration (chapter 5)
nickel [M]	$5 \cdot 10^{-6}$	$2.8 \cdot 10^{-7}$
goethite [g/L]	0.5	0.5
ionic strength (KNO <sub>3</sub> ) [M]	0.01	0.01

**Table 2.11:** Constants used to calculate nickel speciation in solution

Species	log K <sup>[1]</sup>
NiOH <sup>+</sup>	4.0
Ni(OH) <sub>2</sub>	7.8
Ni(OH) <sub>3</sub> <sup>-</sup>	11.0

[1]: association constants as defined in Smith and Martell (1976 and 1982) and corrected for the ionic strength ( $I = 0.01$  M) with Davies equation ( $b=0.2$ ) (Stumm and Morgan, 1996). The components needed to define the equations are Ni<sup>2+</sup> and OH<sup>-</sup>.

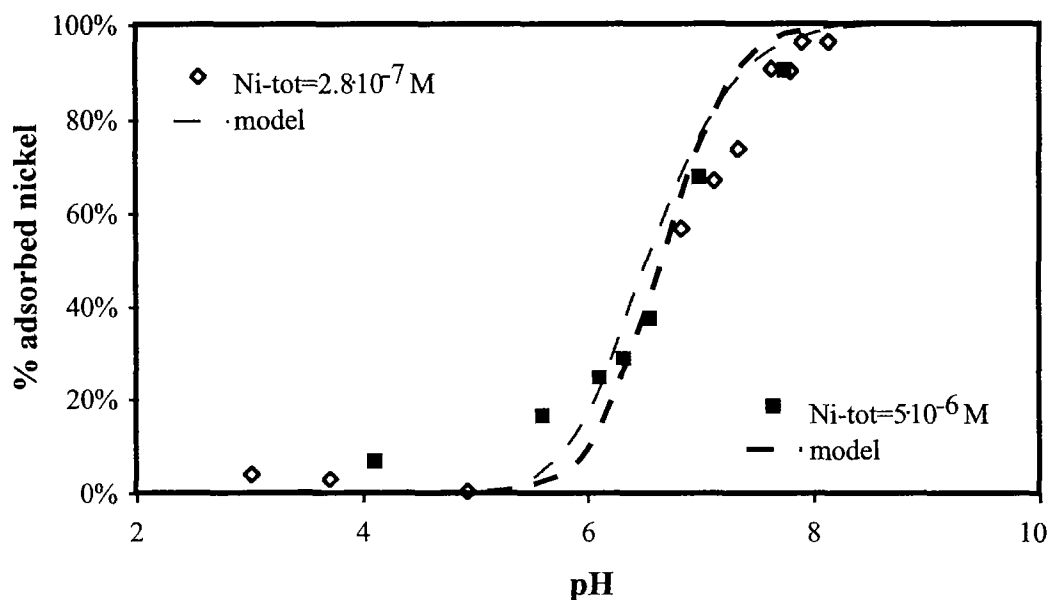


**Fig. 2.10:** pH dependence of nickel adsorption as calculated with a surface complexation model using the double layer model for electrostatic interactions. ( $[Ni]_{tot} = 5 \cdot 10^{-6}$  M)

**Table 2.12:** Adsorption constant of nickel on goethite as estimated by our model.

[Ni] [M]	log K	WSOS/DF
$5 \cdot 10^{-6}$	-0.08	0.92
$2.8 \cdot 10^{-7}$	0.46	0.36

## 2.8.4 Variations of the adsorption constant with metal concentration

It is striking that the adsorption constants defined for all three metals increased with decreasing initial total metal concentration. Considering the small variations in the concentration range, the constant should by definition of a constant not change. This phenomenon, however, can be explained by the presence of weaker and stronger sites on the surface. The strong surface sites are occupied first, as the surface is progressively occupied, lower reactivity sites are left. This has as a consequence that adsorption constants decrease with increasing total metal concentrations.

## 2.9 Modelling of Oxalate, Salicylate, and Pyromellitate on Goethite

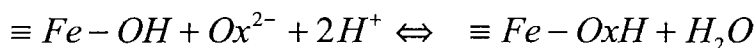
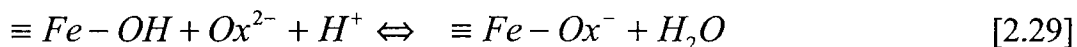
### 2.9.1 Oxalate-Goethite System

The experimental procedure to determine the pH dependence of oxalate adsorption is explained in detail in chapter 4.2. The most important parameters are summarized in Tab. 2.13.

**Table 2.13:** Parameters used for calculating oxalate adsorption on goethite

Parameter	concentration
oxalate [M]	$1 \cdot 10^{-6}$
goethite [g/L]	0.33
ionic strength (NaNO <sub>3</sub> ) [M]	0.01

Two surface species were necessary to model oxalate adsorption sufficiently well (Eq 2.29)



Oxalate speciation in solution was defined by the constants given in Tab. 2.14. The WSOS/DF factor was determined to be 0.049. The results are listed in Table 2.15 and shown in Fig. 2.11.

**Table 2.14:** Constants used to describe oxalate speciation in solution

Species	pK <sub>a</sub> <sup>[1]</sup>
H <sub>2</sub> Ox	1.208
HOx <sup>-</sup>	4.133

<sup>[1]</sup>: acidity constants as defined in Smith and Martell (1977 and 1982), corrected with Davies equation (b = 0.2) (Stumm and Morgan, 1996) for I=0.01 M. The components needed to define the equations are Ox<sup>2-</sup> and H<sup>+</sup>.

**Table 2.13:** Adsorption constants of oxalate on goethite as defined by DLM model

Surface species	log K
≡Fe-Ox <sup>-</sup>	9.9
≡Fe-OxH	14.5

The constants fitted in this study are comparable to constants defined in the literature, e.g. in Mesuere and Fish (1992), and make sense, as the pK<sub>a</sub> of the adsorbed oxalate is 4.6. This value is comparable to the value for aqueous oxalate.

By definition of only one species, no convergence of the optimization procedure could be achieved. ≡Fe-OxH defines the adsorption behavior in the acidic pH range and ≡Fe-Ox<sup>-</sup> is the species responsible for adsorption at pH values about pH 6.

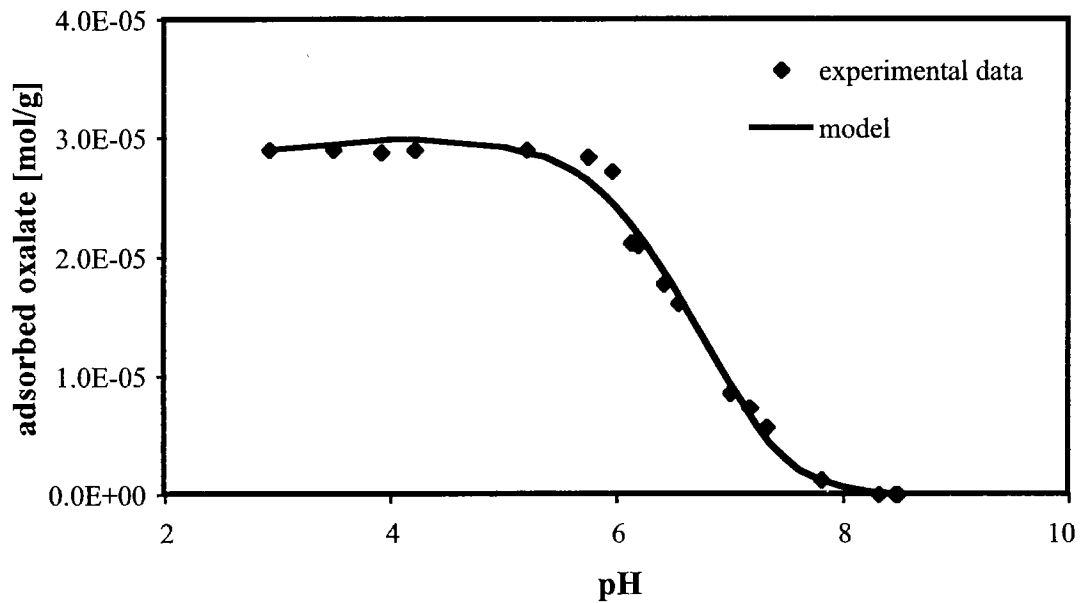


*Fig. 2.11: pH dependence of oxalate adsorption on goethite calculated with a surface complexation model with a double layer model for electrostatic interactions*

## 2.9.2 Salicylate-Goethite System

Salicylate adsorption was not measured in our system. However, calculations of the salicylate adsorption could be performed by using data from the literature which were determined under a similar ligand/goethite ratio as in our study (Evanko and Dzombak, 1999). Modelling was performed with the generalised two layer model (G-TLM). However, no difference between strong and weak adsorption sites was made, so this model is identical to the double layer model used in this study and the constants could be used directly. 2 surface species listed in Tab. 2.14 were defined by parameter estimation. Salicylate adsorption onto goethite is shown in Fig. 2.12.

**Table 2.14:** Surface complexation reactions to describe salicylate adsorption on goethite. Constants were taken from Evanko and Dzombak (1999).

Surface reactions	log $K_{int}$
$\equiv Fe-OH + HSal^- + H^+ \Leftrightarrow \equiv Fe-HSal + H_2O$	8.55
$\equiv Fe-OH + HSal^- \Leftrightarrow \equiv FeO-Sal^{3-} + 2H^+$	-12.92

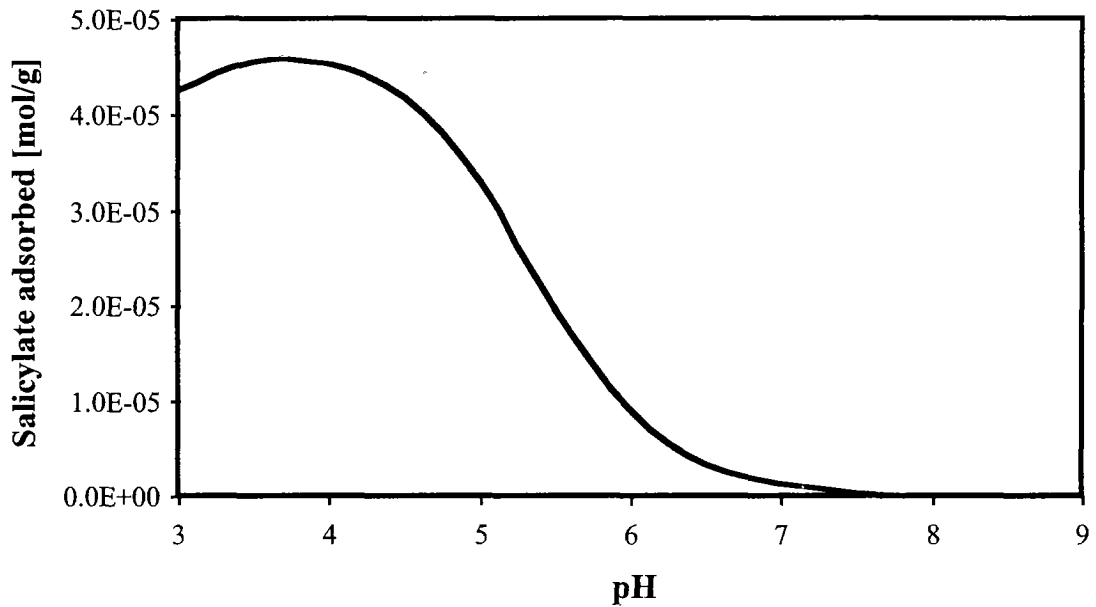


*Fig. 2.12: pH dependence of salicylate adsorption on goethite as calculated by a surface complexation model with a double layer model for electrostatic interactions. Surface complexation constants were taken from Evanko and Dzombak (1999).*

### 2.9.3 Pyromellitate-Goethite System

Pyromellitate adsorption was not measured in our system. However, data to model pyromellitate adsorption on goethite could be found in the literature (Evanko and Dzombak, 1999). In this study, modelling was performed for a broad range of pyromellitate/goethite concentration ratios, including also a ratio close to that used in our study. Modelling was performed with G-TLM, however, no difference was made between weak and strong adsorption sites and thus the G-TLM becomes identical to the double layer model used in this study. Fitting was performed by defining 6 different pyromellitate-goethite surface complexes (Tab. 2.15). Pyromellitate adsorption on goethite is represented in Fig. 2.13.



**Table 2.15:** Surface complexation reactions to describe pyromellitate adsorption on goethite. Constants were taken from Evanko and Dzombak (1999).

Reactions	log $K_{int}$
$\equiv Fe-OH + H_3Pyr^- + H^+ \Leftrightarrow \equiv Fe-H_3Pyr + H_2O$	11.91
$\equiv Fe-OH + H_3Pyr^- \Leftrightarrow \equiv Fe-H_2Pyr^- + H_2O$	9.15
$\equiv Fe-OH + H_3Pyr^- \Leftrightarrow \equiv Fe-HPyr^{2-} + H^+ + H_2O$	4.70
$\equiv Fe-OH + H_3Pyr^- \Leftrightarrow \equiv Fe-Pyr^{3-} + 2H^+ + H_2O$	-1.25
$\equiv Fe-OH + H_3Pyr^- \Leftrightarrow \equiv FeOH-Pyr^{4-} + 3H^+$	-6.61
$\equiv Fe-OH + H_3Pyr^- \Leftrightarrow \equiv FeO-Pyr^{5-} + 4H^+$	-13.12

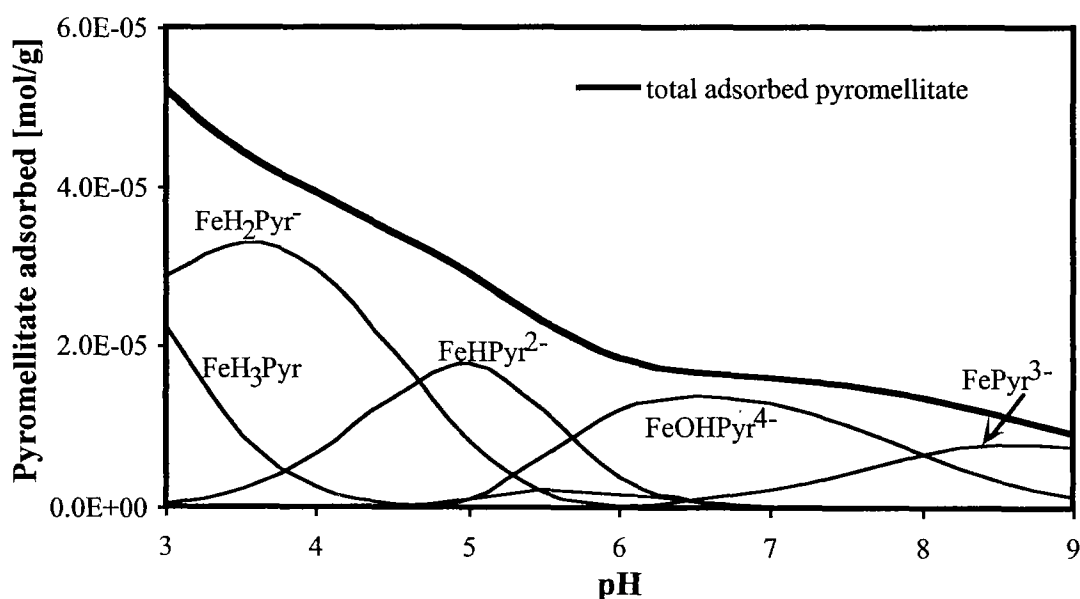


**Fig. 2.13:** pH adsorption edge of pyromellitate adsorption calculated by a surface complexation model with the double layer model for electrostatic interactions. Surface complexation constants were taken from Evanko and Dzombak (1999).

Seite Leer /  
Blank leaf

# *Characterisation of Goethite*

## **3.1 Introduction**

In this study, goethite, a crystalline iron oxide, was used as solid phase, as we wanted to have a well characterised surface. Goethite is a very stable surface, which makes it an ideal solid phase for adsorption experiments (Schwertmann and Cornell, 1991). A further reason for this choice was the fact that iron oxides are known to be strong adsorbents in natural systems and goethite is a wide spread iron oxide in natural systems (Schwertmann and Cornell, 1991).

## **3.2 Description of Goethite**

The goethite used in this study was produced by BASF in large quantities and is used industrially as pigments.

By scanning microscopic studies (SEM), the crystal morphology of this goethite was deduced to have the form of needles (Fig. 3.1). Further SEM pictures of the BASF goethite are shown in the report by Ehrhardt (1999). This is also the normal shape normally observed for goethite (Schwertmann and Cornell, 1991). The dimensions of these needles have been determined to be  $1000 \times 150 \times 30$  nm (Ehrhardt, 1999). The specific surface area was determined with the BET method with  $N_2$  to be  $21.4 \text{ m}^2/\text{g}$ , which is within the normal range defined for goethite. Measurements have been performed with Sorptomatic 1990 by Daniel Kobler (EAWAG, Dübendorf). BET measurements of the same goethite have also been performed by other groups, e.g., by the Laboratoire Environnement et Minéralurgie (LEM) in Nancy. They defined the specific surface with  $N_2$  to be  $18.6 \text{ m}^2/\text{g}$ , and with Ar to be  $15.3 \text{ m}^2/\text{g}$  (Ehrhardt, 1999). Furtheron it has been shown that 40 vol-%

of the pores of the BASF goethite are between 33 and 97 nm (Ehrhardt, 1999), which means that our goethite was highly crystallised.

In general, it has been shown by electron microscopy (EM) that the main plane of goethite is  $\{110\}$ . At the end of the needles, a  $\{021\}$  layer can be defined (Cornell and Schwertmann, 1996; Weidler et al., 1996) (Fig. 3.2). The length of the crystal defines the relative abundance of the  $\{021\}$  plane, which is often less than 10% of the total surface area.

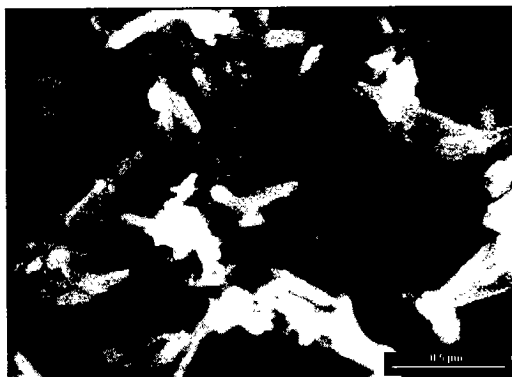


*Fig. 3.1: SEM pictures of BASF goethite after the washing procedure*

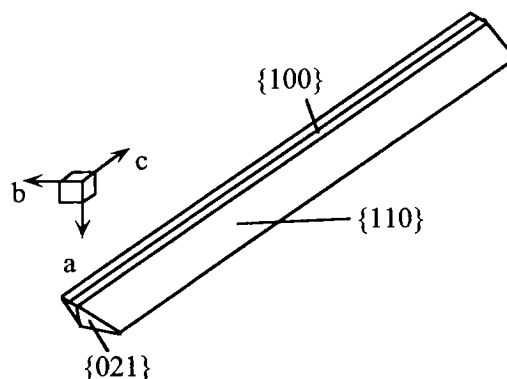


*Fig. 3.2: Goethite crystallographic planes*

- The  $\{110\}$  plane is characterised on a unit cell basis by 3 rows of triply coordinated surface  $\text{Fe}_3\text{O}(\text{H})$  groups, one row with singly coordinated  $\text{FeOH}(\text{H})$  groups, and one row with doubly coordinated surface groups  $\text{Fe}_2\text{OH}$ . The goethite surface is dominated by triply coordinated surface  $\text{Fe}_3\text{O}(\text{H})$  groups. This is reflected by the high value for the  $\text{pH}_{\text{pzc}}$  of the goethite, which is obtained by the elevated  $\log K$  of the protonation of the triply coordinated surface groups. Two types of triply coordinated groups are found, one protonated ( $\text{Fe}_3\text{OH}$ ) and one nonprotonated ( $\text{Fe}_3\text{O}$ ). The non protonated ( $\text{Fe}_3\text{O}^{1/2-}$ ) species are the low affinity sites and the protonated ( $\text{Fe}_3\text{OH}^{1/2-}$ ) represent the high affinity sites (Hiemstra, 1989 a and 1996).

- The  $\{021\}$  plane is characterised by alternating rows of singly and doubly coordinated surface groups (Hiemstra et al., 1989 b).

- The  $\{100\}$  plane is less important for adsorption reactions, because it is uncharged (Hiemstra et al., 1989 b).

### 3.3 Determination of Acidity Constants

By potentiometric measurements it has been shown that the  $\text{pH}_{\text{pzc}}$  of the BASF goethite (after the washing procedure, see section 3.4) was 8.2 (Morsad, 1999). However potentiometric titrations of goethite are quite delicate and values for the  $\text{pK}_a$  values have been taken from the literature (Mesuere and Fish, 1992; Robertson, 1998) (Tab. 3.1).

**Table 3.1:**  $\text{pK}_a$  values of goethite as used in this study

surface species	$\text{pK}_a$
$\equiv\text{Fe-OH}_2^+$	7.9
$\equiv\text{Fe-OH}$	10.5

The  $\text{pK}_a$  values, as defined in Tab. 3.1 result in a  $\text{pH}_{\text{pzc}}$  value of 9.2, which is above the experimental value determined for the BASF goethite. The choice of these constants to characterise our goethite surface was not ideal, as the difference has an influence on our calculations. However, the difference in the acidity constants will not change the main conclusions of this study. The error lies in the fact that in our calculations the surface was slightly more positively charged, which has as consequence that the surface was a less strong ligand. However, as parameter estimation for the determination of the adsorption constants of metals and ligands was performed with the acidity constants from Tab 3.1, an error in the calculations may only occur in the estimation of the electrostatic attraction of the positively charged groups of goethite. This influence, however, is minute in comparison with the others.

### 3.4 Treatment of Goethite

#### *Impurities on the Surface*

It has been shown by ICP-OES measurements that certain impurities are present on the goethite surface (Tab. 3.2) (Ehrhardt, 1999). Furtheron, anions like sulphate have been shown by XPS (X-ray Photo Electron Spectroscopy) to be present on the surface (Ehrhardt, 1999; Morsad, 1999). Sulphate measurements were also performed with ion-chromatography (Dionex, column As11) in suspensions of

goethite at pH 9 that were filtered. Only a qualitative analysis was performed for this task. In order to eliminate these impurities, the goethite was washed.

More details about the characterisation of the BASF goethite are given in the studies of Ehrhardt (1999) and Morsad (1999).

**Table 3.2:** List of impurities on the goethite surface

Impurity	Concentration [ $\mu\text{g/g}$ ]
Ba	8
Ca	650
Cu	70
Mg	80
Mn	150
Na	500
Sr	4
Ti	2

### ***Washing Procedure***

50 g of goethite were weighted into a 500 ml polypropylene centrifugation tube. The tube was soaked first in 0.1 M  $\text{HNO}_3$  for at least 2 days and afterwards for 2 days in nanopure water. Several washing steps were necessary. The volume of solution added was always 250 ml. Goethite was washed successively with  $10^{-3}$  M NaOH (prepared from Baker Analysed<sup>®</sup>, 50 %,  $\text{CO}_2$ -free (see section 4.2.1)), nanopure water,  $10^{-3}$  M  $\text{HNO}_3$  (prepared from Merck suprapur<sup>®</sup>, 65 %), and twice with 0.01 M  $\text{NaNO}_3$  (Fluka, grade Biochemika). For each washing step, the suspension was equilibrated for about 2 h. After each washing step, the suspension was centrifugated (Centrikon T124 Kontron Instruments) at 7800 U/min at  $15^\circ\text{C}$  for 30 min. The rotor used for centrifugation was A 6.9. Centrifugation parameters were the same for all the washing steps. At the end, goethite was dried for 24 h at  $80^\circ\text{C}$  and crushed in an agate mortar. For storage, suspensions of 20 g/l were prepared, which were treated for 10 minutes with ultrasound in order to disperse goethite particle homogeneously. This solutions were aged for at least 2 days before use.

Similar washing procedures for goethite are reported in Ehrhardt (1999) and Morsad (1999).

# *Adsorption of Cu, Cd, and Ni on Goethite in the Presence of Simple Organic Ligands*

## **4.1 Introduction**

Natural organic ligands have an important influence on the transport of heavy metals in infiltration groundwater systems (Stumm, 1996; Stumm and Morgan, 1996). A variety of models has been developed to describe the complexation and adsorption properties of natural organic substances with high molecular weight (Bartschat et al., 1992; Benedetti et al., 1995; Dzombak et al., 1986; Tipping, 1993, 1986, 1994; Tipping and Hurley, 1992; Tipping and Woof, 1990). However, a detailed, quantitative description is still difficult as the knowledge about structure and chemical behaviour of humic substances and hydrophilic acids is still quite limited. Organic ligands of lower molecular weight have the advantage not to present this kind of problems. It has been shown that natural organic ligands are mostly bound to mineral surfaces through a ligand exchange mechanism, at least at pH values below  $\text{pH}_{\text{pzc}}$  (Gu et al., 1994). Therefore, simple organic ligands with carboxylic groups and/or phenolic groups, which represent major functional groups in natural organic ligands (Aiken et al., 1985; Stevenson, 1982), are very promising for a better understanding of mineral-ligand-metal interactions (Ali and Dzombak, 1996 b).

In this study, oxalate, salicylate, and pyromellitate (Fig. 4.1-4.3) were chosen as simple organic ligands. These ligands have carboxylic functional groups and

salicylate has also a phenolic group. The compounds have often been described in the literature to be good representatives for natural organic matter.

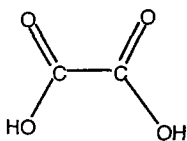


**Fig. 4.1:** oxalic acid

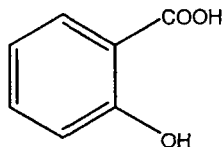


**Fig. 4.2:** salicylic acid

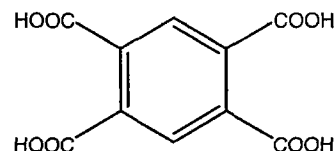


**Fig. 4.3:** pyromellitic acid

Oxalic acid (ethanedioic acid) is often selected to represent the aliphatic part of humic substances (Elliott and Denney, 1982; Filius et al., 1997; Huang, 1977; Lamy et al., 1991; Ragnarsdottir et al., 1998; Violante et al., 1996). Oxalate is one of the most abundant organic ligands of low molecular weight in soils and is particularly concentrated in the rhizosphere.

Salicylic acid (2-hydroxybenzoic acid) is an important component of dissolved humic substances and is important to define acidity and complexation properties of fulvic acids (Leenheer et al., 1995).

Pyromellitic acid (1,2,4,5-benzenetetracarboxylic acid) is a good chelating agent with two identical carboxylic groups located on both sides of the benzene ring. Pyromellitate has been used in the last few years as a representative for natural organic ligands in several studies (Angove et al., 1999; Evanko and Dzombak, 1998, Boily et al., 2000 a, b, c).

These three ligands can be expected to represent quite a broad range of possible influences of natural organic ligands on the adsorption of heavy metals on goethite. Oxalate is a strong complexing agent and is therefore likely to compete with the surface groups to complex heavy metals at elevated pH values. Formation of ternary complexes of type B in the acidic pH range can be expected with pyromellitate. The carboxylic groups on one side of the aromatic ring can form complexes with the surface groups, while the carboxylic groups on the other side can complex heavy metals on the bulk solution side. Both types of reactions are not expected with salicylate, as it is a less strong ligand and competition reactions with the surface are not likely at the surface/ligand concentration ratios used in this study.

The objective of this chapter was to study the influence of these three ligands on the adsorption of copper, cadmium, and nickel on goethite. By stepwise inclusion of the different modules, which define interactions of organic ligands with metal adsorption (see chapter 1) into the surface complexation model, the effects of the various complexation reaction could be analysed individually. The modules



considered competition reactions with aqueous organic ligands, electrostatic attraction of the metal cation on the surface due to adsorbed ligands, and formation of ternary complexes. The probability of formation of ternary complexes of type A or B were discussed. Consideration of the properties of the metals and the ligands helped to explain the adsorption data obtained in the nine different systems.

## 4.2 Experimental Conditions

### 4.2.1 Chemicals

Metal solutions were prepared from metal stock standards from Baker Analyzed<sup>®</sup> (copper, nickel, cadmium: 1000 $\mu$ g/mL Baker Instra-Analyzed<sup>®</sup>). Following chemicals were from Fluka: Biochemika grade: HEPES (4-(2-hydroxyethyl)-piperazine-1-ethane-sulfonic acid), MES (2-morpholinoethane-sulfonic acid monohydrate), oxalic acid sodium salt, and NaNO<sub>3</sub>, Chemika grade: sodium salicylate. KNO<sub>3</sub> was used from Merck suprapur<sup>®</sup> and pyromellitic acid from Merck (synthesis grade).

All nitric acid dilutions were prepared from HNO<sub>3</sub> 65%, Merck suprapur<sup>®</sup>. All NaOH dilutions were prepared CO<sub>2</sub>-free from 50% NaOH solutions (Baker Analyzed<sup>®</sup>). In such solutions, carbonate precipitates as Na<sub>2</sub>CO<sub>3</sub> and can thus be eliminated by filtration (Öhman and Sjöberg, 1996). The polypropylene bottles and the nanopure water used for the dilutions were purged previously to use with argon and nitrogen, respectively. In order to prevent the NaOH solution to come into contact with air, mixing as well as storage was done under argon atmosphere. NaOH solutions were only used for 24 h.

All solutions were prepared with deionized water (18M $\Omega$  Q-H<sub>2</sub>O grade Barnstead Nanopure) in bottles soaked for at least 24 h in 0.1 M HNO<sub>3</sub>. For metal, NaOH, and HEPES solutions, polypropylene bottles were used. All other solutions were prepared in glass ware.

### 4.2.2 Treatment of Goethite

Goethite purchased from BASF was treated as described in Chapter 3. It was stored in suspensions of 20 g/L in polyethylene bottles. Before use, goethite suspensions were thoroughly shaken. Pipetting of goethite into the bottles used for the experiments was done with an error smaller than 4%.

### 4.2.3 General Experimental Setup

Experiments were performed at 25°C as batch systems in 100 mL polypropylene beakers, which had been soaked for at least 24 h in 0.1 M HNO<sub>3</sub> and rinsed before use with nanopure water.

pH between 5.2 and 7.2 was buffered with MES and between pH 7.2 and 7.8 with HEPES. Below pH 5.2 and above pH 7.8, no buffers were used. pH values were adjusted by adding HNO<sub>3</sub> or NaOH.

To remove CO<sub>2</sub>, all samples were purged with nitrogen for at least 30 min before the adsorption reaction and whenever the bottles were opened. All solutions used were either purged with nitrogen or prepared CO<sub>2</sub> free (see chapter 4.2.1).

Because of possible photoreduction of goethite by organic ligands, experiments were carried out under red light at  $\lambda > 560$  nm (Siffert and Sulzberger, 1991; Sulzberger et al., 1989).

Because the order of addition of the different reagents may show that kinetic effects are important, different systems were investigated.

#### ***System "metal-ligand-together"***

Metal and ligand were equilibrated for 30 min under nitrogen atmosphere at the desired pH value. The ionic strength was adjusted with KNO<sub>3</sub> (if not specified otherwise). Afterwards, goethite was added and the samples were allowed to equilibrate in the dark on a side to side shaker for 4 h. Concentrations are listed in Tab. 4.1.

#### ***System "metal-first"***

Metal and goethite were first equilibrated for 2 h at the desired pH and ionic strength. Afterwards, the ligand was added. The pH was controlled and the samples were equilibrated for 4 h.

#### ***System "ligand-first"***

Ligand and goethite were first equilibrated for 2 h at the desired pH value and ionic strength prior to addition of the metal. The pH was then checked and the samples were equilibrated for 4 h.

**Table 4.1:** *Experimental conditions used in the experiments unless specified otherwise*

pH	3-9
Metal <sup>[1]</sup> [M]	$5 \cdot 10^{-6}$
Ligand <sup>[2]</sup> [M]	$5 \cdot 10^{-4}$
goethite [g/L]	0.5
I [M]	0.01
buffer <sup>[3]</sup> [M]	$5 \cdot 10^{-3}$

<sup>[1]</sup>: copper, cadmium, or nickel

<sup>[2]</sup>: oxalate, salicylate, or pyromellitate

<sup>[3]</sup>: MES or HEPES

After the final equilibration step, the pH was measured again under nitrogen atmosphere. This equilibrium pH value, which was slightly lower in both binary and ternary systems compared to the one measured before the adsorption reaction, was used for data evaluation. Afterwards, the samples were filtered (0.45  $\mu\text{m}$ , either Acrodisc Gelman Science or Titan Nylon from Schmidlin Labor & Service AG) and acidified to 0.01 M  $\text{HNO}_3$  for metal analysis. For oxalate analysis, the pH of the filtrate was set to pH 10.

The amount of metal or ligand adsorbed was calculated from the difference between the total initial concentration and the measured concentration in the filtrate after the adsorption reaction.

In order to see the effect of the organic ligands on the adsorption of metals on goethite, reference samples without organic ligands were measured. In the experiments described in this chapter, the reference was always measured in a simple ionic medium (0.01 M  $\text{KNO}_3$  if not specified otherwise).

#### 4.2.4 Analytical Methods

Within one week, the metal samples were analysed with ICP–OES (Spectroflame). Analytical methods were checked with standard addition in the matrix. Detection limits ( $3 \cdot \sigma$ ) are listed in Tab. 4.2.

Blanks of filters, bottles, and goethite suspensions were measured to control that samples were not contaminated. No problems arose for the concentrations used in this study.

**Table 4.2:** Detection and quantification limits for measurements with ICP-OES

Element	Detection limit [M]
Cu	$7.8 \cdot 10^{-8}$
Cd	$8.9 \cdot 10^{-8}$
Ni	$8.5 \cdot 10^{-7}$

pH was measured with an Orion combination electrode (Ross electrode, model 81-02) connected to an Orion pH meter (model 420A). The electrode was calibrated with 3 pH buffers from Hamilton Bonaduz AG with pH  $4.01 \pm 0.02$ ,  $7.00 \pm 0.02$ , and  $9.21 \pm 0.02$ .

Oxalate concentrations in the filtrate were measured by ion chromatography (Dionex, column As11).

### 4.3 Modelling

The constants used for modelling are summarized in Table 4.3. Modelling calculations were performed with the speciation programme ChemEQL (Müller, 1996).

<sup>[1]</sup>: association constants as defined in Smith and Martell (1976, 1977 and 1982), corrected with Davies equation ( $b = 0.2$ ) (Stumm and Morgan, 1996) for  $I = 0.01$  M. The components to describe the equations are  $\text{Cu}^{2+}$ ,  $\text{Cd}^{2+}$ ,  $\text{Ni}^{2+}$ ,  $\text{Ox}^{2-}$ ,  $\text{Sal}^{2-}$ ,  $\text{Pyr}^{4-}$ ,  $\equiv\text{Fe-OH}$ , and  $\text{H}^+$ , except for the formation of the metal hydroxo complexes, where the components are the free metal cation and  $\text{OH}^-$ .

<sup>[2]</sup>: from Giammar and Dzombak (1998), corrected with Davies equation ( $b = 0.2$ ) for  $I = 0.01$  M

<sup>[3]</sup>: from Evanko and Dzombak (1999), corrected with Davies equation ( $b = 0.2$ ) for  $I = 0.01$  M. Details are given in chapter 2.

<sup>[4]</sup>: this study. Details are given in chapter 2.

<sup>[5]</sup>: from Mesuere and Fish (1992) and Robertson (1998). Details are given in chapter 3.

<sup>[6]</sup>: no data could be found in the literature for nickel-pyromellitate complex formation constant

**Table 4.3: Equilibrium constants (log K) used in the calculations performed in this chapter (Foot notes page 56).**

pK <sub>a</sub> ligand/surface		Copper		Cadmium		Nickel		
Metal hydroxo complexes		Cu(OH) <sup>+</sup>	6.1 <sup>[1]</sup>	CdOH <sup>+</sup>	3.8 <sup>[1]</sup>	NiOH <sup>+</sup>	4.0 <sup>[1]</sup>	
		Cu(OH) <sub>2</sub>	11.6 <sup>[1]</sup>	Cd(OH) <sub>2</sub>	7.5 <sup>[1]</sup>	Ni(OH) <sub>2</sub>	7.8 <sup>[1]</sup>	
		Cu(OH) <sub>3</sub> <sup>-</sup>	14.5 <sup>[1]</sup>	Cd(OH) <sub>3</sub> <sup>-</sup>	10.2 <sup>[1]</sup>	Ni(OH) <sub>3</sub> <sup>-</sup>	11.0 <sup>[1]</sup>	
		Cu(OH) <sub>4</sub> <sup>2-</sup>	16.4 <sup>[1]</sup>					
Oxalate	H <sub>2</sub> Ox	1.208 <sup>[1]</sup>	CuOx	5.87 <sup>[1]</sup>	CdOx	3.53 <sup>[1]</sup>	NiOx	4.8 <sup>[1]</sup>
	HOx <sup>-</sup>	4.133 <sup>[1]</sup>	Cu(Ox) <sub>2</sub>	9.74 <sup>[1]</sup>				
			CuHOx <sup>+</sup>	2.87 <sup>[1]</sup>				
Salicylate	H <sub>2</sub> Sal	2.9 <sup>[1]</sup>	CuSal	11.14 <sup>[1]</sup>	CdSal	5.9 <sup>[1]</sup>	NiSal	7.5 <sup>[1]</sup>
	HSal <sup>-</sup>	13.61 <sup>[1]</sup>	Cu(Sal) <sub>2</sub> <sup>2-</sup>	19.4 <sup>[1]</sup>	CdHSal <sup>+</sup>	15.8 <sup>[1]</sup>	Ni(Sal) <sub>2</sub> <sup>2-</sup>	12.2 <sup>[1]</sup>
Pyromellitate	H <sub>4</sub> Pyr	0.99 <sup>[1]</sup>	CuPyr <sup>2-</sup>	4.95 <sup>[2]</sup>	CdPyr <sup>2-</sup>	3.82 <sup>[1]</sup>	[6]	
	H <sub>3</sub> Pyr <sup>-</sup>	2.45 <sup>[1]</sup>			Cd(Pyr) <sub>2</sub> <sup>6-</sup>	5.28 <sup>[1]</sup>		
	H <sub>2</sub> Pyr <sup>2-</sup>	4.39 <sup>[1]</sup>			CdHPyr <sup>-</sup>	-3.76 <sup>[1]</sup>		
	HPyr <sup>3-</sup>	5.92 <sup>[1]</sup>			Cd <sub>2</sub> (Pyr) <sub>2</sub> <sup>4-</sup>	9.48 <sup>[1]</sup>		
Goethite	≡Fe-O-H <sub>2</sub> <sup>+</sup>	7.9 <sup>[5]</sup>	≡Fe-O-Cu <sup>+</sup>	1.9 <sup>[4]</sup>	≡Fe-O-Cd <sup>+</sup>	-0.81 <sup>[4]</sup>	≡Fe-O-Ni <sup>+</sup>	-0.08 <sup>[4]</sup>
	≡Fe-OH	10.5 <sup>[5]</sup>						
Adsorption of ligands	Oxalate		Salicylate		Pyromellitate			
					≡Fe-H <sub>3</sub> Pyr	24.67 <sup>[3]</sup>		
					≡Fe-H <sub>2</sub> Pyr <sup>-</sup>	21.91 <sup>[3]</sup>		
	≡Fe-Ox <sup>-</sup>	9.9 <sup>[4]</sup>	≡Fe-HSal	22.16 <sup>[3]</sup>	≡Fe-Hpyr <sup>2-</sup>	17.46 <sup>[3]</sup>		
	≡Fe-OxH	14.5 <sup>[4]</sup>	≡Fe-O-Sal <sup>3-</sup>	0.687 <sup>[3]</sup>	≡Fe-Pyr <sup>3-</sup>	11.51 <sup>[3]</sup>		
				≡Fe-OH-Pyr <sup>4-</sup>	6.75 <sup>[3]</sup>			
				≡Fe-O-Pyr <sup>5-</sup>	-0.36 <sup>[3]</sup>			

Characterisation of the goethite surface is described in detail in chapter 3, details to the adsorption reactions of the ligands and the metals are given in chapter 2. Constants for cadmium and nickel bisoxalate complexes could not be found. Probably, the bisoxalate complexes are weaker for these metals than for copper and therefore, constants were not determined. The complexation of copper, cadmium, and nickel by oxalate, salicylate, and pyromellitate is shown in Fig. 4.4-4.6.

Copper, cadmium, and nickel adsorption on goethite in the presence of the organic ligands was calculated with two different surface complexation models with a double layer model to consider the electrostatic interactions:

- model 1: To the surface complexation model for the adsorption of the metal (as described in chapter 2) was added the module considering competition reactions between the surface functional groups and the aqueous ligands.
- model 2: To the surface complexation model for the adsorption of the metal were added the modules considering competition reactions between the surface functional groups and the aqueous ligands, and electrostatic attraction of the metal by the adsorbed ligand.

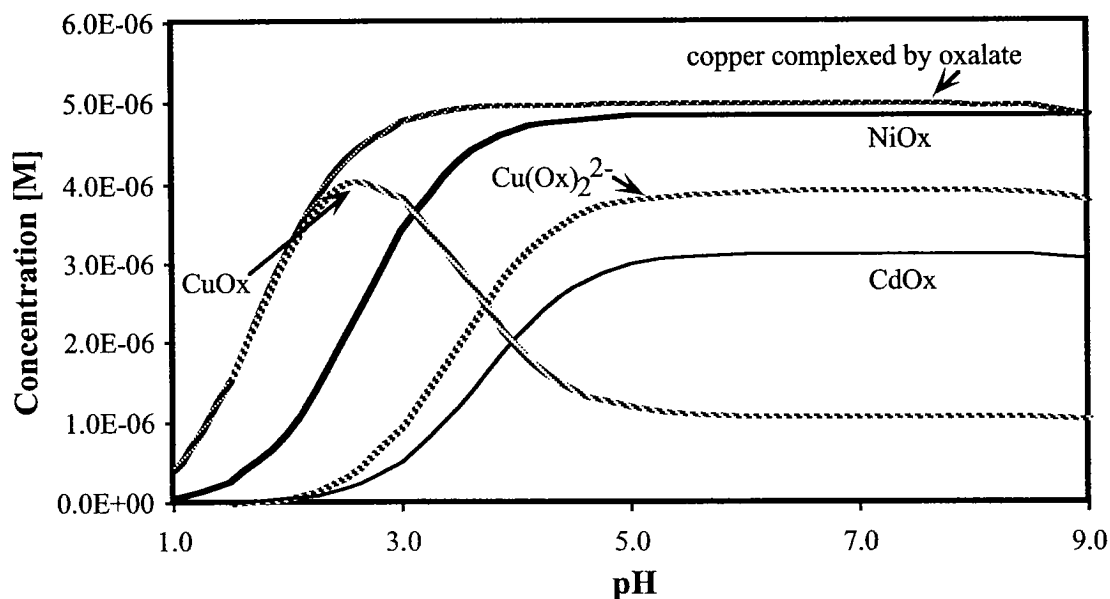


*Fig. 4.4: Speciation of copper, cadmium, or nickel in an oxalate solution. For each metal, an oxalate concentration of 0.5 mM was considered, and the concentrations of the three metals were each 5  $\mu$ M.*

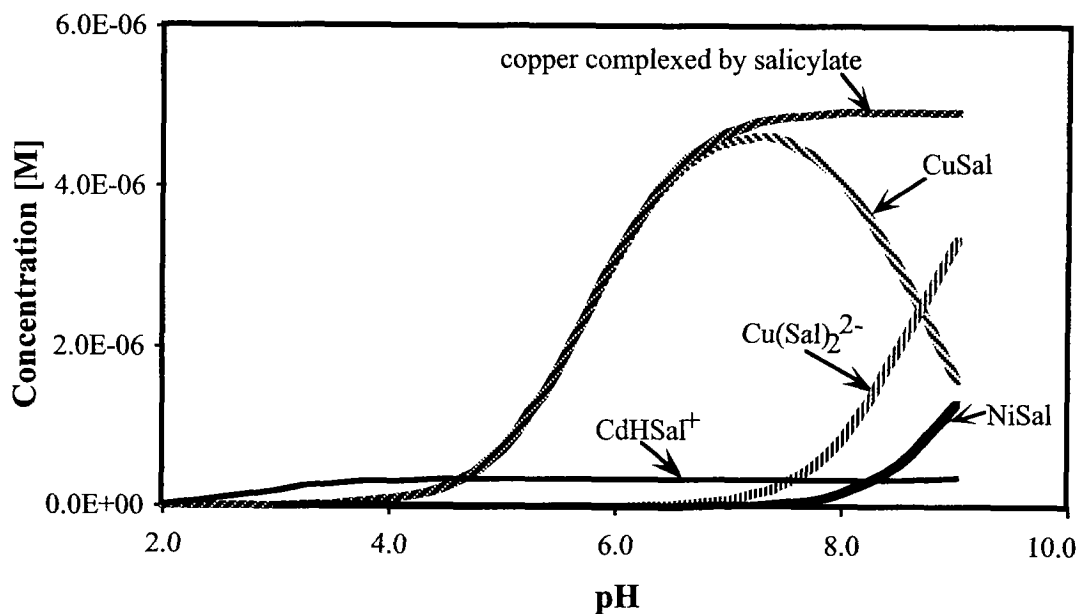


**Fig. 4.5:** Speciation of copper, cadmium, or nickel in a salicylate solution. For each metal, a salicylate concentration of 0.5 mM was defined, and the concentrations of the three metals were each 5  $\mu\text{M}$ . (Metal complexes defined in Tab. 4.3, but not shown on this figure, are only present in negligible concentrations.)

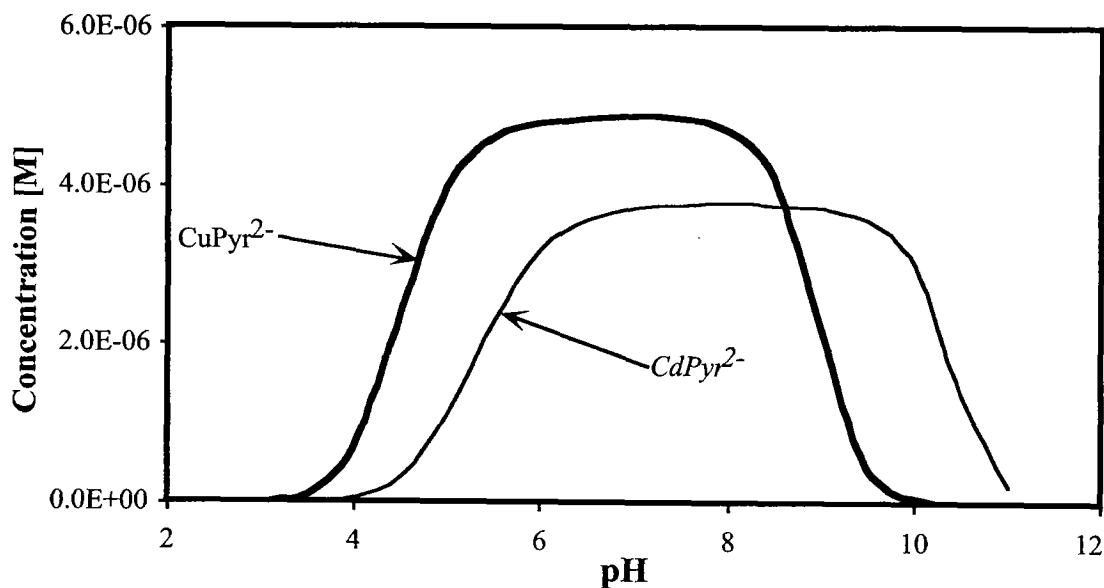


**Fig. 4.6:** Speciation of copper and cadmium in a pyromellitate solution. For each metal, a pyromellitate concentration of 0.5 mM was defined, and the concentrations of the metals were each 5  $\mu\text{M}$ . (The cadmium-pyromellitate complexes not shown in this figure are only present in small negligible concentrations.)

## 4.4 Influence of Oxalate on the Adsorption of Copper, Cadmium, and Nickel on Goethite

### 4.4.1 Copper-Oxalate-Goethite System

The pH dependence of the adsorption of copper on goethite in the presence of oxalate is shown in Fig. 4.7. For these experiments, copper concentrations were  $5 \cdot 10^{-6}$  M, oxalate concentrations amounted to  $1 \cdot 10^{-3}$  M. The other concentrations were as defined in Table 4.1. A reference adsorption edge, without oxalate, was measured in 0.01 M  $\text{KNO}_3$ .

Considerably less copper was adsorbed at pH values between 5 and 8 in the presence of oxalate. Oxalate is a strong complexant and competes with surface groups for complexation of copper.

Experiments to study kinetic effects were performed by changing the order of addition of the components. No difference in the adsorption of copper could be observed (Fig. 4.7), thus it can be concluded that equilibrium was reached within the equilibration times used in the experiments.

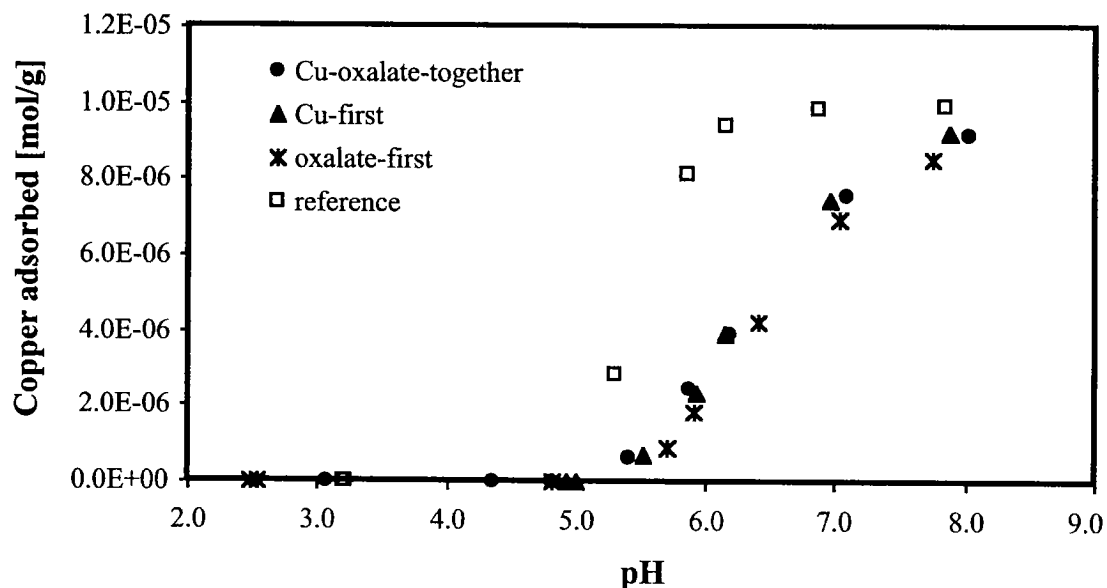


*Fig. 4.7: pH adsorption edge of copper on goethite in the presence of oxalate. The adsorption of copper onto goethite in the presence of oxalate was examined in different systems to study possible kinetic effects. ( $[\text{Cu}]_{\text{tot}}=5 \mu\text{M}$ ,  $[\text{Oxalate}]_{\text{tot}}=1 \text{ mM}$ ,  $[\text{goethite}]=0.5 \text{ g/L}$ ).*



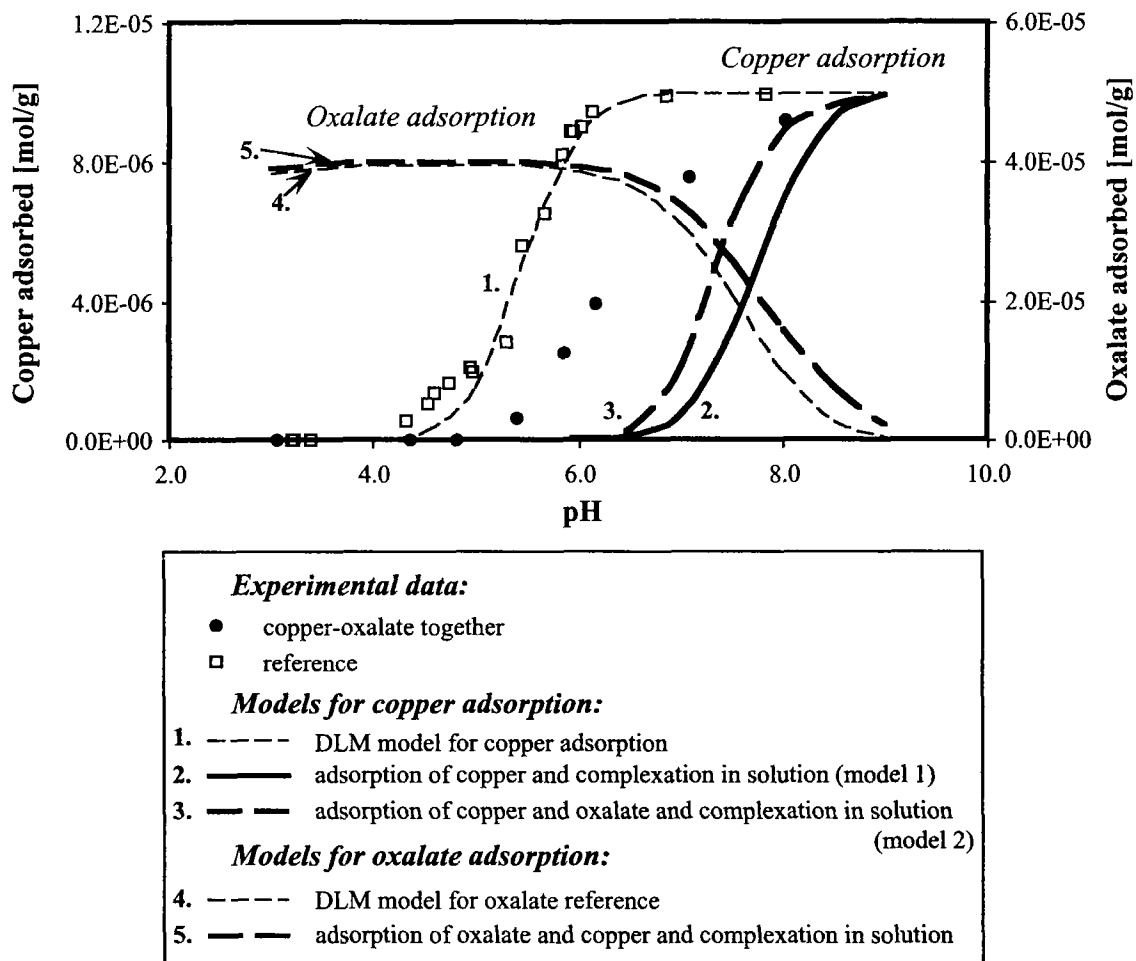


**Fig. 4.8:** pH adsorption edge of copper on goethite in the presence of oxalate. For comparison, a reference in 0.01 M  $\text{KNO}_3$ , fitted with the DLM model, is shown. Calculation of the copper adsorption in the presence of oxalate was performed with models 1 and 2. The oxalate adsorption edge, calculated by model 2 is also shown. ( $[\text{Cu}]_{\text{tot}}=5 \mu\text{M}$ ,  $[\text{Oxalate}]_{\text{tot}}=1 \text{mM}$ ,  $[\text{goethite}]=0.5 \text{g/L}$ ).

### Modelling Results

The results calculated by models 1 and 2 are reported in Fig. 4.8. The adsorbed copper concentration as well as the calculated adsorbed oxalate are shown.

First, the adsorption of copper in the presence of oxalate was calculated by model 1, where the adsorption of the metal on the surface and the complexation of the metal in solution were considered (curve 2 in Fig. 4.8). The adsorption of copper in the presence of oxalate is clearly underestimated compared to the experimental data because of complexation of copper by oxalate in solution. Since between pH 5 and 7, co-adsorption of copper and oxalate occurs (Fig. 4.8), interactions between

these two components on the surface are possible. The simplest interactions are of electrostatic nature and they are taken into account in model 2 (curve 3 in Fig. 4.8). Due to specific adsorption of oxalate, the surface gets more negatively charged, which increases copper adsorption. However, adsorption of copper is still underestimated. Thus, further interactions between oxalate and copper on the surface are probable, like e.g., formation of ternary complexes. Possible structures of these ternary complexes will be discussed in section 4.7.5.

According to the model calculations, oxalate adsorption was slightly increased at pH values above 6 in the presence of copper (curve 5 in Fig. 4.8). Due to adsorption of copper, the positive charge on the surface is increased at higher pH values and oxalate is thus attracted electrostatically on the surface.

#### 4.4.2 Cadmium-Oxalate-Goethite System

The pH dependence of the adsorption of cadmium on goethite in the presence of oxalate is shown in Fig. 4.9. A reference adsorption edge without oxalate was measured in 0.01 M  $\text{KNO}_3$ . The concentrations used were as defined in Tab. 4.1.

There seems not to be a clear difference between the two adsorption edges. Possibly, a small enhancement of cadmium adsorption in the presence of oxalate could be observed in the pH range of about 6-7. At the conditions used in our experiments, no clear decrease in cadmium adsorption could be observed at higher pH values.

##### *Modelling Results*

Model 1 could describe the pH dependence of cadmium on goethite in the presence of oxalate sufficiently well (curve 2 in Fig. 4.9). However, in comparison with the calculated reference curve, it seems that in the model a small amount of cadmium is complexed by oxalate, which could not be seen in the experiments. As there is co-adsorption of cadmium and oxalate at pH values between 6 and 8, an influence of oxalate on the adsorption is likely. Electrostatic attraction of cadmium due to adsorbed oxalate is taken into account in model 2 (curve 3 in Fig. 4.9). In fact including the adsorption of oxalate into the model enhanced even slightly cadmium adsorption compared to the reference adsorption edge.

The calculated curve is steeper than the experimental one because less than one proton is liberated per adsorbed cadmium. More details are given in chapter 2.

The adsorption of oxalate is also presented in Fig. 4.9. According to the model, oxalate adsorption is slightly enhanced compared to the reference at pH values above 7, due to electrostatic attraction of adsorbed cadmium (curve 5).

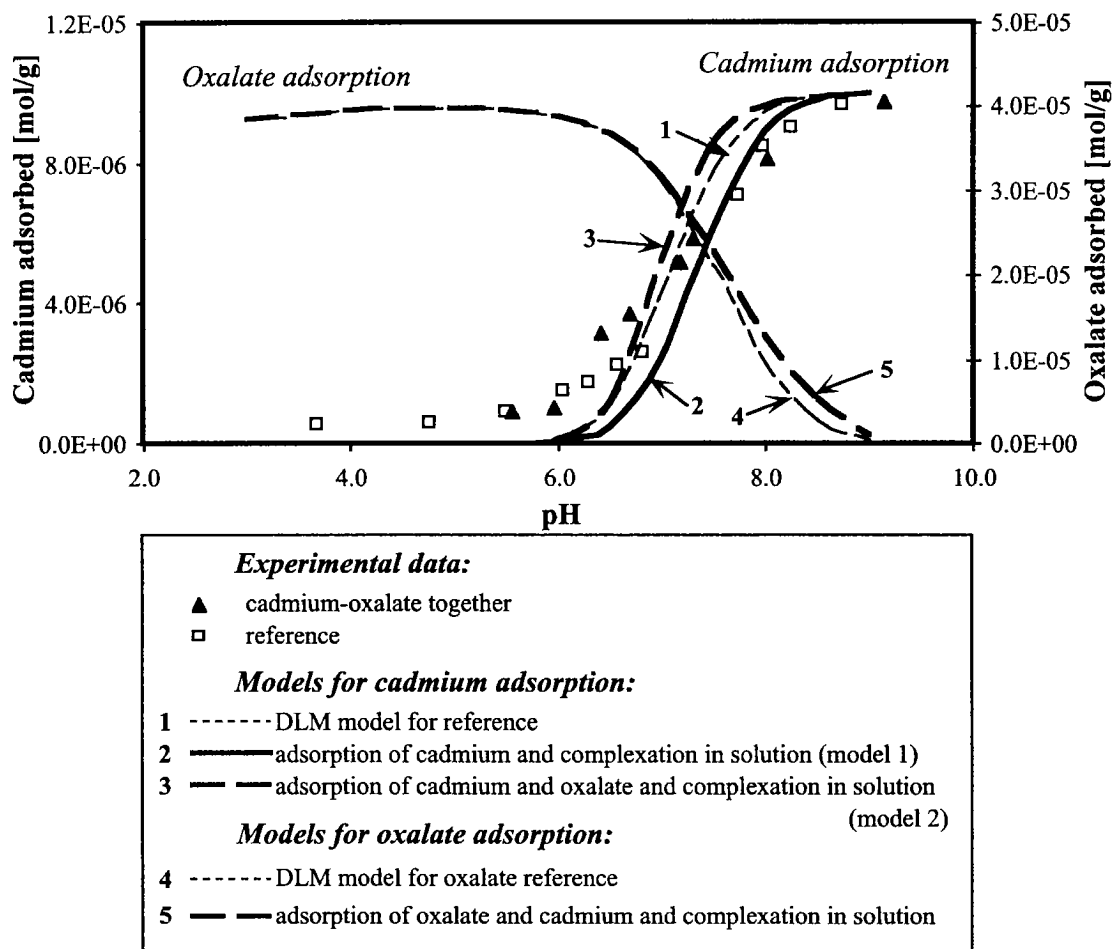


**Fig. 4.9:** pH adsorption edge of cadmium on goethite in the presence of oxalate. For comparison, a reference in 0.01 M  $\text{KNO}_3$ , calculated with the DLM model, is shown. Cadmium adsorption in the presence of oxalate was calculated by models 1 and 2. The pH adsorption edge of oxalate, calculated by model 2, is also shown. ( $[\text{Cd}]_{\text{tot}} = 5 \mu\text{M}$ ,  $[\text{Oxalate}]_{\text{tot}} = 0.5 \text{ mM}$ ,  $[\text{goethite}] = 0.5 \text{ g/L}$ ).

### Adsorption of Oxalate in the Presence of Cadmium

The pH adsorption edge of oxalate on goethite in the presence of cadmium is shown in Fig. 4.10. A reference adsorption edge was measured in the absence of cadmium in electrolyte medium (0.01 M  $\text{NaNO}_3$ ). For these experiments, the cadmium concentration was set to 1.45  $\mu\text{M}$ , oxalate to 10  $\mu\text{M}$ , and goethite to 0.04 g/L. Competition reactions between cadmium and oxalate for goethite

functional groups could be expected, as the oxalate concentration was in excess to the concentration of surface groups. However, the adsorption of oxalate on goethite seemed to be unaffected by the adsorption of cadmium. The slight enhancement of oxalate adsorption in the presence of cadmium at pH above 7, observed in the calculations (Fig. 4.9) could not be distinguished clearly under these conditions.

The oversaturation of the surface by oxalate made a description of these experiments by a surface complexation model impossible. The concentrations of adsorbed oxalate were more elevated than the concentration of surface sites, thus formation of more than one monolayer was possible. The concentration of one monolayer would equal  $2.4 \mu\text{M}$  and calculations showed that approximately 4 monolayers could be formed. No explanation could be found for this phenomenon.

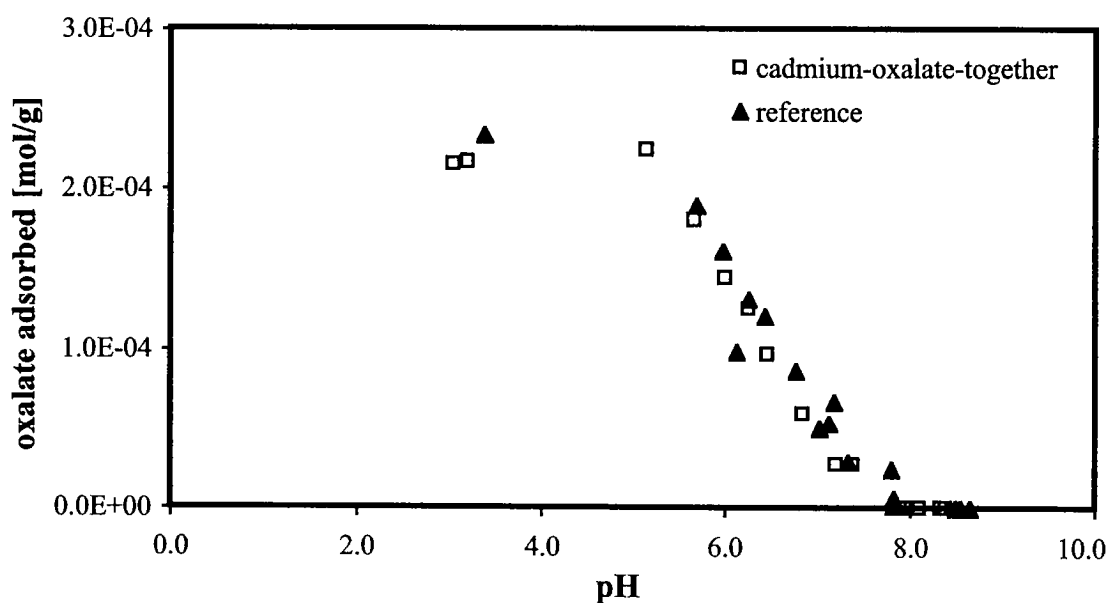


*Fig. 4.10: pH adsorption edge of oxalate on goethite ( $[\text{Cd}]_{\text{tot}} = 1.45 \mu\text{M}$ ,  $[\text{oxalate}] = 10 \mu\text{M}$ ,  $[\text{goethite}] = 0.04 \text{ g/L}$ )*

#### 4.4.3 Nickel-Oxalate-Goethite System

The pH dependence of the adsorption of nickel on goethite in the presence of oxalate is shown in Fig. 4.11. A reference adsorption edge, without oxalate, was measured in  $0.01 \text{ M KNO}_3$ .

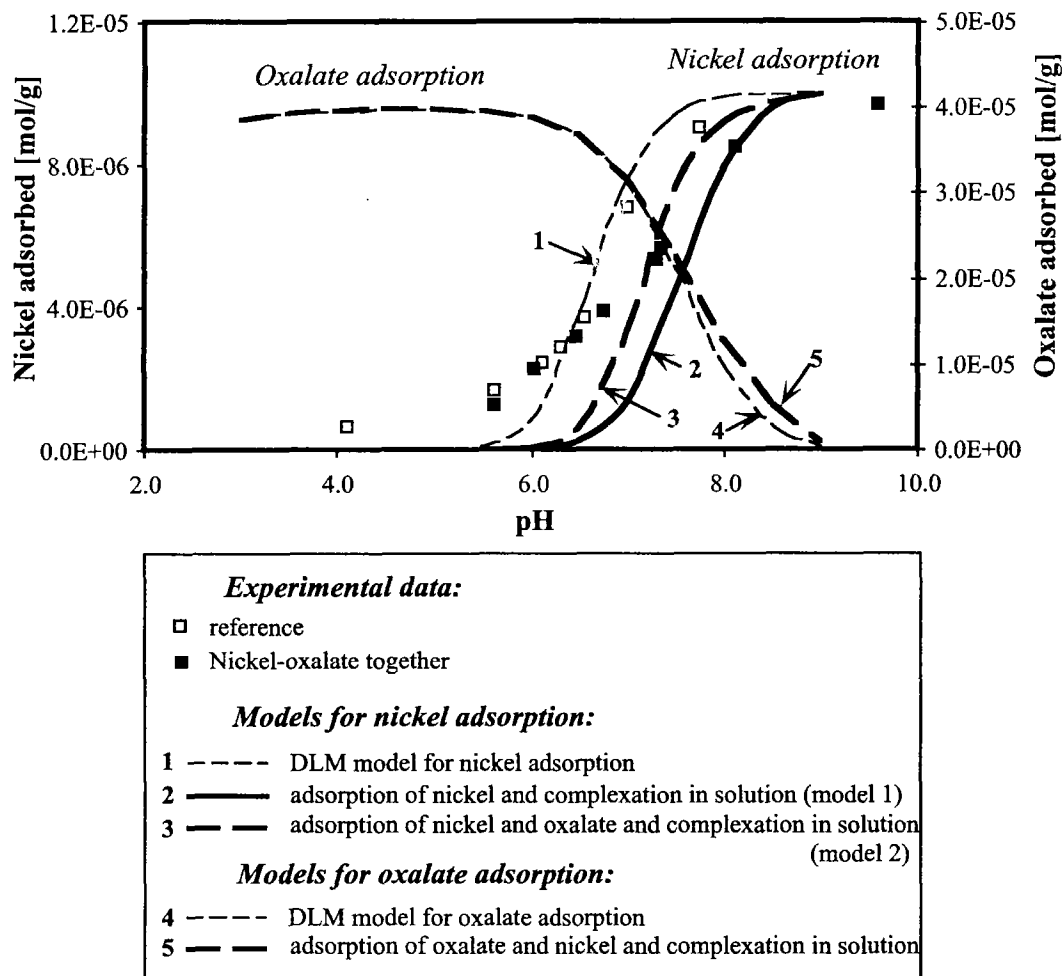


**Fig. 4.11:** pH adsorption edge of nickel on goethite in the presence of oxalate. For comparison, a reference in 0.01 M  $\text{KNO}_3$ , calculated with the DLM model, is shown. Nickel adsorption on goethite in the presence of oxalate was calculated by models 1 and 2. The pH dependence of oxalate adsorption calculated with model 2 is shown as well. (Equilibration time for nickel and oxalate before addition of goethite: 0.5 h, adsorption time: 24 h,  $[\text{Ni}]_{\text{tot}} = 5 \mu\text{M}$ ,  $[\text{Oxalate}] = 0.5 \text{ mM}$ ,  $[\text{goethite}] = 0.5 \text{ g/L}$ ).

At pH values above 7, a decrease in nickel adsorption was observed, whereas at pH values lower than 7, no influence of oxalate on nickel adsorption could be observed directly from the experimental adsorption edges. In this system, the ratio oxalate/nickel equaled 100. However, if this ratio decreased to a value of 1.43, the adsorption of nickel in the pH range below 6 was clearly increased. (Fig. 4.12).

### ***Modelling Results***

At high pH values, the decrease of nickel adsorption compared to the reference could not be adequately described by both models, and in the acidic pH range, the adsorption of nickel was underestimated (Fig. 4.11). A possible explanation is that the nickel-oxalate complexes which form at pH values above 4 (Fig. 4.4), adsorb at acidic pH values on the goethite surface and form a ternary complex such as  $\equiv\text{Fe-Ox-Ni}^+$ .

For an oxalate/nickel ratio of 1.43, nickel adsorption on goethite was even more underestimated by both models (Fig. 4.12). Thus, electrostatic interactions due to adsorbed oxalate were not likely to be the reason for enhancing nickel adsorption but rather specific interactions between nickel and oxalate on the surface, i.e., formation of a ternary complex, occurred.

Prior to addition of goethite, nickel and oxalate were equilibrated together. At such a low ratio of oxalate/nickel, the main oxalate species in solution at pH values above 4 is the nickel-oxalate complex. At pH values below 6, oxalate readily adsorbed on the surface (Fig. 4.13). Thus, upon addition of goethite, the nickel-oxalate complex, formed previously in solution, adsorbed probably as metal complex on the surface to form a ternary complex of type B. The effect was more pronounced at this low oxalate/nickel ratio, as the main oxalate species at  $\text{pH} > 4$  in solution is the nickel-oxalate species, whereas under the conditions of Fig. 4.11 only about 10% of the oxalate formed a complex with nickel.

Another hint for another reaction mechanism in the nickel/oxalate system lies in the fact that the slope of the adsorption edge changed (Fig. 4.12). In the presence of oxalate, the adsorption edge was less steep which indicated that less protons were released per adsorbed nickel. For formation of a ternary complex of type B protons are even consumed. For more details, see the discussion in section 4.7.2.

Kinetic effects will be discussed in section 4.7.4.

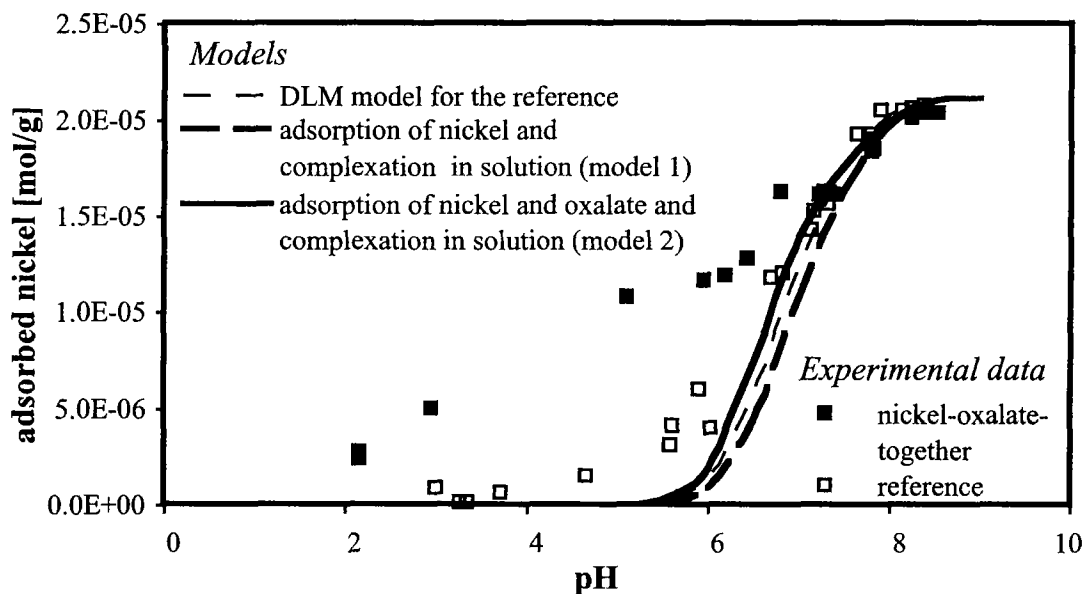


**Fig. 4.12:** pH adsorption edge of nickel on goethite in the presence of oxalate (oxalate/nickel ratio = 1.43). The reference (0.01 M NaNO<sub>3</sub>) was calculated with the DLM model. Nickel adsorption calculations were performed by models 1 and 2. (Equilibration time for nickel and oxalate before addition of goethite: 24 h, adsorption time: 24h, [Ni]<sub>tot</sub> = 7 μM, [oxalate] = 10 μM, [goethite] = 0.33 g/L)

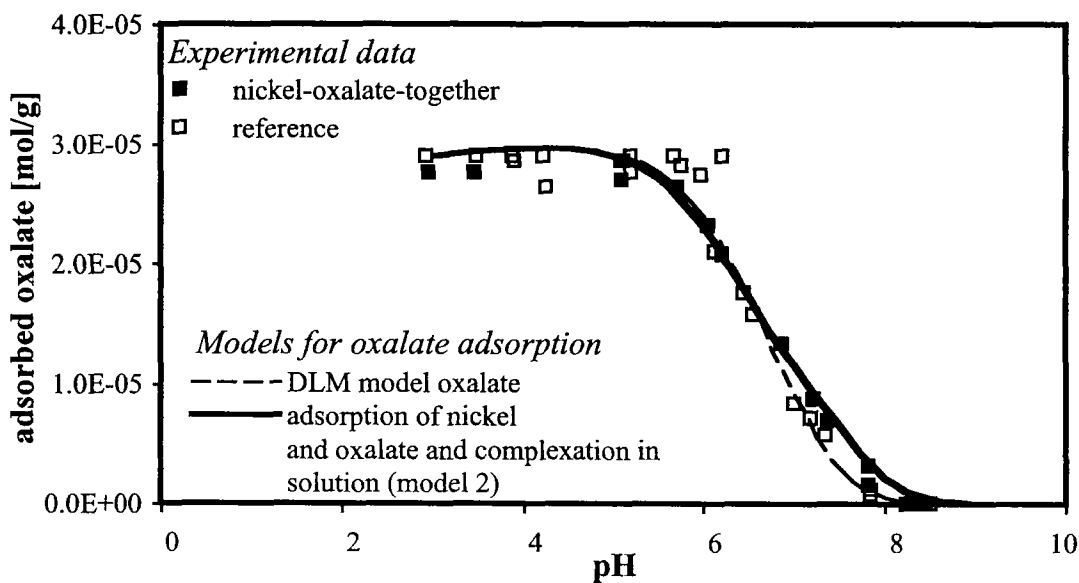


**Fig. 4.13:** pH adsorption edge of oxalate on goethite in the presence of nickel. The reference (0.01 M NaNO<sub>3</sub>) was calculated with the DLM model. Oxalate adsorption was calculated by model 2. (Equilibration time for nickel and oxalate before addition of goethite: 24 h, adsorption time: 24h, [Ni]<sub>tot</sub> = 7 μM, [oxalate] = 10 μM, [goethite] = 0.33 g/L)

### ***Adsorption of Oxalate in the Presence of Nickel***

The adsorption of oxalate was measured in the system nickel-oxalate-together (oxalate/nickel ratio =1.43). The adsorption edge could be described by model 2 (Fig. 4.13). The slight enhancement of the oxalate adsorption, compared to the reference oxalate adsorption edge in 0.01 M NaNO<sub>3</sub>, at pH values above pH 7 was interpreted by electrostatic attraction. At pH 7, more than 50% of the nickel were adsorbed and could thus decrease the negative charge on the surface, which enhanced the adsorption of oxalate in this pH range.

#### **4.4.4 Summary of the Oxalate System**

At pH values above 5, copper and nickel were totally complexed by oxalate in the absence of goethite. Estimation of the metal adsorption in the presence of oxalate was performed by two different models. In model 1, considering only metal adsorption and complexation in solution, metal adsorption was clearly underestimated. Including the adsorption of oxalate into the model (model 2) shifted the calculated adsorption edge to the left. Thus, electrostatic interactions due to the adsorbed oxalate could enhance copper and nickel adsorption on goethite, but could not account for all the metal adsorbed in the experiments. The difference between the experimental and the calculated curves can possibly be explained by further interactions of oxalate and the metal cation on the surface, like formation of ternary complexes. Oxalate is a strong ligand for copper and nickel at pH values above 3. Thus, it is possible that copper-oxalate or nickel-oxalate complexes were adsorbed on the goethite surface.

The influence of oxalate on cadmium adsorption was not pronounced. Complexation of cadmium by oxalate is weaker than for copper or nickel (Fig. 4.4), and thus competition reactions between the surface functional groups and oxalate in solution are essentially not of importance. In the acidic pH range, however, a small enhancement of cadmium adsorption could be observed. This enhancement could be represented sufficiently well by calculating the adsorption of cadmium with the model considering cadmium and oxalate adsorption onto goethite and complexation of cadmium by oxalate in solution. This leads to the conclusion that electrostatic interactions due to adsorbed oxalate might possibly explain an enhanced cadmium adsorption.



## 4.5 Influence of Salicylate on the Adsorption of Copper, Cadmium, and Nickel on Goethite

### 4.5.1 Copper-Salicylate-Goethite System

The pH dependence of the adsorption of copper on goethite in the presence of salicylate is shown in Fig. 4.14. A reference adsorption edge, without salicylate, was measured in 0.01 M  $\text{KNO}_3$ . For these experiments, concentrations were as defined in Tab. 4.1.

In the experimental points, no clear difference could be observed between the adsorption edge of copper in the presence of salicylate and the reference adsorption edge (Fig. 4.14).

#### *Modelling Results*

Modelling of the adsorbed copper concentrations, as well as the calculated salicylate adsorption, are shown in Fig. 4.14. Salicylate adsorption calculations with the constants from Tab. 4.3 are explained in detail in chapter 2.

According to the model calculations performed with models 1 and 2, copper adsorption should be slightly suppressed in the presence of salicylate (curves 2 and 3 in Fig. 4.14), which, however, could not be observed in the experimental data. This is a hint that possibly further interactions occur on the surface. Calculations with the assumption of the formation of ternary complexes are shown in section 4.7.2.

According to model 2, the increase in negative charge of the surface due to specifically adsorbed salicylate was not large enough to enhance copper adsorption. This is probably due to the fact that the adsorption of salicylate was maximal at a pH of about 4 and thus, in the pH range of copper adsorption the electrostatic effect was not so pronounced.

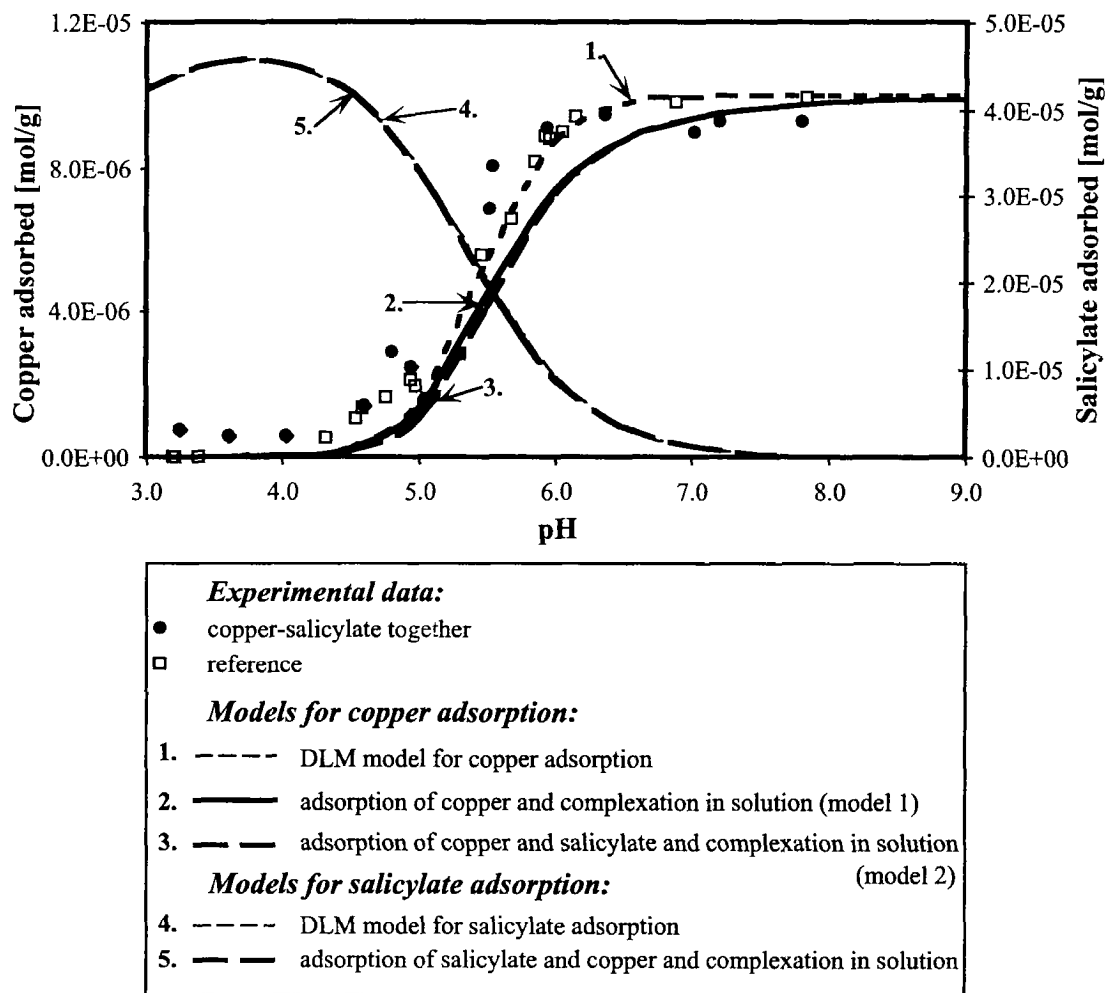


**Fig. 4.14:** pH adsorption edge of copper on goethite in the presence of salicylate. For comparison, a reference in 0.01 M  $\text{KNO}_3$ , calculated with the DLM model, is shown. Copper adsorption in the presence of salicylate was estimated by models 1 and 2. The pH dependence of salicylate adsorption, calculated by model 2, is also shown. ( $[\text{Cu}]_{\text{tot}} = 5 \mu\text{M}$ ,  $[\text{salicylate}] = 0.5 \text{ mM}$ ,  $[\text{goethite}] = 0.5 \text{ g/L}$ )

#### 4.5.2 Cadmium-Salicylate-Goethite System

The pH dependence of the adsorption of cadmium on goethite in the presence of salicylate is shown in Fig. 4.15. A reference adsorption edge, without salicylate, was measured in 0.01 M  $\text{KNO}_3$ . For these experiment, concentrations were as defined in Tab. 4.1.

No decrease in cadmium adsorption in the presence of salicylate was observed at high pH values. Between pH 5 and 7, however, the adsorption of cadmium was enhanced compared to the reference system.

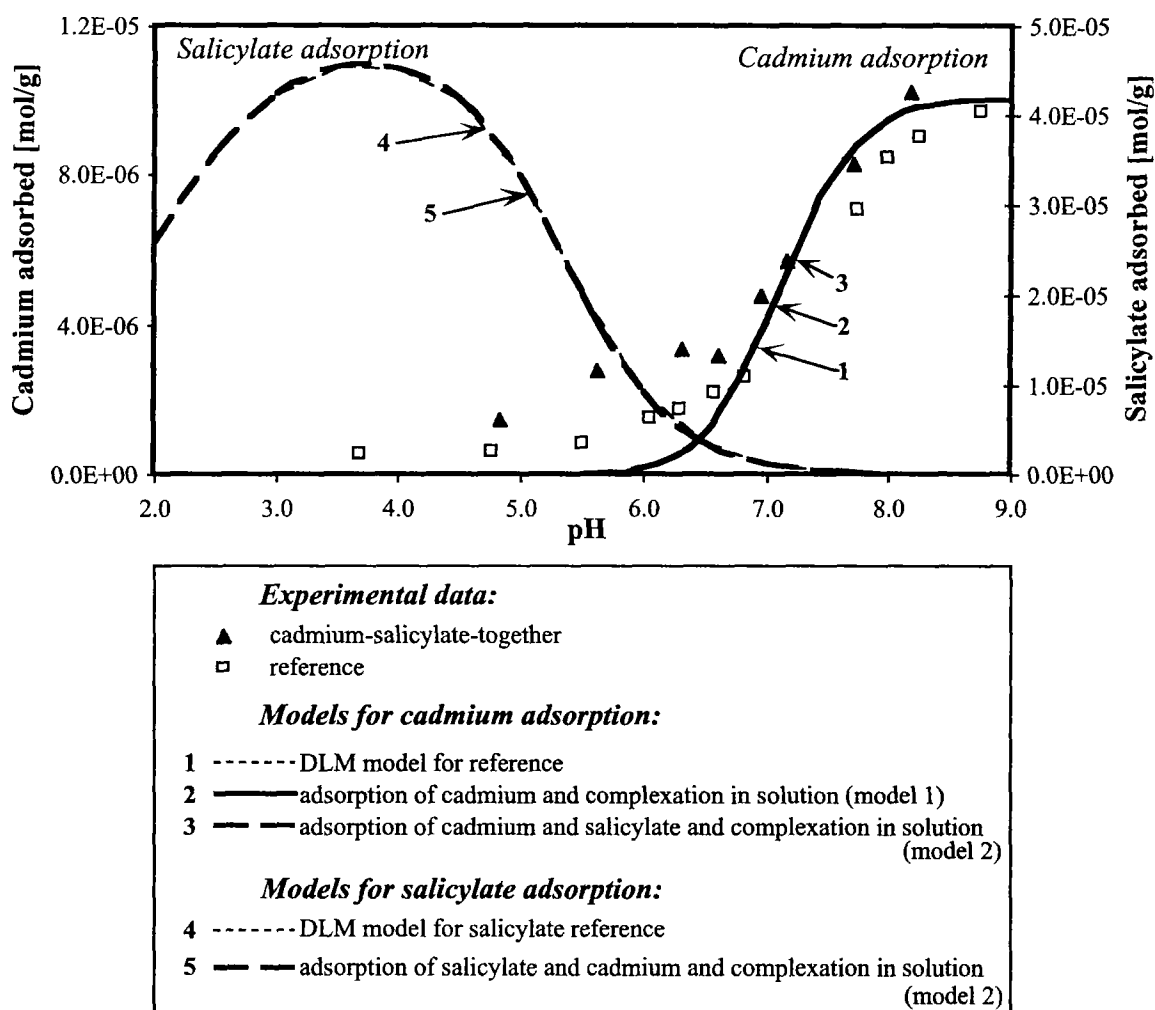


**Fig. 4.15:** pH adsorption edge of cadmium on goethite in the presence of salicylate. For comparison, a reference in 0.01 M  $KNO_3$ , calculated with the DLM model, is shown. Cadmium adsorption on goethite in the presence of salicylate was described by models 1 and 2. The pH adsorption edge of salicylate, calculated by model 2, is also shown. ( $[Cd]_{tot} = 5 \mu M$ ,  $[salicylate] = 0.5 mM$ ,  $[goethite] = 0.5 g/L$ )

### Modelling Results

The adsorption edge of cadmium in the presence of salicylate as calculated by models 1 (curve 2 in Fig. 4.15) and 2 (curve 3 in Fig. 4.15) was equal to the adsorption edge calculated in the absence of salicylate. This is not astonishing, since complexation of cadmium by salicylate is quite weak (Fig. 4.5), and thus a decrease of cadmium adsorption due to salicylate was unlikely at high pH values.

The adsorption of salicylate is not likely to enhance cadmium adsorption through electrostatic effects, because salicylate and cadmium adsorb at different pH regions (curve 3 in Fig. 4.15).

The enhanced cadmium adsorption in the acidic pH range cannot be explained by models 1 and 2. Further possible interactions like formation of ternary complexes will be discussed later (section 4.7.2).

### 4.5.3 Nickel-Salicylate-Goethite System

The pH dependence of the adsorption of nickel on goethite in the presence of salicylate is shown in Fig. 4.16. A reference adsorption edge, without salicylate, was measured in 0.01 M  $\text{KNO}_3$ . For these experiments, concentrations were as defined in Tab. 4.1.

No influence of salicylate on the adsorption of nickel on goethite could be seen in this system (Fig. 4.16). Neither a decreased nickel adsorption at high pH values, nor an enhanced nickel adsorption in the acidic pH range could be observed.

#### *Modelling Results*

As well in the experimental data as in the calculations performed with models 1 and 2, no difference between the adsorption edge of nickel in the presence of salicylate and the reference adsorption edge could be observed (curves 2 and 3 in Fig. 4.16). Salicylate is quite a weak ligand and cannot compete with the surface ligands for complexation of nickel. Thus, nickel is essentially not complexed by salicylate in solution even at high pH values (Fig. 4.5).

The adsorption of salicylate is not likely to have an electrostatic effect on the adsorption of nickel (curve 3 in Fig. 4.16), because the pH regions, where salicylate and nickel adsorb, were different.

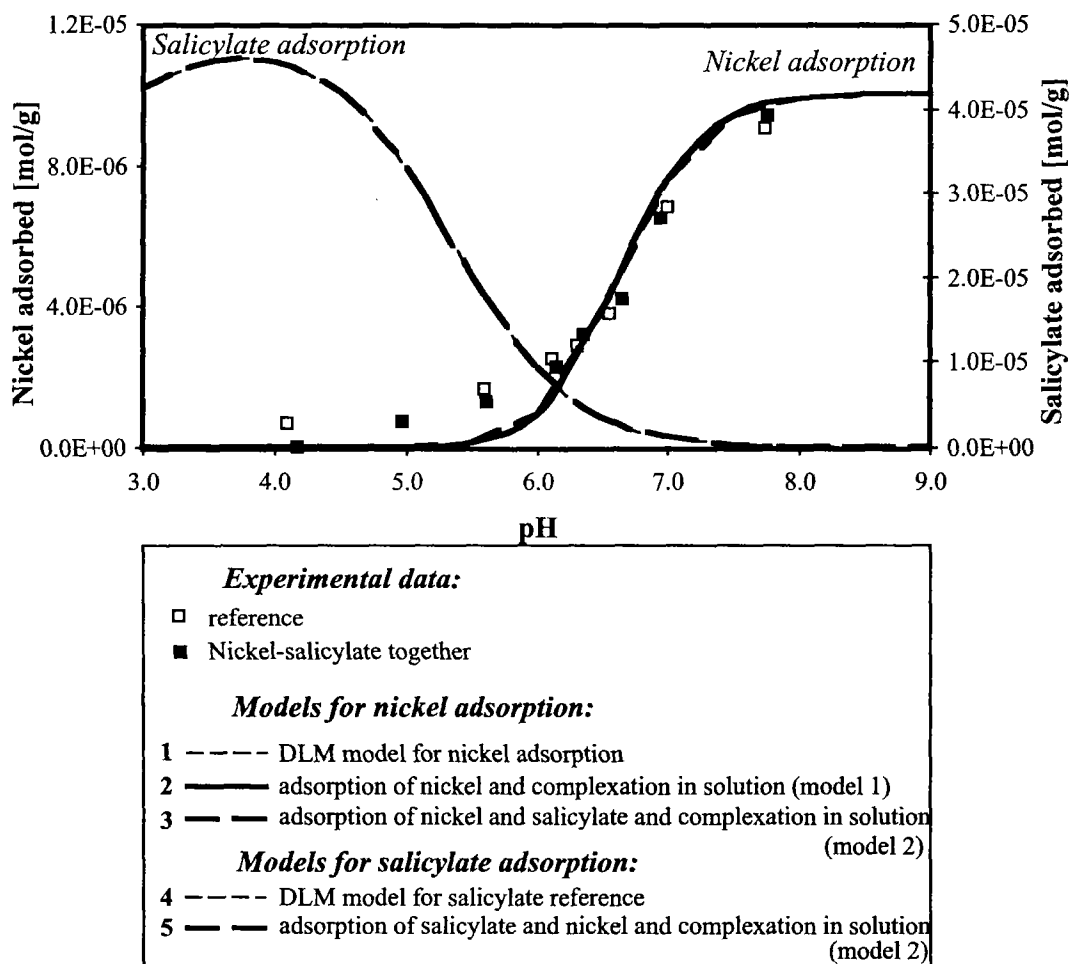


**Fig. 4.16:** pH adsorption edge of nickel on goethite in the presence of salicylate. For comparison, a reference in 0.01 M  $KNO_3$ , calculated with the DLM model, is shown. Nickel adsorption on goethite in the presence of salicylate was calculated by models 1 and 2. The salicylate adsorption (as calculated by model 2) is also shown. ( $[Ni]_{tot} = 5 \mu M$ ,  $[salicylate] = 0.5 mM$ ,  $[goethite] = 0.5 g/L$ )

#### 4.5.4 Summary of the Salicylate System

In the experiments shown above, the ligand concentration was always in excess of the metal concentration, the ratio salicylate/metal was 100. No major influence of salicylate on the metal adsorption could be observed under these conditions. Adsorption was not suppressed clearly for any of the three metals analysed. Only a slight decrease of copper adsorption in the presence of salicylate was calculated with the models 1 and 2. This is consistent with the complexation behaviour of salicylate (Fig. 4.5). Cadmium and nickel are only weakly complexed by salicylate.

In the experiments, a slight increase of cadmium adsorption in the presence of salicylate in the acidic pH range was observed. This increase could not be represented by either model, which is a hint that the increase is due to some interactions not taken into account by the models. Specific interactions with salicylate and cadmium, e.g., formation of ternary complexes, can most probably be excluded as the binding of cadmium by salicylate is weaker than the one of copper and nickel. For these metals, however, no increased adsorption could be observed.

## 4.6 Influence of Pyromellitate on the Adsorption of Copper, Cadmium, and Nickel on Goethite

### 4.6.1 Copper-Pyromellitate-Goethite System

The pH dependence of the adsorption of copper on goethite in the presence of pyromellitate is shown in Fig. 4.17. A reference adsorption edge, without pyromellitate, was measured in 0.01 M  $\text{KNO}_3$ . For these experiments, concentrations were as defined in Tab. 4.1.

Essentially no decrease of copper adsorption by pyromellitate could be observed at high pH values. At pH values between 4 and 5, however, the adsorption of copper was clearly enhanced in the presence of pyromellitate compared to the reference system.

#### *Modelling Results*

Modelling of the adsorbed copper concentrations as well as the calculated pyromellitate adsorption, are shown in Fig. 4.17. Pyromellitate adsorption calculations are shown in chapter 2.

According to the calculations performed with model 1 (curve 2 in Fig. 4.17), a clear decrease in copper adsorption can be expected at pH values above 5. By doing calculations with model 2 (curve 3 in Fig. 4.17), the adsorption edge was shifted to the left with regard to that calculated with model 1. However, adsorption of copper was still underestimated. Therefore, it is probable that some other interactions between copper and pyromellitate occurred on the goethite surface, e.g., formation of ternary complexes.

Pyromellitate forms strong complexes with copper between pH 5 and 9 (Fig. 4.6). These complexes may adsorb on the goethite surface to form ternary complexes of type B or of type A. This assumption will be discussed in section 4.7.2.

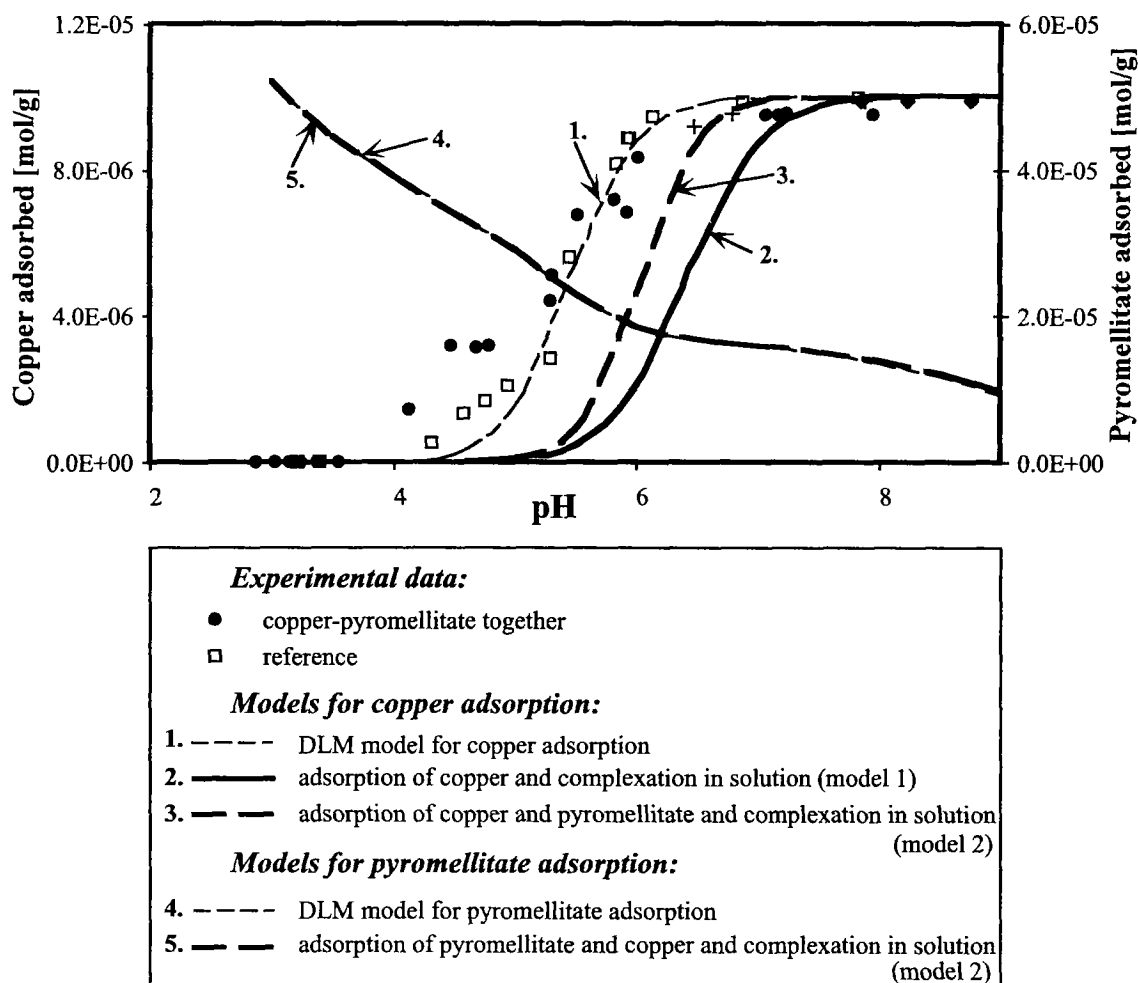


**Fig. 4.17:** pH adsorption edge of copper on goethite in the presence of pyromellitate. For comparison, a reference in 0.01 M KNO<sub>3</sub>, calculated with DLM, is shown. Copper adsorption in the presence of pyromellitate was modelled by models 1 and 2. The adsorption of pyromellitate, calculated with model 2, is also shown. ( $[Cu]_{tot} = 5 \mu M$ ,  $[pyromellitate] = 0.5 mM$ ,  $[goethite] = 0.5 g/L$ )

#### 4.6.2 Cadmium-Pyromellitate-Goethite System

The pH dependence of the adsorption of cadmium on goethite in the presence of pyromellitate is shown in Fig. 4.18. A reference adsorption edge, measured in

0.01 M  $\text{KNO}_3$ , is shown as comparison. The concentrations used in these experiments were as defined in Tab. 4.1.

A clear enhancement of the cadmium adsorption could be observed at pH values above pH 5.

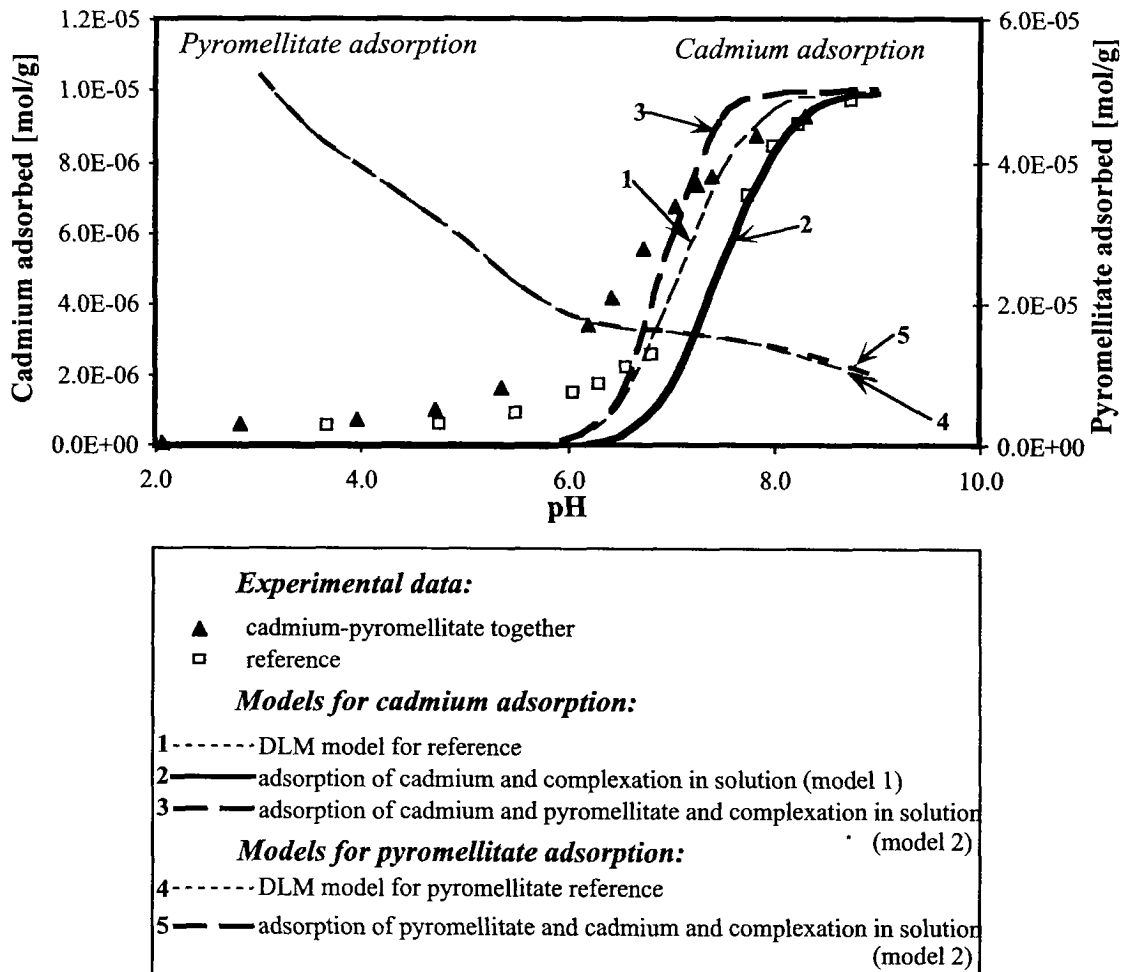


**Fig. 4.18:** pH cadmium adsorption edge on goethite in the presence of pyromellitate. For comparison, a reference in 0.01 M  $\text{KNO}_3$ , calculated with the DLM model, is shown. Cadmium adsorption in the presence of pyromellitate was described with models 1 and 2. The adsorption edge of pyromellitate, calculated by model 2, is also shown. ( $[\text{Cd}]_{\text{tot}} = 5 \mu\text{M}$ ,  $[\text{pyromellitate}] = 0.5 \text{ mM}$ ,  $[\text{goethite}] = 0.5 \text{ g/L}$ )

### Modelling Results

Contrary to the observed adsorption of cadmium on goethite, model 1 (curve 2 in Fig. 4.18) suggested a slight decrease in the adsorption of cadmium. Considering additionally the adsorption of pyromellitate (model 2) resulted in an



enhanced cadmium adsorption. The net surface charge of goethite was lowered due to the specific adsorption of pyromellitate and thus cadmium adsorption was increased. However, in the acidic pH range, the enhanced cadmium adsorption could not be described by this model and other interactions on the surface, e.g., formation of ternary complexes, have to be taken into account. A discussion will follow in section 4.7.2.

### 4.6.3 Nickel-Pyromellitate-Goethite System

The adsorption edge of nickel in the presence of pyromellitate on goethite is shown in Fig. 4.19. For comparison, a reference adsorption edge in 0.01 M  $\text{KNO}_3$  was measured.

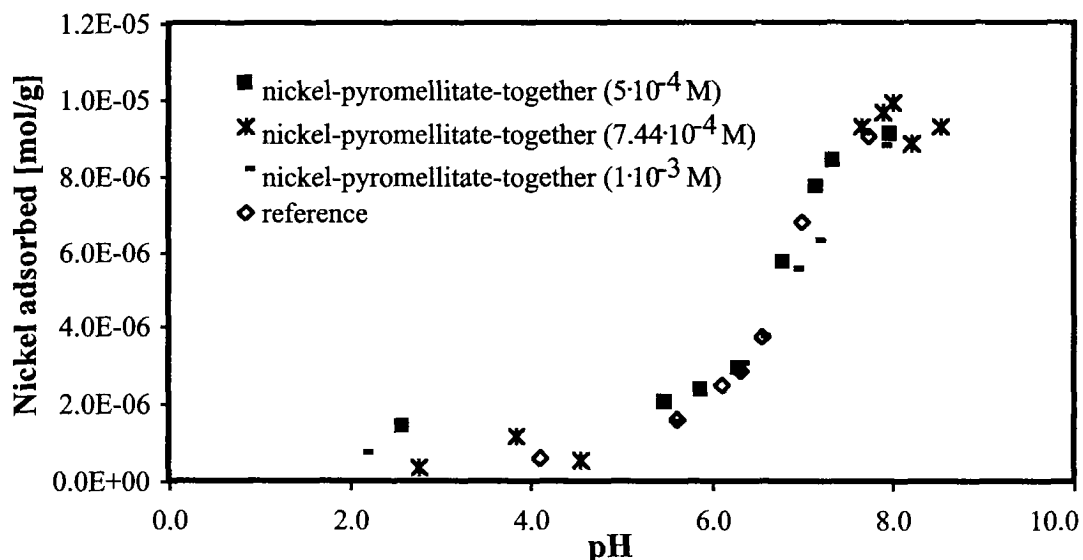


**Fig. 4.19:** pH nickel adsorption edge on goethite in the presence of pyromellitate. Various concentrations of pyromellitate were used. ( $[\text{Ni}]_{\text{tot}} = 5 \mu\text{M}$ ,  $[\text{pyromellitate}] = 5 \cdot 10^{-4} - 1 \cdot 10^{-3} \text{ M}$ ,  $[\text{goethite}] = 0.5 \text{ g/L}$ )

Pyromellitate seemed not to have an influence on the adsorption of nickel on goethite. Increasing pyromellitate concentration did neither enhance nickel adsorption in the acidic pH range, nor suppress nickel adsorption. Unfortunately, complexation constants of pyromellitate with nickel could not be found. However, as nickel has similar complexation and adsorption behaviour as copper, similar results can be expected. In the experimental adsorption edge of copper (Fig. 4.17), no difference in copper adsorption with and without pyromellitate was observed as well. Only the comparison of the experimental data with the modelling results, gave

a hint that some interactions between pyromellitate and copper on the surface are possible. In analogy, the adsorption edge of nickel calculated by model 1 should be shifted to the right of the reference adsorption edge. This shift will probably be less pronounced than for copper since nickel generally forms less stable complexes. Including the adsorption of pyromellitate into the model would increase the negative charge of the surface, and thus probably enhance nickel adsorption. However, as for copper, this model probably would still not be able to account for all nickel adsorbed, which would be a hint for formation of ternary complexes.

Kinetic effects in the adsorption of nickel in the presence of pyromellitate were checked by changing the order of addition of the components (Fig. 4.20). No difference between the different systems could be observed and thus it can be concluded that equilibrium was reached within the equilibration times used in the experiments.

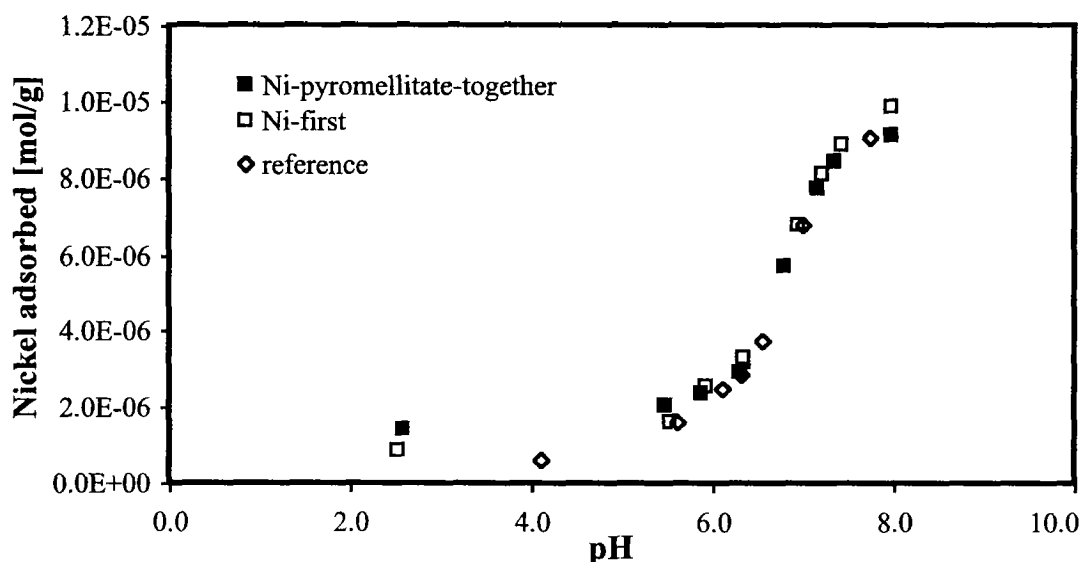


*Fig. 4.20: pH adsorption edge of nickel on goethite in the presence of pyromellitate. For comparison, a reference adsorption edge performed in 0.01 M KNO<sub>3</sub> is shown. The adsorption of nickel onto goethite in the presence of pyromellitate was also studied in the Ni-first system to investigate kinetic effects.*

#### 4.6.4 Summary of the Pyromellitate System

In the experiments shown, the ligand concentration was always in excess of the metal concentration; the ratio of ligand to metal was always 100.

No decrease in the adsorption could be observed experimentally for any of the three metals analysed, although a decrease was calculated by model 1.

Considering pyromellitate adsorption as well (model 2), the adsorption edges of cadmium and copper were shifted to the left, but still, copper adsorption was underestimated. This effect can probably be explained by formation of ternary complexes of type A or B.

Cadmium showed an enhanced adsorption between pH 5 and 8 compared to the reference adsorption edge. However, cadmium forms less strong complexes with pyromellitate than copper (Fig. 4.6), and therefore it is unlikely that more ternary complexes would be formed with cadmium than with copper.

A definitive conclusion for this system could not be given. The cadmium adsorption edge calculated for the reference was too steep (see chapter 2 for more details). Thus, it is also too steep in the ternary system and it was difficult to decide why the calculated curve did not fit to the experimental data. Possibly, cadmium adsorption was only increased through electrostatic attraction on the surface. Another explanation would be the formation of cadmium-pyromellitate surface precipitates.

## 4.7 General Discussion of Adsorption Experiments in the Presence of Simple Organic Ligands

### 4.7.1 Summary of the Main Results

The experiments summarised here were all performed at the same conditions, so that they could be compared with each other. The metal concentrations were  $5\ \mu\text{M}$ , the ligand concentration  $5 \cdot 10^{-4}\ \text{M}$  (except oxalate:  $1\ \text{mM}$ ), and the goethite concentration was  $0.5\ \text{g/L}$ .

#### *High pH Range*

In the presence of oxalate, a clear decrease in the adsorption of copper and nickel was measured, whereas in the presence of pyromellitate, no clear influence could be observed. It could be shown by modelling results, however, that the influence of both ligands on the adsorption of copper and nickel can be explained by two mechanisms. On the one hand, the adsorption was decreased because of complexation of copper or nickel by the respective ligand in solution, and on the other hand it was increased again because of the decreased surface charge due to the

specific adsorption of ligands and probably also because of the formation of ternary complexes. In the presence of oxalate, the decrease in the adsorption of both metals was more pronounced, because oxalate is a stronger complexant in solution than pyromellitate. Kumar and Fish (1996) as well observed a decrease in adsorption of copper on soil in the presence of oxalate. Copper concentrations were varied between 15  $\mu\text{M}$  and 121  $\mu\text{M}$  and oxalate concentrations between 100 and 1000  $\mu\text{M}$ . An increased ratio of oxalate to copper concentrations induced a shift of the adsorption edge to the right, i.e., copper adsorption was decreased.

Both oxalate and pyromellitate did not show a clear effect on the adsorption of cadmium. This can be explained by the fact that cadmium forms less stable complexes with carboxyl groups than copper and nickel and thus, cadmium is less strongly complexed in solution. Competition reactions for binding of cadmium between surface functional sites and the added aqueous ligand occur. Cadmium will be attached to the ligands with the greatest binding strength, which were the goethite functional groups. Similar results for cadmium adsorption on soil samples and goethite in the presence of oxalate at high pH values were reported by Elliott and Denny (1982), Lamy et al. (1991), and Naidu and Harter (1998).

Salicylate, which is a weak ligand compared to oxalate and pyromellitate, did not have a pronounced influence on the adsorption of cadmium and nickel. Only for copper, a slight decrease in adsorption was found.

### ***Low pH Range***

In the presence of oxalate and pyromellitate, the adsorption of copper and of nickel on goethite was enhanced at low pH values. This effect was particularly pronounced according to model 2 for copper adsorption on goethite in the presence of pyromellitate. Pyromellitate was shown to adsorb on goethite also at elevated pH values, thus formation of ternary complexes would be theoretically possible over a large pH range (Evanko and Dzombak, 1999). Nordin et al. (1998) have shown by modelling of FTIR studies that pyromellitate adsorbs as inner- and outersphere complexes on boehmite. Outersphere complexes were found to dominate over the whole pH range, but an increasing amount of innersphere complexes was found at pH values below 5.5. These results indicate that pyromellitate is not a very effective ligand to form ternary complexes, except in the acidic pH range. Applying this information to our system, it is possible that in the acidic pH range an innerspherical ternary complex is formed and that at pH values between 5.5 and 7  $\text{CuPyr}^{2-}$  may be

attracted electrostatically to the still positively charged surface ( $\text{pH}_{\text{pzc}}=9.2$ , see chapter 3).

In the experiments performed with an oxalate/nickel ratio of 1.43, nickel adsorption was drastically enhanced, which can probably be explained by formation of ternary complexes. Similarly, ternary complexes in a system at equimolar concentrations of EDTA and nickel have been reported by other authors (Bowers and Huang, 1986; Bryce et al., 1994; Nowack et al., 1996 b).

No effect of salicylate could be observed on the adsorption of both copper and nickel.

Surprisingly, the adsorption of cadmium was enhanced by all three ligands. The effect was weak in the presence of oxalate and most pronounced in the presence of pyromellitate. An enhanced cadmium adsorption in the presence of organic ligands was reported before in several studies.

Lamy et al. (1991) observed a distinct shift to the left of the adsorption edge of cadmium on goethite in the presence of oxalate, i.e., an enhanced cadmium adsorption in the acidic pH range. Both cadmium and oxalate concentrations were  $10 \mu\text{M}$ , and the surface sites were in excess. The authors postulated some interactions of oxalate with cadmium on the goethite surface. However, they did not give precisions whether cadmium binding occurred via chemical bonding, i.e., formation of a ternary complex of type B, or whether there was only a coulombic interaction with an oxalate surface group.

In their experiments performed with surface soils, Naidu and Harter (1998) explained the enhanced cadmium adsorption in the presence of oxalate by the formation of ternary complexes.

An enhanced adsorption of cadmium on alumina in the presence of salicylate was observed by Benyahya and Garnier (1999). In their experiments the salicylate/cadmium ratio was about 10. The effect was explained by the formation of ternary complexes, although no spectroscopic evidence for their existence could be given.

However, as cadmium forms the weakest complexes with all three ligands, it is improbable that more ternary complexes are formed with this metal than with copper or nickel. Possibly another mechanism than formation of ternary complexes has to be considered to explain the enhanced cadmium adsorption.

In the work of Collins et al. (1999), the enhanced cadmium uptake on goethite at pH 5 was shown by EXAFS measurements to be due to the formation of a cadmium oxalate precipitate. However, the concentrations used in this study were

about 4 mM and 2 mM for cadmium and oxalate, respectively. As the concentrations of this study were much lower, it remains unsure whether surface precipitation can explain the enhanced uptake of cadmium at low pH.

It has been shown in several studies that oxalate and salicylate can reduce goethite photochemically (Siffert and Sulzberger, 1991; Sulzberger et al., 1989). As our experiments were performed in the dark, dissolution is kinetically very slow and can be neglected within the equilibration times used in this study.

In general, the following simplified conclusions of the metal adsorption reactions, performed in the presence of different organic ligands, can be drawn:

- Oxalate is the ligand with the highest tendency to mobilise metals at elevated pH values.
- Salicylate has no pronounced effect on the adsorption of the metals over the whole pH range.
- Pyromellitate is the ligand with the strongest tendency of the analysed ligands to enhance metal adsorption over the whole pH range.

In the following section, effects of the ligands shall be discussed by including ternary complexes into the model.

#### **4.7.2 Formation of ternary complexes**

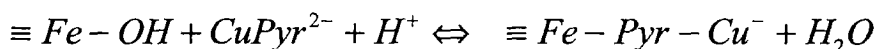
In the presence of strong organic ligands such as oxalate, metal adsorption was underestimated in the model calculations, i.e., the calculated adsorption edges were shifted to higher pH values. The difference between calculated and experimental adsorption edge could probably be explained by the formation of ternary complexes. In this section it will be discussed, how formation of the two possible types of ternary complexes influences the adsorption of metals.

The formation of a ternary complex was included into model 2, using plausible formation constants in the calculations with the programme ChemEQL. The goal of this section was further to discuss under which conditions which type of ternary complex was possibly formed. To achieve this purpose, calculations were performed over a range of possible constants. This allowed to see clearly, how the shape of the curve changed with the definition of a ternary complex.

### **Formation of ternary complexes of type B**

As the formation of this type of ternary complex is ligand-like, metal adsorption will be enhanced in the acidic pH range. The following reactions were defined in:

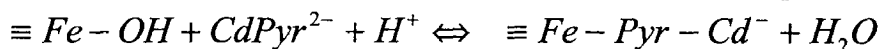
the **copper** system:



the **nickel** system:



and in the **cadmium** system:



A first estimation for the formation constant of the ternary complexes was calculated by the sum of the adsorption constant of the ligand onto goethite and the complexation constant of the metal by the ligand in solution. The results of these calculations are shown in Fig. 4.21 a-e.

In the model calculations, metal adsorption is enhanced if the following statements are true:

- a high amount of ligand is adsorbed in this pH range,
- the metal is strongly complexed in this pH range.

---

**Fig. 4.21:** pH adsorption edge of copper, cadmium, and nickel in the presence of the organic ligand was calculated by including the equation for the formation of a ternary complex of type B into model 2. Calculations were performed over a range of constants for the formation of ternary complexes.

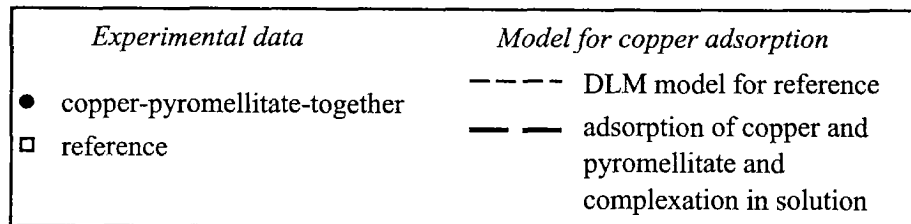
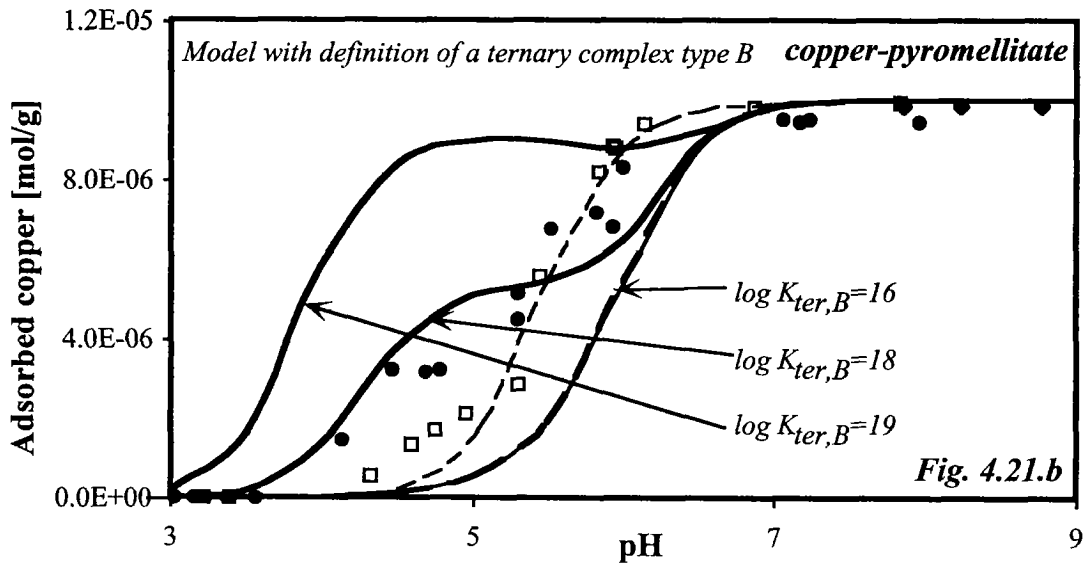
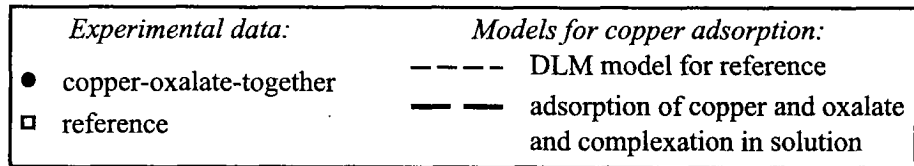
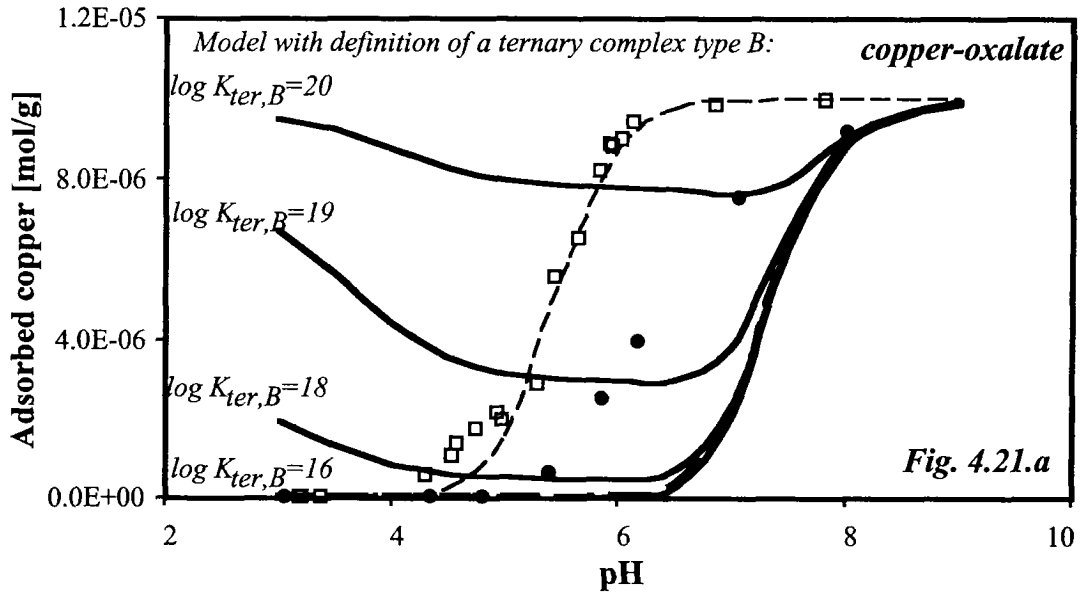
**a:** copper-oxalate-system

**b:** copper-pyromellitate system

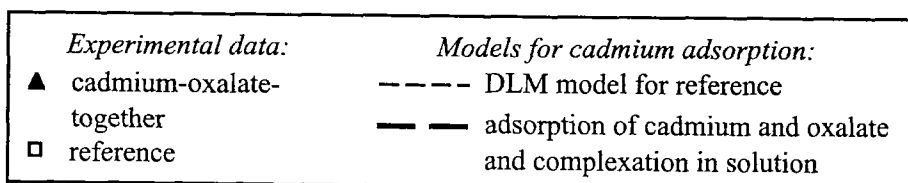
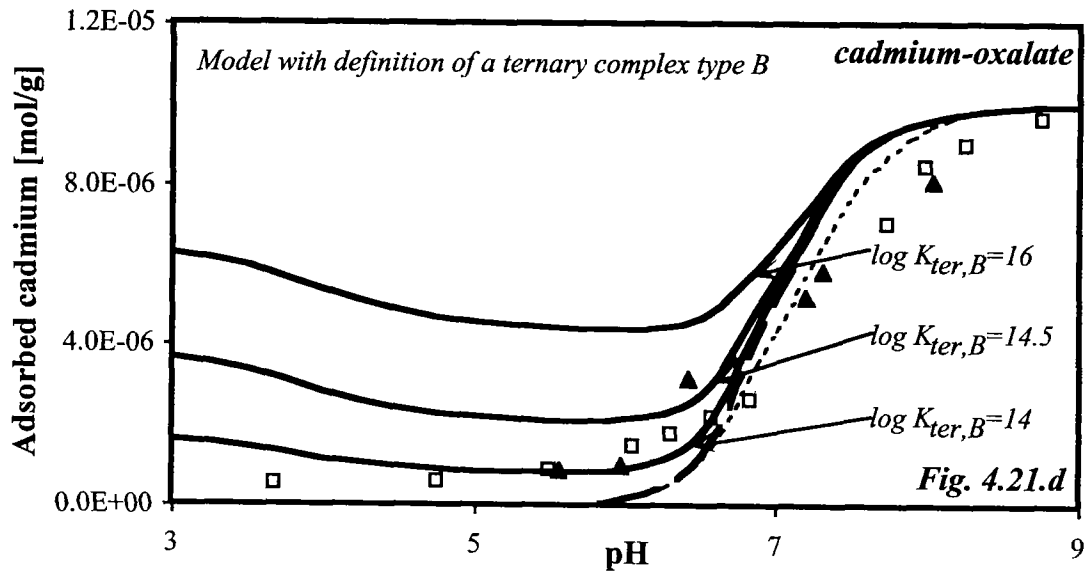
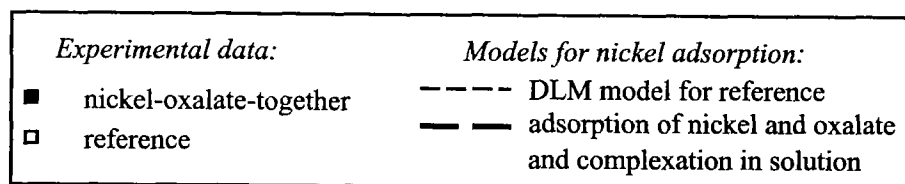
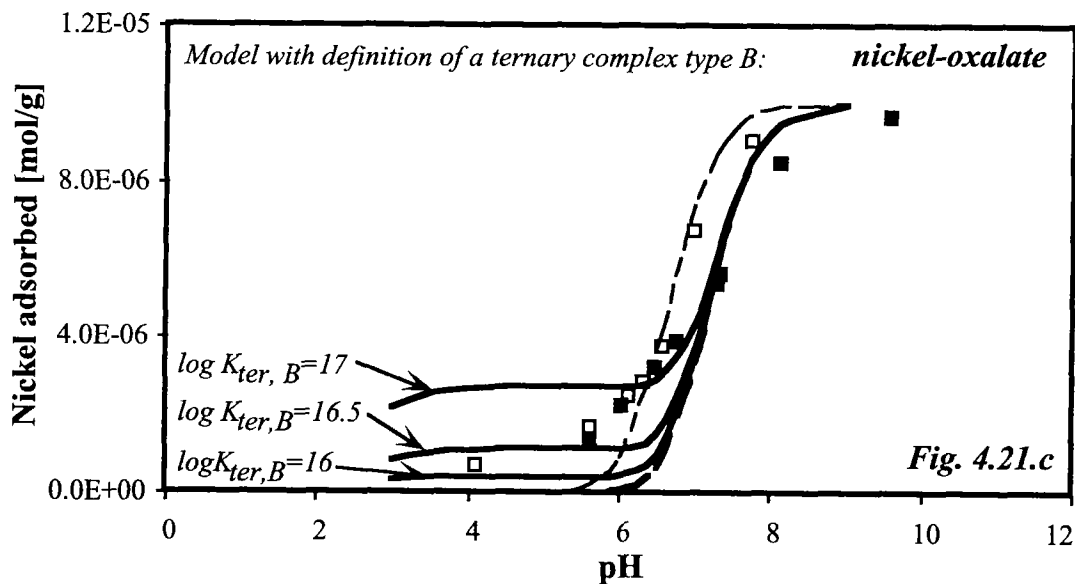
**c:** nickel-oxalate system

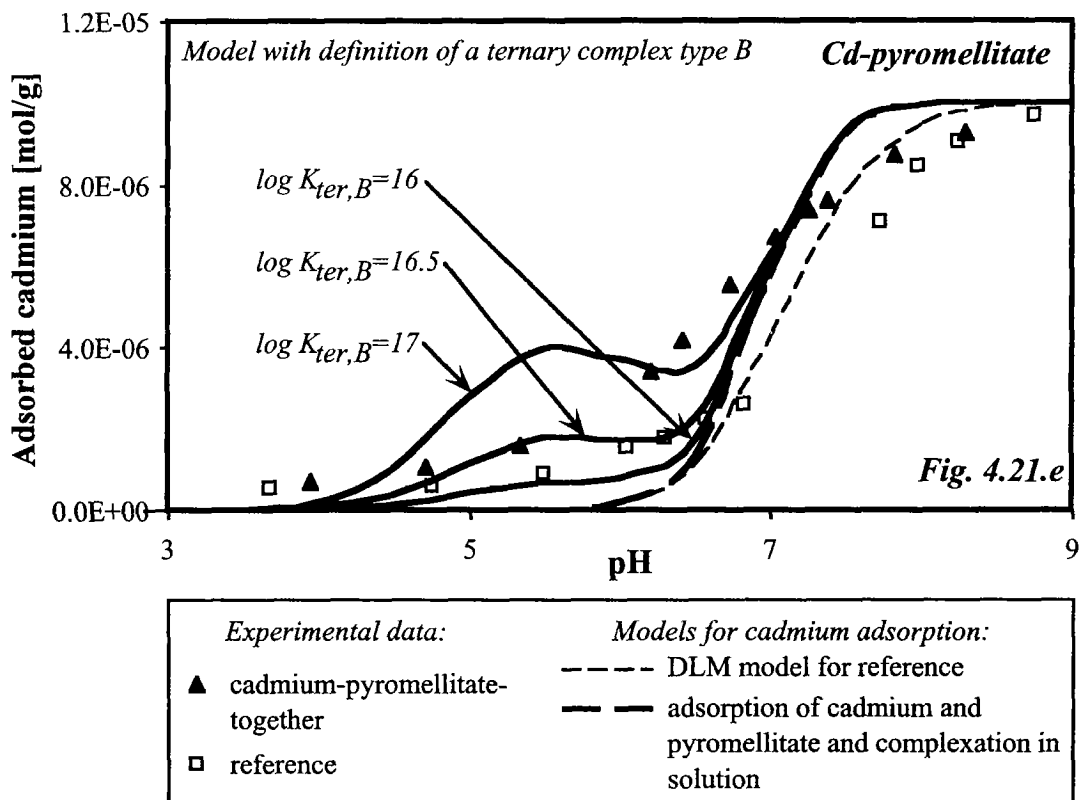
**d:** cadmium-oxalate system

**e:** cadmium-pyromellitate system









In the copper-pyromellitate and the nickel-oxalate system, the experimental points follow the same trend as the calculated adsorption edge. As a consequence, it can be assumed that copper and nickel are adsorbed in these systems as a ternary complex of type B in the acidic pH range.

In the copper-oxalate system, the experimental copper adsorption edge had a totally different shape than the calculated one. According to the calculations, copper adsorption should reach a maximum at a pH value of about 2, where both conditions, described above, become true. Copper adsorption in this system cannot be described by this model. This is probably due to the fact that goethite-oxalate-copper complexes are not stable.

Similar reflections can be made for the cadmium-oxalate system, where the enhancement of the cadmium adsorption as calculated by the model is too pronounced.

In the cadmium-pyromellitate system, cadmium adsorption was indeed slightly enhanced at pH values around 5, which could be described by the model calculations. Altogether, at higher pH values, the adsorption of cadmium could not be described sufficiently well.

In all these examples, where the definition of a ternary complex of type B helped to describe the data, the equilibrium constant for the formation of the ternary complex can be estimated by the following empirical relationship:

$$\log K_{ter} = \log K_{\equiv Fe-L} + \log K_{MeL} + y$$

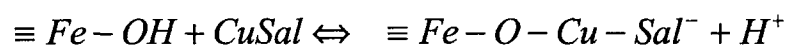
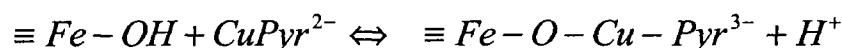
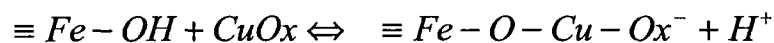
where  $y$  is an empirically defined constant

In our case, the value for  $y$  was always about 2. Similar results for the definition of the formation constant for a ternary complex were found e.g., by Ali and Dzombak (1996a) and Lövgren (1991).

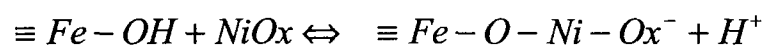
### **Formation of ternary complexes of type A**

This type of ternary complex, which is metal-like, will enhance heavy metal adsorption at high pH values. The following reactions were defined

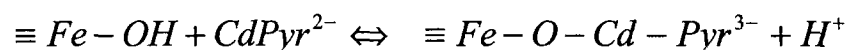
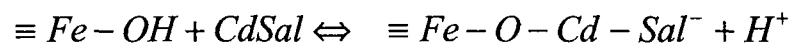
for the **copper** system:



for the **nickel** system:



and for the **cadmium** system:



Calculations were performed by assuming different values for the stability constant of the ternary complex of type A. A first value was estimated by taking the sum of the adsorption constant of the metal onto goethite and the complexation constant of the metal by the ligand in solution. The results of the calculations are shown in Fig. 4.22 a-f.

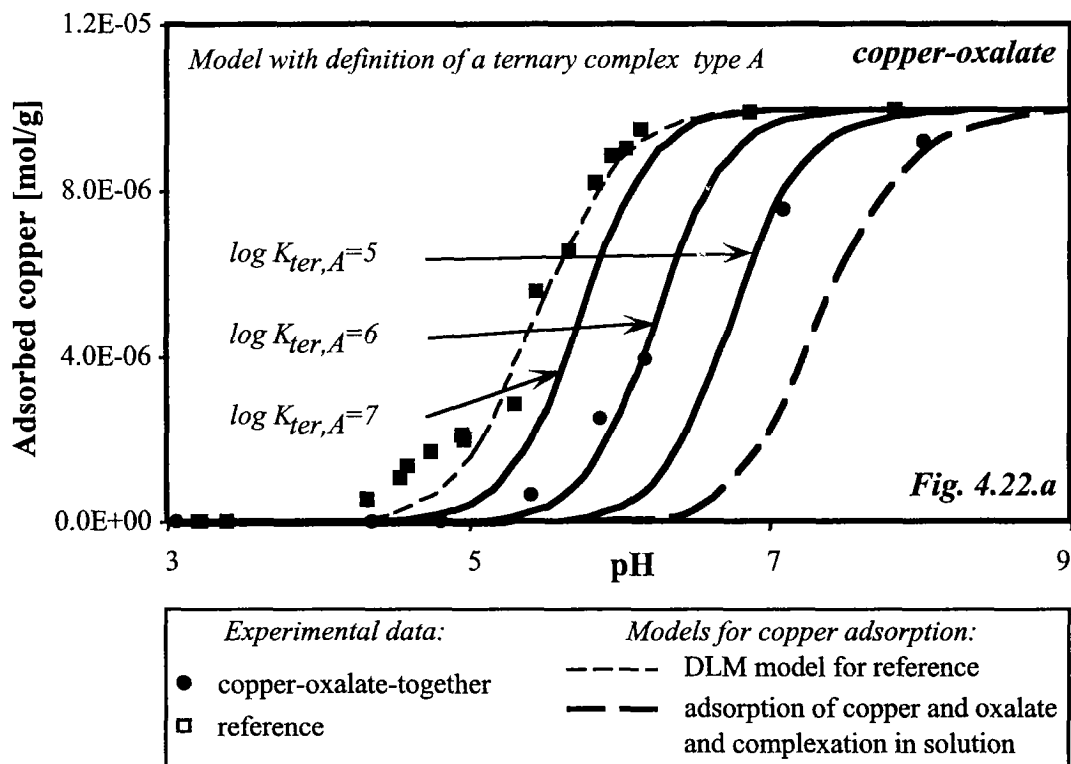


**Fig. 4.22:** pH adsorption edge of copper, cadmium, and nickel adsorption in the presence of organic ligands was calculated by including the equation for the formation of a ternary complex of type A. Calculations were performed by assuming different values for the formation of a ternary complex.

**a:** copper-oxalate-system

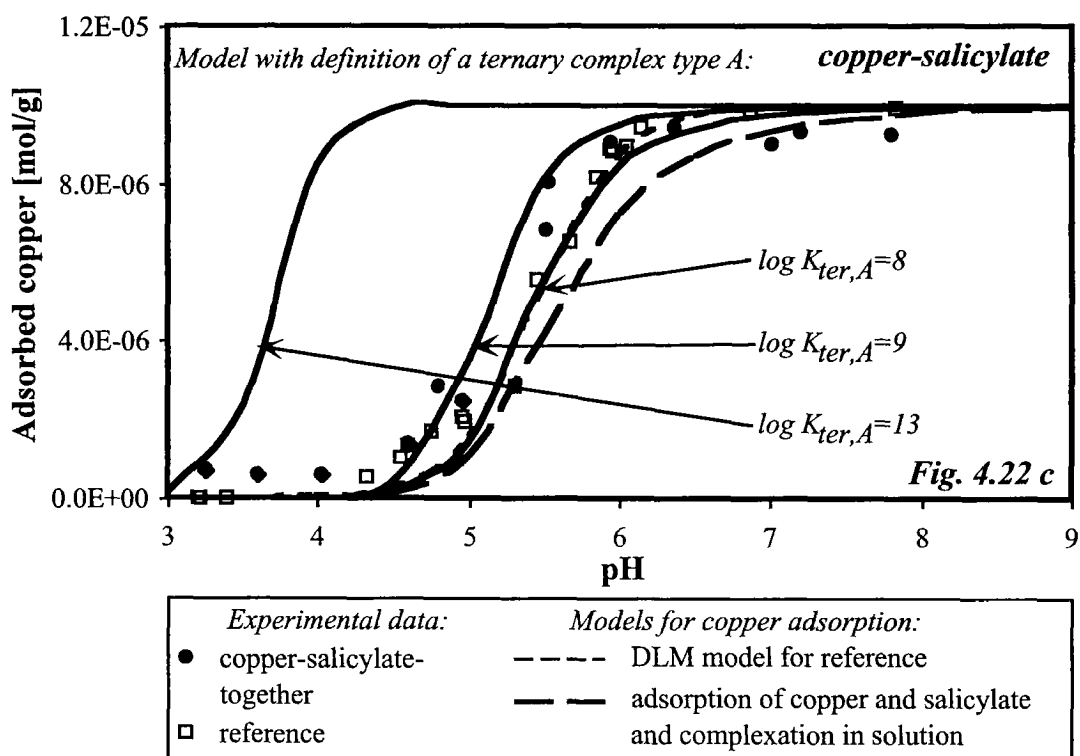
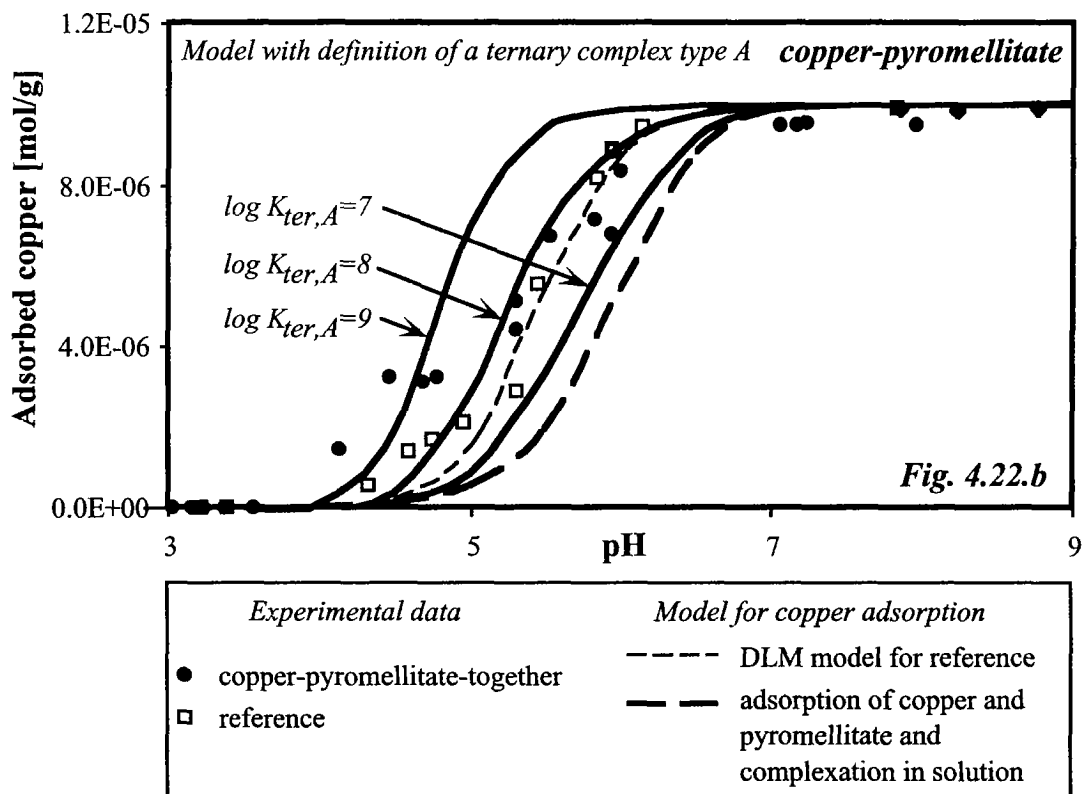
**b:** copper-pyromellitate system

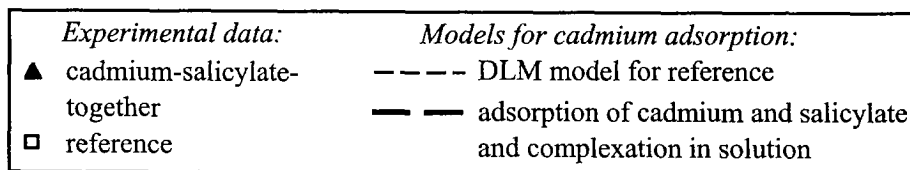
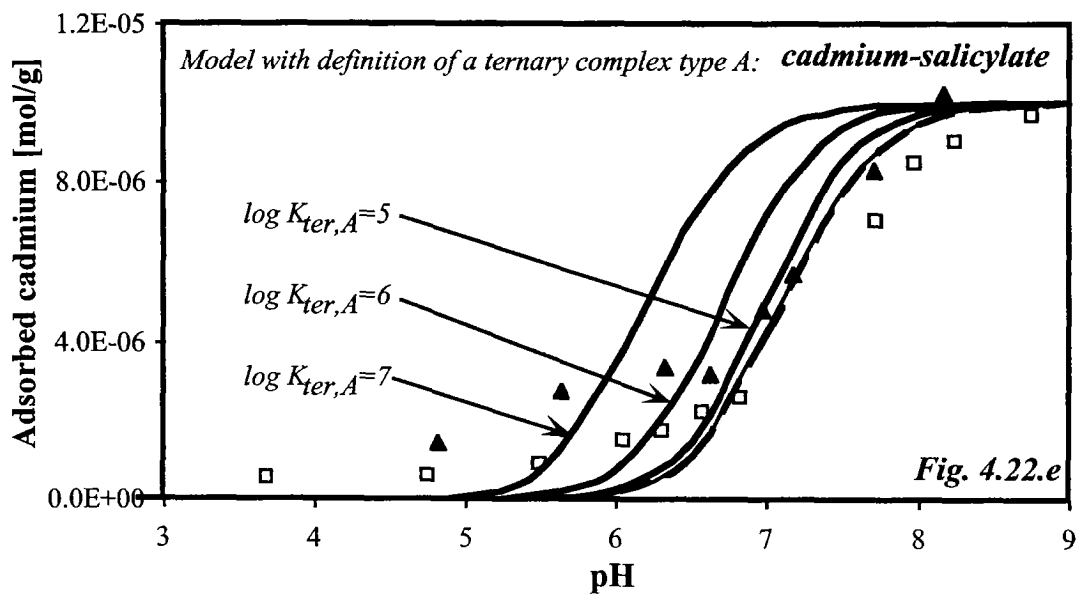
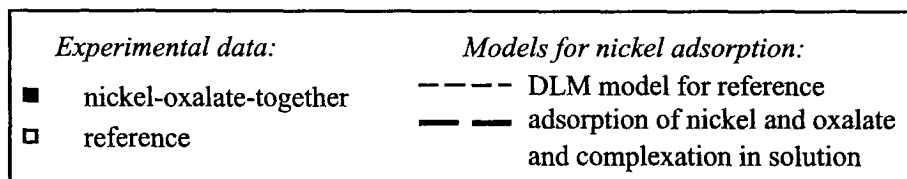
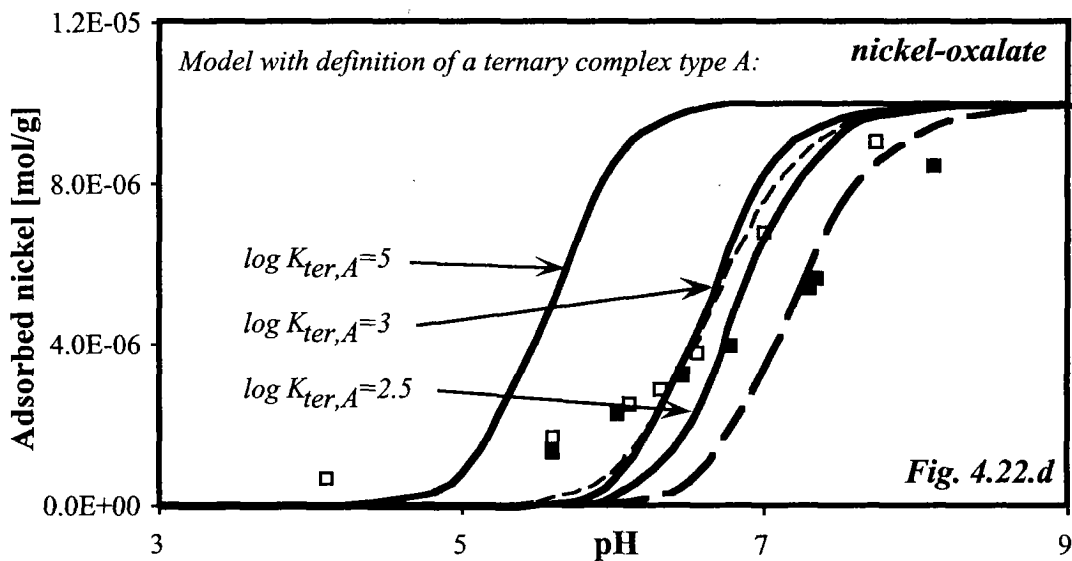
**c:** copper-salicylate system

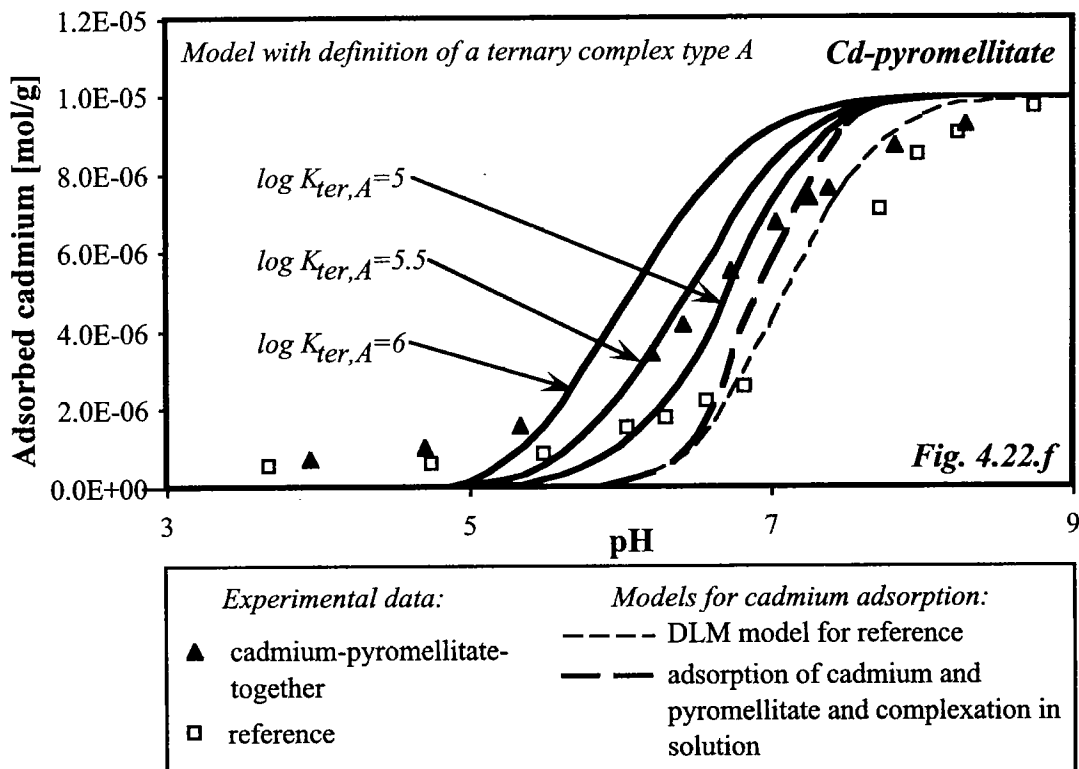
**d:** nickel-oxalate system

**e:** cadmium-salicylate system

**f:** cadmium-pyromellitate system







In the copper-oxalate, nickel-oxalate, and cadmium-salicylate systems, the definition of ternary complexes of type A did not improve the fit of the model to describe the experimental data. The adsorption behaviour of copper in the presence of salicylate could be described sufficiently well by forming a ternary complex of type A. At high pH values, the adsorption of copper in the pyromellitate system could be described adequately. However, in the acidic pH range, adsorption was underestimated for the cadmium-pyromellitate system. A definitive conclusion cannot be drawn, because the calculated cadmium adsorption edge was too steep (details to this problem are given in section 2.7). For this reason, it is difficult to decide whether the calculated adsorption edge in the presence of cadmium can describe the data.

### 4.7.3 Discussion

The models presented here, although simple, are useful to estimate the influence of the different effects on the adsorption of metals in the presence of organic ligands. Calculations were started in the ternary system by considering the most simple model, i.e., the adsorption of the metal onto goethite and the complexation of the metal by the ligand in solution. In the systems, where the metal

was strongly complexed by the ligand, i.e., copper- and nickel-oxalate systems and copper-pyromellitate system (and probably nickel-pyromellitate system), the adsorption of the metal was underestimated just by considering the competition reactions between the surface functional groups and the ligand. Including the adsorption of the ligand increased metal adsorption in the systems, where considerable amounts of the ligand and the metal were adsorbed in the same pH range, i.e., in the oxalate and pyromellitate systems. Altogether, metal adsorption was still underestimated. The definition of ternary complexes of type B helped to describe the adsorption of copper in the pyromellitate and of nickel in the oxalate system, whereas a ternary complex of type A seems to be more adequate to represent copper adsorption in the presence of salicylate. Possibly both types of ternary complexes may be formed, e.g., in the copper-pyromellitate system with a ternary complex of type A at high pH values and type B at low pH values. This would be consistent with the studies of Nordin et al. (1998), who showed by FT-IR, that pyromellitate adsorbs innerspherically on boehmite only at low pH values.

Of course, these models are not a proof for the existence of ternary complexes. Other interactions, which could not be represented by a double layer model, are possible, e.g., the outersphere adsorption of metal-pyromellitate complexes or surface precipitation. The outersphere adsorption of CuOx is unlikely as this complex is uncharged.

To verify the formation of ternary complexes, spectroscopic measurements would be necessary. By FT-IR and EXAFS measurements it is in general possible to determine the structural identity and to distinguish between innersphere or outersphere coordination (Davis and Kent, 1990; Hug, 1994, 1997).

#### 4.7.4 Kinetic effects

Striking is the fact that a ternary complex of type B may help to describe adsorption of nickel in the presence of oxalate, but fails to represent copper adsorption. Possibly, this difference can be explained by kinetic effects. Nickel kinetics are known to be slow due to its electron configuration (Wilkins, 1991). It has been shown e.g., by Xue et al. (2000), that it takes about 20 h to reach equilibrium to form Ni(DMG)<sub>2</sub> (nickel-dimethylglyoxime) complexes at pH 7.6 in a system containing 6 μM DMG and 100 nM nickel.

It is possible that the nickel-oxalate complex, formed prior to the addition of goethite, adsorbs on the surface in the acidic pH range and that the



thermodynamically more stable binary oxalate surface complex (Schindler, 1990) is formed by slow desorption of nickel.

Similar kinetic effects were also observed by (Bryce et al., 1994; Nowack et al., 1996 b) for nickel adsorption on hydrous ferric oxide in the presence of EDTA. In the system Ni-EDTA-together, an enhanced adsorption of nickel in the presence of EDTA was observed, which could be modelled by the definition of ternary complexes of type B. However, in the systems Ni-first and EDTA-first, no enhanced nickel adsorption could be observed which the author explained by kinetic effects.

#### 4.7.5 Influence of the structure of the ligands

Ternary complexes of type B are unlikely with salicylate because of the unfavourable position of the functional groups. By CIR-FTIR and ATR-FTIR (cylindrical internal reflection, respectively attenuated total reflection Fourier transform infrared) measurements, it has been shown, that salicylate adsorbs on goethite by forming a six-membered ring involving one oxygen from the carboxyl and the phenolic group and one Fe atom from the surface (Biber and Stumm, 1994; Yost et al., 1990) (Fig. 4.23). Once adsorbed on the surface, no functional group is free to complex with a metal cation. Formation of ternary complexes of type A, however, is possible.

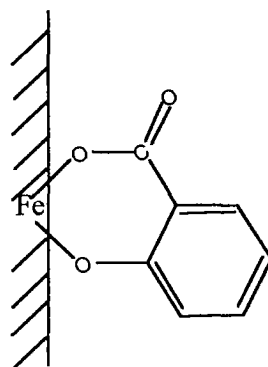


*Fig. 4.23: Possible structure of salicylate on goethite*

Oxalate and pyromellitate, on the other hand, can probably form ternary complexes both of type A and B, as their functional groups are more favourably localised.

Oxalate can possibly adsorb on the goethite surface by forming a five-membered ring or by forming a surface complex with two iron atoms (Fig. 4.24)

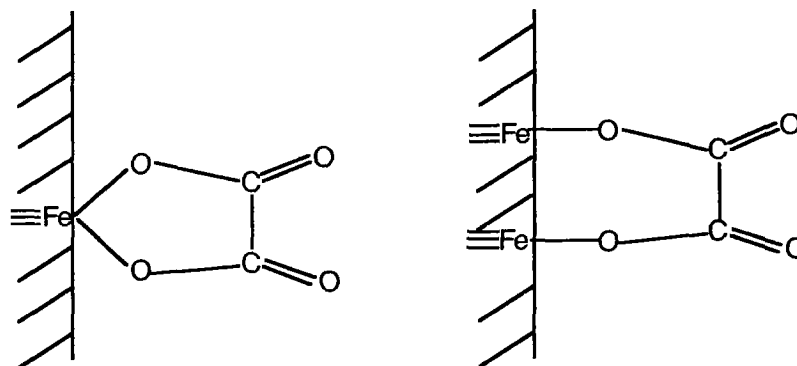


*Fig. 4.24: Possible structures of oxalate on goethite*

Other structures, like those defined for oxalate adsorption on  $\text{TiO}_2$ , are possible (Hug, 1994), but the exact structures of oxalate on a goethite surface could not be defined till now. These structures shown in Fig. 4.24, however, are not favourable for the formation of ternary B complexes.

It has been shown with IR spectroscopy by Boily et al. (2000), that pyromellitate adsorbs on goethite as an outersphere complex in the pH range from 3 – 9. Below pH 6 additional IR spectroscopic features appeared, which were assigned to innersphere complexes. Similar results have been obtained by Nordin et al. (1998) who showed that pyromellitate adsorbs innerspherically on boehmite at pH values below 5 and outerspherically at pH values above 5. Adsorption experiments performed with simple aromatic acids can also give information on how pyromellitate may adsorb. Evanko and Dzombak (1998) showed that with increasing number of carboxylic groups, the sorption increased and extended over a wider pH range. This suggests that pyromellitate adsorbs on the goethite surface by binding with two carboxylic groups. Formation of ternary complexes of type B is possible, as the two carboxylic groups on the other side of the ring can complex metals.

Although the structures of the ligand complexes on the surface are still not definitively known, it can be assumed that those shown in Fig. 4.23 and 4.24 are stable. A ligand probably forms complexes with an adsorbed metal in a similar way as it does with an iron atom belonging to the goethite crystal. Thus, merely from the structure of these complexes, it cannot be explained why formation of ternary complexes of type A is possible for copper in the salicylate system, but not in the oxalate system. Additional effects, such as charge transfer have to be taken into account.

# *Adsorption of Cu, Cd, Ni on Goethite in the Presence of Natural Groundwater Ligands*

## **5.1 Introduction**

A lot of work has been done to investigate the influence of simple organic ligands on the adsorption of heavy metals on solid phases, e.g. protocatechuic acid and salicylate by Davis and Leckie (1978 and 1979), oxalate by Collins et al. (1999), Lamy et al. (1991) and Ragnarsdottir et al. (1998), salicylate by Benyahya and Garnier (1999), or citrate by Boily and Fein (1996) and Ragnarsdottir et al. (1998). Recently, interest increased to study the effect on heavy metal adsorption by natural organic ligands, like humic and fulvic acids (Davis and Bhatnagar, 1995; Hering and Morel, 1988; Jordan et al., 1997; Koopal et al., 1994; Lo et al., 1992; Murphy and Zachara, 1995; Temminghoff et al., 1997; Tipping et al., 1991). However, few studies have been done using unfractionated natural organic matter (NOM). Humic and fulvic acids represent only a part (about 50%) of the total DOC (Thurman, 1985). Hydrophilic compounds (about 30% of the total DOC) are not taken into account when investigating only the humic and fulvic fraction. Although the chemical nature of these acids is hardly known, they are thought to be similar to humic material, with more  $-\text{COOH}$  and  $-\text{OH}$  groups and lower molecular weights (Aiken et al., 1985). As proton and metal binding properties are assumed to be similar to the fulvic fraction (Christensen et al., 1999), the complexation capacities of the hydrophilic acids must be taken into account when investigating complexation

of metals by DOC in a natural water. The other 20 % of the DOC are simple molecules like glucides, or amino acids. The properties of these components are poorly characterised.

In this study, the influence of a natural unfractionated groundwater DOC at environmental concentrations on the adsorption of copper, cadmium, and nickel on goethite was investigated in detail. Groundwater, which was sampled from a river water infiltration site in Switzerland, was filtered and degased and used without further treatment. Important points of this work were that unfractionated DOC without preconcentration was used for the experiments and that metal concentrations as well were close to environmental conditions. As experiments were performed in the natural groundwater matrix interactions with other ions, such as calcium, magnesium, or phosphate could also be analysed. Furthermore, the adsorption of other trace metals, such as chromium, lead, and cobalt could be determined simultaneously at their natural concentrations. Experiments were performed with batch laboratory systems, using as a simplification for this rather complex system a synthetic solid phase, a goethite sample which had been well characterised in collaboration with other groups (Ehrhardt, 1999). Models for estimating metal adsorption in the presence of natural organic ligands will be presented, in which interactions with other anions and cations will also be taken into account.

## 5.2 Sampling site and methods

### *Description of Sampling Site*

The field site is located in Glattfelden in the lower Glatt Valley, Switzerland. The river water is a typical calcium carbonate water, about 40% from its discharge originate from lake Greifen, and about 15 % from several sewage treatment plants located upstream of the field site (von Gunten et al., 1991). In the region of Glattfelden, the Glatt is hydraulically connected to shallow groundwater and infiltrates permanently into the top layer of the saturated aquifer (von Gunten and Kull, 1986) at a flow rate of 0.4 – 0.8 m<sup>3</sup>/d per square meter of infiltration area (Hoehn and Santschi, 1987; Hoehn and von Gunten, 1989). The aquifer in the Glatt Valley consists of tightly packed glacio-fluvial outwash deposits of gravel and interbedded layers of sand (von Gunten et al., 1991). Quartz and calcite contribute to more than 60 % of the mineral composition of the aquifer (von Gunten and Kull, 1986).

A scheme of the sampling site is shown in Fig. 5.1. The groundwater flow in the aquifer is indicated with arrows. Three groundwater layers can be distinguished at this site (Hoehn et al., 1983):

- Zone B: freshly infiltrated river water. This water can be found up to a distance of 13 m from the river.
- Zone C: river water infiltrated further upstream
- Zone D: deep groundwater. Due to the stratification of the sediments, only little mixing of infiltrated river water with deep groundwater occurs (von Gunten and Kull, 1986). This water does not show any seasonal variations.

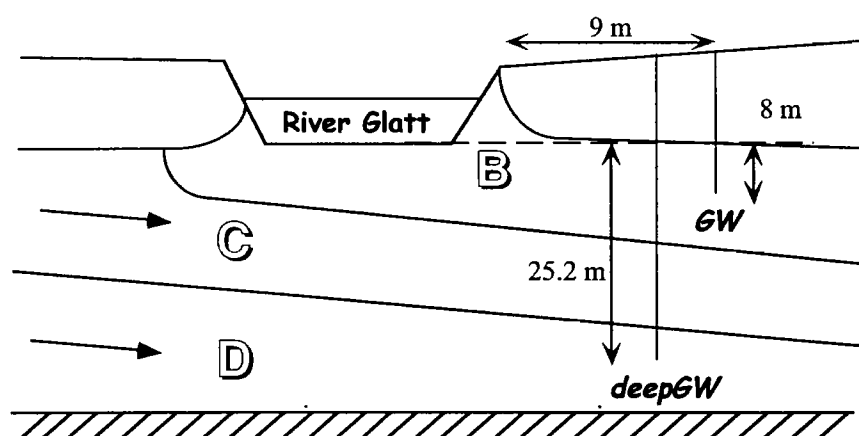


**Fig. 5.1:** Infiltration Site of water from River Glatt in Glattfelden (Switzerland) (adapted from Hoehn et al. (1983))

A network of observation wells was laid over the whole area. They allow sampling at different depths and distances from the river. In this study, groundwater samples were taken in the upper infiltration groundwater (GW) and from the deep groundwater (deepGW). The sites are shown in Fig. 5.1 and characteristics of the corresponding wells are listed in Tab. 5.1.

At this site, the behaviour of contaminants during infiltration of the river water in unconfined groundwater has been extensively studied (Jacobs et al., 1988; Schaffner et al., 1986; Schwarzenbach et al., 1983; Schwarzenbach and Westall, 1981; von Gunten and Kull, 1986).

**Table 5.1: Technical details of the wells (from Hoehn et al. (1983))**

Water	Well	Distance from river [m]	Depth from river [m] <sup>[2]</sup>	Depth of infiltration <sup>(1)</sup>
GW	PZ3	9	8	B
deepGW	Kb1T	-	25.2	D

<sup>[1]</sup> letters defined in Fig. 5.1

<sup>[2]</sup>: from bottom of Glatt

### **Description of Sampling Campaigns**

Samples were collected from the wells PZ3 (GW) and KB1T (deepGW) in February 1999, and from well PZ3 in May 1999 and November 1999. Results of the three sampling campaigns are presented in Table 5.2.

In February, the Glatt had a normal water discharge rate and the concentrations were comparable to previous measurements (Nowack, 1996). Groundwater from the well PZ3 contained much more particulate matter than usually observed. We could not find any explanations for this phenomenon, which had not been observed in previous, nor in following sampling campaigns.

In May 1999, the whole site had been inundated and infiltration groundwater had mixed with deep groundwater. As a consequence, the concentrations of DOC and heavy metals in the infiltration groundwater were lower than expected.

In November 1999, the Glatt had a normal water discharge and concentrations were comparable to previous measurements (Nowack, 1996).

The depth of the groundwater was determined with an electric tape, and water was pumped 50 cm below the surface of the groundwater with a submerged pump (Whale), which was operated at a flow of 1 l/min. Prior to sampling, water was pumped for at least 20 minutes to remove old water from the pipe.

Special precautions were taken to avoid contamination in trace metal sampling. Bottles, syringes, and filters were soaked for at least 3 days in 0.1 M HNO<sub>3</sub> suprapure. Bottles were transported to and from the field site wrapped in two plastic bags. The outer bag was removed immediately after arrival in the laboratory. For taking all samples, plastic gloves were worn. To detect any systematic contamination, blanks were taken on the field. These were nanopure water and were treated in exactly the same manner as the samples. Two replicates of each sample were taken. Values shown in this study represent an average of these measurements.

The samples were taken directly at the outflow of the pump and metal and EDTA samples were filtered on site in precleaned PE-tubes through 0.45 $\mu$ m filters (Acrodisc, Gelman Science).

### ***Analytical Methods***

Samples for total metal analysis were acidified with HNO<sub>3</sub> to a final concentration of 0.01M. Total concentrations of heavy metals were measured with ICP-MS (ELAN 5000), except for iron which was measured with GF-AAS (Perkin Elmer 5100 ZL). Ca and Mg were analysed with ICP-OES (Spectroflame).

Samples for EDTA were stored in dark bottles in order to prevent photolytically induced degradation. EDTA concentrations were determined by HPLC (Nowack et al., 1996 a).

Samples for DOC and major anions (NO<sub>3</sub><sup>-</sup>, SO<sub>4</sub><sup>2-</sup>, Cl<sup>-</sup>, PO<sub>4</sub><sup>3-</sup>) were collected in glassware and filtered in the laboratory (0.45 $\mu$ m cellulose nitrate filters, Sartorius (February and May) or Acrodisc, Gelman Science (November)). DOC measurements were performed on a Shimadzu 500 TOC Analyzer. Nitrate, sulphate, and chloride were measured by ion chromatography (Dionex, column AS11), and phosphate by a colorimetric method with ascorbic acid on a Technicon<sup>®</sup> Auto Analyzer<sup>®</sup> II. Alkalinity was determined by Gran plot titration (Stumm and Morgan, 1996).

Oxygen was determined with an oxygen electrode in the respective well. In February, the water was pumped at a reduced flow rate before measuring the oxygen concentration. In May, the oxygen content was measured directly in the well by descending the sensor. pH (with a WTW pH 323 meter) and conductivity (with a testo<sup>®</sup> 240 conductivity meter) were measured on site. Temperature could be measured with either the pH- or the conductivity meter. The pH meter was calibrated with two buffers of pH 7.00 and 10.01. No corrections were made for the temperature.

**Table 5.2:** Mean dissolved (< 0.45µm) concentrations in the groundwater during the sampling periods of February, May, and November 1999

Parameter	Unit	GW (February)	GW (May)	GW (November)	DeepGW (February)
pH		7.61	7.35	7.18	7.17
Temperature	°C	5.6	15	14.3	10.8
Depth	m	6.4	4.13	5.01	5.27
Conductivity	µS/cm	632	503	637	719
Oxygen	mg/L	4.56	2.28	-	7.21
Total Alkalinity	mM	4.44	4.28	4.9	6.06
Ca	mM	2.3	1.89	2.24	2.9
Mg	mM	0.74	0.6	0.85	1.08
B	M	$1.3 \cdot 10^{-5}$	-	-	$4.6 \cdot 10^{-6}$
Mn	M	$2.9 \cdot 10^{-8}$	$5.5 \cdot 10^{-10}$	$1.69 \cdot 10^{-9}$	$4.9 \cdot 10^{-10}$
Zn	M	$3.9 \cdot 10^{-8}$	$3.2 \cdot 10^{-8}$	$5.5 \cdot 10^{-9}$	$3.8 \cdot 10^{-8}$
Pb	M	$2.6 \cdot 10^{-10}$	$6.7 \cdot 10^{-10}$	$4.8 \cdot 10^{-10}$	$9.6 \cdot 10^{-10}$
Cu	M	$3.8 \cdot 10^{-8}$	$6.1 \cdot 10^{-8}$	$6.07 \cdot 10^{-8}$	$9.4 \cdot 10^{-9}$
Ni	M	$1.4 \cdot 10^{-8}$	$1.9 \cdot 10^{-8}$	$2.3 \cdot 10^{-8}$	$7.2 \cdot 10^{-9}$
Cd	M	$3.6 \cdot 10^{-10}$	$1.8 \cdot 10^{-10}$	$6.5 \cdot 10^{-10}$	$< 9 \cdot 10^{-11}$
Co	M	$1.3 \cdot 10^{-8}$	$1.5 \cdot 10^{-8}$	$8.14 \cdot 10^{-9}$	-
Cr	M	$4.02 \cdot 10^{-8}$	$7.4 \cdot 10^{-8}$	-	-
Fe	M	$3.1 \cdot 10^{-7}$	-	-	$1.64 \cdot 10^{-8}$
Cl	mM	1.14	0.57	1.1	0.68
NO <sub>3</sub>	mM	0.33	0.25	0.45	0.44
PO <sub>4</sub>	M	-	$5.6 \cdot 10^{-6}$	$9.34 \cdot 10^{-6}$	-
SO <sub>4</sub>	mM	0.72	0.57	0.94	0.79
DOC	mg/L	1.9	2.3	1.5	<0.5
EDTA	M	-	-	$6.14 \cdot 10^{-8}$	-

∴ not analysed



## 5.3 Experimental Conditions

### 5.3.1 Chemicals

Metal solutions were prepared from metal stock standards from Baker Analyzed<sup>®</sup> (copper, nickel, cadmium, and magnesium: 1 mg/L Baker Instra-Analyzed<sup>®</sup>, calcium: 10 mg/L Baker Instra-Analyzed<sup>®</sup>). Following chemicals were from Fluka: Biochemika grade: KCl, HEPES (4-(2-hydroxyethyl)-piperazine-1-ethane-sulfonic acid), MES (2-morpholinoethanesulfonic acid monohydrate, and grade Chemika: K<sub>2</sub>SO<sub>4</sub> and K<sub>3</sub>PO<sub>4</sub>). KNO<sub>3</sub>, HCl (30%), and H<sub>2</sub>O<sub>2</sub> (30%) were used from Merck suprapur<sup>®</sup>.

All nitric acid dilutions were prepared from HNO<sub>3</sub>, 65%, Merck suprapur<sup>®</sup>. All NaOH dilutions were prepared from 50% NaOH solutions (Baker Analysed<sup>®</sup>). In such solutions, carbonate precipitates as Na<sub>2</sub>CO<sub>3</sub> and can thus be eliminated by filtration (Öhman and Sjöberg, 1996). The polypropylene bottles and the nanopure water used for the dilution were purged previously to use with argon and nitrogen, respectively. In order to prevent the NaOH solution to come into contact with air, mixing as well as storage was done under argon atmosphere. NaOH solutions were only used for 24 h.

All solutions were prepared with deionized water (18MΩ Q-H<sub>2</sub>O grade Barnstead Nanopure) in bottles soaked for at least 24 hours in 0.1M HNO<sub>3</sub>. For metal, NaOH, and HEPES solutions, polypropylene bottles were used. All other solutions were prepared in glass ware.

### 5.3.2 Pretreatment of groundwater

Groundwater was sampled from the sites described in the previous section. This water was transported within 3 h to the laboratory where it was filtered immediately (0.45μm, Sartorius Cellulose Nitrate filters). Filters were soaked for at least 24 h in 0.1M HNO<sub>3</sub> and rinsed with nanopure water before use. After filtration the groundwater was acidified with HNO<sub>3</sub> to pH 4.3 and degased with nitrogen. It was stored in the dark at 4°C.

There are different reasons to degas. First, it is easier to maintain a constant and well-defined pH in a carbonate-free system. Secondly, carbonate is known to interact electrostatically with oxide surfaces, change their surface charge and thus to have an influence on the adsorption of cations (Balistrieri and Murray, 1982; Sunda

and Hanson, 1979; van Geen et al., 1994). Thirdly, the precipitation of metal carbonates could be hindered (Cowan et al., 1991).

The experiments with natural groundwater were all performed within three weeks. DOC and total metal concentrations were repeatedly measured during this time to make sure that their concentrations remained constant.

### 5.3.3 Treatment of Goethite

Goethite purchased from BASF was treated as described in Chapter 3. It was stored in suspensions of 20 g/L in polyethylene bottles. Because acid-base equilibria on solid surfaces are slowly established, suspensions were equilibrated at least 24 h at the pH values of the following experiments (pH 3.5, acidified with HNO<sub>3</sub>, and 7.35, pH adjusted with NaOH). Before use, goethite suspensions were thoroughly shaken. Pipetting of goethite into the bottles used for the experiments was done with an error smaller than 4 %.

### 5.3.4 General Experimental Setup

Experiments were performed at 25 °C as batch systems in 100 mL polypropylene beakers (Semadeni Art. Nr. 2064), soaked for at least 24 hours in 0.1 M HNO<sub>3</sub> and rinsed before use with nanopure water.

pH between 5.2 and 7.2 was buffered with MES (concentration 5·10<sup>-3</sup> M) and between pH 7.2 and 7.8 with HEPES (concentration 5·10<sup>-3</sup> M). Below pH 5.2 and above pH 7.8, no buffers were used and the pH was adjusted by adding HNO<sub>3</sub> or NaOH.

To remove CO<sub>2</sub>, all samples were purged with nitrogen before the adsorption reaction for at least 30 min and whenever the bottles were opened. All solutions used were either purged with nitrogen, or prepared CO<sub>2</sub>-free (see section 5.3.1).

Because of possible photoreduction of goethite by organic ligands, experiments were carried out under red light ( $\lambda > 560$  nm) (Siffert and Sulzberger, 1991; Xyla et al., 1992).

Because the order of addition of the different components may show that kinetic effects are important, different systems were investigated (Fig. 5.2). Metal stands for copper, cadmium, or nickel. Adsorption edges were measured between pH 3 and 9. The goal of these experiments was to analyse the pH dependence of the metal adsorption. In order to get more experimental points at one pH value,

adsorption isotherms were recorded at pH 3.5 and pH 7.35. pH 3.5 was chosen as this pH is easy to adjust without buffers and thus it is possible to avoid interferences. pH 7.35 was the natural infiltration groundwater pH in May 1999 (Tab. 5.2).

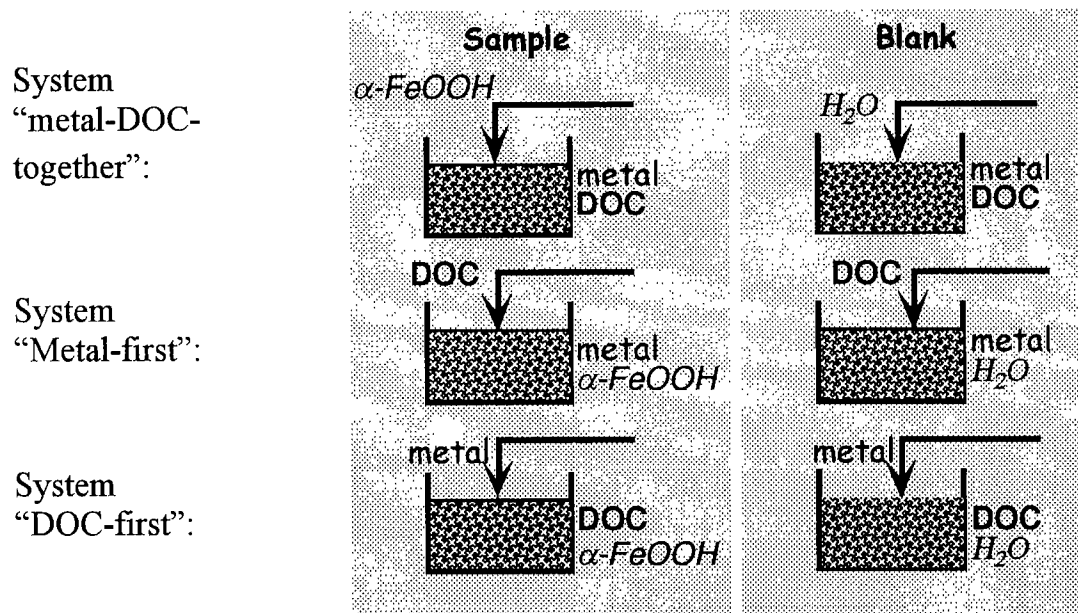


*Fig. 5.2: Several systems were analysed in order to investigate the effect of the order of addition of the different components. For every second sample, a blank, without goethite, was analysed in order to consider metal losses on beaker walls and contamination problems. Blanks were treated in exactly the same manner as the samples.*

### **System "metal-DOC-together"**

The groundwater was first equilibrated with the metals (cadmium, copper, or nickel) at the desired pH value. The ionic strength was adjusted to 0.01 M with  $\text{KNO}_3$ . Afterwards goethite was added and the samples were equilibrated in the dark on a side-to-side shaker. Concentrations and equilibration times are listed in Tab. 5.3 - 5.6.

### **System "metal-first"**

Goethite, metal, and buffer (concentrations in Tab. 5.3 - 5.5) were allowed to equilibrate. Afterwards 50 mL groundwater and the electrolyte,  $\text{KNO}_3$ , were added. The pH was verified and the samples could equilibrate again. Equilibration times are listed in Tab. 5.6.

### ***System "DOC-first"***

50 mL groundwater, goethite and electrolyte, KNO<sub>3</sub>, were allowed to equilibrate at the desired pH value before the addition of the metals. Then the metals were added to concentrations listed in Tab. 5.3 – 5.5 and the samples were allowed to equilibrate again. Equilibration times are reported in Tab. 5.6.

The system "metal-DOC-together" was analysed as well in acidic conditions as at pH-values above 7, whereas the systems "metal-first" and "DOC-first" were only analysed at pH 7.35 and pH 3.5, respectively.

These experiments were all carried out in the natural groundwater. This water includes besides the concentrations of the major anions and cations also trace concentrations of heavy metals, like chromium, cobalt, or lead (Tab. 5.2). The adsorption of these metals at their natural concentrations, i.e., without any further addition, in a natural groundwater matrix could be determined in the "Ni-DOC-together", "Cu-DOC-together"; and "Cd-DOC-together" systems by using ICP-MS for the simultaneous measurement of several metals (see section 5.12).

After the final equilibration step, pH was measured again under nitrogen atmosphere. This value was used for the data evaluation. Afterwards samples were filtered (0.45µm, Acrodisc Gelman Science) and acidified to 0.01 M HNO<sub>3</sub>.

**Table 5.3: Parameters for Copper Experiments**

<b>Systems</b>	<b>"Cu-DOC-together"</b>	<b>"Cu-first"</b>	<b>"DOC-first"</b>
<b>pH</b>	<b>3.5 ± 0.05</b>		<b>3.5 ± 0.05</b>
Cu [M]	6·10 <sup>-8</sup> – 3·10 <sup>-7</sup>		6·10 <sup>-8</sup> – 3·10 <sup>-7</sup>
I [M]	0.01		0.01
goethite conc. [g/L]	0.1		0.1
<b>pH</b>	<b>7.35 ± 0.05</b>	<b>7.35 ± 0.05</b>	
Cu [M]	8·10 <sup>-8</sup> – 3·10 <sup>-7</sup>	8·10 <sup>-8</sup> – 3·10 <sup>-7</sup>	
I [M]	0.01	0.01	
goethite conc. [g/L]	0.1	0.1	
<b>pH</b>	<b>3-9</b>	<b>3-9</b>	<b>3-9</b>
Cu [M]	3.03·10 <sup>-7</sup>	3.03·10 <sup>-7</sup>	3.03·10 <sup>-7</sup>
I [M]	0.01	0.01	0.01
goethite conc. [g/L]	0.5	0.5	0.5

**Table 5.4: Parameters for Cadmium Experiments**

Systems	“Cd-DOC-together”	“Cd-first”	“DOC-first”
<i>pH</i>	$7.35 \pm 0.05$	$7.35 \pm 0.05$	
Cd [M]	$8.8 \cdot 10^{-10} - 7 \cdot 10^{-9}$	$8.8 \cdot 10^{-10} - 7 \cdot 10^{-9}$	
I [M]	0.01	0.01	
goethite conc. [g/L]	0.1	0.1	
<i>pH</i>	$2.4 - 8.2$	$2.4 - 8.2$	$2.4 - 8.2$
Cd [M]	$1.3 \cdot 10^{-9}$	$1.3 \cdot 10^{-9}$	$1.3 \cdot 10^{-9}$
I [M]	0.01	0.01	0.01
goethite conc. [g/L]	0.1	0.1	0.1

**Table 5.5: Parameters for Nickel Experiments**

Systems	“Ni-DOC-together”	“Ni-first”	“DOC-first”
<i>pH</i>	$3.5 \pm 0.05$		$3.5 \pm 0.05$
Ni [M]	$5.7 \cdot 10^{-8} - 2 \cdot 10^{-7}$		$5.7 \cdot 10^{-8} - 2 \cdot 10^{-7}$
I [M]	0.01		0.01
goethite conc. [g/L]	0.1		0.1
<i>pH</i>	$7.35 \pm 0.05$	$7.35 \pm 0.05$	
Ni [M]	$5.5 \cdot 10^{-8} - 2 \cdot 10^{-7}$	$5.5 \cdot 10^{-8} - 2 \cdot 10^{-7}$	
I [M]	0.01	0.01	
goethite conc. [g/L]	0.1	0.1	
<i>pH</i>	$2.8 - 8.2$	$2.8 - 8.2$	$2.8 - 8.2$
Ni [M]	$2.8 \cdot 10^{-7}$	$2.8 \cdot 10^{-7}$	$2.8 \cdot 10^{-7}$
I [M]	0.01	0.01	0.01
goethite conc. [g/L]	0.5	0.5	0.5

**Table 5.6:** *Equilibration in the different systems. Metal stands for copper, cadmium, or nickel.*

<b>System “metal-DOC together”</b>	
Equilibration time metal-DOC	0.5 hours
Adsorption on goethite	4 hours
<b>System “metal-first”</b>	
Adsorption time of metal on goethite	2 hours
Equilibration time with DOC	4 hours
<b>System “DOC-first”</b>	
Adsorption time of DOC on goethite	2 hours
Equilibration time with metal	4 hours

### ***Additional precautions to be taken when working with low metal concentrations***

In order not to saturate the complexation capacities of the ligands by addition of metals, experiments were done at low metal concentrations. Hence, contamination problems and metal losses on beaker walls had to be considered. Blanks were analysed for every second sample. These were samples without goethite, to which an equivalent volume of nanopure water was added instead of goethite. They were treated in exactly the same manner as the corresponding samples. A control of the initial metal concentration in the samples was achieved by measurements of the total metal concentration in the blanks. In the absence of contamination and metal losses on beaker walls, these concentrations should equal the calculated initial concentration of the corresponding sample. If these two concentrations differed by more than 10% further investigations were necessary, or the sample was rejected. Furtheron, blanks of the bottles, goethite suspensions, and the filters had been analysed. The former two did not present any problems, whereas blanks of the filters were determined to contain about  $1 \cdot 10^{-8}$  M copper and  $5.65 \cdot 10^{-9}$  M nickel. Cadmium was below the detection limit.

### ***Reference Samples***

In order to see the effect of the organic ligands on the adsorption of metals on goethite, references were measured. References are samples without DOC, and three types of them were analysed:

- **Simple ionic medium**  
The ionic strength was adjusted to 0.01 M with KNO<sub>3</sub>.
- **Irradiated groundwater**  
H<sub>2</sub>O<sub>2</sub> was added to a concentration of 0.05 M to filtered groundwater. The water was filled into quartz tubes and irradiated with a Hg-lamp during 18 hours. UV-oxidation with H<sub>2</sub>O<sub>2</sub> is a powerful method to oxidize DOC in natural waters (Pisch et al., 1993). After this treatment, no DOC could be detected (Detection limit: 0.5 mg/L).
- **Synthetic groundwater**  
A synthetic groundwater was made up with nanopure water containing the major anions (Cl<sup>-</sup>, SO<sub>4</sub><sup>2-</sup>, PO<sub>4</sub><sup>3-</sup>) and cations (Ca<sup>2+</sup>, Mg<sup>2+</sup>) (Tab. 5.7). The ionic strength was adjusted with KNO<sub>3</sub> to 0.01 M. Depending on the experiments, either sulphate or phosphate were added to the synthetic groundwater.

**Table 5.7: Concentrations of cations and anions in synthetic groundwater**

<b>Parameters</b>	<b>with Sulphate<sup>[1]</sup></b>	<b>with Phosphate<sup>[1]</sup></b>
Ca <sup>2+</sup> [M]	1.89·10 <sup>-3</sup>	1.89·10 <sup>-3</sup>
Mg <sup>2+</sup> [M]	6·10 <sup>-4</sup>	6·10 <sup>-4</sup>
Cl <sup>-</sup> [M]	5.6·10 <sup>-4</sup>	5.6·10 <sup>-4</sup>
SO <sub>4</sub> <sup>2-</sup> [M]	1.9·10 <sup>-4</sup>	-
H <sub>x</sub> PO <sub>4</sub> <sup>x-3</sup> [M]	-	9.3·10 <sup>-6</sup>

<sup>[1]</sup>: ions are counterbalanced by addition of KNO<sub>3</sub> in order to get a total ionic strength of 0.01 M

### 5.3.5 Analytical Methods

#### **Total Metal Concentration Measurements**

Within one week, the samples were analysed with ICP-MS (ELAN 5000). Rh was used as internal standard. The isotopes measured were <sup>65</sup>Cu, <sup>60</sup>Ni, <sup>112</sup>Cd, <sup>53</sup>Cr, <sup>208</sup>Pb, and <sup>59</sup>Co. Analytical methods were checked with standard addition in the groundwater ionic medium and with external standards (Certified Reference Material SLRS-3, riverine water, National Research Council Canada, Institute for Environmental Chemistry, Ottawa, Canada). Detection limit (3·σ) and quantification limit (10·σ) are listed in Table 5.8.

**Table 5.8:** *Detection and quantification limits for measurements with ICP-MS*

Element	Detection limit [M]	Quantification limit [M]
<sup>65</sup> Cu	$3.15 \cdot 10^{-10}$	$1.1 \cdot 10^{-9}$
<sup>60</sup> Ni	$3.14 \cdot 10^{-10}$	$9.54 \cdot 10^{-10}$
<sup>114</sup> Cd	$8.89 \cdot 10^{-11}$	$1.78 \cdot 10^{-10}$
<sup>53</sup> Cr	$2.7 \cdot 10^{-9}$	$8.85 \cdot 10^{-9}$
<sup>208</sup> Pb	$9.1 \cdot 10^{-12}$	$9.65 \cdot 10^{-11}$
<sup>59</sup> Co	$1.7 \cdot 10^{-10}$	$5.09 \cdot 10^{-10}$

The amount of metal sorbed was calculated from the difference between the initial concentration, i.e., the concentration measured in the blank, and the measured concentration in the filtrate after the adsorption reaction.

### ***Metal Complexation in Solution***

In order to estimate metal complexation constants with the natural ligands, metal titration curves of groundwater were analysed. These experiments were carried out with a ligand exchange DPCSV method (differential pulse cathodic stripping voltammetry) for copper and nickel, and a ligand exchange DPASV method (differential pulse anodic stripping voltammetry) for cadmium. The methods have been described in detail by Xue et al. (1996) (copper), Xue and Sunda (1997) (copper and cadmium) and by Jansen (1998) and Prasch (1999) (nickel). The total metal concentration ranges analysed by the voltammetric methods were for copper:  $6 \cdot 10^{-8}$  M to  $1 \cdot 10^{-7}$  M, for cadmium:  $1.78 \cdot 10^{-10}$  M to  $9.12 \cdot 10^{-9}$  M, and for nickel:  $1.5 \cdot 10^{-8}$  to  $5 \cdot 10^{-8}$  M.

Copper complexation measurements were performed additionally with a copper ion selective electrode (Cu-ISE) in the concentration range  $8 \cdot 10^{-8}$  M to  $8 \cdot 10^{-6}$  M. A detailed description of the method has been given by Hari (1998).

## **5.4 Modelling description**

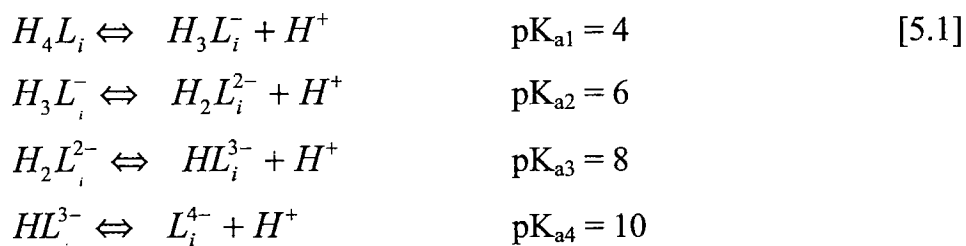
### **5.4.1 Metal Complexation by Infiltration Groundwater Organic Ligands**

Although it is widely recognised by now that complexation properties of natural ligands are best described by a continuous distribution of complexation



constants, we decided to use a discrete model that is easier to combine with the adsorption model.

In order to minimise the degrees of freedom and to keep the model as simple as possible, parameters were estimated with a minimum number of metal ligands. For each of these ligands, four  $pK_a$  values were fixed (Eq. 5.1):



Carboxylic acids are represented by  $pK_a$  4 and 6, amino acids by  $pK_a$  8 and phenolic groups by  $pK_a$  10. A  $\Delta pK_a$  of 2 is a good compromise between good convergence when a small  $\Delta pK_a$  is chosen and a systematic set of parameters if a large  $\Delta pK_a$  is used (Westall et al., 1995).

Parameter estimation was performed with the programme FitEQL (Herbelin and Westall, 1994). The relative error of the total metal concentration was fixed to 10 % and the absolute error of total metal concentration was defined to be 10 % of the initial total metal concentration, i.e., for copper:  $5 \cdot 10^{-9}$  M, for cadmium:  $2.8 \cdot 10^{-10}$  M, and for nickel:  $5 \cdot 10^{-9}$  M. The goodness of fit was mainly checked by the WSOS/DF factor (weighted sum of squares divided by the degrees of freedom. For more information see chapter 2 and the description from Herbelin and Westall (1994)).

Complexation of copper, cadmium, and nickel was described with the lowest necessary number of ligands in the respective titration range.

#### 5.4.2 Metal Adsorption on Goethite in the Presence of Groundwater Organic Ligands

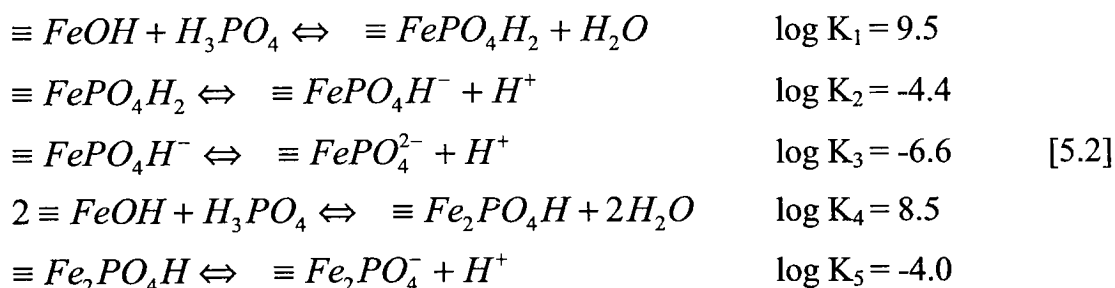
By combining the surface complexation model for the metals in the absence of ligands with the complexation model of the metals by organic ligands as defined in the previous paragraph, metal adsorption on goethite in the presence of the natural organic ligands could be calculated. Constants used for these calculations were determined independently. Parameter estimation for metal adsorption on goethite was described in chapter 2. Calculations were performed with the speciation programme ChemEQL (Müller, 1996). The constants used for modelling are listed in Tab. 5.9.

**Table 5.9:** Constants used to calculate metal adsorption on goethite in the presence of groundwater organic ligands (Footnote page 111).

<b>pK<sub>a</sub> ligand/surface</b>		<b>Copper</b>		<b>Cadmium</b>		<b>Nickel</b>	
<b>metal hydroxo complexes</b>		Cu(OH) <sup>+</sup>	6.1 <sup>[1]</sup>	CdOH <sup>+</sup>	3.8 <sup>[1]</sup>	NiOH <sup>+</sup>	4.0 <sup>[1]</sup>
		Cu(OH) <sub>2</sub>	11.6 <sup>[1]</sup>	Cd(OH) <sub>2</sub>	7.5 <sup>[1]</sup>	Ni(OH) <sub>2</sub>	7.8 <sup>[1]</sup>
		Cu(OH) <sub>3</sub> <sup>-</sup>	14.5 <sup>[1]</sup>	Cd(OH) <sub>3</sub> <sup>-</sup>	10.2 <sup>[1]</sup>	Ni(OH) <sub>3</sub> <sup>-</sup>	11.0 <sup>[1]</sup>
		Cu(OH) <sub>4</sub> <sup>2-</sup>	16.4 <sup>[1]</sup>				
<b>infiltration groundwater ligands</b>	H <sub>4</sub> L <sub>x</sub> <sup>[2]</sup>	4		CuL <sub>1</sub> <sup>2-</sup>	16.3 <sup>[3]</sup>		
	H <sub>3</sub> L <sub>x</sub> <sup>-[2]</sup>	6		CuL <sub>2</sub> <sup>2-</sup>	14.6 <sup>[3]</sup>		
	H <sub>4</sub> L <sub>x</sub> <sup>2-[2]</sup>	8		CuL <sub>3</sub> <sup>2-</sup>	11.0 <sup>[3]</sup>		
	HL <sub>x</sub> <sup>3-[2]</sup>	10				NiL <sub>1</sub> <sup>2-</sup>	17.4 <sup>[3]</sup>
<b>deep groundwater ligands</b>	H <sub>4</sub> L <sub>x</sub> <sup>[2]</sup>	4		CuL <sub>1</sub> <sup>2-</sup>	15.7 <sup>[3]</sup>		
	H <sub>3</sub> L <sub>x</sub> <sup>-[2]</sup>	6		CuL <sub>2</sub> <sup>2-</sup>	14.5 <sup>[3]</sup>		
	H <sub>4</sub> L <sub>x</sub> <sup>2-[2]</sup>	8		CuL <sub>3</sub> <sup>2-</sup>	8.7 <sup>[3]</sup>		
	HL <sub>x</sub> <sup>3-[2]</sup>	10					
<b>Goethite</b>	≡Fe-O-H <sub>2</sub> <sup>+</sup>	7.9 <sup>[4]</sup>		≡Fe-O-Cu <sup>+</sup>	2.93 <sup>[4]</sup>	≡Fe-O-Cd <sup>+</sup>	-0.18 <sup>[4]</sup>
	≡Fe-OH	10.5 <sup>[4]</sup>				≡Fe-O-Ni <sup>+</sup>	0.46 <sup>[4]</sup>
<b>Phosphate</b>	H <sub>3</sub> PO <sub>4</sub>	2.104 <sup>[1]</sup>		CuHPO <sub>4</sub>	15.85 <sup>[1]</sup>		
	H <sub>2</sub> PO <sub>4</sub> <sup>-</sup>	7.07 <sup>[1]</sup>		CuH <sub>2</sub> PO <sub>4</sub> <sup>+</sup>	20.89 <sup>[1]</sup>		
	HPO <sub>3</sub> <sup>2-</sup>	12.13 <sup>[1]</sup>				NiHPO <sub>4</sub> <sup>[1]</sup>	21.67

### 5.4.3 Influence of Phosphate on Metal Adsorption on Goethite

Phosphate has been assumed to adsorb innerspherically (Ding et al., 2000; Hawke et al., 1989; Nilsson, 1995; Parfitt and Atkinson, 1976; Parfitt et al., 1977; Sigg, 1979; Tejedor-Tejedor and Anderson, 1990), and may thus lower the surface charge and have an influence on metal adsorption (see section 1.5). Phosphate adsorbs over a wide pH range (Fig. 5.3), and the main phosphate species on the surface are  $\equiv\text{Fe-PO}_4\text{H}^-$  at  $\text{pH} < 4$ , and  $\equiv\text{Fe-PO}_4^{2-}$  at pH values above 4. Following adsorption reactions were considered for the calculations (Sigg, 1979):



Influence of phosphate on metal adsorption was estimated by combining the DLM metal adsorption model with the complexation of the metal by the organic ligands and phosphate (Tab. 5.9) and by including phosphate adsorption (reaction [5.2]). Calculations were performed with the speciation programme ChemEQL (Müller, 1996).

[1]: association constants as defined in Smith and Martell (1976, 1977, and 1982), corrected with Davies equation ( $b = 0.2$ ) (Stumm and Morgan, 1996) for  $I = 0.01$  M. The components to describe the equations are  $\text{Cu}^{2+}$ ,  $\text{Ni}^{2+}$ ,  $\text{PO}_4^{3-}$ , and  $\text{H}^+$ , except for the formation of the metal hydroxo complexes, where the components are the free metal cation and  $\text{OH}^-$ .

[2]:  $x = 1, 2$ , or  $3$ , according to the number of ligands needed to describe metal complexation.

[3]: defined in this study. Details are given in this chapter.

[4]: defined in this study. Details are given in chapter 2.

[5]: from Mesuere and Fish (1992a); Robertson (1998).

[6]: no parameter estimation was performed for these systems.

[7]: no data found

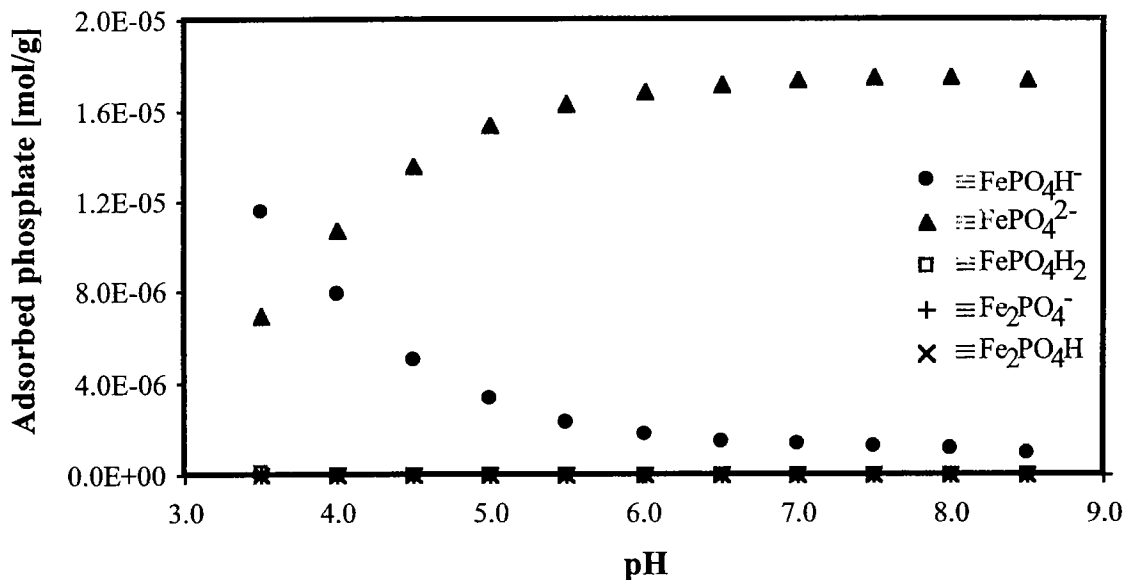
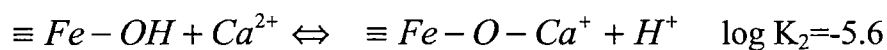
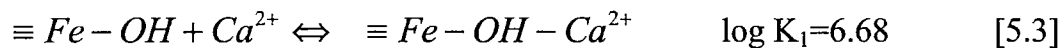


*Fig. 5.3: Phosphate adsorption on goethite. Modelling was performed by using the surface complexation model with the DLM for electrostatic interactions. The reactions [5.2] were used for calculations. (Assumed concentrations:  $[H_xPO_4^{x-3}] = 9.34 \cdot 10^{-6}$ ,  $[goethite] = 0.1$  g/L)*

#### 5.4.4 Influence of Calcium and Magnesium on Metal Adsorption on Goethite

As concentrations of calcium and magnesium were several orders of magnitude higher than the concentration of copper, competition reactions for surface sites could be expected (see section 1.5). Model calculations, where the adsorption of calcium on goethite was considered, were performed. Following reactions were used to describe calcium adsorption on goethite (Dzombak and Morel, 1990) (they have been defined for a double layer model for amorphous iron oxide):



By adding these reactions to those of Tab. 5.9, metal pH adsorption edges were estimated in the presence of calcium. Calculations were performed with the speciation programme ChemEQL (Müller, 1996).

## 5.5 Influence of a Groundwater Matrix on the Adsorption of Copper on Goethite

### 5.5.1 pH Adsorption Edge of Copper on Goethite in an Infiltration Groundwater Matrix

The pH dependence of the adsorption of copper on goethite in the presence of natural organic ligands was measured in the three systems defined in Fig. 5.2. As reference, without DOC, copper adsorption was measured in 0.01 M KNO<sub>3</sub>.

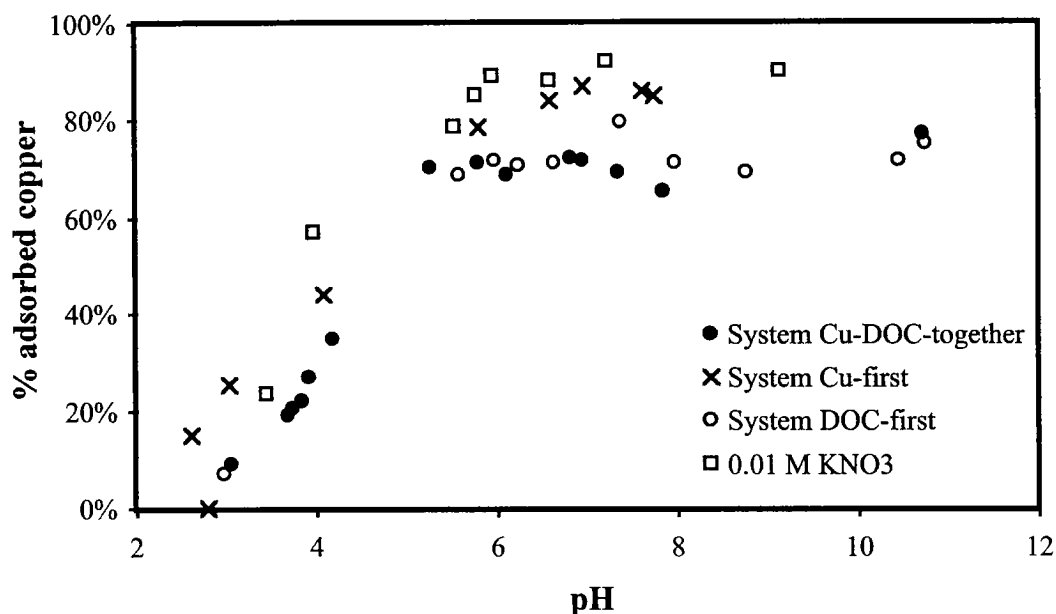


*Fig. 5.4: pH adsorption edge of copper on goethite in the presence of infiltration groundwater organic ligands measured in 3 different systems. (Sampling Campaign February 1999). ( $[Cu]_{tot} = 3.03 \cdot 10^{-7} M$ ).*

Clearly less copper was adsorbed at pH-values above 6 in the systems “Cu-DOC-together” and “DOC-first” than in the reference system without DOC (Fig. 5.4). This could be explained by competition reactions between complexation in solution and adsorption on the surface. Specific ligands in solution complexed copper strongly enough to mobilise it. In the system “Cu-first”, apparently more copper was adsorbed than in the two other systems, which could be explained by kinetic effects. In these experiments, copper was adsorbed on the surface prior to addition of DOC, i.e., in the absence of competition reactions. Desorption kinetics of copper are slow and the ligands, added after 2 hours, were not capable to completely remobilise the copper within the equilibration time of 4 hours. Competition reactions between the

surface and the solution ligands could be studied in more detail with the adsorption isotherm at pH 7.35. (see section 5.5.3).

### **5.5.2 Adsorption of Copper on Goethite in an Infiltration Groundwater Matrix at pH 3.5**

In the absence of organic ligands, copper is supposed not to adsorb at pH 3.5. This was confirmed by recording an adsorption isotherm in 0.01 M KNO<sub>3</sub>. In the presence of the infiltration groundwater organic ligands, however, a clear adsorption can be observed (Fig. 5.5).

In reference experiments performed with UV-irradiated groundwater, i.e., without DOC, the adsorption was comparable to that in presence of organic ligands. This means that organic ligands were not responsible for the enhanced adsorption in our system. Interferences with inorganic ligands of the groundwater matrix like sulphate or phosphate were postulated. Experiments with a synthetic groundwater made up of the major cations (calcium and magnesium), chloride, and sulphate (Tab. 5.7) showed only a weak adsorption (Fig. 5.6). Adsorption of sulphate could not be measured at our conditions. However, synthetic groundwater made up of the major cations, chloride, and phosphate showed an adsorption behaviour similar to that of irradiated groundwater (Fig. 5.6).

The adsorption curves shown in Fig. 5.5 were measured with a groundwater sampled in May 1999, experimental data reported in Fig 5.6 were performed with a groundwater sampled in November 1999. Contrary to what would be expected, a higher adsorption could be observed in the water sampled in May when phosphate concentrations (0.57 mM) were lower than in November (0.94 mM). However, additional interference reactions are likely in such a complex system. Specific organic ligands could possibly complex the metal in solution and thus have a negative effect on the adsorption. Another possibility could be competition reactions of copper with calcium. Indeed calcium concentrations were about 25% higher in November (2.2 mM) than in May (1.9 mM).

The slight shift of the isotherms to the right could be explained by blank problems during filtration as explained in section 5.3.4.

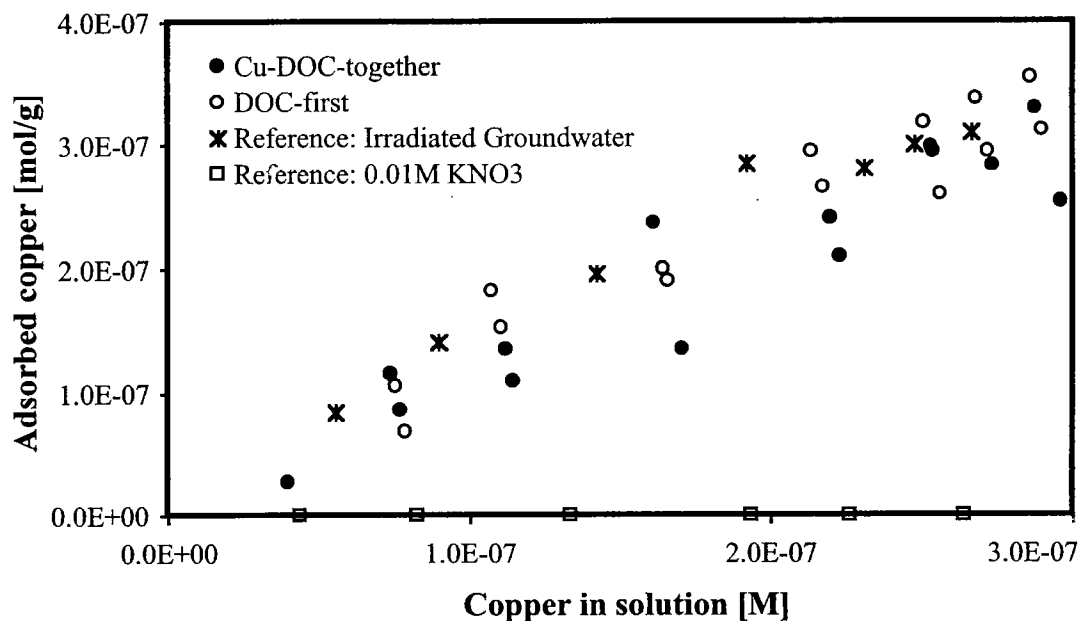


*Fig. 5.5: Copper adsorption isotherm at pH 3.5 in the presence of infiltration groundwater organic ligands. (sampling campaign May 1999). ( $[Cu]_{tot} = 6 \cdot 10^{-8} M - 3 \cdot 10^{-7} M$ ).*

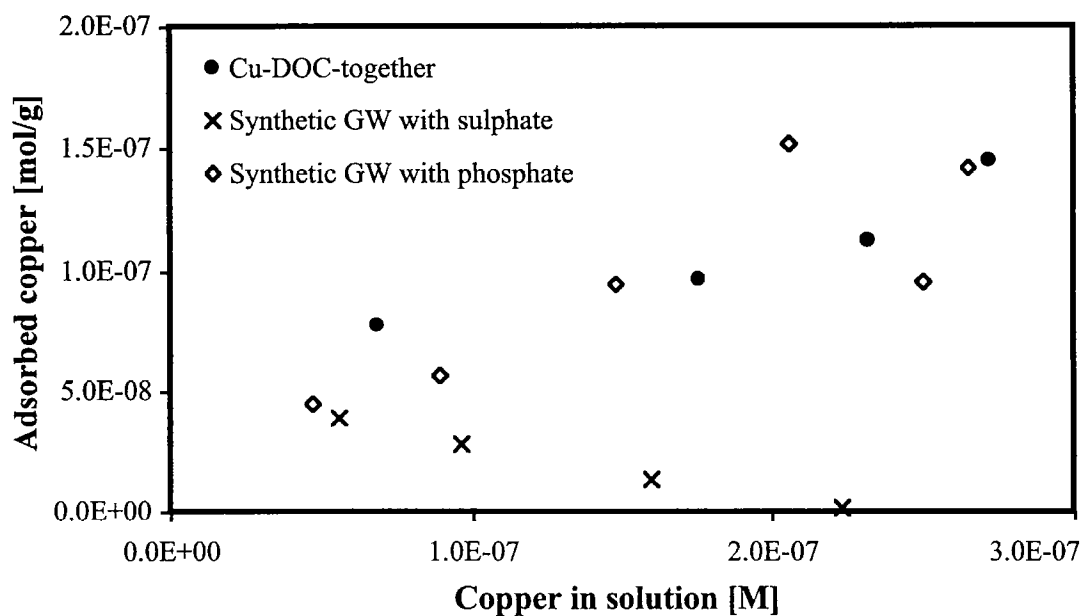


*Fig. 5.6: Influence of sulphate and phosphate on the adsorption of copper at pH 3.5. Sulphate and phosphate concentrations in the synthetic groundwaters were the same as in the natural groundwater ( $[H_xPO_4^{x-3}] = 9.34 \cdot 10^{-6} M$  and  $[SO_4^{2-}] = 1.9 \cdot 10^{-4} M$ ). (Sampling campaign November 1999). ( $[Cu]_{tot} = 6 \cdot 10^{-8} M - 3 \cdot 10^{-7} M$ ).*

### 5.5.3 Adsorption of Copper on Goethite in an Infiltration Groundwater Matrix at pH 7.35

pH 7.35 was the pH of the natural groundwater in May 1999 (Tab. 5.2). Adsorption experiments were conducted with two reference samples, an irradiated natural groundwater and a synthetic groundwater with sulphate (Tab. 5.7), and in the systems “Cu-DOC-together” and “Cu-first” (Fig. 5.7).

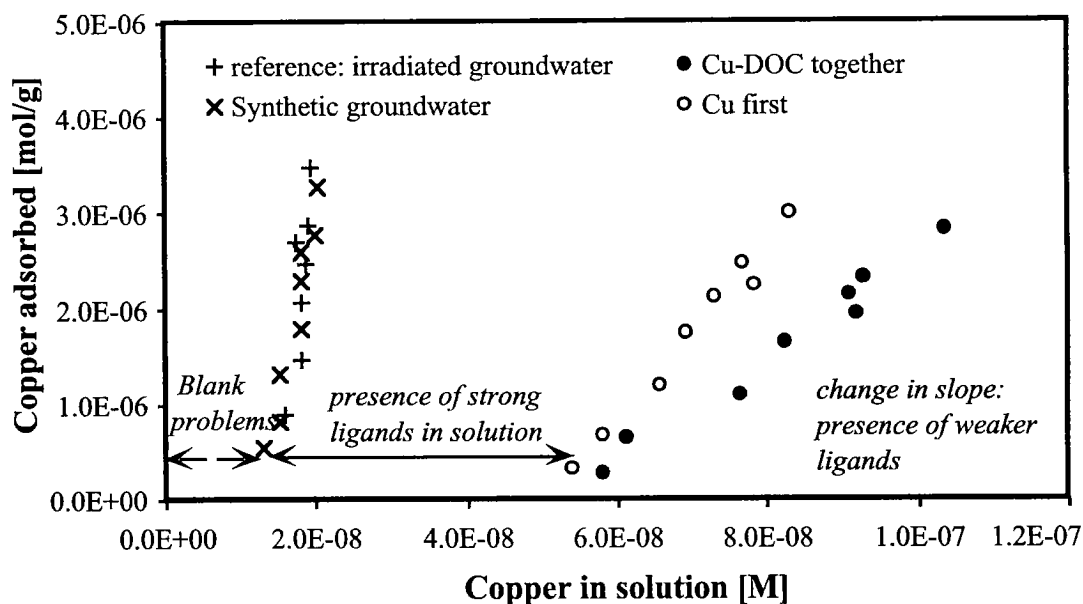


*Fig. 5.7: Copper adsorption isotherms on goethite at pH 7.35 in the presence of infiltration groundwater natural organic ligands (sampling campaign May 1999).  $[Cu_{tot}] = 6 \cdot 10^{-8} - 3 \cdot 10^{-7} M$ .*

Clearly less copper was adsorbed in the presence of organic ligands than in the reference systems, which is comparable with the results shown in Fig. 5.4. Most striking was the fact that the adsorption isotherms in the presence of organic ligands cut the x-axis at a value of about  $5.5 \cdot 10^{-8} M$  and not at the origin as would be expected for a “normal” adsorption isotherm. This shift could be explained by the presence of specific ligands in solution which formed very strong complexes with copper. Such complexation reactions, which completely hinder adsorption reactions, can only be due to chelating ligands. Once these ligands were saturated, copper adsorption on goethite increased linearly with the concentration of copper in solution. Copper concentration was too low to saturate the surface (concentration of surface groups:  $8.2 \cdot 10^{-5} mol/g$ ). Competition reactions between less specific complexants in solution and the surface groups lowered the adsorption of copper as



well. This could be deduced from the smaller slope of the adsorption isotherm in the presence of organic ligands compared to the slope of the reference system.

A small difference could be observed between the adsorption isotherms in the systems “Cu-first” and “Cu-DOC-together”. This phenomenon probably was due to kinetic effects and is discussed in section 5.5.1.

The slight shift to the right of the reference isotherms could be explained by blank problems during filtration (see section 5.3.4).

### 5.5.4 Adsorption of Copper on Goethite in a Deep Groundwater Matrix at pH 7.6

The adsorption isotherm of copper in the presence of deep groundwater organic ligands is shown in Fig. 5.8. pH 7.6 was the natural pH of the deep groundwater (Tab. 5.2).

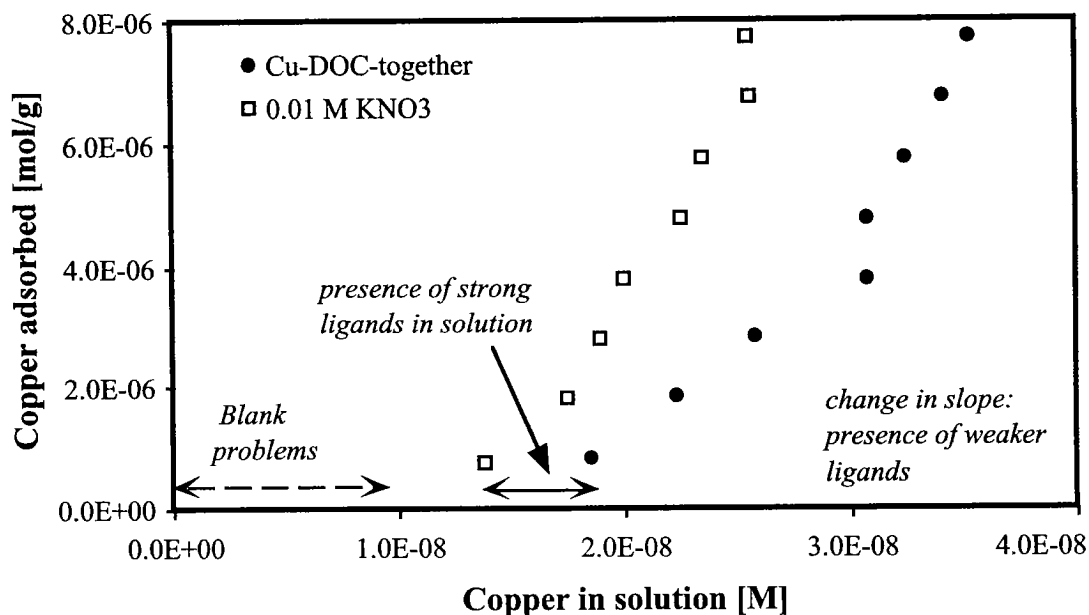


**Fig. 5.8:** Adsorption isotherm of copper on goethite at pH 7.6 in the presence of deep groundwater organic ligands. ( $[Cu]_{tot} = 9 \cdot 10^{-8} - 8 \cdot 10^{-7} M$ ).

The isotherm of the reference system did not cut the origin, possibly because of blank problems due to filtration (see section 5.3.4). The adsorption isotherm of the “Cu-DOC-together” system cuts the x-axis at a higher value than the reference system. The difference between these two intersections probably represented the concentration of strong complexing ligands. In addition further ligands seemed to be

present, since the slope of the adsorption isotherm in the presence of organic ligands was slightly lower than that in the reference system.

## 5.6 Modelling of Copper Experiments

### 5.6.1 Adsorption of Copper in the Presence of Infiltration Groundwater Organic Ligands

#### *Copper Complexation by Infiltration Groundwater Organic Ligands*

A titration curve of the ligands with copper is shown in Fig. 5.9. Measurements were performed with two analytical methods: an ion selective electrode and a voltammetric method (section 5.3.5).

In the total copper concentration range of  $8 \cdot 10^{-8}$  M to  $1.2 \cdot 10^{-7}$  M total copper, free copper concentrations measured with the electrode were higher than those measured with the voltammetric method. It is advisable to use ion selective electrodes only in solutions containing total copper concentrations higher than  $1 \cdot 10^{-7}$  M (Avdeef et al., 1983; Gulens, 1987). Otherwise interference problems with other cations, like  $Zn^{2+}$ , are likely to occur and thus the free copper concentration may be overestimated. As a consequence, the voltammetric method seemed the most reliable to us in the low copper concentration range ( $< 1.8 \cdot 10^{-7}$  M), although this method is known to rather underestimate free metal concentrations (Xue and Sunda, 1997). For total copper concentrations below  $1.8 \cdot 10^{-7}$  M, only polarographic measurements were considered for parameter estimation (black triangles in Fig. 5.9). For total copper concentrations higher than  $1.8 \cdot 10^{-7}$  M, measurements performed with the Cu-ISE were used for parameter estimation (black circles in Fig. 5.9). Analyses performed with DPCSV at concentrations higher than  $1.8 \cdot 10^{-7}$  M were not considered for modelling (open triangles in Fig. 5.9), because the added ligand, catechol, was almost saturated and according to our experience, measurements seemed less reliable than those done with the Cu-ISE in this range.

For copper, three ligands had to be defined for parameter estimation of the complexation constants (model description in section 5.4.1). Ligand concentrations and complexation constants had to be calculated separately. First, the concentration of the strong ligand was fixed at a value of  $5.5 \cdot 10^{-8}$  M, which is the intercept of the isotherm with the x-axis (Fig. 5.7). First estimations for the complexation constants

with reasonable values from literature were made. The concentrations of the ligands  $L_2$  and  $L_3$  were optimised over the WSOS/DF factor. The best estimation was  $L_2 = 1.03 \cdot 10^{-7}$  M and  $L_3 = 2.22 \cdot 10^{-6}$  M (WSOS/DF = 2.68).

Once these two concentrations were known, optimisation over the concentration of the strong ligand  $L_1$  was performed. No convergence could be achieved with ligand concentrations below  $4 \cdot 10^{-8}$  M, and the model was best at a concentration of  $7 \cdot 10^{-8}$  M (WSOS/DF = 2.47).

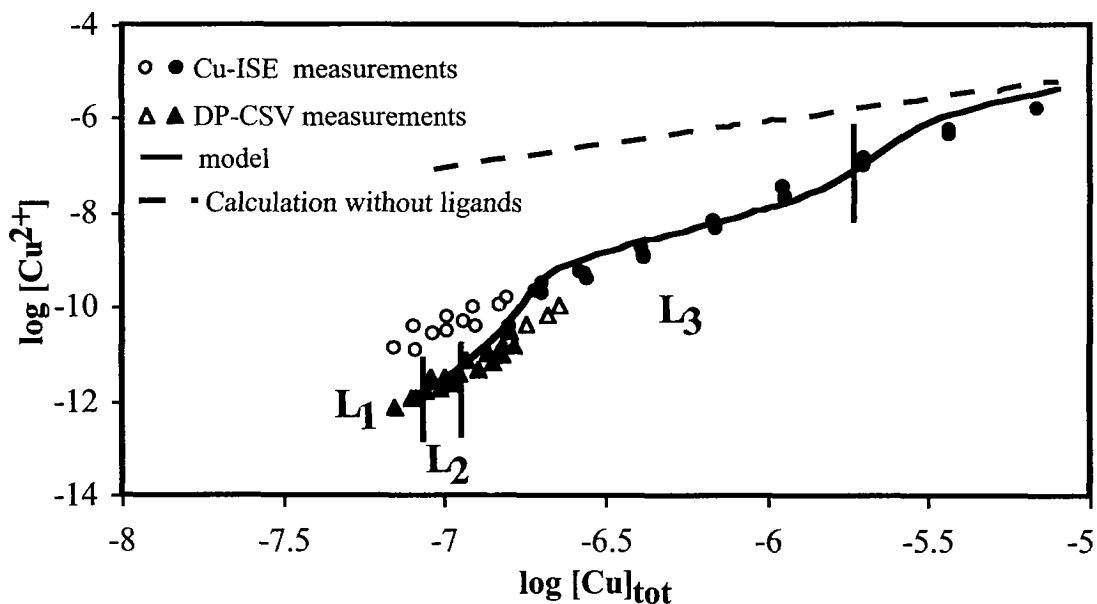
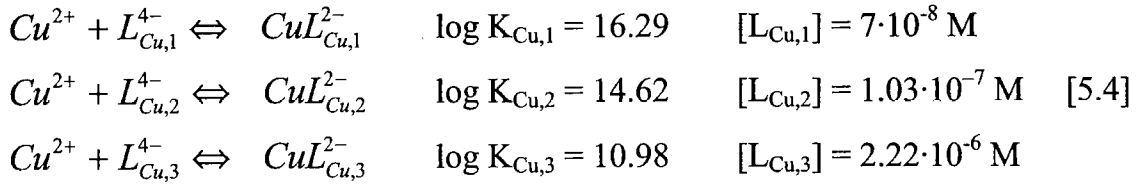


**Fig. 5.9:** Titration curve of infiltration groundwater organic ligands with copper at pH 7.35 (water sampled in May 1999). Measurements were performed with two different analytical methods: DPCSV measurements by Hanbin Xue (EAWAG, Kastanienbaum) and Cu-ISE measurements by Renata Hari (EAWAG, Dübendorf). This curve could be modelled by defining three ligands ( $L_1$ ,  $L_2$ ,  $L_3$ ), each with 4  $pK_a$ -values. The concentration ranges of copper, in which each of the ligands predominate, are indicated in the figure. Open circles and triangles represent experimental points that were not considered for parameter estimation. The dashed curve represents speciation of copper in the absence of organic ligands. The point where this estimated curve intercepts the experimental curve yields the maximum total copper concentration that the natural ligands are able to complex (section 5.13.1).

As a next step, the ligand concentrations were fixed and the corresponding complexation constants were estimated. The best results were obtained with the following complexation constants and ligand concentrations for the complexation properties of the DOC in the water sampled in May 1999 (Fig. 5.9):



The pH dependence of copper complexation by natural infiltration groundwater organic ligands was measured with the copper ion selective electrode (Fig. 5.10). In the acidic pH-range, complexation was weak, but at pH values above 7, complexation became stronger. An increase of one unit in pH (e.g. from pH 7 to 8) gave a decrease of 2 logarithmic units in the free copper concentration.

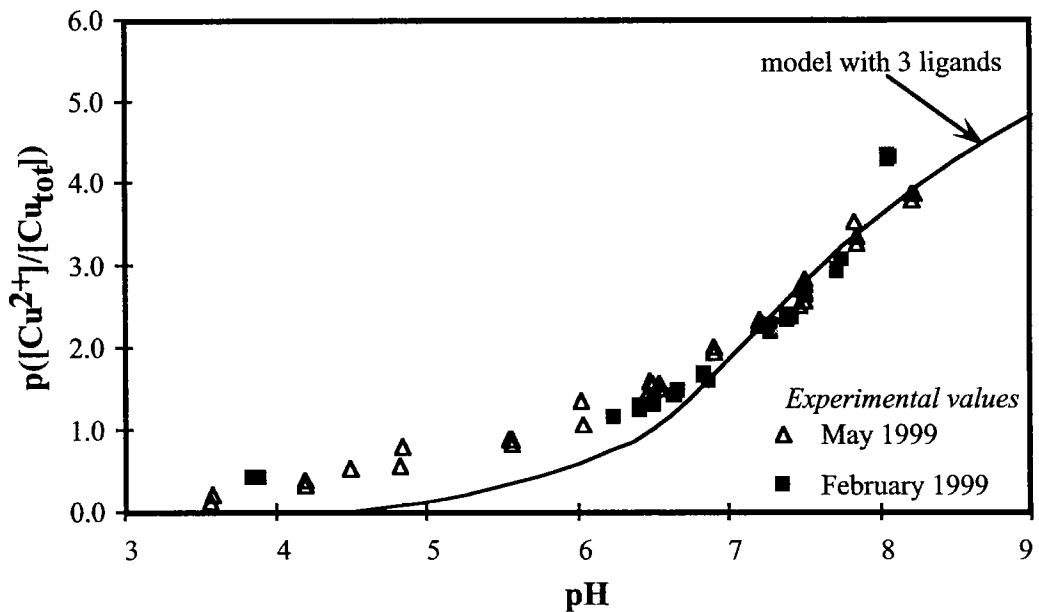


**Fig. 5.10:** pH dependence of copper complexation by natural organic ligands from an infiltration groundwater. The negative logarithm of the ratio between the free copper concentration and the total copper concentration is plotted versus pH, i.e., low values mean high free copper concentrations. Experiments were performed with a Cu-ISE by Renata Hari (EAWAG, Dübendorf). Data from May 1999 ( $[\text{Cu}_{\text{tot}}] = 2 \cdot 10^{-7} \text{ M}$ ) and February 1999 ( $[\text{Cu}_{\text{tot}}] = 2.2 \cdot 10^{-7} \text{ M}$ ).

The complexation properties do not seem to differ a lot in February 1999 and May 1999 (Fig. 5.10). Calculations with the 3 ligand model described above are shown. This model using parameters estimated from the titration curve at pH 7.35 could describe the pH dependence of the copper complexation sufficiently well, although at pH values below 7, the calculated complexation behaviour was slightly weaker than the one measured in the experiment. As experiments were performed at copper concentrations close to the saturation of the second ligand, calculations were

very sensitive to variations of the total copper concentration (Fig. 5.11). This might explain the difference observed between the experimental points and our model calculations.

The fact that the pH dependence of copper complexation could be described adequately with our 3 ligand model is a proof that the  $pK_a$  values defined were appropriate (Fig. 5.10).

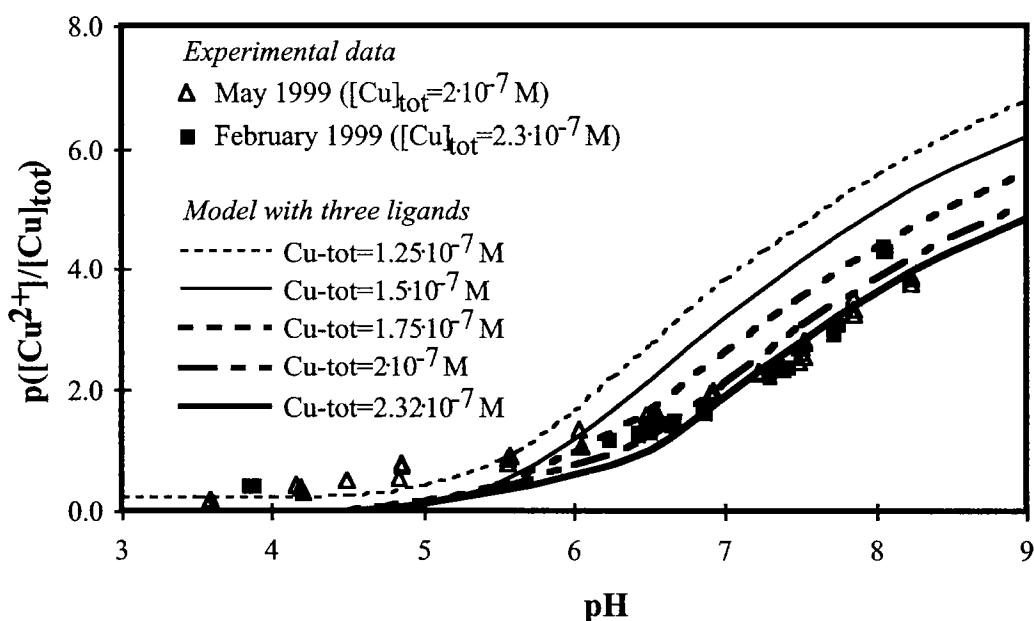


**Fig. 5.11:** Sensitivity of the total initial copper concentration on modelling the pH dependence of copper complexation by natural organic ligands. Model calculations with different total copper concentrations are shown.

### ***Copper Adsorption on Goethite in the Presence of Infiltration Groundwater Organic Ligands***

Calculations were performed as described in section 5.4.2 and the results are shown in Fig. 5.12.

Considering the simplicity of the model, the adsorption behaviour of copper in such a system was astonishingly well described. However, at pH values about 7, more copper was complexed by the ligands in solution in the calculations than in the experiments. One explanation for this enhanced adsorption may be that continuously varying complexation properties were described by defining only 3 ligands. As a consequence, the complexation properties of the ligand  $L_2$  may be overestimated, and thus copper adsorption underestimated. Another explanation would be, that the adsorption of copper was enhanced by reactions not yet considered in the

calculations, e.g., formation of ternary complexes or influences of anions contained in the groundwater matrix (see section 5.14).

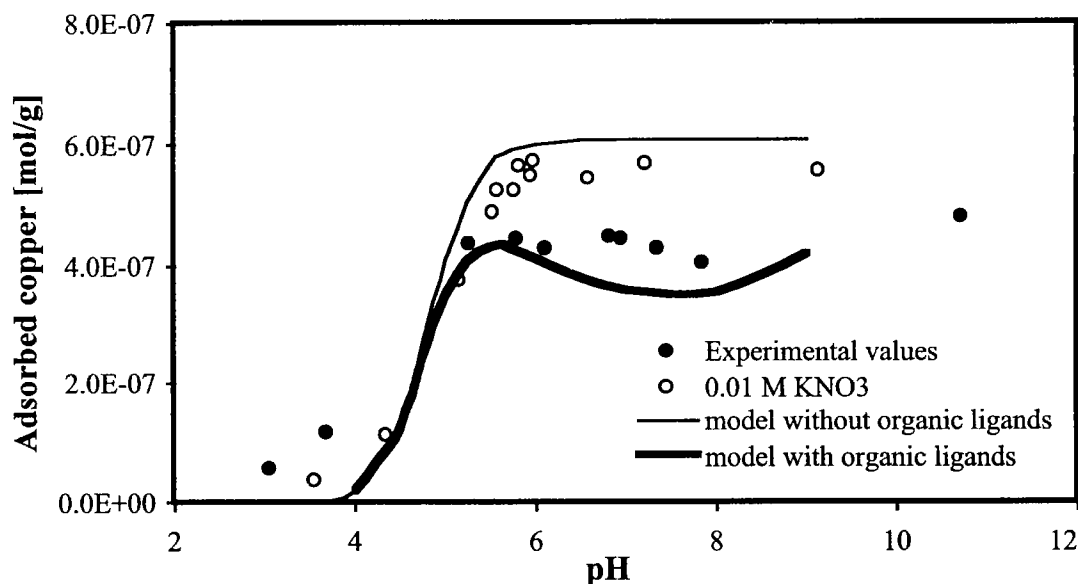


*Fig. 5.12: pH adsorption edge of copper in the presence of infiltration groundwater organic ligands. The reference data was fitted with the DLM model. By combination of the model for the adsorption of copper on goethite in the absence of organic ligands and the model for copper complexation in solution, copper adsorption in the presence of organic ligands was calculated.*

### ***Copper Adsorption in an Infiltration Groundwater at Environmental Concentrations***

Fig. 5.13 represents the pH adsorption edge of copper adsorption on goethite in the presence of natural ligands at environmental copper concentrations. No copper was added to the system to measure this adsorption edge and total initial copper concentration was  $4.6 \cdot 10^{-8}$  M. The experiment was performed in the “Cd-DOC-together” system, i.e., small increments of cadmium were added to the system. Cadmium was shown in section 5.11 to have no influence on copper adsorption.

Modelling of copper adsorption was done with the model described in section 5.4.2 and the constants defined in Tab. 5.9. At low pH values, phosphate probably influenced copper adsorption (section 5.14.2). These interactions were not taken into account by the model. At pH values above 6.5, copper adsorption was suppressed by the organic ligands. This effect was described very well by the model and shows that this model can be adequately used over a wide range of copper

concentrations to describe competition reactions between the ligand and the surface functional groups at pH values above 6.5. However at pH values between 4 and 6, the model could not represent the data.

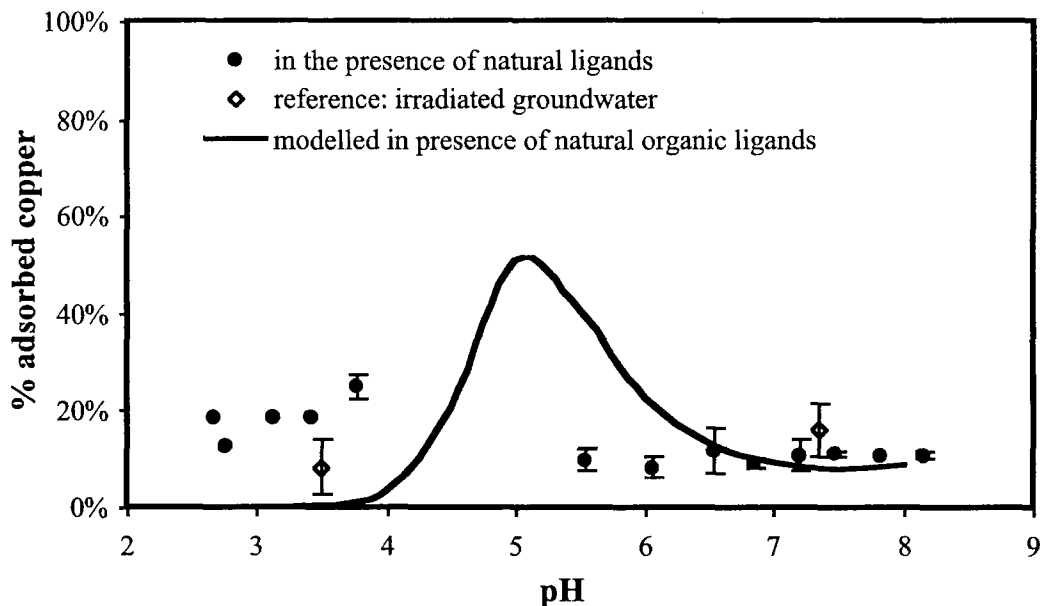


**Fig. 5.13:** Copper adsorption on goethite in a natural groundwater matrix at environmental concentrations. Experiments were performed in the “Cd-DOC-together” system (Sampling Campaign May 1999). ( $[Cu]_{tot}=4.6 \cdot 10^{-8} M$   $[goethite] = 0.1 g/L$ ).

## 5.6.2 Adsorption of Copper in the Presence of Deep Groundwater Organic Ligands

### *Copper Complexation by Deep Groundwater Organic Ligands*

As for the infiltration water, complexation of copper in solution was determined by titration curves analysed with DPCSV and Cu-ISE (Fig. 5.14). Total copper concentration varied between  $1 \cdot 10^{-8}$  and  $4.8 \cdot 10^{-5} M$ .

Modelling was performed exactly as described in section 5.6.1. Parameter estimation was done by using data at different pH values (Fig. 5.14). With the definition of three ligands, the following fitting results were obtained (WSOS/DF=53.2):

$$\begin{array}{ll}
 \log K_1=15.74 & [L_1]=1 \cdot 10^{-8} M \\
 \log K_2=14.47 & [L_2]=5 \cdot 10^{-8} M \\
 \log K_3=8.73 & [L_3]=7 \cdot 10^{-5} M
 \end{array} \tag{5.5}$$

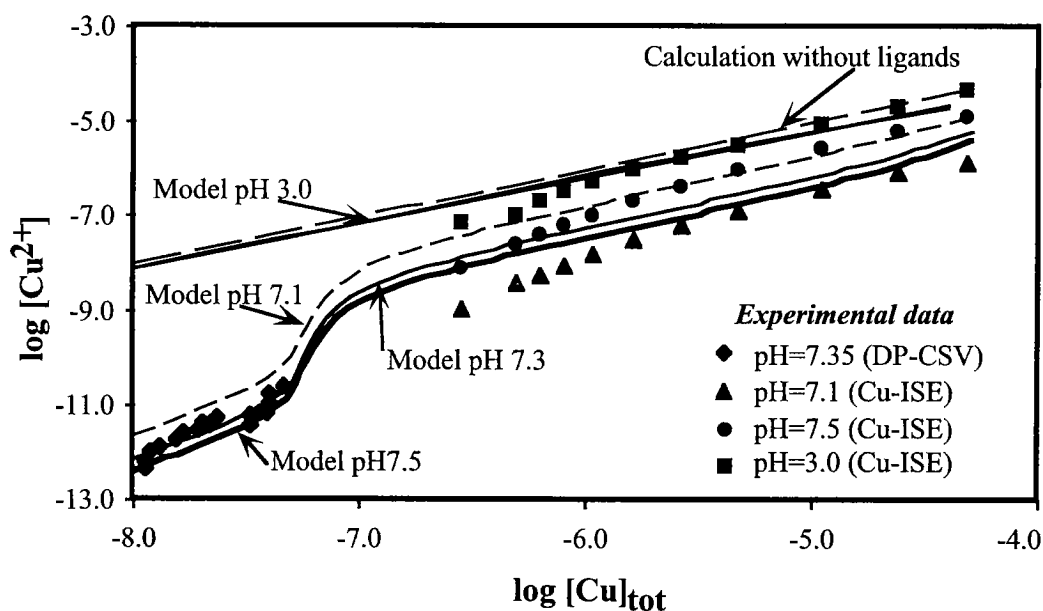


**Fig. 5.14:** Titration curve of copper in a deep groundwater sample at different pH values. Measurements were performed with two different analytical methods: DPCSV measurements by Hanbin Xue (EAWAG, Kastanienbaum) and Cu-ISE measurements by Renata Hari (EAWAG, Dübendorf). These curves were fitted by defining three ligands ( $L_1$ ,  $L_2$ ,  $L_3$ ), each with 4 acidity constants. The fine dashed curve represents speciation of copper in the absence of organic ligands. The point where this estimated curve intercepts the experimental curve yields the maximum total copper concentration that the natural ligands are able to complex.

### **pH dependence of Copper Complexation by Deep Groundwater Ligands**

The pH dependence of copper complexation by deep groundwater organic ligands is similar to that in the infiltration groundwater, weak complexation was observed for low pH values, and at pH values above 7, the complexation capacity increased strongly (Fig. 5.15).

The 3 ligand model, presented in this study can describe the data sufficiently well, although at pH values above 8, complexation capacity was underestimated.

Complexation capacities were lower in the deep groundwater (Fig. 5.15) than in the infiltration groundwater (Fig 5.10). Nowack (1996) has postulated that the weak ligands were degraded first and that in older water only strong complexes remained. This seems to be in opposition to the results obtained in this study. Xue and Sigg (1999) have argued that specific ligands were most likely of recent biological origin. These assumptions are consistent with our results: in the deep



groundwater mainly refractory less specific ligands, or else ligands in smaller concentrations were present.

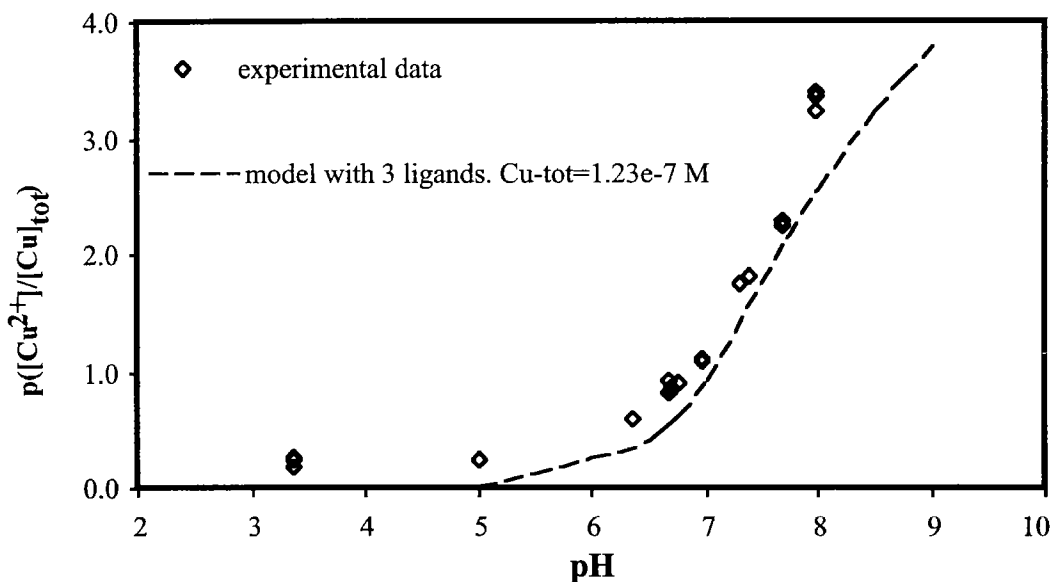


*Fig. 5.15: pH dependence of copper complexation by deep groundwater organic ligands. Measurements were performed with a Cu-ISE by Renata Hari (EAWAG, Dübendorf).*

### ***Copper Adsorption on Goethite in the Presence of Deep Groundwater Organic Ligands***

The results of the combination model as described in section 5.4.2 are shown in Fig. 5.16. The model could describe the adsorption in the presence of deep groundwater organic ligands sufficiently well. The fact that suppression of adsorption at pH values about 7 was overestimated, could be explained by competition reactions between the surface functional groups and the ligands in solution to complex copper. Probably, the ligand L<sub>2</sub> as defined in our model was too strong, or else interactions of copper adsorption with other cations or anions contained in the deep groundwater occurred. Similarly as for the infiltration groundwater, a specific interaction with phosphate could be possible, i.e. formation of ternary complexes.

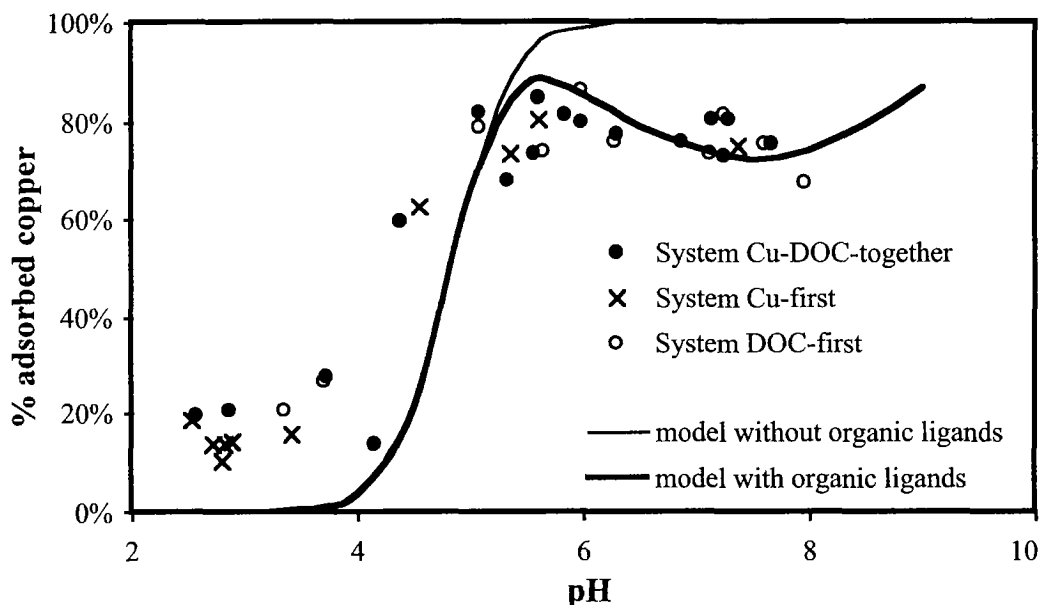


*Fig. 5.16: pH adsorption edge of copper on goethite in the presence of deep groundwater organic ligands. As comparison, a reference in 0.01 M  $KNO_3$  is shown. These reference data were fitted with the DLM model. By combination of the model for the adsorption of copper on goethite in the absence of organic ligands and the model for copper complexation in solution, copper adsorption in the presence of organic ligands was calculated.*

## 5.7 Influence of a Groundwater Matrix on the Adsorption of Cadmium on Goethite

### 5.7.1 pH Adsorption Edge of Cadmium on Goethite in an Infiltration Groundwater Matrix

The pH dependence of the adsorption of cadmium on goethite in the presence of natural organic ligands was measured in the three systems defined in Fig. 5.2. (Fig. 5.17). As reference without DOC, cadmium adsorption was measured in a synthetic groundwater made up with calcium, magnesium, chloride, and sulphate concentrations (Table 5.7).

At pH values above 8, slightly less cadmium was adsorbed in the presence of organic ligands, which could be explained by competition reactions between complexation in solution and adsorption on the surface.

At pH values in the acidic pH range, no significant adsorption could be observed. Adsorption isotherms at pH 3.5 were performed. For initial total cadmium

concentrations varied between  $7.5 \cdot 10^{-10}$  and  $1.4 \cdot 10^{-9}$  M, no adsorption could be noticed (data not shown).

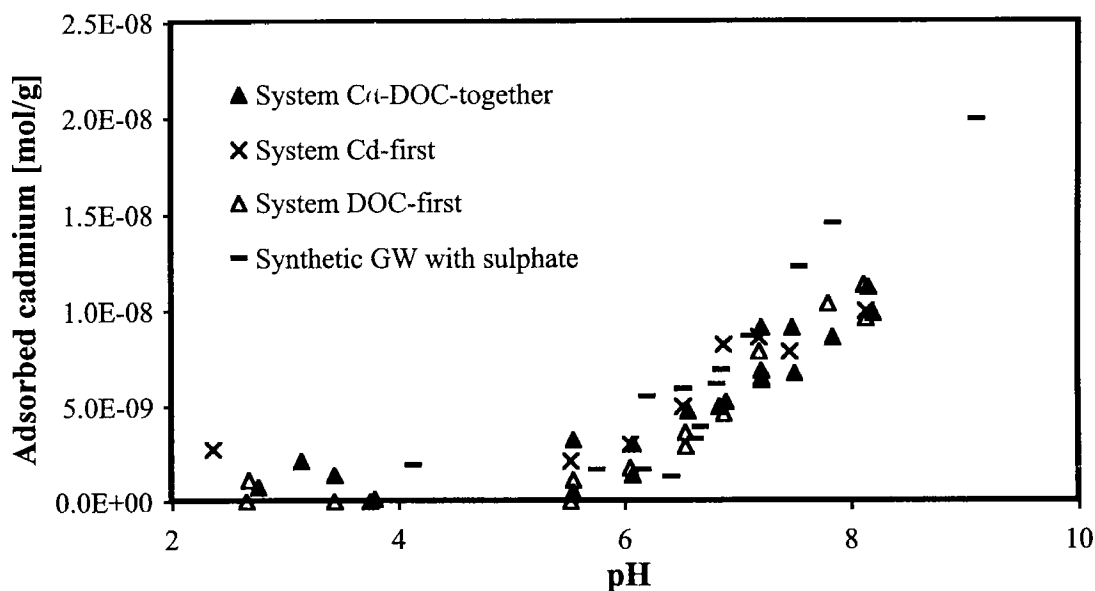


*Fig. 5.17: pH adsorption edge of cadmium on goethite in the presence of natural infiltration groundwater. (Sampling campaign May 1999). ( $[Cd_{tot}] = 1.3 \cdot 10^{-9}$  M).*

### 5.7.2 Adsorption of Cadmium on Goethite in an Infiltration Groundwater Matrix at pH 7.6

The following experiments were carried out with groundwater sampled in February 1999 at pH 7.6, the pH of the infiltration groundwater (Tab. 5.2). Adsorption experiments were done for the system “Cd-DOC-together”. A reference in 0.01 M  $KNO_3$  was investigated for comparison (Fig. 5.18).

Clearly less cadmium was adsorbed in the presence of organic ligands compared to the reference system and the adsorption isotherm seemed to cut the x-axis at a concentration of  $5 \cdot 10^{-10}$  M (estimation directly from Fig. 5.18), which was a hint to the presence of strong cadmium specific ligands in solution.

### 5.7.3 Adsorption of Cadmium in a Deep Groundwater Matrix at pH 7.6

An adsorption isotherm of cadmium at pH 7.6 in the presence of deep groundwater organic ligands is shown in Fig. 5.19. As reference an adsorption isotherm in 0.01 M  $KNO_3$  was measured. As for the infiltration groundwater, a

suppression of cadmium adsorption could be observed in the presence of these ligands. This suppression seemed to be even more pronounced in the presence of the deep groundwater organic ligands than in the presence of infiltration groundwater organic ligands.

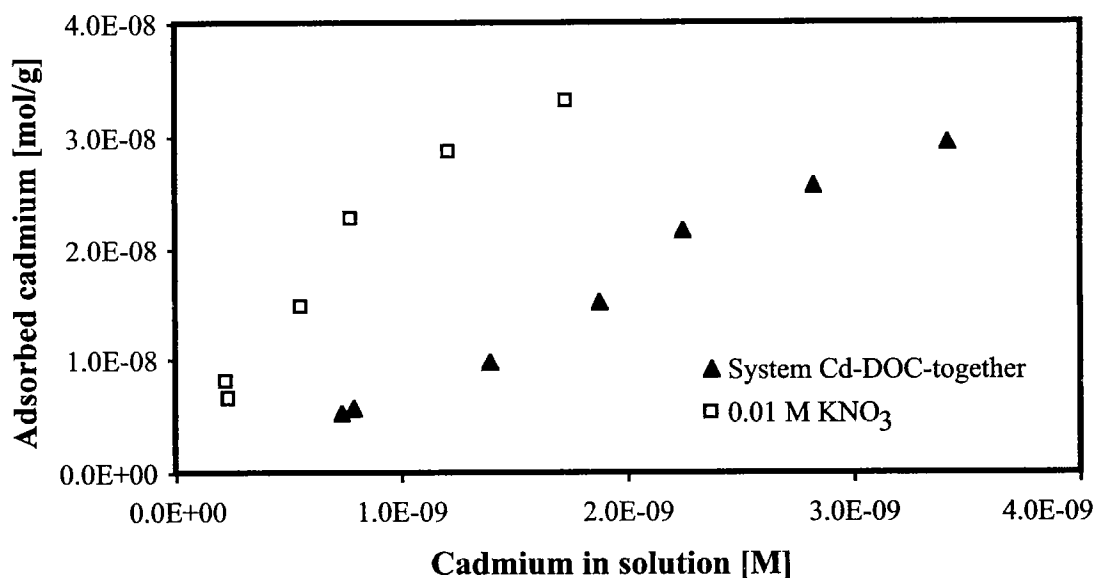


*Fig. 5.18: Cadmium adsorption isotherms on goethite at pH 7.6 in the presence of infiltration groundwater natural organic ligands. (Sampling Campaign February 1999). ( $[Cd_{tot}] = 8.8 \cdot 10^{-10} - 7 \cdot 10^{-9} M$ ).*

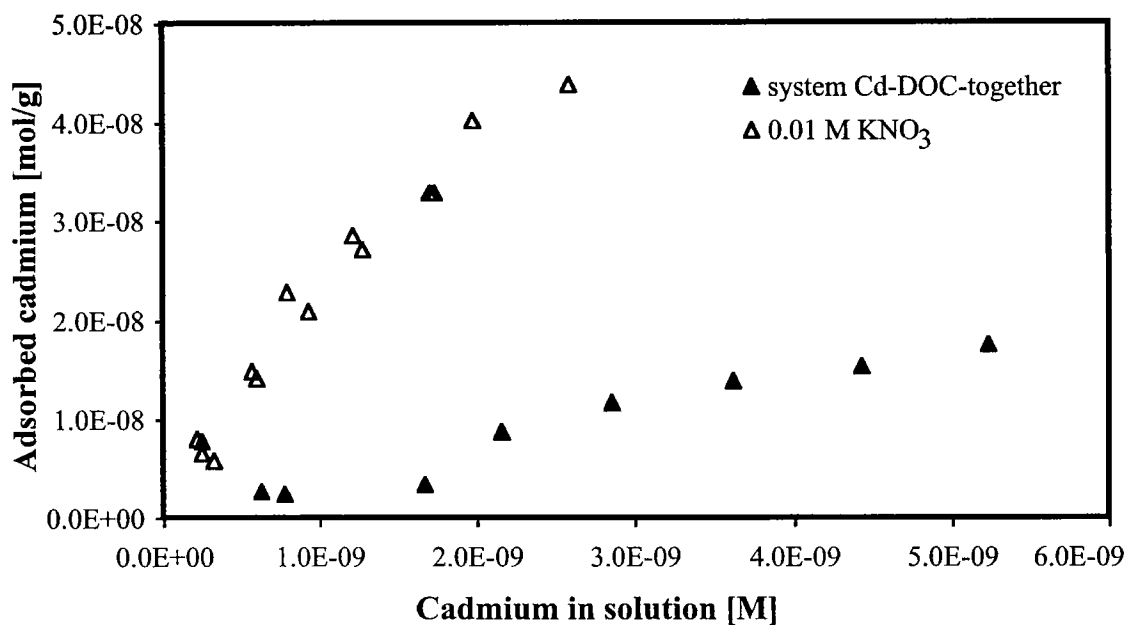


*Fig. 5.19: Cadmium adsorption isotherm on goethite at pH 7.6 in the presence of deep groundwater natural organic ligands. ( $[Cd]_{tot} = 8 \cdot 10^{-10} M$  and  $7 \cdot 10^{-9} M$ ).*

## 5.8 Modelling of Cadmium Experiments

### 5.8.1 Adsorption of Cadmium in the Presence of Infiltration Groundwater Organic Ligands

#### *Cadmium Complexation by Infiltration Groundwater Organic Ligands*

Groundwater samples were titrated with cadmium in the concentration range  $2 \cdot 10^{-10}$  to  $9 \cdot 10^{-9}$  M (Fig. 5.20).

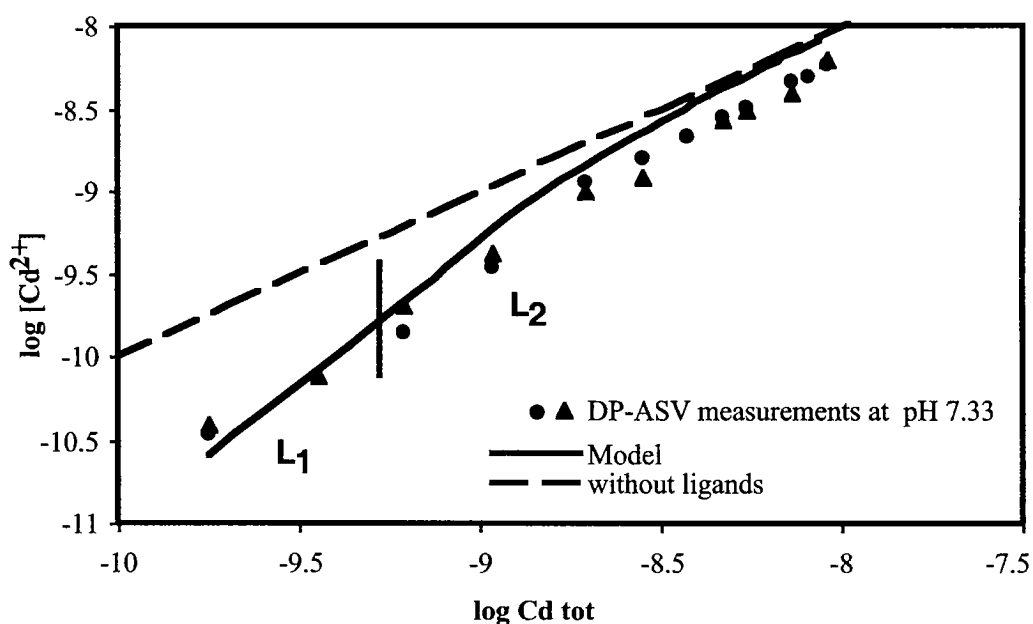


**Fig. 5.20:** Titration curve of infiltration groundwater with cadmium (Water sampled in May 1999). Measurements were performed at  $\text{pH } 7.33 \pm 0.05$  with a voltammetric method (DPASV) by Hanbin Xue (EAWAG, Kastanienbaum). This curve could be modelled by defining two ligands ( $L_1$  and  $L_2$ ), both with 4  $\text{p}K_a$ -values. The concentrations of cadmium, in which each of the ligands predominate, are depicted in the figure. The dashed curve represents speciation of cadmium in the absence of organic ligands. The point, where this estimated curve intercepts the experimental one yields the maximum total cadmium concentration that natural ligands are able to complex (section 5.13.1).

Modelling was performed with the discrete model described in section 5.4.2. The presence of 2 cadmium ligands was assumed. All 4 parameters, i.e., complexation constants and concentration of the ligands  $L_1$  and  $L_2$ , could be estimated in one run (WSOS/DF = 0.32). Following complexation constants and

ligand concentrations were defined for the complexation properties of DOC with cadmium in the water sampled in May 1999:

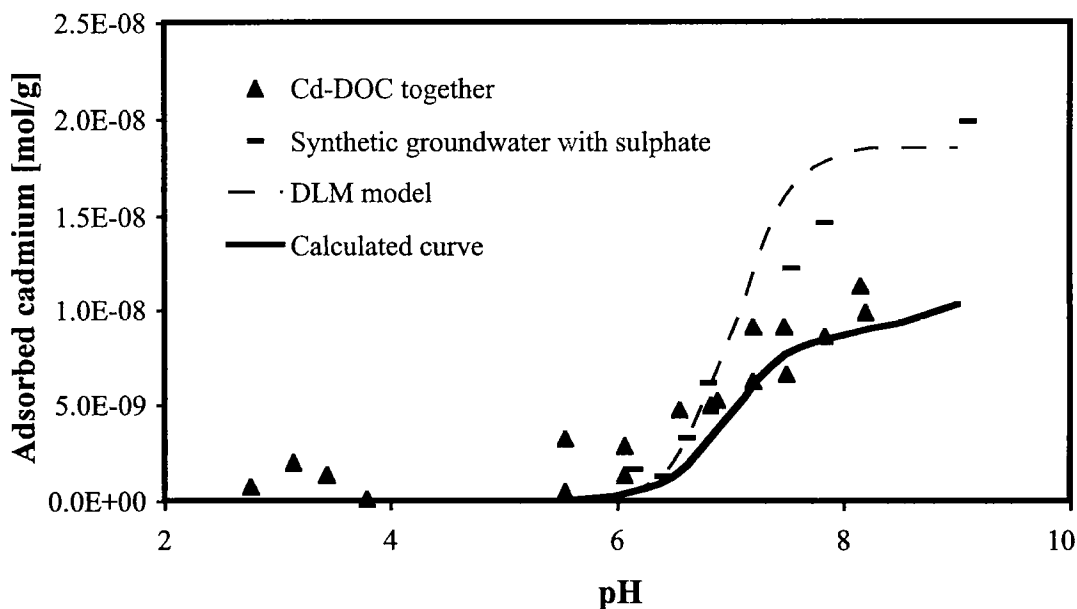
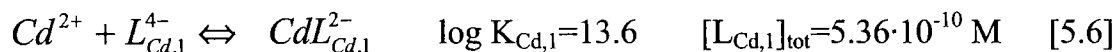


*Fig. 5.21: pH cadmium adsorption edge on goethite in the presence of organic ligands. For comparison, a synthetic groundwater with sulphate was measured. These reference data were modelled with the DLM-model. By combination of the model for the adsorption of cadmium on goethite in the absence of organic ligands and the model for cadmium complexation in solution, cadmium adsorption in the presence of organic ligands could be calculated.*

### ***Cadmium Adsorption on Goethite in the Presence of Infiltration Groundwater Organic Ligands***

With the combination model described in section 5.4.2, the adsorption of cadmium on goethite in the presence of groundwater organic ligands could adequately well be described (Fig. 5.21).

## 5.9 Influence of a Groundwater Matrix on the Adsorption of Nickel on Goethite

### 5.9.1 pH Adsorption Edge of Nickel on Goethite in an Infiltration Groundwater Matrix

The pH dependence of the adsorption of nickel on goethite in the presence of groundwater ligands was measured in the systems “Ni–DOC–together” and “DOC–first” (Fig. 5.22). As a reference without DOC, the nickel adsorption was studied in 0.01 M  $\text{KNO}_3$ .

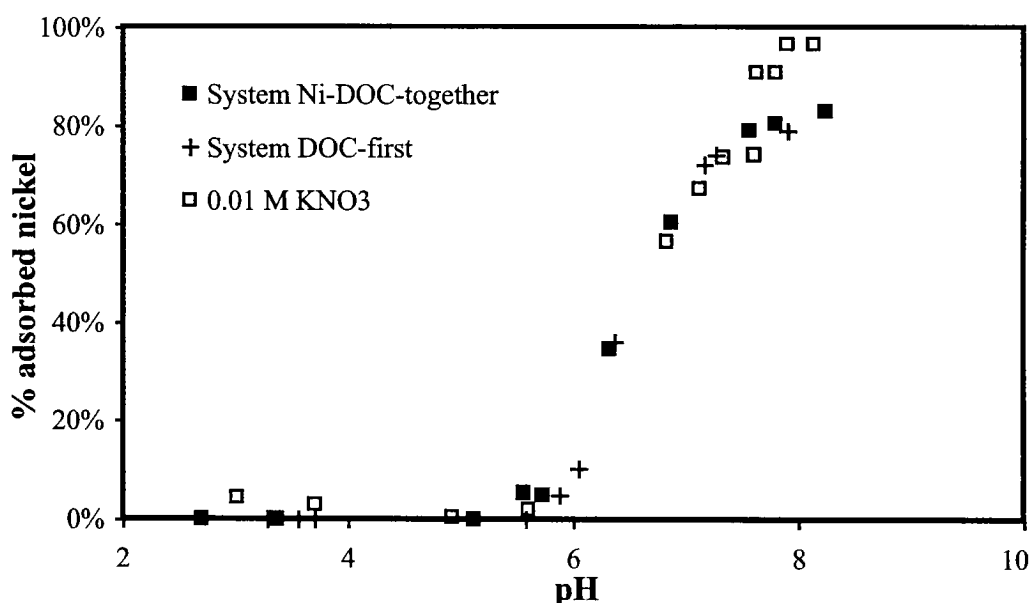


*Fig. 5.22: pH nickel adsorption edge on goethite in the presence of groundwater organic ligands. Sampling Campaign February 1999. ( $[\text{Ni}]_{\text{tot}}=2.8 \cdot 10^{-7} \text{ M}$ )*

Less nickel was adsorbed at pH values above 7.5 in the systems with organic ligands than in the reference system without DOC. This was explained by the presence of specific ligands in solution, which complex nickel strong enough to mobilise it.

In the acidic pH range, no adsorption of nickel on goethite could be observed. The same result was obtained by recording isotherms at pH 3.5 with equilibration times of up to 5 days (data not shown).

## 5.9.2 Adsorption of Nickel on Goethite in an Infiltration Groundwater Matrix at pH 7.35

pH 7.35 was the pH of the natural groundwater sampled in May 1999 (Tab. 5.2). Adsorption experiments were performed for a reference system (0.01 M  $\text{KNO}_3$ ) and in the systems “Ni–DOC–together” and “Ni–first” (Fig. 5.23).

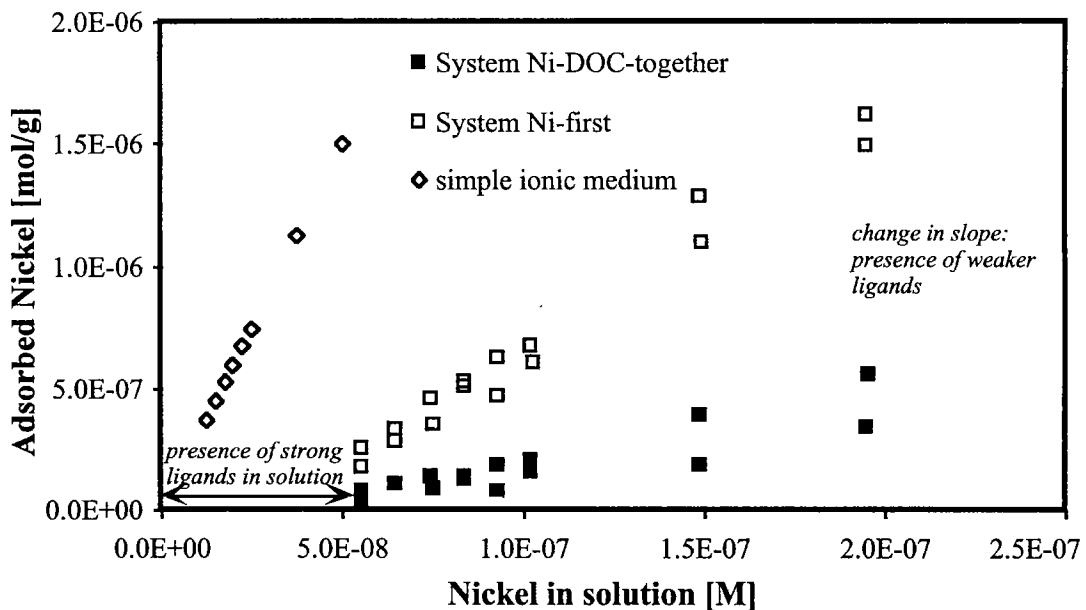


**Fig. 5.23:** Nickel adsorption isotherms on goethite at pH 7.35 in the presence of infiltration groundwater organic ligands. Sampling campaign May 1999. ( $[\text{Ni}]_{\text{tot}} = 5 \cdot 10^{-8} - 2 \cdot 10^{-7} \text{ M}$ )

The same remarks can be made to the shape of the isotherms as for copper (section 5.5.4). Nickel experiments were performed at concentrations which did not allow saturation of the surface sites.

Clearly less nickel was adsorbed in the presence of organic ligands than in the reference system. Nickel isotherms cut the x-axis at a value about  $2\text{--}3 \cdot 10^{-8} \text{ M}$ . This indicated that DOC contained strong specific ligands for nickel, which could completely hinder the adsorption of nickel. Moreover, weaker nickel ligands could be assumed, as the slope of the isotherms in presence of the ligands was lower than that of the reference curve.

A clear difference could be seen between the isotherms in the system “Ni–first” and the system “Ni–DOC–together”. This phenomenon was likely due to kinetic effects as described for copper in section 5.5.1. The difference between the adsorption isotherms in the systems “Ni–first” and “Ni–DOC–together” could be



due to slow nickel desorption reactions (Fig. 5.23). The water exchange rate for nickel is  $3 \cdot 10^4 \text{ s}^{-1}$  (Morel and Hering, 1993), which shows that complexation reactions with nickel are slow. Another explanation would be that nickel slowly diffuses into the mineral and becomes thus unavailable for the aqueous complexants in solution (Fischer et al., 1997; Fischer et al., 1998; Gerth and Brümmer, 1981).

## 5.10 Modelling of Nickel Experiments

### 5.10.1 Adsorption of Nickel in the Presence of Infiltration Groundwater Organic Ligands

#### *Nickel Complexation by Infiltration Groundwater Ligands*

The titration curve of the organic ligands with nickel was modelled as described in section 5.4.1 (Fig. 5.24) (WSOS/DF=0.2). The measurement range was very narrow, therefore only one nickel ligand was defined. The complexation constant and ligand concentration estimated were:

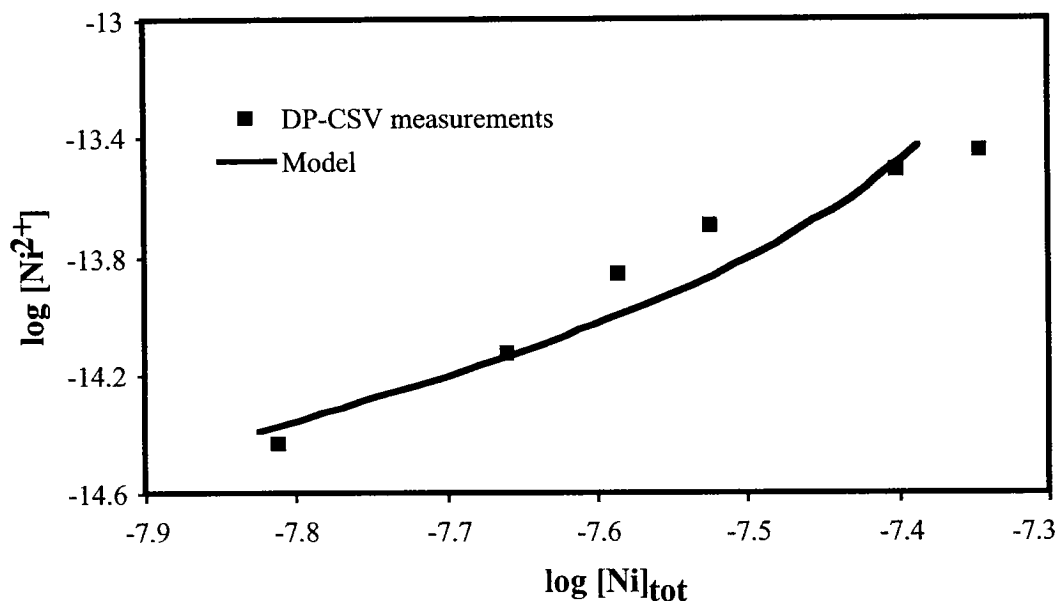
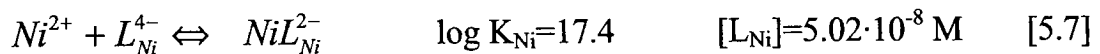


**Fig. 5.24:** Titration curve of infiltration groundwater organic ligands with nickel (Water sampled in May 1999). Measurements were performed at pH 7.35 with a voltammetric method (DPCSV) by Andreas Prasch (EAWAG, Kastanienbaum). This curve was modelled by using one ligand only with 4  $pK_a$  values.

### *Nickel Adsorption on Goethite in the Presence of Infiltration Groundwater Organic Ligands*

Modelling was performed as described in section 5.4 (Fig. 5.25). This model can well describe the nickel adsorption edge under the influence of organic ligands.

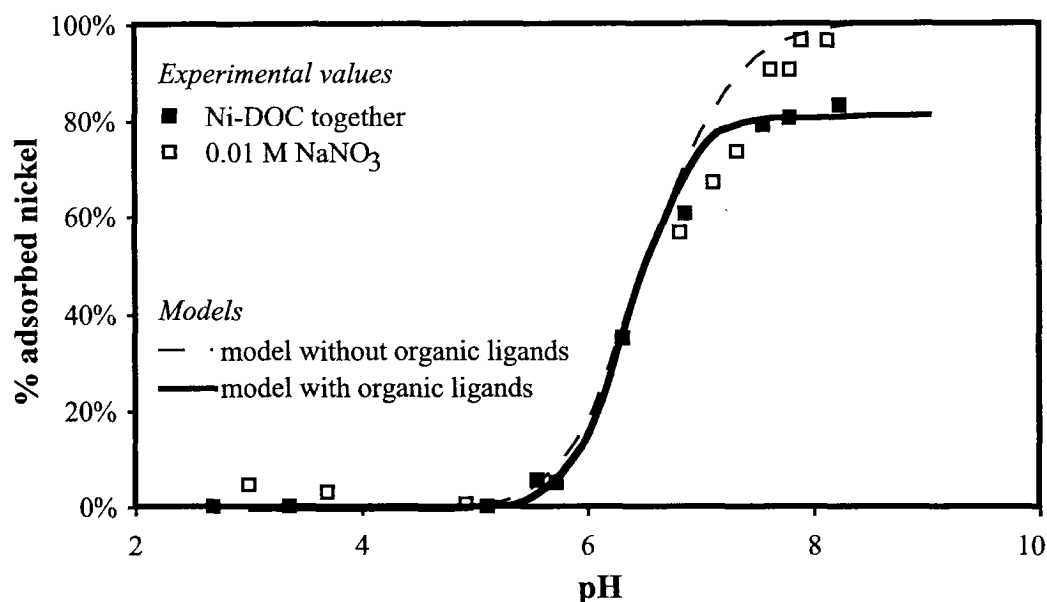


*Fig. 5.25: pH nickel adsorption edge on goethite in the presence of groundwater organic ligands. ( $[Ni]_{tot} = 2.8 \cdot 10^{-7} M$ ,  $[goethite] = 0.5 g/L$ )*

## **5.11 Competitive Adsorption of Cu and Ni on Goethite in the Presence of Natural Organic Ligands**

In this section, competition between copper and nickel for their adsorption on goethite in the presence of natural organic ligands is discussed. Experiments were carried out in the systems “metal–DOC–together” and “metal–first” at pH 7.35. Two types of experiments were thus performed (Tab. 5.10): variable copper concentration at constant nickel concentration in order to study the effect of nickel on the adsorption of copper and vice versa.

**Tab. 5.10:** *Experimental conditions for the two types of competition reactions*

	<b>Effect of nickel on copper adsorption</b>	<b>Effect of copper on nickel adsorption</b>
pH	7.35	7.35
KNO <sub>3</sub> [M]	0.01	0.01
Cu [M]	$7.7 \cdot 10^{-8} - 3.3 \cdot 10^{-7}$	$1.2 \cdot 10^{-7}$
Ni [M]	$6.7 \cdot 10^{-8}$	$3 \cdot 10^{-8} - 1.5 \cdot 10^{-7}$
DOC [mg/L]	1.5	1.5
goethite [g/L]	0.1	0.1

### **System "Cu-Ni-DOC-together"**

Copper adsorption on goethite in competition with nickel in the presence of natural organic ligands is represented in Fig. 5.26. A slightly enhanced adsorption of copper could be observed. The adsorption isotherm and the intercept with the x-axis were shifted to the left, which was a hint that less copper was complexed in solution by strong ligands. This could probably be explained by the fact that copper and nickel were competing for the same specific ligand in solution.

No interactions between nickel and copper on the surface occurred, as nickel adsorption did not clearly decrease by increasing copper concentration (Fig. 5.27). Nickel adsorption as well was enhanced in the presence of copper: the fraction of nickel adsorbed in the presence of increasing copper concentrations was about 40%, whereas in the absence of copper it amounted to less than 20%. This means that less nickel was complexed in solution in the presence of copper, which corroborates the statement that specific strong ligands for nickel were also specific for copper.

Corresponding results have been obtained by recording the nickel isotherm at pH 7.35 in the presence of a constant copper concentration (Tab. 5.10). The nickel adsorption isotherm and the intercept with the x-axis were shifted clearly to the left (Fig. 5.28), i.e., less nickel was complexed in solution by strong ligands due to competition reactions with copper. The adsorbed copper concentration on goethite did not clearly decrease with an enhanced concentration of adsorbed nickel, which was expected as the surface sites were in excess of the metal concentrations (Fig. 5.29). Similarly as described before, copper adsorption was increased in the presence of nickel: the fraction of adsorbed copper was about 55% whereas in the

absence of nickel it was about 44%. This observation showed that all results for the competition experiments were consistent.

The effect of competition of copper on the adsorption of nickel on goethite was more pronounced than vice versa. This could probably be explained by the fact that nickel concentrations were lower than that of copper and that nickel complexation was relatively slow (Jansen, 1998; Prasad, 1999).

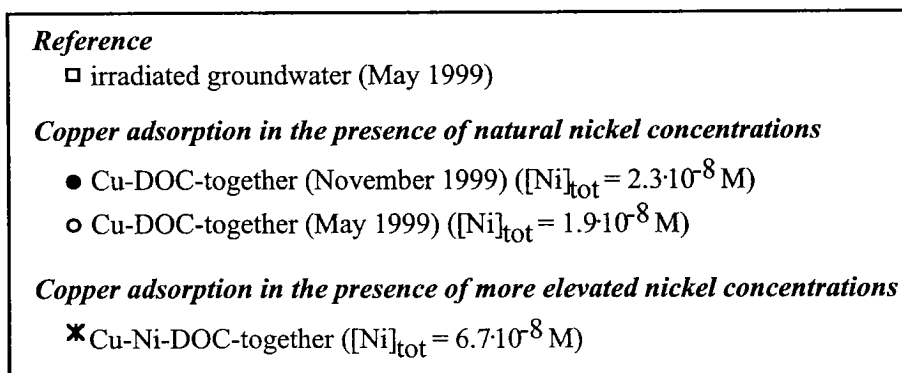
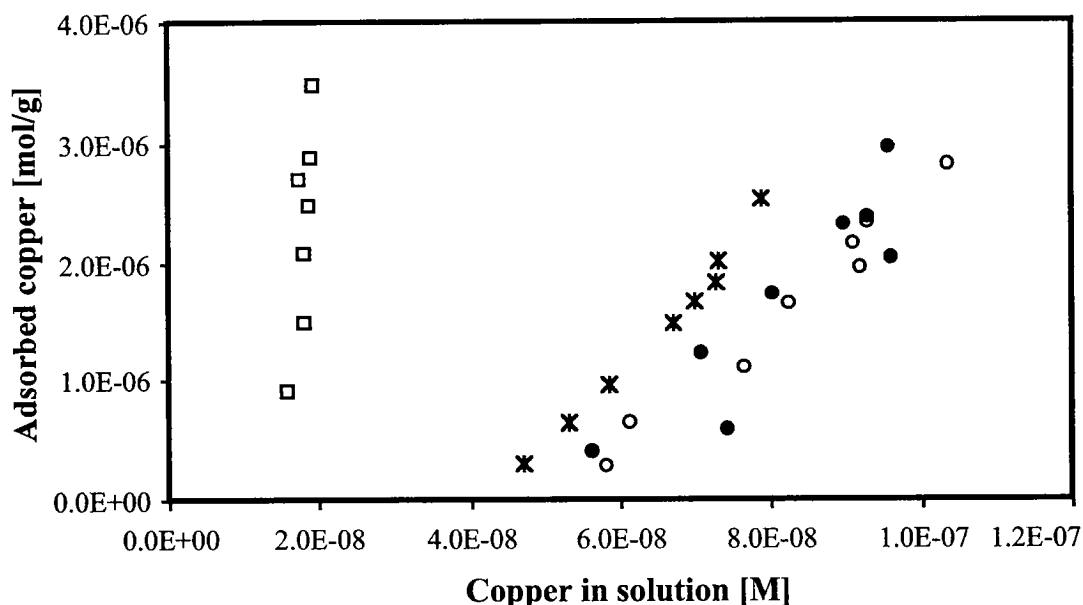


**Fig. 5.26:** Effect of nickel on the adsorption of copper on goethite in the presence of natural organic ligands at  $\text{pH} = 7.35$ . For comparison the adsorption of copper on goethite without competition reactions with nickel is shown. ( $[\text{Cu}]_{\text{tot}} = 7.7 \cdot 10^{-9} - 3.3 \cdot 10^{-7} \text{ M}$ ,  $[\text{Ni}]_{\text{tot}} = 6.7 \cdot 10^{-8} \text{ M}$ ).

**Fig. 5.28 (bottom):** Effect of copper on the adsorption of nickel on goethite in the presence of natural organic ligands. For comparison the adsorption isotherm of nickel on goethite without competition reactions with copper is shown. ( $[\text{Ni}]_{\text{tot}} = 3 \cdot 10^{-8} - 1.5 \cdot 10^{-7} \text{ M}$ ,  $[\text{Cu}]_{\text{tot}} = 1.2 \cdot 10^{-7} \text{ M}$ ).

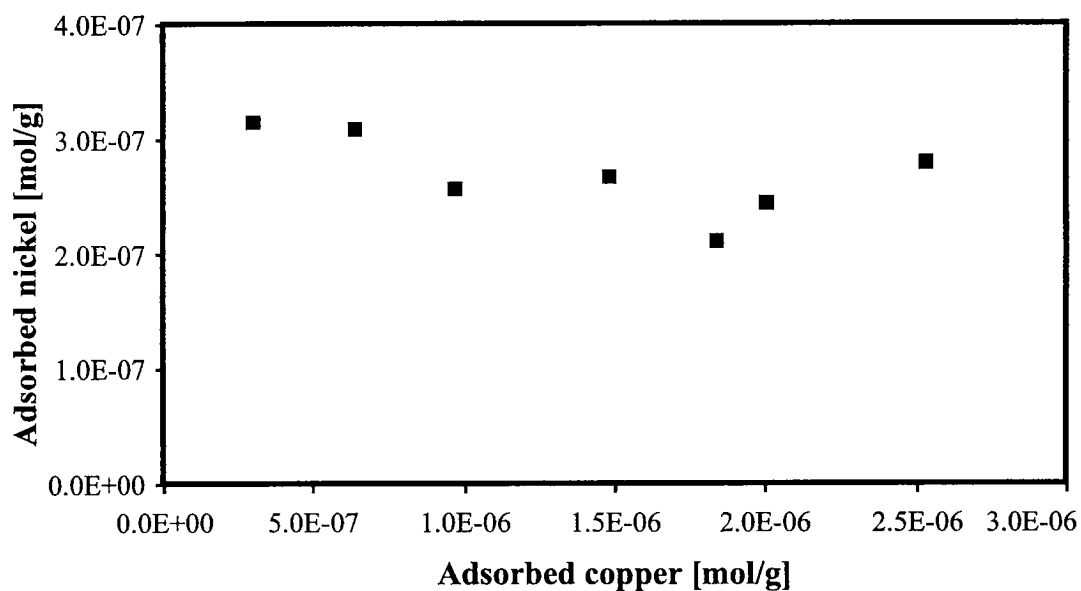
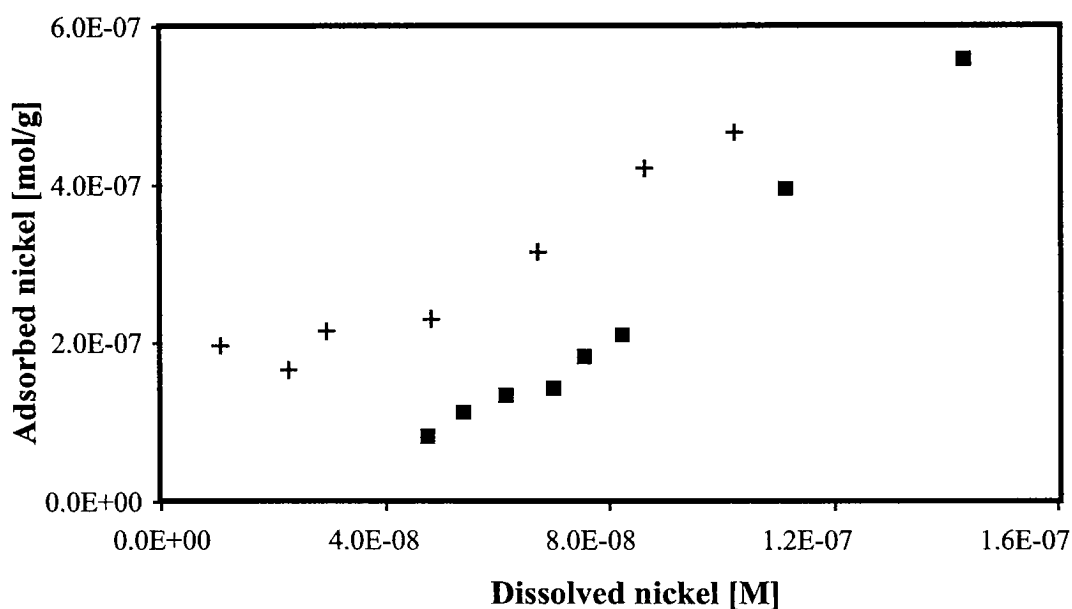


*Fig. 5.27: Influence of the copper adsorption on the nickel adsorption. ( $[Cu]_{tot} = 7.7 \cdot 10^{-9} - 3.3 \cdot 10^{-7} M$ ,  $[Ni]_{tot} = 6.7 \cdot 10^{-8} M$ ,  $pH = 7.35$ ).*



*Nickel adsorption in the presence of natural copper concentrations*

■ Ni-DOC-together (May 1999) ( $[Cu]_{tot} = 1.2 \cdot 10^{-8} M$ )

*Nickel adsorption in the presence of more elevated copper concentrations*

+ Ni-Cu-DOC together (November 1999) ( $[Cu]_{tot} = 6.1 \cdot 10^{-8} M$ )

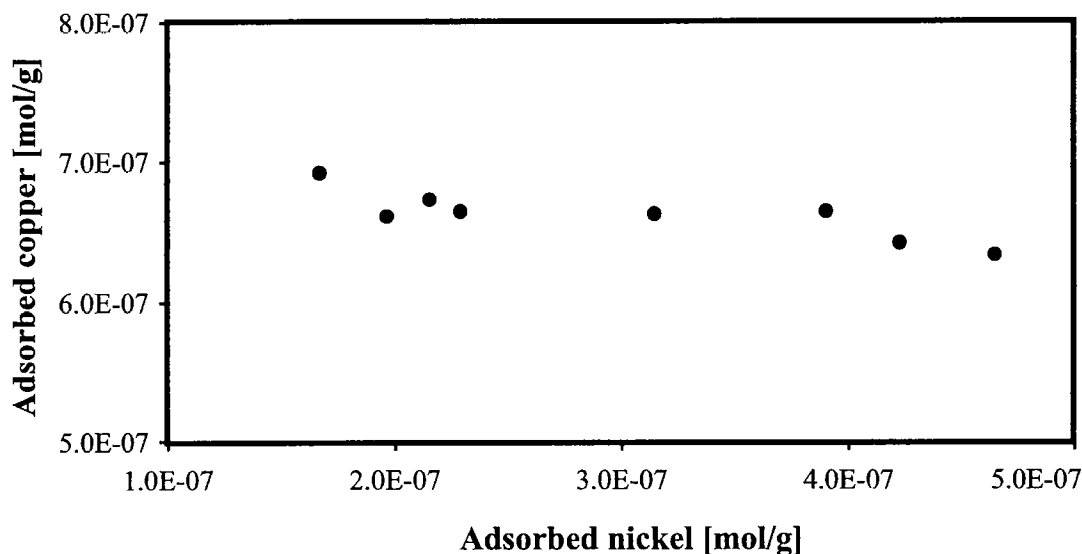
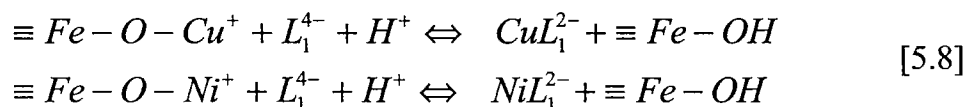


**Fig. 5.29:** Adsorption of copper on goethite in the presence of nickel. ( $[Ni]_{tot} = 3 \cdot 10^{-8} - 1.5 \cdot 10^{-7} M$ ,  $[Cu]_{tot} = 1.2 \cdot 10^{-7} M$ ,  $pH = 7.35$ ).

### System "Metal-first"

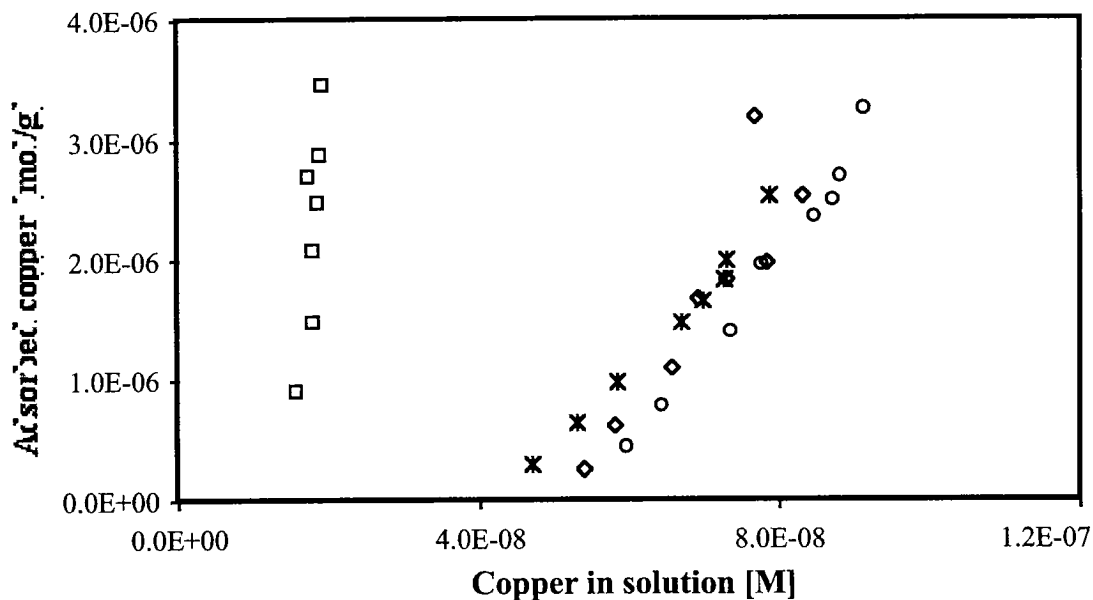
In this system, no effect on the adsorption of copper was observed in the presence of nickel (Fig. 5.30).

These results are probably explained by slow kinetics of nickel complexation. Nickel and copper were adsorbed prior to the addition of natural organic ligands. After their addition, metal desorption reactions occurred (Eq. 5.8). Nickel is known to slowly exchange complexed ligands (Margerum et al., 1978; Wilkins, 1991), thus mainly copper desorbed from the surface and essentially no competition reactions in the solution could occur.



For the nickel adsorption in this case, we would expect an adsorption of nickel in competition with copper in the presence of natural organic ligands similar to the adsorption in a system without DOC.

A comparison between isotherms recorded in May 1999 and November 1999, as it is done in Fig. 5.30 is allowed. It has been shown that the two water samples behave in the same way, and that no difference between the isotherms performed in May 1999 and November 1999 could be seen (Fig. 5.26).

**Reference**

□ irradiated groundwater (May 1999) ( $[\text{Ni}]_{\text{tot}} = 1.9 \cdot 10^{-8} \text{ M}$ )

**Copper adsorption in the presence of natural nickel concentrations**

◇ Cu-first (May 1999) ( $[\text{Ni}]_{\text{tot}} = 1.9 \cdot 10^{-8} \text{ M}$ )

**Copper adsorption in the presence of more elevated nickel concentrations**

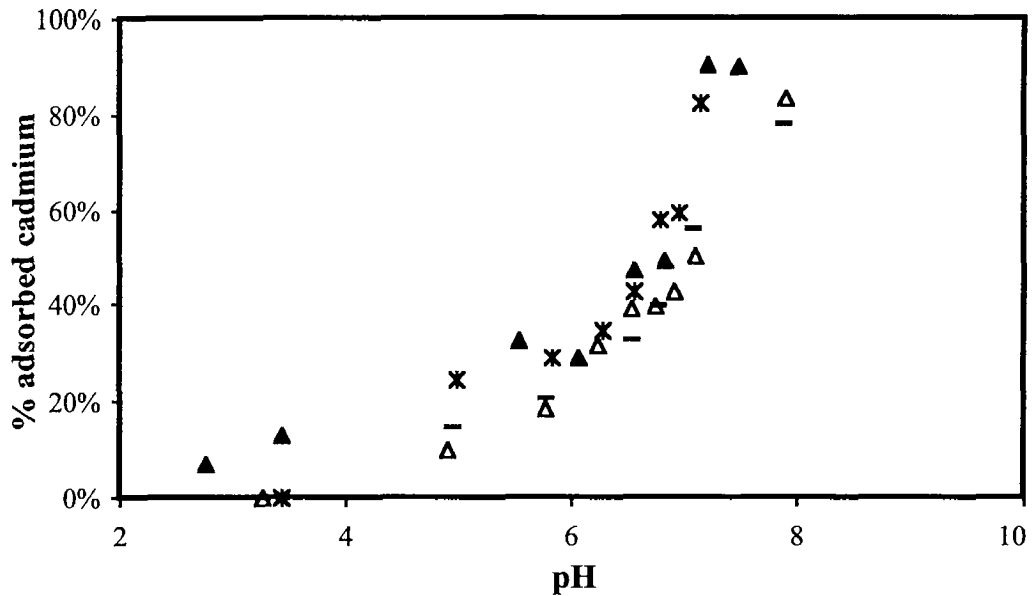
○ Cu-Ni-first (November 1999) ( $[\text{Ni}]_{\text{tot}} = 6.7 \cdot 10^{-8} \text{ M}$ )

\* Cu-Ni-DOC-together (November 1999) ( $[\text{Ni}]_{\text{tot}} = 6.7 \cdot 10^{-8} \text{ M}$ )

**Fig. 5.30:** Effect of nickel on the adsorption of copper on goethite in the presence of natural organic ligands in the system "metal-first". For comparison the adsorption of copper on goethite without competition reactions with nickel and the adsorption of copper on goethite in the presence of nickel in the system "metal-DOC-together" are represented. (Adsorption time of metals on goethite: 2 h, and equilibration time with DOC: 4 h).

### ***Influence of nickel and copper on the adsorption of cadmium***

In Fig. 5.31, the pH adsorption edge of cadmium in the presence of copper and nickel is shown. Cadmium adsorption on goethite was not influenced by copper or nickel whatever the pH. This result could be expected, as surface functional groups were in large excess of the total metal concentrations. In addition, cadmium may be bound to other ligands or adsorption sites than nickel or copper.



**Cadmium adsorption in the presence of copper and nickel at natural concentrations**

▲ Cd-DOC-together (May 1999)

( $[Cu]_{tot} = 6.4 \cdot 10^{-8} M$ ,  $[Ni]_{tot} = 1.9 \cdot 10^{-8} M$ )

**Cadmium adsorption in the presence of copper and nickel at higher concentrations**

△ Cd-Cu-Ni DOC together

\* Cd-Cu-Ni-first

- DOC-first

}  $[Cu]_{tot} = 1 \cdot 10^{-7} M$ ,  $[Ni]_{tot} = 1 \cdot 10^{-7} M$

**Fig. 5.31:** Influence of copper and nickel on the pH adsorption edge of cadmium on goethite. ( $[Cd] = 1 \cdot 10^{-9} M$ ,  $[Cu] = 1 \cdot 10^{-7} M$ , and  $[Ni] = 1 \cdot 10^{-7} M$ ,  $[goethite] = 0.1 g/L$ . Equilibration times as listed in Tab. 5.6)

## 5.12 Adsorption of Several Metals on Goethite in the Groundwater Matrix

### *Adsorption of Chromium on Goethite in an Infiltration Groundwater Matrix*

In natural systems, chromium is stable in two oxidation states, Cr(III) and Cr(VI). Cr(III) is an essential trace element for human and animals and is generally associated with solid phases, whereas Cr(VI) is a priority pollutant and relatively mobile in soils and aquifers.



The adsorption edge of chromium on goethite was measured in the presence of organic ligands in the system “Cu-DOC-together”, i.e., small increments of copper were added (section 5.5.1). Experiments were carried out with initial total chromium concentrations of  $7.4 \cdot 10^{-8}$  M (Fig. 5.32). Standard deviations calculated from the variations between different samples are represented with bars in the figure.

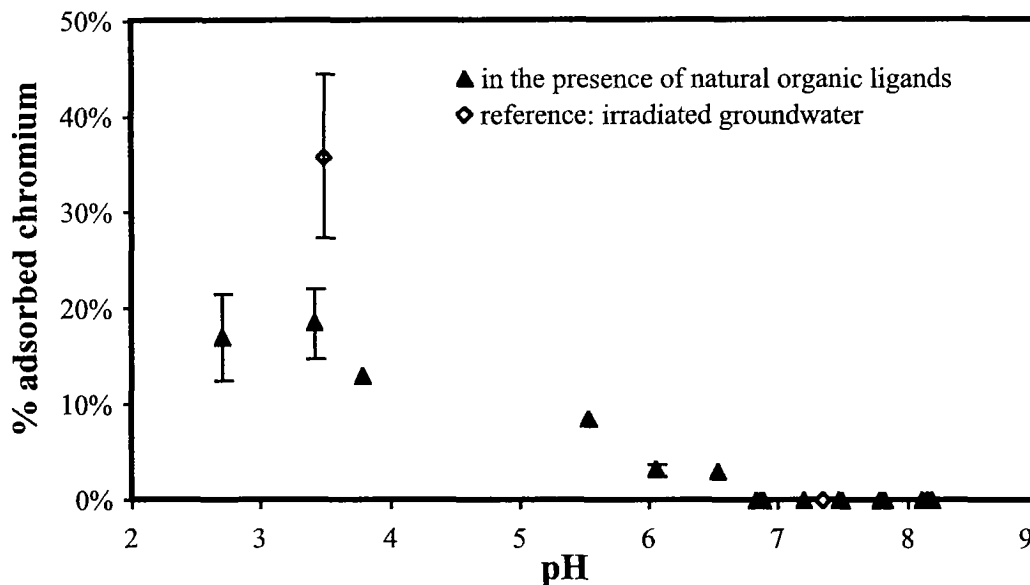


**Fig. 5.32:** Chromium pH adsorption edge on goethite in a natural groundwater matrix. Experiments were performed in the “Cu-DOC-together” system (Sampling campaign May 1999). Total chromium concentration was  $7.4 \cdot 10^{-8}$  M. Adsorption of chromium in the reference (irradiated groundwater) was measured at pH 3.5 and pH 7.35. The standard deviations are represented in the figure.

The shape of the adsorption isotherm corresponded to the adsorption of an anion. This means that chromium was adsorbed most probably as  $H_xCr^{VI}O_4^{x-2}$ . As reference, chromium adsorption was measured at pH 3.5 (average over 7 data points) and pH 7.35 (average over 8 data points) in UV-irradiated groundwater, i.e., in the absence of organic ligands. Mesuere and Fish (1992a and b) have observed that chromate adsorption on goethite was significantly inhibited at low pH values in the presence of oxalate, by increasing the ratio of  $[Ox]_{tot}/[Cr]_{tot}$  from 1 to about 20. The authors have explained this effect by competition reactions between oxalate and chromate for surface sites. A similar type of competition reaction between the adsorption of chromate and the natural organic ligands could possibly be observed in our system, since slightly more chromate was adsorbed in the reference system as in the presence of organic ligands.

In addition, co-adsorption of other inorganic anions like sulphate or phosphate has been reported to mobilise Cr(VI) (Music et al., 1986; Zachara et al., 1987 and 1989), which also possibly explains the relatively low adsorption of Cr(VI) in the irradiated groundwater at low pH.

### ***Adsorption of Lead on Goethite in an Infiltration Groundwater Matrix***

Two lead adsorption edges, determined in the systems “Cu-DOC-together” and “Cd-DOC-together” were performed at a total lead concentration of  $1.9 \cdot 10^{-9}$  M (Fig. 5.33). Standard deviations taking into account the variations between the samples are represented with bars in the figure.

The adsorption edge in the presence of organic ligands was obtained from 4 independent experiments, the adsorption of lead in the reference system at pH 7.35 is an average of 8 independent experimental data points, measured in the UV-irradiated “Cu-DOC-together” system. In this set of experiments, although copper concentration was increased from sample to sample, the fraction of adsorbed lead remained constant, i.e., copper did not influence the adsorption of lead. Similarly, Christl and Kretzschmar (1999) have not observed competition between copper and lead adsorption on hematite and Benjamin and Leckie (1981) could not see any significant competition effects in experiments with Cd, Cu, Zn, and Pb with amorphous iron oxyhydroxide.

At pH 7.35, adsorption of lead on goethite seemed to be decreased in the presence of natural organic ligands, compared to the reference system. Enhanced mobility of lead in the presence of organic ligands was reported by Coughlin and Stone (1995), Jordan et al. (1997) and Mason et al. (1999). Competition reactions with magnesium have been reported for lead (Balistrieri and Murray, 1982), which might explain the fact that also in the reference system only 80% of the total lead concentration was adsorbed. Calcium may thus as well decrease lead adsorption in our system.

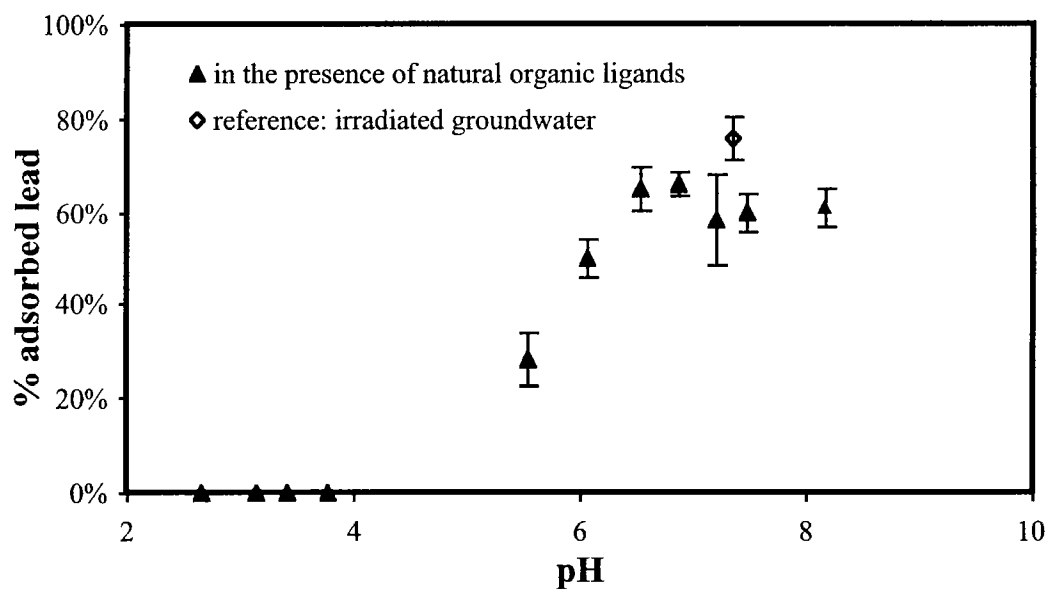


*Fig. 5.33: Adsorption edge of lead on goethite in a natural groundwater matrix. Experiments were performed in the “Cu-DOC-together” system (Sampling campaign May 1999). The adsorption of lead in the reference system (irradiated groundwater) was measured at pH 7.35. Total lead concentration was  $1.9 \cdot 10^{-9}$  M.*

### ***Adsorption of Cobalt on Goethite in an Infiltration Groundwater Matrix***

At typical environmental pH and  $E_H$ -values, cobalt can exist in two oxidation states, Co(II) and Co(III). Co(II) is the predominant oxidation state in natural waters (Qian et al., 1998) and forms strong, but labile complexes. Co(III) can only form strong organic complexes and is associated with particulate matter, especially  $MnO_2$  (Moffett and Ho, 1996; Murray and Dillard, 1979).

The cobalt adsorption edge on goethite was measured in the systems “Cu-DOC-together” and “Ni-DOC-together”, i.e., small increments of copper, and nickel had been added to the system, respectively. Experiments were performed at total concentration of  $9 \cdot 10^{-9}$  M cobalt.

No difference between the adsorption edge measured with natural organic ligands and with the UV-irradiated groundwater could be observed (Fig. 5.34). For pH values above 7, this observation might be explained by the fact that only small concentrations of specific Co(II) ligands were present (Qian et al., 1998) and that these ligands were not capable of mobilising Co(II).

In the acidic pH range, quite a high fraction of cobalt was adsorbed, but again, no difference between the reference and the system with natural organic acids

could be observed. Phosphate can form relatively stable complexes with Co(II) (Bürgisser and Stone, 1997). The cobalt adsorption in the acidic pH range could possibly be explained by the formation of ternary goethite-phosphate-cobalt(II) complexes.

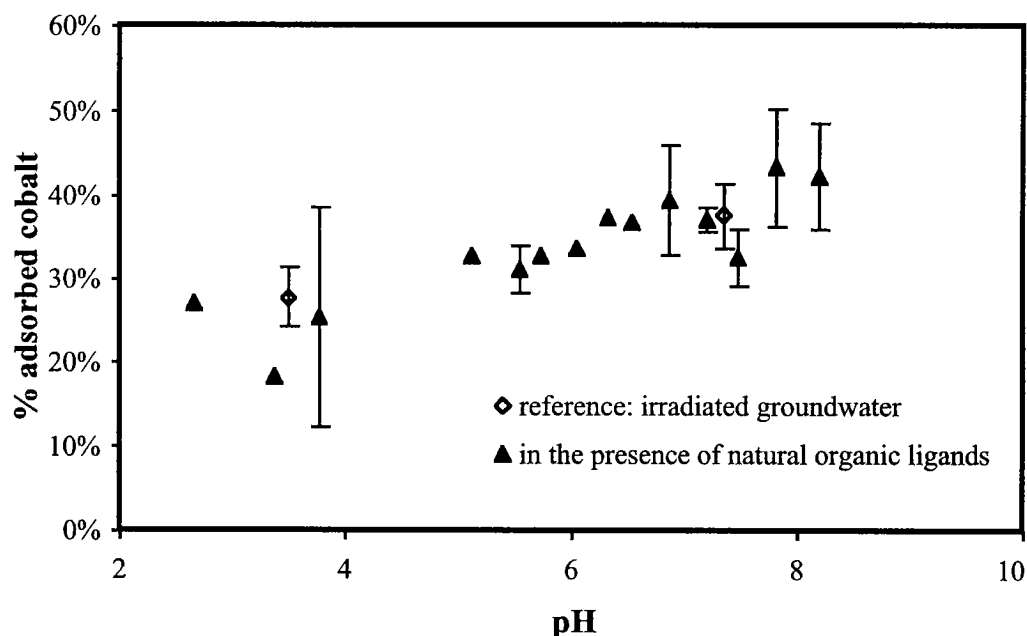


*Fig. 5.34: Cobalt adsorption edge on goethite in a natural groundwater matrix. Experiments were performed in the “Cu-DOC-together” and the “Ni-DOC-together” systems (Sampling campaign May 1999). Total initial cobalt concentration was  $9 \cdot 10^{-9}$  M.*

## 5.13 Discussion of Metal Complexation with Natural Groundwater Organic Ligands

### 5.13.1 Total Ligand Concentration in Natural Groundwater

Free metal concentration in the respective groundwater matrix was calculated assuming that no organic ligands were present. The point, where this curve intercepts the experimental titration curve yields the maximum total copper concentration that the natural ligands are able to complex. Thus the total ligand concentration for this metal can be deduced, assuming the formation of 1:1 metal-ligand complexes.

The total copper ligand concentration could be estimated to be  $1.3 \cdot 10^{-5}$  M (Fig. 5.9). The third ligand  $L_3$  defined in our model, however, was already saturated

at a concentration about  $2.2 \cdot 10^{-6}$  M, and at least one more ligand would have been necessary to define the whole complexation behaviour of the DOC. However, we decided not to introduce more ligands, because they would not be strong complexants, and thus would not have a strong influence on the adsorption of copper onto goethite in our system.

The concentration of complexation groups of all the copper ligands defined with this 3 ligand model amounted to  $1.04 \cdot 10^{-6}$  mol/mg C. This is in the range normally assumed for the concentration of complexation groups in fulvic acids. Cabaniss and Shuman (1988) have found a value of  $16 \cdot 10^{-6}$  mol/mg C and Tipping and Hurley (1992) have defined it with their Model V to be  $7 \cdot 10^{-6}$  mol/mg C. It has to be considered that in the model presented in this study, only part of the ligands was taken into account as the weaker ligands were not fully saturated.

The total ligand concentration in the deep groundwater could not be calculated as the DOC concentration in the deep groundwater was below our detection limit (0.5 mg/L).

The total cadmium ligand concentration was defined to be  $4.4 \cdot 10^{-7}$  M (Fig. 5.20). The concentration of complexation groups of all the cadmium ligands defined with this model amounted to  $1.1 \cdot 10^{-7}$  mol/mg C, which is in the range normally assumed for the concentration of complexation groups in fulvic acids.

The titration curve of nickel was measured in a very narrow concentration range (Fig. 5.24). At these small concentrations, only the stronger ligands were saturated, and therefore the total concentration of the complexation groups could not be estimated.

### 5.13.2 WHAM model calculations

One has to be very careful to compare complexation constants defined with different models. The constants strongly depend on the parameters defined in the model, i.e., number and values of acidity constants, and number of ligands as well as the concentrations of the ligands. One possibility to compare the complexation capacity of the ligands defined in this study with that of other ligands is by doing calculations with the WHAM model. This model defines metal complexation by humic and fulvic acids, which uses a discrete ligand approach. It has been developed by Tipping (1994).

The concentrations of the major cations and anions (calcium, magnesium, sulphate, phosphate, nitrate, and chloride) were considered for calculations. We

assumed that 1 g DOC represented 2 g FA or 2 g HA (Thurman, 1985). Calculations were performed assuming 3 different cases:

- 100 % of the DOC are 100 % FA.
- 100 % of the DOC are 80 % FA and 20 % HA. This is a typical ratio between HA and FA, as it occurs in average waters (Thurman, 1985).
- 100 % of the DOC are 100 % HA.

### ***Complexation of Copper by Natural Organic Ligands***

If we assume that 100 % of the DOC were composed of 100% FA or of 80% FA and 20% HA, the calculated curves could describe the experimental one adequately for total copper concentrations above  $2 \cdot 10^{-7}$  M (Fig. 5.35). For lower concentrations, complexation was underestimated. Similar results have been observed by Xue and Sigg (1999). In a work by Christensen et al. (1999) the complexation of Cu by DOC in a polluted groundwater has been overestimated by WHAM calculations, but this was probably due to the fact that high DOC concentrations (up to 200mg/L) were investigated. The assumption that 100 % of the DOC consist of 100% HA overestimated copper complexation for total copper concentrations above  $2 \cdot 10^{-7}$  M (Fig. 5.35). At lower copper concentrations again, complexation was underestimated, which is a hint for the presence of very strong complexing ligands. These strong ligands were responsible for the total suppression of copper adsorption at low concentrations (Fig. 5.7).

Higher DOC and higher metal concentrations than those in our study were used to develop this model. At high total metal concentrations, the model can describe the data excellently.

### ***Complexation of Cadmium by Natural Organic Ligands***

By assuming that 100 % of the DOC were either 100 % FA or else 80 % FA and 20 % HA, the complexation of cadmium, as calculated by the WHAM model, was slightly underestimated at total cadmium concentrations above  $3 \cdot 10^{-9}$  M, but clearly underestimated at lower concentrations (Fig. 5.36). This is a hint that the strong natural organic ligands in the groundwater were stronger than fulvic acids.

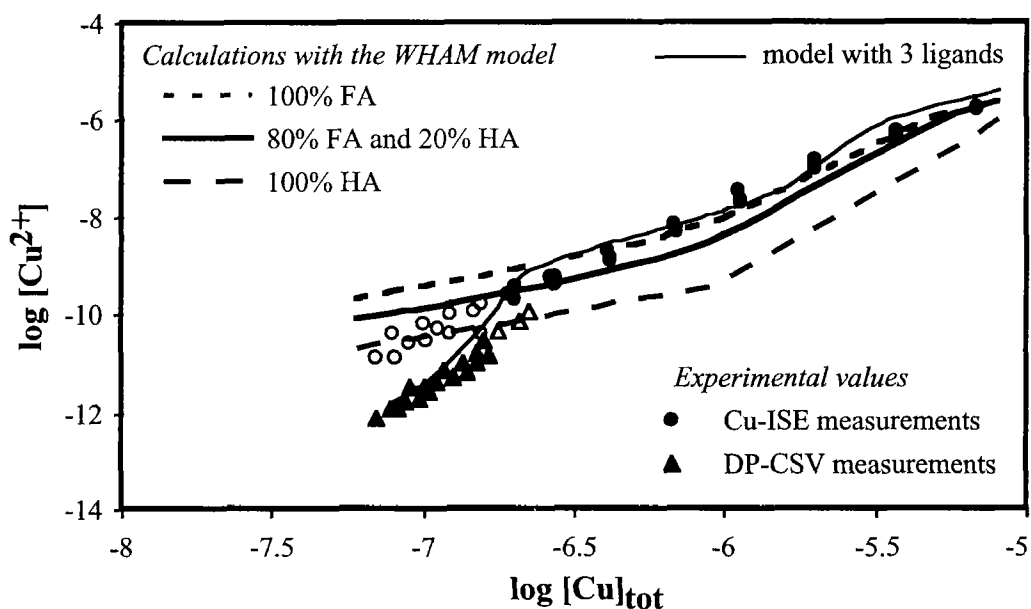


**Fig. 5.35:** Calculation of the titration curve of copper in the infiltration groundwater with the WHAM model. For calculations, it was assumed that 1 mg DOC represented 2 mg FA or HA.

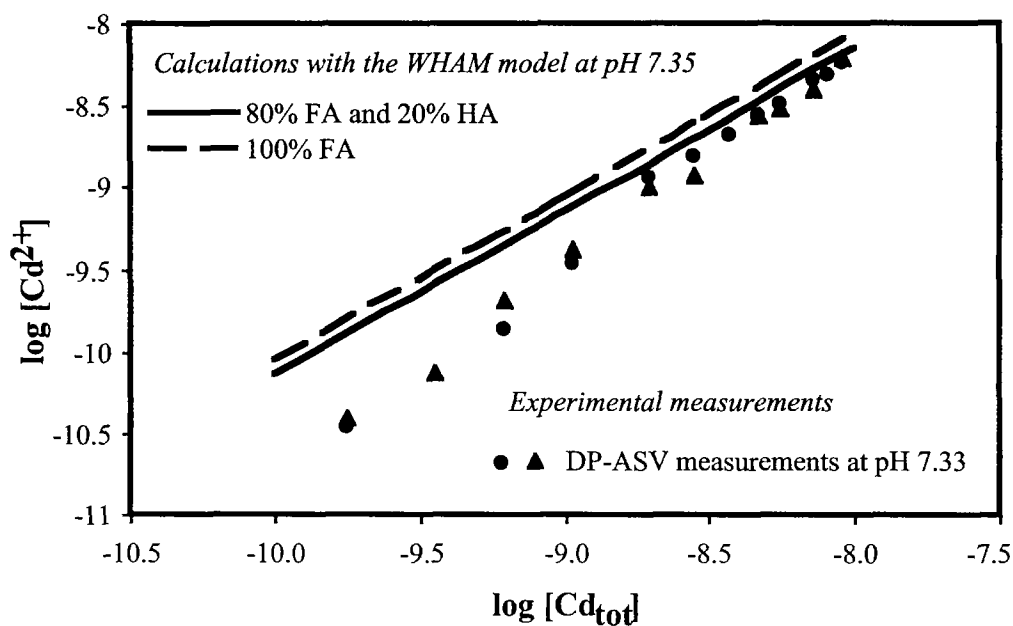


**Fig. 5.36:** Calculation of the titration curve of cadmium in the infiltration groundwater with the WHAM model. For the calculations, it was assumed that 1 mg DOC represented 2 mg FA or HA.

### ***Complexation of Nickel by Natural Organic Ligands***

In the analysed concentration range, the WHAM model completely underestimates the complexation capacity of the natural ligands (Fig. 5.37). At these low total nickel concentrations, ligands were stronger than calculated with the model. These strong ligands were responsible for the suppression of nickel adsorption on goethite in the groundwater matrix (Fig. 5.23).

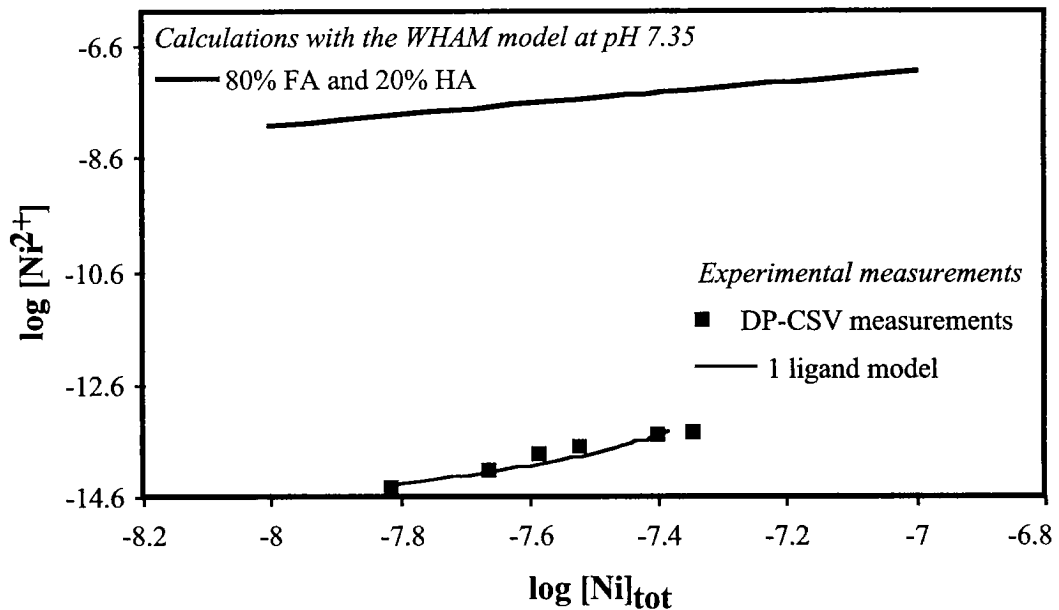


**Fig. 5.37:** Calculation of the titration curve of nickel in the infiltration groundwater with the WHAM model. For the calculations, it was assumed that 1 mg DOC represented 2 mg FA or HA.

### ***pH Dependence of Copper Complexation by Infiltration Groundwater Organic Ligands***

Calculation of the pH dependence of copper complexation by natural organic ligands with the WHAM model underestimated the complexation properties of the ligands at pH values above 7.5. This is again a hint to the presence of strong complexing ligands in our system, and is consistent with the data presented above.



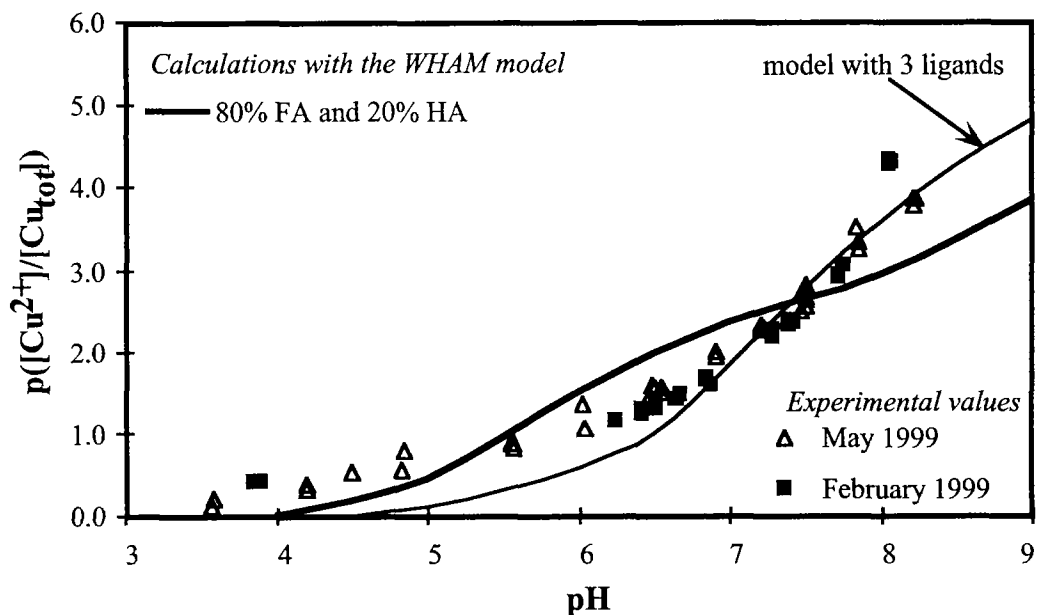


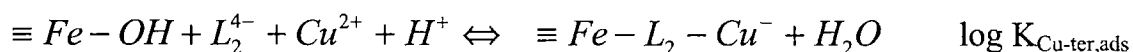
**Fig. 5.38:** pH dependence of copper complexation by natural infiltration groundwater organic ligands. On the y-axis is depicted the negative logarithm of the ratio between the free copper activity and the total copper concentration, i.e., low values mean high free copper concentrations. Measurements were performed with a Cu-ISE by Renata Hari (EAWAG, Dübendorf). Data from May 1999 ( $[Cu_{tot}] = 2 \cdot 10^{-7} M$ ) and February 1999 ( $[Cu_{tot}] = 2.2 \cdot 10^{-7} M$ ) are shown.

## 5.14 Discussion of Metal Adsorption Modelling

### 5.14.1 Formation of Ternary Complexes

The potential formation of ternary complexes is discussed in the system copper-infiltration groundwater organic ligands. Ligands are often adsorbed on the surface at pH values around 7 (Evanko and Dzombak, 1998; Gu et al., 1994, 1995; Nilsson, 1995; Stone, 1988; Stone et al., 1993; Tipping, 1981), and at pH values above 7, these ligands complex copper very strongly (Fig. 5.37). Thus, it can be assumed that these ligands complex copper as well if they are adsorbed on the surface, in other words form ternary complexes of type B. As we wanted to limit the degrees of freedom, we assumed only formation of ternary complexes with  $L_2$  for our model calculations.

For parameter estimation of the equilibrium constant of the ternary complex, the constants listed in Tab. 5.9 were used, with additionally the following reaction:



The constant  $\log K_{\text{Cu-ter,ads}}$  was determined to be 7.99 (WSOS/DF=9.46), and this calculated pH adsorption edge perfectly described the experimental data (data not shown).

The formation of such complexes is of course theoretically possible and they have been postulated by Ali and Dzombak (1996b), Davis and Leckie (1978) and Schindler (1990). Still, one has to be always aware that these model calculations are not a proof for the existence of such ternary complexes. The definition of additional species increases the number of degrees of freedom of the system, which results in a better fit. Boily (1999) has argued that in most systems the formation of ternary complexes of type B is not necessary to define a system. For further investigations, surface spectroscopic measurements would be needed, e.g., EXAFS or ATR-FTIR. However, the low concentrations used in this study were under the detection limit of such methods.

#### **5.14.2 Influence of Phosphate on Metal Adsorption on Goethite**

Metal adsorption in the presence of phosphate was calculated with a DLM model as described in section 5.4.3. Model calculations yielded phosphate adsorption of about 50% at pH 3.5, which was consistent with experimental measurements performed in our system.

According to the calculations, adsorption of both copper and cadmium was enhanced at pH values above 6 in the presence of phosphate (Fig. 5.39 – 5.40). The formation of the phosphate surface species  $\equiv\text{Fe-PO}_4\text{H}^-$  and  $\equiv\text{Fe-PO}_4^{2-}$  could decrease the surface charge enough to enhance electrostatically metal adsorption.

At acidic values, phosphate did not have any influence on copper and cadmium adsorption according to the calculations. Thus the elevated adsorption of copper at pH 3.5 in the presence of phosphate observed in the isotherms (Fig. 5.6) was most probably due to some specific interactions not yet considered in the model. This could also be deduced directly from the experiments, as phosphate did not influence nickel adsorption (section 5.9.1), although copper and nickel are supposed to react in a similar way. Possibly copper-phosphate complexes are very stable, because of the Jahn-Teller distortion of the copper ion (Schosseler, 1998; Schosseler et al., 1997), and can thus adsorb on goethite to form ternary complexes of type B.

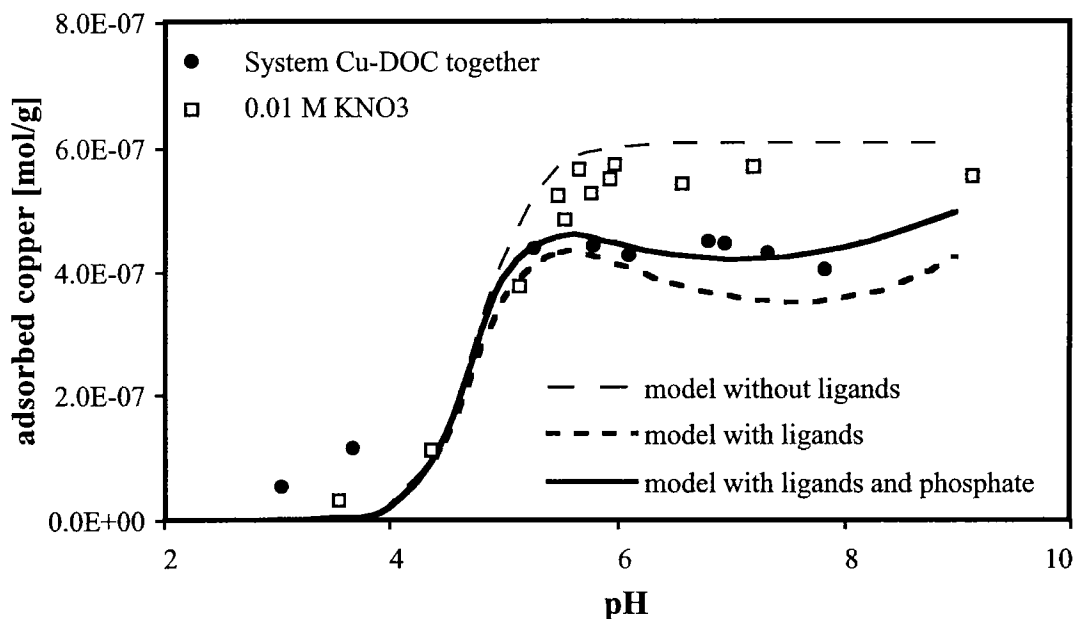


*Fig. 5.39: pH adsorption edge of copper in the presence of organic ligands and phosphate. In this model the adsorption of copper and phosphate on goethite and the complexation of copper by natural organic ligands and phosphate were taken into account. Calculations were performed with the DLM model.*

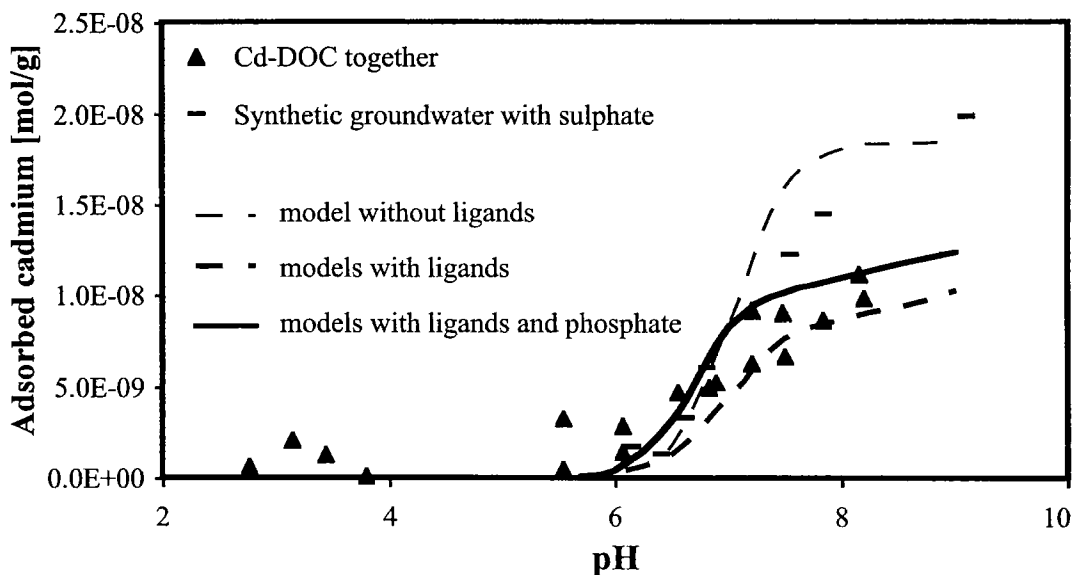


*Fig. 5.40: pH adsorption edge of cadmium in the presence of organic ligands and phosphate. In this model the adsorption of cadmium and phosphate on goethite and the complexation of cadmium by natural organic ligands and phosphate were taken into account. Calculations were performed with the DLM model.*

In opposition to the results obtained in the calculations for copper and cadmium, phosphate seemed to have no influence on the adsorption of nickel onto

goethite (Fig. 5.41). However, these results have to be analysed carefully. Due to adsorption of phosphate, the surface charge is lowered, and as a consequence the surface got a stronger ligand to compete with the solution ligands to complex the metal. This is the reason why adsorption of the metal was enhanced in the presence of phosphate in the copper and cadmium system. For nickel complexation in solution, however, only the strong ligand was defined, and thus no competition reactions between the weaker ligand and the surface functional groups to complex nickel could be considered, and thus nickel adsorption did not increase in our model calculations.

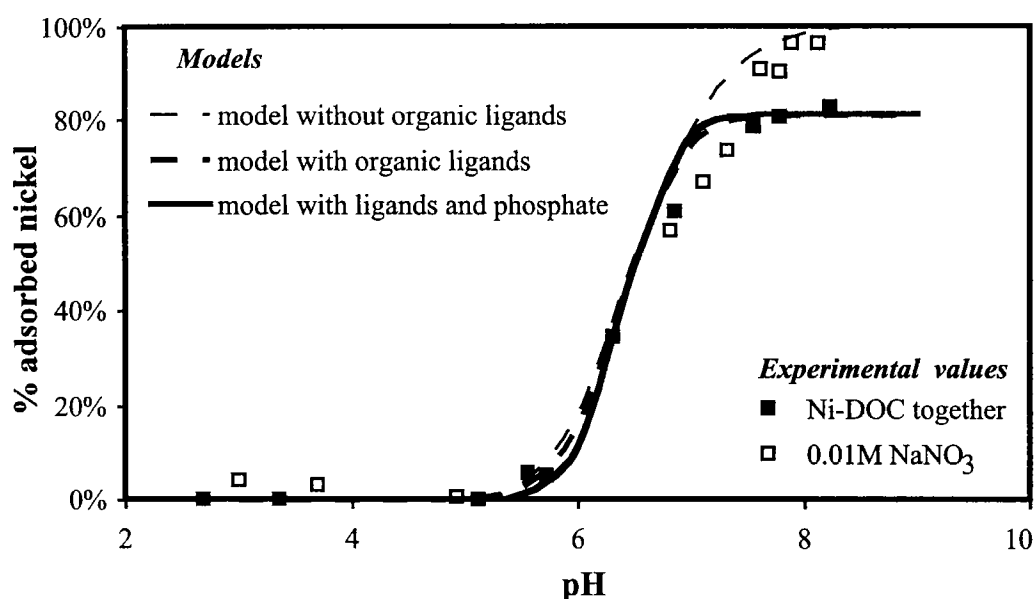


**Fig. 5.41:** pH nickel adsorption edge in the presence of organic ligands and phosphate. In this model the adsorption of nickel and phosphate on goethite and the complexation of nickel by the natural organic ligands and phosphate was taken into account (section 5.4.4).

### 5.14.3 Influence of Calcium and Magnesium on Metal Adsorption on Goethite

Metal adsorption in the presence of organic ligands and calcium was calculated as described in section 5.4.4. Calcium did not interfere with the adsorption of copper according to our calculations (data not shown). This result could be expected, as calcium adsorption was weak, and according to our calculations only about 1 % of the total calcium was adsorbed. The surface site

concentration was in large excess with respect of the adsorbed calcium and copper concentrations. Thus no competition reactions were probable (section 1.4).

Experimentally, the influence of calcium on the copper adsorption could also be checked by comparing the adsorption isotherms obtained in the irradiated and synthetic groundwater with calcium (Fig. 5.7), with the adsorption isotherm in 0.01 M KNO<sub>3</sub> without calcium (Fig. 5.4) (Table 5.11). The amount of copper adsorbed in both systems was nearly equal, so probably, calcium did not have any effect on the adsorption of copper on goethite under these conditions.

**Table 5.11: Influence of calcium on the adsorption of copper**

		Cu-tot [M]	pH	Adsorbed copper [%]
With Ca	Irradiated GW	$3.45 \cdot 10^{-7}$	7.28	94
	Synthetic GW	$2.36 \cdot 10^{-7}$	7.3	92
Without Ca	0.01 M KNO <sub>3</sub>	$3.4 \cdot 10^{-7}$	7.21	93

The calculated cadmium adsorption on goethite, however, clearly decreased in the presence of calcium ([Ca] = 1.89 mM) (Fig. 5.42). Balistreri and Murray (1982) have observed a strong influence of magnesium (0.054 M) on the adsorption of cadmium ([Cd]<sub>tot</sub> =  $3 \cdot 10^{-5}$  M) on goethite. In the presence of magnesium, cadmium adsorption was decreased, which was explained by competition reactions for surface sites. The ratios cadmium/goethite and magnesium/cadmium were similar as in our study, so a negative interaction of magnesium and calcium with the adsorption of cadmium could be expected in our system. Interactions of cadmium adsorption with calcium have also been observed on amorphous iron oxide by Cowan et al. (1991).

Nickel adsorption as well was decreased in the presence of calcium at pH values above 6 (Fig. 5.43). Since surface sites were in excess of the total nickel and calcium concentrations, competition for complexation with the surface sites were unlikely to be responsible for this effect. Possibly calcium could increase the positive charge of the surface and thus electrostatically inhibit nickel adsorption.

The influence of magnesium on metal adsorption was not calculated. However, as magnesium adsorbs a little stronger than calcium (Sigg, 1979), but is present in a lower concentration as calcium, its effect can be predicted to be comparable to the one of calcium.

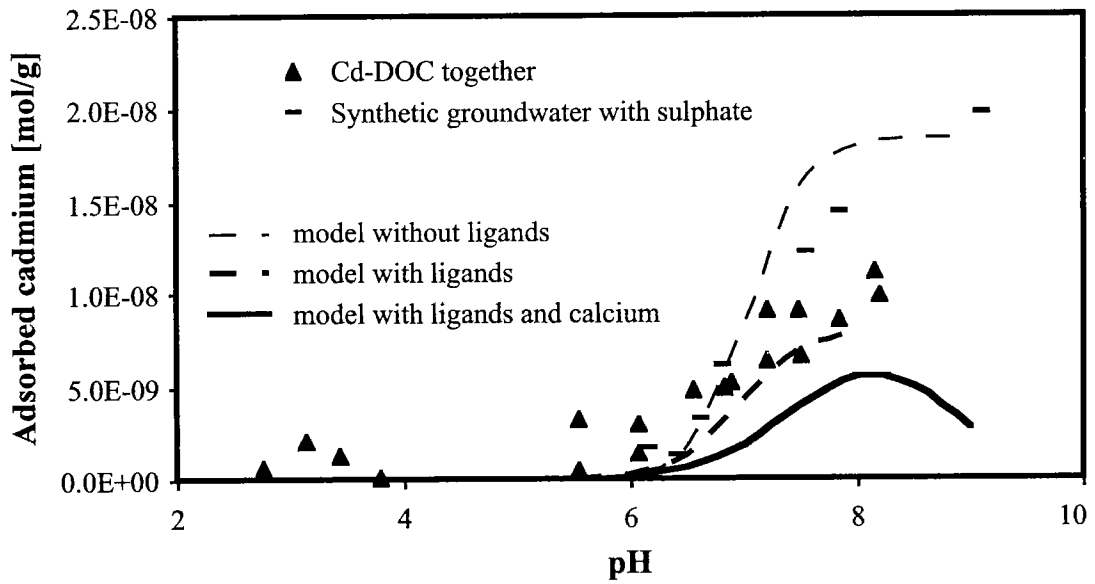


**Fig. 5.42:** pH adsorption edge of cadmium in the presence of infiltration groundwater organic ligands. The interaction of calcium with cadmium adsorption on goethite are analysed. ( $[Cd_{tot}] = 1.3 \cdot 10^{-9} M$ ).

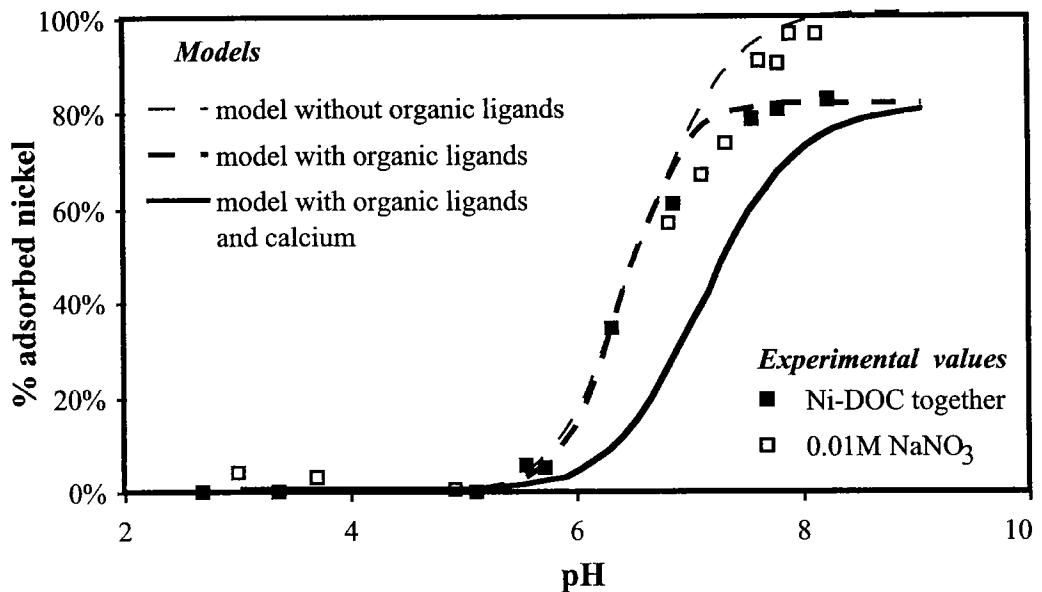


**Fig. 5.43:** pH adsorption edge of nickel in the presence of organic ligands and calcium. In this model, the adsorption of nickel and calcium on goethite and the complexation of nickel by natural organic ligands were considered.

#### 5.14.4 Effect of $\log K_1$ and $[L_1]$ on Metal Adsorption

Complexation in solution could also be described by defining other values for either the complexation constant or the ligand concentration, as long as the product

$\log K \cdot [L]$  remains constant. Metal adsorption, however, varies in function of both the complexation constant and the ligand concentration (Fig. 5.44). Calculations of copper adsorption were performed exactly as described in section 5.4 with the only difference that the values of  $K_1$  and  $[L_1]$  were changed. The product  $\log K_1 \cdot [L_1]$  was kept constant for calculations.

Elevated complexation constants hindered copper adsorption till the corresponding ligand, present only in very small concentrations, was saturated. These isotherms were very steep, as the other ligands  $L_2$  and  $L_3$  were either not strong enough or else not concentrated enough to suppress metal adsorption in a high amount. Elevated concentrations of  $L_1$ , and thus lower complexation constants, clearly decreased the slope of the adsorption isotherm. This means that there are competition reactions between the ligand in solution and the surface in this concentration range.

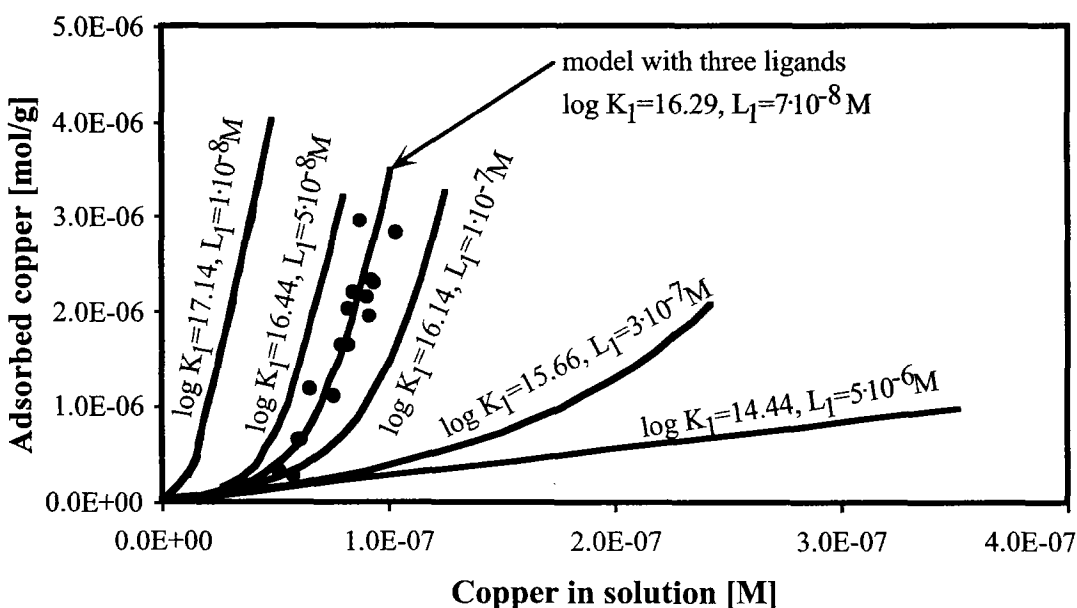


**Fig. 5.44:** Copper adsorption isotherm at pH 7.35 in the presence of infiltration groundwater organic ligands. The dependence of the copper adsorption on goethite in the presence of organic ligands on the complexation constants and the ligand concentration is analysed.

The ligand  $L_1$  was responsible for most ligand effects on metal adsorption. That is why it is interesting to estimate what influence would have either variations of its complexation constant or its concentration on metal adsorption. Calculations were performed with the DLM model as described in section 5.4.

### Effect of $\log K_1$ on Copper Adsorption

Keeping the concentration of the copper ligand  $L_1$  constant ( $[L_1] = 7 \cdot 10^{-8} \text{ M}$ ) and increasing its complexation constant  $\log K_1$  did not effect copper adsorption (data not shown). Thus  $\log K_1$ , as defined in our model, was already so strong that the ligand  $L_1$  was saturated.

As the value of the first complexation constant was decreased ( $[L_1] = 7 \cdot 10^{-8} \text{ M}$ ), competition effects between the ligand and the surface could clearly be observed at a constant of  $\log K_1 = 14.5$  (now complexation strength can be compared to that of the second ligand  $L_2$ ), as the curve was no longer a straight line at pH values above 6. Up to pH 7.9, complexation strength of the ligand was stronger than that of the surface. At pH values above 7.9, the complexation strength of the surface got stronger. Above pH 7.9, the first  $\text{pK}_a$  value of the surface, the concentration of  $\equiv\text{Fe-OH}$  surface species got bigger. If complexation constants were decreased to about 13, the ligand had no longer an effect on copper adsorption (Fig. 5.45). For these calculations, only the ligand  $L_1$  was considered, i.e.,  $L_2$  and  $L_3$  were omitted in order to distinguish the effects of the strong ligands only. As a consequence the adsorption edge became a straight line at pH values above 5, as no competition reactions with the second ligand occurred.

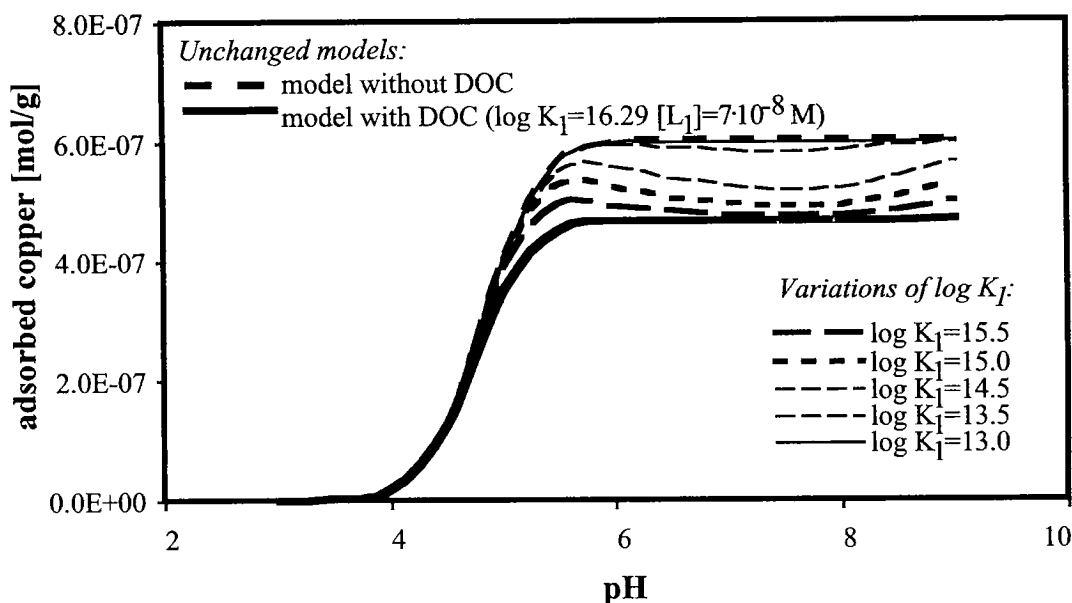


**Fig. 5.45:** pH adsorption edge of copper in the presence of infiltration groundwater organic ligands. The influence of the complexation constant of the strong copper ligand on copper adsorption was analysed.



Changing the concentration of  $L_1$  ( $\log K_1=16.29$ ) had a negative effect on copper adsorption, and at concentrations higher than  $5 \cdot 10^{-7}$  M, all copper was mobilised (Fig. 5.46).

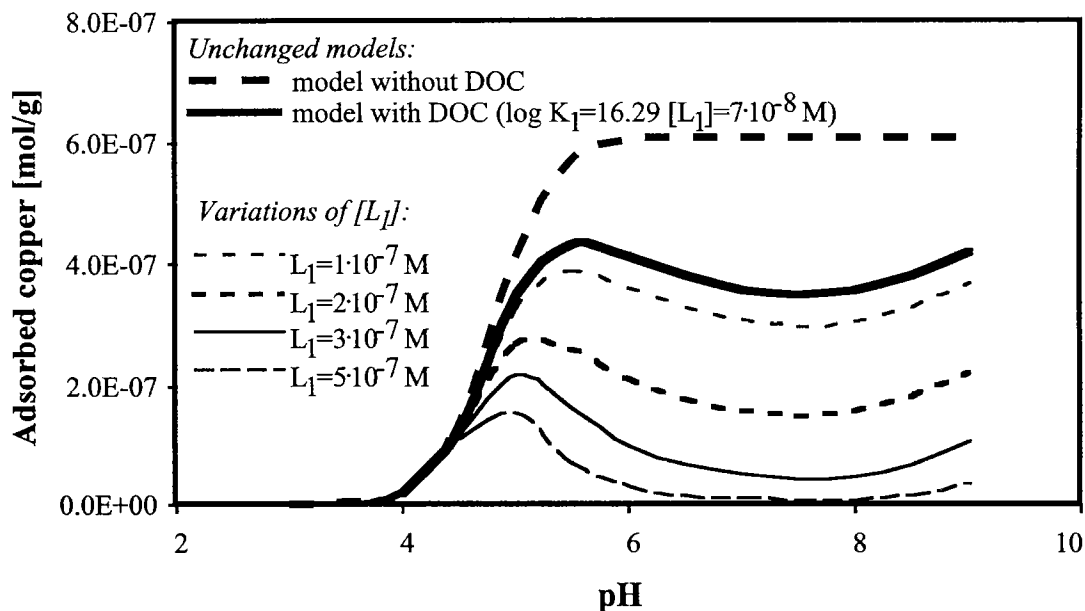


*Fig. 5.46: pH adsorption edge of copper in the presence of infiltration groundwater organic ligands. The influence of the strong ligand concentration on copper adsorption was analysed.*

### **Effect of $[L_1]$ on Cadmium Adsorption**

Keeping the concentration of the ligand  $L_1$  constant ( $[L_1] = 5.36 \cdot 10^{-10}$  M) and increasing its complexation constant, decreased cadmium adsorption (Fig 5.47). If the  $\log K_1$  value was increased to a value between 15 and 16, the strong cadmium ligand  $L_1$  was saturated. Up to this value competition reactions between the strong ligand and the surface occurred. By decreasing the value of  $\log K_1$ , another effect could be observed. At a  $\log K_1$  value of about 12, competition reactions between the second ligand  $L_2$  and the strong ligand occurred and adsorption was no longer affected by variations of the strong ligand.

Increasing the concentration of  $L_1$  had a negative effect on cadmium adsorption. At concentrations above  $1 \cdot 10^{-8}$  M, all cadmium was complexed by the organic ligands (Fig. 5.48).

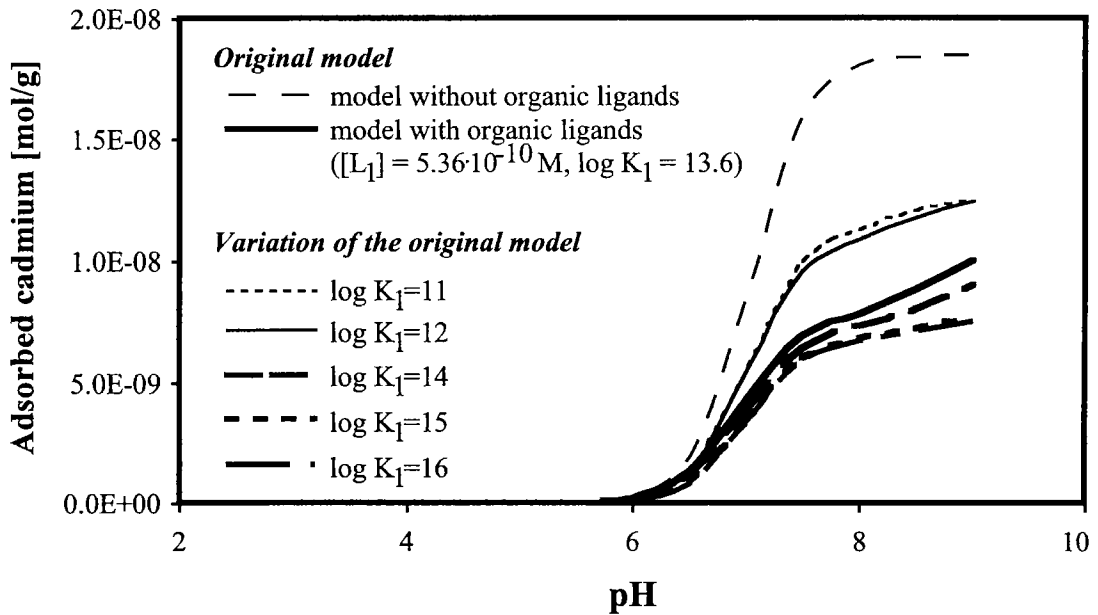


*Fig. 5.47: pH cadmium adsorption edge in the presence of infiltration groundwater organic ligands. The influence of the complexation constant of the strong cadmium ligand on the adsorption of cadmium on goethite is analysed.*

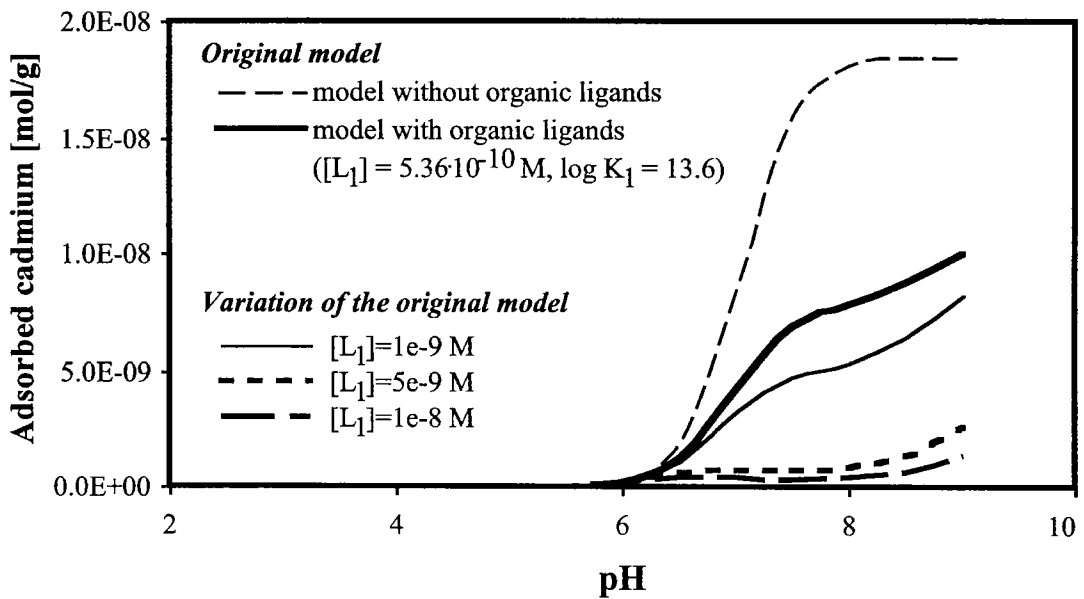


*Fig. 5.48: pH cadmium adsorption edge in the presence of infiltration groundwater organic ligands. The influence of the concentration of the strong cadmium ligand on the adsorption of cadmium on goethite is analysed.*

## 5.15 Conclusions

A total inhibition of adsorption due to organic ligands which was found in this study at low metal concentrations had not been observed till now. A first explanation may be that most studies were carried out at higher copper concentration, where this effect was camouflaged due to saturation of strong, specific ligands. Another explanation would be that most studies were carried out with the humic or the fulvic fraction. However, the strong complexation capacities necessary for this effect could not be observed in this fraction (Xue and Sigg, 1999). This result was also shown by calculations with the WHAM model.

Nothing more is known about the structure and nature of these strong organic ligands, but we have to keep in mind, that also anthropogenic ligands, like e.g., EDTA, were present in this groundwater (Tab. 5.2). EDTA is known to be a strong complexant, and it could be possible, that adsorption inhibition at low metal concentrations was at least partly due to this strong ligand. Nowack et al. (1997) made studies in the same infiltration groundwater and showed that CuEDTA complexes were present in this groundwater. Less NiEDTA complexes were found than expected according to equilibrium calculations. At  $\text{pH} > 7$ , remobilization of adsorbed metals by exchange with Fe(III)-EDTA is thus possible.

No ternary complexes were needed to model metal adsorption in the presence of natural organic ligands. Probably the strong organic ligands  $L_1$  are low-molecular weight ligands, which do not have a high affinity for the surface at higher pH values. Further on the complexation with the metals in solution may keep this ligand in solution. The weaker ligands probably are higher molecular weight organic ligands and adsorb on the surface. However, as goethite is a very strong adsorbent, metals preferentially react with the surface functional groups instead with the adsorbed organic ligands.

## *Summary and Outlook*

The goal of this study was to find a method that allows the systematic description of the influence of organic ligands on the adsorption of copper, cadmium, and nickel. For this purpose, experiments were performed with simple organic ligands as well as with natural, unfractionated organic material. It was our aim to show that complex natural systems could as well be described by simple models and it will be shown in section 6.1 that the behaviour of the natural organic ligands can be compared to that of simple organic ligands. The present laboratory experimental results were important to study on the one hand the competition between adsorption and aqueous complexation reactions, and on the other hand electrostatic interaction of metal cations by adsorbed ligands. The significance and applicability of the results in environmental systems will be discussed in section 6.2. However, limitations to transfer the information from the laboratory experiments to the transport of metals in a natural groundwater still exist. An outlook to further studies necessary to understand such a complex system will be given in section 6.3.

### **6.1 Main Results**

In a first part, experiments were performed with simple organic ligands (oxalate, salicylate, and pyromellitate). As a summary of the adsorption experiments, following statements could be made. Salicylate, which is the weakest ligand, had no pronounced effect on heavy metal adsorption. Oxalate, a strong complexant, tended to suppress metal adsorption. Pyromellitate, because of favourable position of the functional groups and strong complexation capacities, formed in addition to complexation in solution also ternary surface complexes.

The influence of these ligands on the adsorption of metals could be described by simple models, which were refined by successive addition of surface reactions.

*First*, metal adsorption estimations started with the most simple model, considering only metal adsorption and complexation of the metal in solution. This model described competition reactions between the organic ligands in solution and the surface functional groups. Calculations performed with this model underestimated metal adsorption in the presence of strong ligands. However, in the presence of weak ligands, like salicylate, the description of metal adsorption was adequate.

*Secondly*, ligand adsorption was included into the model. In this way, the electrostatic attraction of the metal by the adsorbed ligand could be described. In all systems, the calculated adsorption edge was shifted to the left of the one estimated with the first model, but still metal adsorption was underestimated in the oxalate and pyromellitate systems.

*Thirdly*, formation of ternary surface complexes of type A and B was assumed. Adsorption of copper in the pyromellitate system and of nickel in the oxalate system could be described by ternary surface complexes of type B, whereas copper adsorption in the salicylate system could be improved by assuming a ternary surface complex of type A. The advantage of this stepwise modelling method is that the single effects of the ligands on metal adsorption, i.e., competition reactions, electrostatic and specific interactions on the surface could be separately defined .

In a second part, experiments were carried out with natural infiltration groundwater ligands. The experiments were performed with batch laboratory experiments, where the conditions were kept as close as possible to the environmental ones, by using an unfractionated DOC and by keeping DOC as well as metal concentrations close to environmental conditions. All these experiments could be interpreted in a similar way to above described experiments, using a discrete model taking into account the complexation behaviour of the dissolved organic ligands and a surface complexation model for the description of the metal adsorptions. Using these two modules, all metal adsorption data could be described adequately. The major influence of the organic ligands on metal adsorption, i.e., suppression of metal adsorption at low metal concentrations, was explained by a very strong specific ligand ( $L_1$ ). The presence of weaker ligands ( $L_2$  and possibly  $L_3$ ) did not affect adsorption in a pronounced way. Concentrations and complexation properties of these ligands were determined from metal titration curves.

Surprising is the fact that no ternary surface complexes with the natural organic ligands had to be invoked to explain the results. Similar results could have been expected with these multifunctional ligands as with pyromellitate. This observation can be explained by analysing the properties of the organic ligands. The weaker ligands  $L_2$  and  $L_3$  are expected to sorb onto the goethite surface. Their molecular weight distribution can probably be compared to that of high molecular weight humic acids, which have a great affinity for the surface. The surface functional groups, which are in excess of the organic ligand and metal concentrations, compete with the adsorbed ligands for complexation of the metal. As goethite is a very strong adsorbent, metals preferentially adsorb onto the free goethite functional groups (Lewis base) rather than complex to the organic ligands. The strong ligand  $L_1$ , on the other hand, is probably of lower molecular weight. As a consequence, it does not have a high affinity for the surface at high pH values, but forms instead complexes with the metals in solution and in this way decreases adsorption.

Combining the results obtained in the presence of natural organic ligands with those obtained in the presence of simple organic ligands, it can be concluded that the influence of DOC on copper adsorption in our system can be described by a model system including salicylate at a concentration which equals the sum of the concentrations of the weak ligands  $L_2$  and  $L_3$  and an additional strong ligand,  $L_1$ . Calculations were performed in the natural system with copper, where the ligands  $L_2$  and  $L_3$  were replaced by salicylate ( $[\text{salicylate}] = 2.3 \cdot 10^{-6} \text{ M}$ ). The ligand  $L_1$  was included unchanged into the model, i.e.,  $[\text{L}_1] = 7 \cdot 10^{-8} \text{ M}$  and  $\log K_1 = 16.3$  (Fig. 6.1).

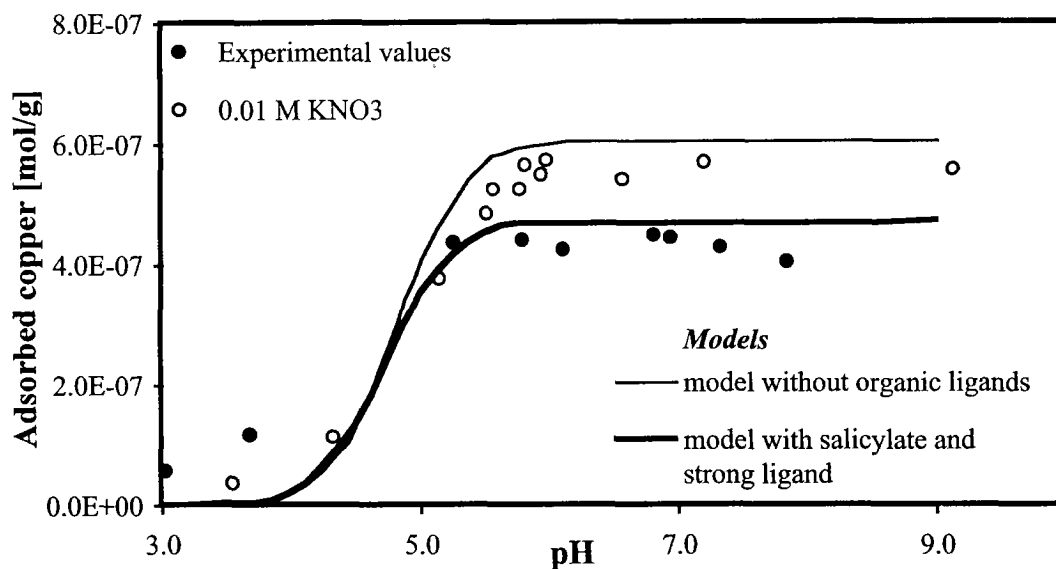


*Fig. 6.1: pH adsorption edge of copper in the presence of infiltration groundwater organic ligands in comparison to adsorption in absence of organic ligands. Modelling of copper adsorption in the presence of natural organic ligands was performed by representing the weak natural organic ligands  $L_2$  and  $L_3$  by salicylate and by considering additionally a strong organic ligand  $L_1$ .*

## 6.2 Environmental Significance

The infiltration groundwater used in this study comes from the river Glatt and can be considered to be typical for the Swiss plateau. Typical agglomerations and industrial areas within the Glatt catchment area and several water treatment plants discharge their water into the river. Thus, the composition of the river water, and as a consequence, that of the infiltration groundwater, can be considered to be representative of many other groundwaters that are in contact with anthropogenically slightly contaminated surface waters.

The solid phase goethite used as adsorbent in this study can adequately represent sorbents in natural groundwater systems. Fe(II), which may be formed in reduced spots, is reoxidized again once it comes into contact with oxygenated water. Fe(III), which is formed by this oxidation reaction, precipitates as amorphous iron (hydr)oxide. Iron (hydr)oxides are often found as coatings on other minerals. They are excellent sorbents, which can well be represented by goethite.

As the flow rate in natural groundwaters is normally quite small, it can be assumed in a first estimation, that our results from the batch experiments are also applicable to a natural aquifer system. In the groundwater, analysed in this study, with quite a low DOC content, metal adsorption is strongly suppressed at low metal

concentrations due to complexation of the metal by the dissolved ligands. Once these strong aqueous organic ligands are saturated, metals adsorb onto the surface, as the surface functional groups become then the strongest complexants. At ambient metal concentrations of the Glatt groundwater, metals would be complexed by the strong ligand  $L_1$  and thus would probably be mobilised. The nature of these strong ligands, responsible in our system for mobilisation, is yet unknown. They may either be natural ligands of low molecular weight, or else anthropogenic organic ligands, as e.g., EDTA or NTA (Nowack et al., 1997).

Further on, metal mobilisation depends on the ratio ligand to metal. Although humic substances are considered to be weaker ligands, mobilisation of metals in waters rich in humic substances is still possible.

As a consequence, metals, which are previously immobilised in a soil, can be remobilised due to the presence of strong organic ligands. Thus they may become bioavailable and toxic to certain organisms or may reach deeper groundwater systems.

### 6.3 Limitations and Outlook

One major limitation in this study is that no information is available on the structure of the surface complexes formed. In order to refine the models, however, more mechanistic information would be of prime importance. Thus, it would be helpful to do surface spectroscopic and microscopic measurements at least on the model ligands. With these analyses, it could be deduced whether innersphere or outersphere surface complexes were formed and whether there was formation of ternary surface complexes.

In order to better represent reactions in natural groundwater systems, the kinetics of the interactions between metals, ligands, and solid phases have also to be considered. The best way to do this would be to carry out column experiments. Of main interest would be experiments, where the order of addition of the components into the columns was changed. This would give information under which conditions adsorbed metal cations could be remobilised by organic ligands. As metals get bioavailable or may reach deep groundwaters, this knowledge would be of high importance in the study of the environmental impact of heavy metals in groundwater systems.

In order to be able to describe other groundwater sites as well, e.g., with higher DOC content, older groundwaters, or acidic groundwaters, more knowledge



---

should be obtained about DOC, as the properties of the organic ligands play an essential role in the distribution of heavy metals. This is a very difficult task, but redoing similar experiments as in this study with DOC coming from different groundwater sites would be helpful. Further characterisation of DOC, like e.g., molecular weight distribution and the characterisation of functional groups, would be interesting.

# References

## A

- Achterberg E. P. and van den Berg C. M. G. (1997) Chemical Speciation of Chromium and Nickel in the Western Mediterranean. *Deep Sea Research II* **4**(3-4), 693-720.
- Aiken G. R., McKnight D. M., Wershaw R. L., and Mac Carthy P. (1985) *Humic Substances in Soil, Sediment, and Water. Geochemistry, Isolation, and Characterization*. John Wiley & Sons. New York.
- Ali M. and Dzombak D. (1996a) Effects of simple organic acids on sorption of  $\text{Cu}^{++}$  and  $\text{Ca}^{++}$  on goethite. *Geochim. Cosmochim. Acta* **60**(2), 291-304.
- Ali M. and Dzombak D. A. (1996b) Competitive Sorption of Simple Organic Acids and Sulfate on Goethite. *Environ. Sci. Technol.* **30**(4), 1061-1071.
- Ali M. A. and Dzombak D. A. (1996c) Interactions of copper, organic acid, and sulfate in goethite suspensions. *Geochim. Cosmochim. Acta* **60**(24), 5045-5053.
- Allison J. D. and Perdue E. M. (1994) Modelling metal-humic interaction with MinteqA2. In *Humic Substances in the Global Environment and Implications on Human Health* (ed. N. Senesi and T. M. Miano), pp. 927-942. Elsevier Science B. V.
- Amtsblatt der Europäischen Gemeinschaften. (1999) Gemeinsamer Standpunkt (EG) Nr. 41/1999. Das Europäische Parlament und der Rat der Europäischen Union.
- Anderson M. and Morel F. M. M. (1982) The influence of aqueous iron chemistry on the uptake of iron by the coastal diatom *Thalassiosira weissflogii*. *Limnol. Oceanogr.* **27**, 789-813.
- Angove M., J., Wells J. D., and Johnson B. B. (1999) Adsorption of cadmium(II) onto goethite and kaolinite in the presence of benzene carboxylic acids. *Colloids and Surf. A: Physicochemical and Engineering Aspects* **146**, 243-251.
- Avdeef A., Zabronsky J., and Stuting H. H. (1983) Calibration of Copper Ion Selective Electrode Response to pCu 19. *Anal. Chem.* **55**, 298-304.

## B

- Balistreri L. S. and Murray J. W. (1982) The Adsorption of Cu, Pb, Zn, and Cd on goethite from major ion seawater. *Geochim. Cosmochim. Acta* **46**, 1233 - 1265.
- Bartschat B. M., Cabaniss S. E., and Morel F. M. M. (1992) Oligoelectrolyte Model for Cation Binding by Humic Substances. *Environ. Sci. Technol.* **26**(2), 284-294.
- Behra Ph. (1986) Evidences for the Existence of a Retention Phenomenon During the Migration of a Mercurial Solution Through a Saturated Porous Medium. *Geoderma* **38**, 209-222.

- Benedetti M. F., Milne C. J., Kinniburgh D. G., van Riemsdijk W. H., and Koopal L. K. (1995) Metal Ion Binding to Humic Substances: Application of the Non-Ideal Competitive Adsorption Model. *Environ. Sci. Technol.* **29**(2), 446-457.
- Benedetti M. F., van Riemsdijk W. H., and Koopal L. K. (1996) Humic Substances considered as a Heterogeneous Donnan Gel Phase. *Environ. Sci. Technol.* **30**(6), 1805-1813.
- Benjamin M. and Leckie J. O. (1981) Competitive Adsorption of Cd, Cu, Zn, and Pb on Amorphous Iron Oxyhydroxide. *J. Colloid Interface Sci.* **86**(2), 410-419.
- Benjamin M. M. and Leckie J. O. (1982) Effects of Complexation by Cl, SO<sub>4</sub>, and S<sub>2</sub>O<sub>3</sub> on Adsorption Behavior of Cd on Oxide Surfaces. *Environ. Sci. Technol.* **16**(3), 162-170.
- Benyahya L. and Garnier J.-M. (1999) Effect of Salicylic Acid upon Trace-Metal Sorption (Cd(II), Zn(II), Co(II), and Mn(II)) onto Alumina, Silica, and Kaolinite as a Function of pH. *Environ. Sci. Technol.* **33**(9), 1398-1407.
- Biber M. and Stumm W. (1994) An In-Situ ATR-FTIR Study: The Surface Coordination of Salicylic Acid on Aluminium and Iron(III) Oxides. *ES&T* **28**(5), 763-768.
- Bockris J. O. M. and Reddy A. K. N. (1976) *Modern Electrochemistry*. A Plenum/Rosetta Edition, New York.
- Boily J.-F. (1999) A Refined Multisite Complexation Model for Cd(II) Surface Complexes on Goethite Particles of different Surface Areas. Ph.D. thesis, Umeå University, Sweden.
- Boily J.-F. and Fein J. B. (1996) Experimental study of cadmium citrate co-adsorption onto  $\alpha$ -Al<sub>2</sub>O<sub>3</sub>. *Geochim. Cosmochim. Acta* **60**(16), 2929-2938.
- Boily J. F., Persson P., and Sjöberg S. (2000) Benzenecarboxalate Surface Complexation at the Goethite/Water Interface.III. The Influence of Particle Surface Area and the Significance of Modelling Parameters. *J Colloid Interface Sci* **227**, 132-140.
- Boily J. F., Nilsson N., Persson P., and Sjöberg S. (2000) Benzenecarboxylate Surface Complexation at the Goethite/Water Interface: I. A Mechanistic Description of Pyromellitate Surface Complexes from the Combined Evidence of Infrared Spectroscopy, Potentiometry, Adsorption Data, and Surface Complexation Modeling. *Langmuir* **16**, 5719-5729
- Bonnissel-Gissinger P., Alnot M., Lickes J.-P., Ehrhardt J.-J., and Behra P. (1999) Modeling the Adsorption of Mercury(II) on (Hydr)oxides II: Goethite and Amorphous Silica. *J. Colloid Interface Sci.* **215**, 313-322.
- Bourg A. C. M., Joss S., and Schindler P. W. (1979) Ternary Surface Complexes 2. Complex Formation in the System Silica-Cu(II)-2,2'-Bipyridyl. *Chimia* **33**(1), 19-21.
- Bourg A. C. M. and Schindler P. W. (1979) Ternary Surface Complexes. 1. Complex Formation in the System Silica-Cu(II)-Ethylenediamine. *Chimia* **32**(5), 166-168.
- Bowers A. R. and Huang C. P. (1986) Adsorption Characteristics of Metal-EDTA Complexes onto Hydrous Oxides. *J. Colloid Interface Sci.* **110**(2), 575-590
- Brown G. E. (1990) Spectroscopic Studies of Chemisorption Reaction Mechanisms at Oxide-Water Interfaces. In *Reviews in Mineralogy, Mineral-Water Interface Geochemistry (Mineral Society of America, Washington, D. C.) Vol. 23*, Vol. 23 (ed. M. F. Hochella and A. F. White), pp. 309-363.

- Bryce A. L., Kornicker W. A., and Elzerman A. W. (1994) Nickel Adsorption to Hydrous Ferric Oxide in the Presence of EDTA: Effects of Component Addition Sequence. *Environ. Sci. Technol.* **28**(13), 2353-2359.
- Buffle J. (1984) Natural Organic Matter and Metal-Organic Interactions in Aquatic Systems. In *Metal Ions in Biological Systems*, Vol. 18 (ed. H. Sigel), pp. 165-213.
- Buffle J. (1988) *Complexation Reactions in Aquatic Systems-an Analytical Approach*. John Wiley & Sons. New York.
- Buffle J. and Altmann R. S. (1987) Interpretation of Metal Complexation by Heterogeneous Complexants. In *Aquatic Surface Chemistry. Chemical Processes at the Particle-Water Interface* (ed. W. Stumm). John Wiley & Sons. New York.
- Bürgisser C. S. and Stone A. T. (1997) Determination of EDTA, NTA, and Other Amino Carboxylic Acids and Their Co(II) and Co(III) Complexes by Capillary Electrophoresis. *Environ. Sci. Technol.* **31**(9), 2656-2664.

**C**

- Cabaniss S. E. and Shuman M. S. (1988a) Copper binding by dissolved organic matter: I. Suwannee River fulvic acid equilibria. *Geochim. Cosmochim. Acta* **52**, 185-193.
- Cabaniss S. E. and Shuman M. S. (1988b) Copper binding by dissolved organic matter: II. Variation in type and source of organic matter. *Geochim. Cosmochim. Acta* **52**, 195-200.
- Christensen J. B., Botma J. J., and Christensen T. H. (1999) Complexation of Cu and Pb by DOC in Polluted Groundwater: A Comparison of Experimental Data and Predictions by Computer Speciation Models (WHAM and MINTEQA3). *Wat. Res.* **33**(15), 3231-3238.
- Christensen J. B. and Christensen T. H. (1999) Complexation of Cd, Ni, and Zn by DOC in Polluted Groundwater: A Comparison of Approaches Using Resin Exchange, Aquifer Material Sorption, and Computer Speciation Models (WHAM and MINTEQA2). *Environ. Sci. Technol.* **33**(21), 3857-3863.
- Christensen J. B., Jensen D. L., and Christensen T. H. (1996) Effect of Dissolved Organic Carbon on the Mobility of Cadmium, Nickel and Zinc in Leachate Polluted Groundwater. *Wat. Res.* **30**(12), 3037-3049.
- Christl I. and Kretzschmar R. (1999) Competitive sorption of copper and lead at the oxide-water interface: Implications for surface site density. *Geochimica et Cosmochimica* **63**(19/20), 2929-2938.
- Collins C. R., Ragnarsdottir K. V., and Sherman D. M. (1999) Effect of inorganic and organic ligands on the mechanism of cadmium sorption to goethite. *Geochim. Cosmochim. Acta* **63**(19/20), 2989-3002.
- Cornell R. M. and Schwertmann U. (1996) *The Iron Oxides. Structure, Properties, Reactions, Occurrence and Uses*. VCH Weinheim.
- Coughlin B. R. and Stone A. T. (1995) Nonreversible adsorption of divalent metal ions (Mn(II), Co(II), Ni(II), Cu(II), and Pb(II)) onto goethite: effects of acidification, Fe(II) addition, and picolinic acid addition. *Environ. Sci. Technol.* **29**(9), 2445-2455.

Cowan C., Zachara J., and Resch C. T. (1991) Cadmium Adsorption on Iron Oxides in the Presence of Alkaline-Earth Elements. *Environ. Sci. Technol.* **25**(3), 437-446.

## D

Dalang F., Buffle J., and Haerdi W. (1984) Study of the Influence of Fulvic Substances on the Adsorption of Copper(II) Ions at the Kaolinite Surface. *Environ. Sci. Technol.* **18**(3), 135-141.

Davis A. P. and Bhatnagar V. (1995) Adsorption of Cadmium and Humic Acid onto Hematite. *Chemosphere* **30**(2), 243-256.

Davis J. A. and Kent D. B. (1990) Surface Complexation Modeling in Aqueous Geochemistry. In *Reviews in Mineralogy, Mineral-Water Interface Geochemistry (Mineralogical Society of America, Washington, D. C.) Vol. 23* (ed. M. F. Hochella and A. F. White).

Davis J. A. and Leckie J. O. (1978) Effect of Adsorbed Complexing Ligands on Trace Metal Uptake by Hydrrous Oxides. *Environ. Sci. Technol.* **12**, 1309-1315.

Davis J. A. and Leckie J. O. (1979) Correspondence. *Environ. Sci. Technol.* **13**(10), 1289-1291.

Ding M., DeJong B. H. W. S., Roosendaal S. J., and Vredenberg A. (2000) XPS studies on the electronic structure of bonding between solid and solutes: Adsorption of arsenate chromate, phosphate, Pb<sup>2+</sup>, and Zn<sup>2+</sup> ions on amorphous black ferric oxyhydroxide. *Geochim. Cosmochim. Acta* **64**(7), 1209-1219.

Dobbs J. C., Susetyo L. A., Knight F. E., Carreira L. A., and Azarraga V. (1989) Characterisation of Metal Binding Sites in Fulvic Acids by Lanthanide Ion Probe Spectroscopy. *Anal. Chem.* **61**, 483-488.

Dzombak D. A., Fish W., and Morel F. M. M. (1986) Metal-Humate Interactions. 1. Discrete Ligand and Continuous Distribution Models. *Environ. Sci. Technol.* **20**(7), 669-675.

Dzombak D. A. and Morel F. M. M. (1990) *Surface Complexation Modeling. Hydrrous Ferric Oxide*. John Wiley & Sons. New York.

## E

Ehrhardt J. J. (Ed). (1999) Proceedings of the Meeting on "Réactivité de surface de goethites". Organisation: GDR CNR PRACTIS-Nancy-May 2 1999. Laboratoire de Chimie Physique pour l'Environnement, Nancy.

Elliott H. A. and Huang C. P. (1979) The Adsorption Characteristics of Cu(II) in the Presence of Chelating Agents. *J. Colloid Interface Sci.* **70**(1), 29-45.

Evanko C. R. and Dzombak D. A. (1998) Influence of Structural Features on Sorption of NOM-Analogue Organic Acids to Goethite. *Environ. Sci. Technol.* **32**(19), 2846-2855.

Evanko C. R. and Dzombak D. A. (1999) Surface Complexation Modeling of Organic Acid Sorption to Goethite. *J. Colloid Interface Sci.* **214**, 189-206.

## F

Filius J. D., Hiemstra T., and Van Riemsdijk W. H. (1997) Adsorption of Small Weak Organic Acids on Goethite: Modeling of Mechanisms. *J. Colloid Interface Sci.* **195**, 368-380.

Fischer L., Brümmer G. W., and Barrow N. J. (1997) Einfluss der Kristallinität von Goethiten auf die Adsorption und Diffusion verschiedener Metalle. *Mitteilgn. Dtsch. Bodenkundl. Gesellsch.* **85**(111), 1501-1504.

Fischer L., Brümmer G. W., and Barrow N. J. (1998) Zur Kinetik der Sorption von Schwermetallen an Bodenkomponenten. I. Sorptions- und Diffusionsprozesse an/in Goethitpartikeln. *Mitteilgn. Dtsch. Bodenkundl. Gesellsch.* **88**, 171-174.

## G

Gerth J. and Brümmer G. (1981) Effect of temperature and reaction time on the adsorption of nickel, zinc, and cadmium, by goethite. *Mitteilungen der Deutschen Bodenkundlichen Gesellschaft* **32**, 229-238.

Giammar D. E. and Dzombak D. A. (1998) Copper complexation with the mellitic acid series. *Journal Of Solution Chemistry* **27**(1), 89-105.

Greenwood N. N. and Earnshaw A. (1985c) Zinc, Cadmium and Mercury. In *Chemistry of the elements*, pp. 1395-1413. Pergamon. Oxford.

Gu B., Schmitt J., Chen Z., Liang L., and McCarthy H. F. (1994) Adsorption and Desorption of Natural Organic Matter on Iron Oxide: Mechanisms and Models. *Environ. Sci. Technol.* **28**, 38-46.

Gu B., Schmitt J., Chen Z., Liang L., and McCarthy H. F. (1995) Adsorption and desorption of different organic matter fractions on iron oxide. *Geochim. Cosmochim. Acta* **59**(2), 219-229.

Gulens J. (1987) Assessment of Research on the Preparation, Response and Application of Solid State Copper Ion-Selective Electrodes. *Ion-Selective Electrode Rev.* **9**, 127-171.

Gunneriusson L. (1993) Aqueous Speciation and surface complexation to goethite of divalent mercury, lead and cadmium. Umeå University, Sweden.

Gunneriusson L. (1994) Composition and Stability of Cd(II)-Chloro and -Hydroxo Complexes at the Goethite ( $\alpha$ -FeOOH)/Water Interface. *J. Colloid Interface Sci.* **163**, 484-492.

**H**

- Hari R. (1998) Effekte von Algen auf die Cu-Spezifizierung in Medien mit tiefem und hohem  $Cu_{tot}$ . Internal report. EAWAG-Dübendorf.
- Hawke D., Carpenter P. D., and Hunter K. A. (1989) Competitive Adsorption of Phosphate on Goethite in Marine Electrolytes. *Environ. Sci. Technol.* **23**(2), 187-191.
- Herbelin A. and Westall J. (1994) FitEQL. A Computer Program for Determination of Chemical Equilibrium Constants from Experimental Data. Version 3.1. Department of Chemistry, Oregon State University. Corvallis.
- Hering J. G. and Morel F. M. M. (1988) Humic Acid Complexation of Calcium and Copper. *Environ. Sci. Technol.* **22**(10), 1234-1237.
- Herrmann R., Daub J., Förster J., and Striebel T. (1994) Chemodynamics of trace pollutants during street runoff. *Wat. Sci. Tech.* **29**(9), 73-82.
- Hiemstra T., van Riemsdijk, W.H., Bolt, G.H. (1989a) Multisite Proton Adsorption Modeling at the Solid/Solution Interface of (Hydr)oxides: A New Approach. *J. Colloid Interface Sci.* **133**(1), 91-104.
- Hiemstra T., van Riemsdijk, W. H. (1996) A Surface Structural Approach to Ion Adsorption: The Charge Distribution (CD) Model. *J. Colloid Interface Sci.* **179**, 488-508.
- Hiemstra T., De Wit F. C. M., and van Riemsdijk W. H. (1989b) Multisite Proton Adsorption Modeling at the Solid/Solution Interface of (Hydr)oxides: A New Approach II: Application to Various Important (Hydr)oxides. *J. Colloid Interface Sci.* **133**(1), 104-117.
- Hoehn E. and Santschi P. H. (1987) Interpretation of tracer displacement during infiltration of river water to groundwater. *Water Resources Res.* **23**, 633-640.
- Hoehn E. and von Gunten H. R. (1989) Radon in Groundwater: A Tool to Assess Infiltration From Surface Waters to Aquifers. *Water Resour. Res.* **25**, 1795 - 1803.
- Hoehn E., Zobrist J., and Schwarzenbach R. P. (1983) Infiltration von Flusswasser ins Grundwasser-hydrogeologische und hydrochemische Untersuchungen im Glattal. *Gas-Wasser-Abwasser* **63**, 401 - 410.
- Hoins U., Charlet, L., Sticher, H. (1993) Ligand Effect on the Adsorption of Heavy Metals: the Sulfate-Cadmium-Goethite Case. *Water Air Soil Pollution* **68**, 241-255.
- Huang C. P., Elliott, H. A., Ashmead, R. M. (1977) Interfacial reactions and the fate of heavy metals in soil-water systems. *WPCF*, 745-756.
- Hug S., Sulzberger, B. (1994) In Situ Fourier Transform Infrared Spectroscopic Evidence for the Formation of Several Different Surface Complexes of Oxalate on  $TiO_2$  in the Aqueous Phase. *Langmuir* **10**, 3587-3597.
- Hug S. (1997) In Situ Fourier Transform Infrared Measurements of Sulfate Adsorption on Hematite in Aqueous Solutions. *J. Colloid Interface Sci.* **188**, 415-422.

**I**

- Internationale Kommission zum Schutze des Rheins (IKSR). (1992) Aktionsprogramm Rhein. Bestandsaufnahme der punktuellen Einleitungen prioritärer Stoffe. IKSR, Koblenz.
- Irwin R. J., van Mouwerik M., Stevens L., Seese M. D., and Basham W. (1997) Environmental Contaminants Encyclopedia. National Park Service, Water Resources Division. Fort Collins, Colorado.

**J**

- Jacobs L. A., von Gunten H. R., Keil R., and Kulsys M. (1988) Geochemical changes along a river-groundwater infiltration flow path: Glattfelden, Switzerland. *Geochim. Cosmochim. Acta* **52**, 2693 - 2706.
- Jansen S. (1998) A ligand exchange and DPCSV study on nickel speciation and related kinetic aspects in freshwater. EAWAG, Dübendorf.
- Jardine P. M., Jacobs G. K., and O'Dell J. D. (1993) Unsaturated Transport Processes in Undisturbed Heterogeneous Porous Media: II. Co-Contaminants. *Soil Sci Soc. Am. J.* **57**, 954-962.
- Jordan R. N., Yonge D. R., and Hathorne W. E. (1997) Enhanced mobility of Pb in the presence of dissolved natural organic matter. *J. Contamin. Hydrology* **29**, 59-80.

**K**

- Koopal W. H., Van Riemsdijk W. H., de Wit J. C. M., and Benedetti M. F. (1994) Analytical Isotherm Equations for Multicomponent Adsorption to Heterogeneous Surfaces. *J. Colloid Interface Sci.* **166**(51), 51-60.
- Kumar A. and Fish W. (1996) Ligands, metals, and metal-ligand complexes as differential probes of soil adsorptive heterogeneity. *Colloids and Surf.* **107**, 111-122.

**L**

- Lamy I., Djafer M., and Terce M. (1991) Influence of Oxalic Acid on the Adsorption of Cadmium at the Goethite Surface. *Water, Air, Soil Poll.* **57-58**, 457-465.
- Leenheer J. A. and Huffman E. W. D., Jr. (1976) Classification of organic solutes in water by using macroreticular resins. *U.S. Geol. Surv. J. Res.* **4**, 737-751.
- Leenheer J. A., Wershaw R., L., and Reddy M. M. (1995a) Strong-Acid, Carboxylic-Group Structures in Fulvic Acid from the Suwannee River, Georgia. 1. Minor Structures. *Environ. Sci. Technol.* **29**(2), 393-398.



- Leenheer J. A., Wershaw R. L., and Reddy M. M. (1995b) Strong-Acid, Carboxyl-Group Structures in Fulvic Acid from the Suwannee River, Georgia. 2. Major Structures. *Environ. Sci. Technol.* **29**(2), 399-405.
- Libes S. M. (1992) *An introduction to Marine Biogeochemistry*. John Wiley & Sons. New York.
- Lo K. S. L., Yang W. F., and Lin Y. C. (1992) Effects of Organic Matter on the Specific Adsorption of Heavy Metals by Soil. *Tox. Environ. Chem.* **34**, 139-153.
- Lövgren L. (1991) Complexation Reactions of phthalic acid and aluminium (III) with the surface of goethite. *Geochim. Cosmochim. Acta* **55**, 3639-3645.
- Ludwig C. and Schindler P. (1995) Surface Complexation on TiO<sub>2</sub>. Ternary surface Complexes: Coadsorption of Cu(II) and Organic Ligands (2,2-Bipyridil, 8-Aminoquinoline, and o-Phenylenediamine) onto TiO<sub>2</sub> (Anatase). *J. Colloid Interface Sci.* **169**, 291-299.
- Lützenkirchen J. (1996) Description des interactions aux interfaces liquide-solide à l'aide des modèles de complexation et de précipitation de surface. Ph.D thesis, Université Louis Pasteur de Strasbourg.
- Lützenkirchen J. (1999) The Constant Capacitance Model and Variable Ionic Strength: An Evaluation of Possible Applications and Applicability. *J. Colloid Interface Sci.* **217**, 8-18.

## M

- Margerum D. W., Cayley G.R., Weatherburn D.C., and Pagenkopf G.K. (1978) *Coordination Chemistry*. Martell, A. E., Ed.; ACS Monograph; American Chemical Society, Washington, DC, Vol.2, 1-220.
- Mason Y., Ammann A., Ulrich A., and Sigg L. (1999) Behavior of Heavy Metals, Nutrients, and Major Components during Roof Runoff Infiltration. *Environ. Sci. Technol.* **33**(10), 1588-1597.
- Mesure K. and Fish W. (1992a) Chromate and Oxalate Adsorption on Goethite. 2. Surface Complexation Modeling of Competitive Adsorption. *Environ. Sci. Technol.* **26**(12), 2365-2370.
- Mesure K. and Fish W. (1992b) Chromate and Oxalate Adsorption on Goethite: 1. Calibration of Surface Complexation Models. *Environ. Sci. Technol.* **26**(12), 2357-2370.
- Moffett J. W. and Ho J. (1996) Oxidation of cobalt and manganese in seawater via a common microbially catalyzed pathway. *Geochim. Cosmochim. Acta* **60**(18), 3415-3424.
- Moore G. L. (1989) *Analytical Spectroscopic Library. Vol 3: Introduction to Inductively Coupled Plasma Atomic Emission Spectrometry*. Elsevier, Amsterdam.
- Moore J. W. and Ramamoorthy S. (1984) *Heavy Metals in Natural Waters. Applied Monitoring and Impact Assessment*. Springer. New York.
- Morel F. M. M. and Hering J. G. (1993) *Principles and Applications of Aquatic Chemistry*. John Wiley & Sons. New York.
- Morsad H. (1999) Caractérisation Physico-chimique d'un sable de quartz et d'un oxyhydroxyde de fer. Report-DEA "Chimie et Microbiologie de l'eau (Université Poitiers, Pau, Nancy)-Institut de Mécanique des Fluides, Université Louis Pasteur, Strasbourg.

- Mottier V., Bucheli T., Kobler D., Ochs M., Zobrist J., Ammann A., Eugster J., Mueller S., Schoenenberger R., Sigg L., and Boller M. (1995) Qualitative aspects of roof runoff. *Eighth Junior European Workshop. Urban rainwater: Resourcefully used. Deventer, the Netherlands.*
- Müller B. (1996) ChemEQL. A Program to Calculate Chemical Speciation, Equilibrium, Titrations, Dissolution, Precipitation, Adsorption, Simple Kinetics, pX-pY Diagrams. Version 2.0. EAWAG Kastanienbaum (Switzerland).
- Murphy E. M. and Zachara J. M. (1995) The role of sorbed humic substance on the distribution of organic and inorganic contaminants in groundwater. *Geoderma* **67**, 103-124.
- Murray J. W. and Dillard J. G. (1979) The oxidation of cobalt(II) adsorbed on manganese dioxide. *Geochim. Cosmochim. Acta* **43**, 781-787.
- Music S., Ristic M., and Tonkovic M. Z. (1986) *Z. Wasser Abwasser Forsch.* **19**, 186.

## N

- Nagashima K. and Blum F. D. (1999) Proton Adsorption onto Alumina: Extension of Multisite Complexation (MUSIC) Theory. *J. Colloid Interface Sci.* **217**, 28-36.
- Naidu R. and Harter R. D. (1998) Effect of Different Organic Ligands on Cadmium Sorption by and Extractability from Soils. *Soil. Sci. Soc. Am. J.* **62**, 644-650.
- National Research Council (United States). Committee on Medical and Biological Effects of Environmental Pollutants - Division of Medical Science. (1975) Nickel. In: *Medical and Biological Effects of Environmental Pollutants*. National Academy of Sciences, Washington, D.C.
- National Research Council (United States). Committee on Medical and Biological Effects of Environmental Pollutants-Division of Medical Science (1977) *Copper*. In *Medical and Biological Effects of Environmental Pollutants*. National Academy of Sciences, Washington, D. C.
- Nilsson N. (1995) Inner/outer sphere complexation of phosphate and organic ligands at the goethite-water interface. Ph. D. thesis, Umeå University, Sweden.
- Nordin J., Persson P., Nordin A., and Sjöber S. (1998) Inner-Sphere and Outer-Sphere Complexation of a Polycarboxylic Acid at the Water-Boehmite ( $\gamma$ -AlOOH) Interface: A Combined Potentiometric and IR Spectroscopic Study. *Langmuir* **14**, 3655-3662.
- Nowack B. (1996) Behavior of EDTA in Groundwater- a Study of the Surface Reactions of Metal-EDTA Complexes. Diss.ETH Nr. 11392.Zürich, Switzerland.
- Nowack B., Kari F. G., Hilger S. U., and Sigg L. (1996a) Determination of Dissolved and Adsorbed EDTA Species in Water and Sediments by HPLC. *Anal. Chem.* **68**(3), 561-566.
- Nowack B., Lützenkirchen J., Behra Ph., and Sigg L. (1996b) Modeling the adsorption of metal-EDTA complexes onto oxides. *Environ. Sci. Technol.* **30**(7), 2397-2405.
- Nowack B. and Sigg L. (1996) Adsorption of EDTA and Metal-EDTA Complexes onto Goethite. *J. Colloid Interface Sci.* **177**, 106-121.
- Nowack B. and Stone A. T. (1999) The Influence of Metal Ions on the Adsorption of Phosphonates onto Goethite. *Environ. Sci. Technol.* **33**(20), 3627-3633.

- Nowack B., Xue H., and Sigg L. (1997) Influence of Natural and Anthropogenic Ligands on Metal Transport during Infiltration of River Water to Groundwater. *Environ. Sci. Technol.* **31**(3), 866-872.
- Nriagu J. O. (1979a) *Copper in the Environment. Part II: Health Effects*. John Wiley and Sons. New York.
- Nriagu J. O. (1979b) *Copper in the Environment. Part I: Ecological Cycling*. John Wiley and Sons.
- Nriagu J. O. (1980) *Nickel in the Environment*. John Wiley and Sons. New York.
- Nriagu J. O. (1981) *Cadmium in the Environment. Part II: Health Effects*. John Wiley and Sons. New York.
- Nriagu J. O. (1989) A global assessment of natural sources of atmospheric trace metals. *Nature* **338**, 47-49.
- Nriagu J. O. and Pacyna J. M. (1988) Quantitative Assessment of Worldwide Contamination of Air, Water and Soils by Trace Metals. *Nature* **333**, 134-139.

## O

- Ochs M. and Sigg L. (1995) Speziierung von Schwermetallen im Dachwasser. EAWAG. Dübendorf. Switzerland.
- Öhman L.-O. and Sjöberg S. (1996) The experimental determination of thermodynamic properties for aqueous aluminium complexes. *Coord. Ch. Re.* **149**, 33-57.

## P

- Parfitt R. L. and Atkinson R. J. (1976) Phosphate adsorption on goethite. *Nature* **264**, 740-741.
- Parfitt R. L., Fraser A. R., Russell J., and Farmer V. C. (1977) Adsorption on Hydrous Oxides II. Oxalate, Benzoate and Phosphate on Gibbsite. *Journal of soil Science* **28**, 40-47.
- Pauling L. (1929) The principles determining the structure of complex ionic crystals. *J. Am. Chem. Soc.* **51**, 1010-1026.
- Pisch J., Schäfer J., and Frahne D. (1993) Voltammetrische Schwermetallbestimmungen in organisch hoch belasteten Flüssigkeiten nach UV-Aufschluss. *FIT Fachzeitschrift für das Laboratorium* **37**, 500-505.
- Plavsic M., Kozar S., Krznaric D., Bilinski H., and Branica M. (1980) The Influence of Organics on the Adsorption of Copper(II) on  $\gamma$ -Al<sub>2</sub>O<sub>3</sub> in Seawater. Model Studies with EDTA. *Marine Chem.* **9**, 175-182.
- Prasch A. (1999) Determination of the Speciation of Nickel in Freshwater with Ligand Exchange and Voltammetric Determination. Diploma thesis, Fachhochschule Isny.

## Q

Qian J., Xue H. B., Sigg L., and Albrecht A. (1998) Complexation of Cobalt by Natural Ligands in Freshwater. *Environ. Sci. Technol.* **32**, 2043-2050.

## R

Ragnarsdottir K. V., Collins C. T., and Sherman D. M. (1998) Mechanisms of cadmium adsorption to goethite in the presence of inorganic and organic ligands. *Goldschmidt Conference*, 1226-1227.

Robertson A. P. (1998) Acid/Base, Copper Binding, and  $\text{Cu}^{++}/\text{H}^{+}$  Exchange Properties of Goethite, an Experimental and Modeling Study. *Environ. Sci. Technol.* **32**(17), 2519-2530.

Robertson A. P. and Leckie J. O. (1997) Cation binding predictions of surface complexation models: effects of pH, ionic strength, cation loading, surface complex, and model fit. *J. Colloid Interface Sci.* **188**(2), 444-472.

## S

Schaffner C., Ahel M., and Giger W. (1986) Behaviour of Organic Micropollutants during Infiltration of River Water into Groundwater: Results of a Field Study in the Glatt Valley, Switzerland. In *Organic Micropollutants in the Aquatic Environment* (ed. R. P. Comp.), pp. 455-458. Bjørseth, A., Angeletti, G.

Schindler P. and Kamber H. R. (1968) Die Acidität von Silanolgruppen. *Helv. Chim. Acta* **51**(7), 1781-1786.

Schindler P. W. (1990) Co-Adsorption of Metal Ions and Organic Ligands: Formation of Ternary Surface Complexes. In *Reviews in Mineralogy, Mineral-Water Interface Geochemistry (Mineralogical Society of America, Washington, D. C.) Vol. 23* (ed. M. F. Hochella and A. F. White), pp. 281-307.

Schindler P. W. and Gamsjäger H. (1972) Acid-base reactions of  $\text{TiO}_2$  (anastase)-water interface and the point of zero charge of  $\text{TiO}_2$  suspensions. *Kolloid-Z. Z. Polym.* **250**, 1781-1786.

Schosseler P. M. (1998) Electron Paramagnetic Resonance Study of the Copper(II) Complexation with Carbonate Ligands in Aqueous Solution and at Calcium Carbonate Surfaces. Diss. ETH No. 12669, ETH Zürich.

Schosseler P. M., Wehrli B., and Schweiger A. (1997) Complexation of Copper(II) with Carbonate Ligands in Aqueous Solution: A CW and Pulse EPR Study. *Inorganic Chemistry* **36**(20), 4490-4499.

Schwarzenbach R. P., Giger W., Hoehn E., and Schneider J. K. (1983) Behaviour of Organic Compounds during Infiltration of River Water to Groundwater. Field Studies. *Environ. Sci. Technol.* **17**(8), 472-479.

- Schwarzenbach R. P. and Westall J. (1981) Transport of Nonpolar Compounds from Surface Water to Groundwater. Laboratory Sorption Studies. *Environ. Sci. Technol.* **15**(11), 1360-1367.
- Schwertmann U. and Cornell R. M. (1991) *Iron Oxides in the Laboratory. Preparation and Characterization*. VCH, Weinheim.
- Siffert C. and Sulzberger B. (1991) Light-Induced Dissolution of Hematite in the Presence of Oxalate: A Case Study. *Langmuir* **7**(8), 1627-1634.
- Sigel H. and Sigel A. (1988) *Nickel and its Role in Biology*. Marcel Dekker, Inc.
- Sigg L. (1979) Die Wechselwirkungen von Anionen und schwachen Säuren mit Goethit in wässriger Lösung. Diss ETH Nr. 6417.
- Sigg L., Behra Ph., and Stumm W. (2000) *Chimie des Milieux Aquatiques. Chimie des eaux naturelles et des interfaces dans l'environnement*. 3rd edition. Dunod, Paris.
- Smith R. M. and Martell A. E. (1976) *Critical Stability Constants. Vol. 4: Inorganic Complexes*. Plenum Press, New York.
- Smith R. M. and Martell A. E. (1977) *Critical Stability Constants. Vol.3: Other Organic Ligands*. Plenum Press, New York.
- Smith R. M. and Martell A. E. (1982) *Critical Stability Constants. Vol. 5: First Supplement*. Plenum Press, New York.
- Sposito G. (1984) *The Surface Chemistry of Soils*. Oxford University Press, New York.
- Stevenson F. J. (1982) *Humus Chemistry: genesis, composition, reactions*. John Wiley & Sons, Inc.
- Stone A. T. (1988) Introduction to Interactions of Organic compounds with Mineral Surfaces. In *Metal Speciation: Theory, Analysis and application*. Lewis Publisher.
- Stone A. T., Torrents A., Smolen J., Vasudevan D., and Hadley J. (1993) Adsorption of Organic Compounds Possessing Ligand Donor Groups at the Oxide/Water Interface. *Environ. Sci. Technol.* **27**, 895-909.
- Stumm W. (1987) *Aquatic Surface Chemistry-Chemical Processes at the Particle-Water Interface*. John Wiley & Sons, New York.
- Stumm W. (1996) *Chemistry of the Solid-Water Interface*. John Wiley & Sons, New York.
- Stumm W. and Morgan J. J. (1996) *Aquatic Chemistry*. 3rd edition. John Wiley and Sons, New York.
- Sulzberger B., Suter D., Siffert C., Banwart S., and Stumm W. (1989) Dissolution of Fe(III) (hydr)oxides in Natural Waters; Laboratory Assessment on the Kinetics Controlled by Surface Coordination. *Marine Chem.* **28**, 127-144.
- Sunda W. and Hanson P. J. (1979) Chemical Speciation of Copper in in River Water: Effect of Total Copper, pH, Carbonate, and Dissolved Organic Matter. In *Chemical Modeling in Aqueous Systems* (ed. E. A. Jenne), pp. 147-180. American Chemical Society.
- Susetyo W., Carreira L. A., Azarraga L. V., and Grimm D. M. (1991) Fate, distribution and metabolism of inorganic pollutants speciation. Fluorescence techniques for metal-humic interactions. *Fresenius J. Anal. Chem.* **339**, 624-635.

**T**

- Tejedor-Tejedor M. I. and Anderson M. A. (1990) Protonation of Phosphate on the Surface of Goethite as Studied by CIR-FTIR and Electrophoretic Mobility. *Langmuir* **6**, 602-611.
- Temminghoff E. H. M., van der Zee S. E. A. T. M., and de Haan F. A. M. (1997) Copper Mobility in a copper-contaminated Sandy Soil as Affected by pH and Solid and Dissolved Organic Matter. *Environ. Sci. Technol.* **31**(4), 1109-1115.
- Thurman E. M. (1985) *Organic Geochemistry of Natural Waters*. Martinus Nijhoff/Dr W. Junk Publishers. Dordrecht.
- Tiffreau, C., Lützenkirchen, J., Behra, Ph.. (1995) Modelling the Adsorption of Mercury(II) on (Hydr)oxides: I: Amorphous Iron Oxide and  $\alpha$ -Quartz. *J. Colloid Interface Sci.* **172**, 82-93.
- Tipping. (1993a) Modelling ion binding by humic acids. *Colloids and Surf. A: Physicochemical and Engineering Aspects* **73**, 117-131.
- Tipping E. (1981) The adsorption of aquatic humic substances by iron oxides. *Geochim. Cosmochim. Acta* **45**, 191-199.
- Tipping E. (1986) Some Aspects of the Interactions between Particulate Oxides and Aquatic Humic Substances. *Marine Chemistry* **18**, 161-169.
- Tipping E. (1994) WHAM-A Chemical Equilibrium Model and Computer Code for Waters, Sediments, and Soils Incorporating a Discrete Site/Electrostatic Model of Ion-Binding by Humic Substances. *Comput. Geosci.* **20**(6), 973-1023.
- Tipping E. and Cooke D. (1982) The effects of adsorbed humic substances on the surface charge of goethite in freshwaters. *Geochim. Cosmochim. Acta* **46**, 75-80.
- Tipping E., Griffith J. R., and Hilton J. (1983) The Effect of Adsorbed Humic Substances on the Uptake of Copper(II) by Goethite. *Croat. Chem. Acta* **56**(4), 613-621.
- Tipping E. and Hurley M. A. (1992) A Unifying Model of Cation Binding by Humic Substances. *Geochim. Cosmochim. Acta* **56**, 3627-3641.
- Tipping E. and Woof C. (1990) Humic substances in acid organic soils: modelling their release to the soil solution in terms of humic charge. *Journal of Soil Science* **41**, 573-586.
- Tipping E., Woof C., and Hurley M. A. (1991) Humic Substances in Acid Surface Waters: Modelling Aluminium Binding, Contribution to Ionic Charge-Balance, and Control of pH. *Wat. Res.* **25**(4), 425-435.
- Turner A., Nimmo M., and Thuresson K. A. (1998) Speciation and Sorptive Behavior of Nickel in an Organic-Rich Estuary (Beaulieu, UK). *Marine Chem.* **63**, 105-118.

**V**

- van Geen A., Robertson A. P., and Leckie J. O. (1994) Complexation of carbonate species at the goethite surface: Implications for adsorption of metal ions in natural waters. *Geochim. Cosmochim. Acta* **58**(9), 2073-2086.

- Venema P., Hiemstra T., and van Riemsdijk W. H. (1996a) Comparison of Different Site Binding Models for Cation Sorption: Description of pH Dependency, Salt Dependency, and Cation-Proton Exchange. *J. Colloid Interface Sci.* **181**, 45-59.
- Violante A., Rao M. A., De Chiara A., and Gianfreda L. (1996) Sorption of phosphate and oxalate by a synthetic aluminium hydroxylsulphate complex. *European Journal of Soil Science* **47**, 241-247.
- von Gunten H. R., Karametaxas G., Krähenbühl U., Kulsys M., Giovanoli R., Hoehn E., and Keil R. (1991) Seasonal biogeochemical cycles in riverborne Groundwater. *Geochim. Cosmochim. Acta* **55**, 3597 - 3609.
- von Gunten H. R. and Kull T. P. (1986) Infiltration of inorganic compounds from the Glatt River, Switzerland, into a groundwater aquifer. *Water Air Soil Poll.* **29**, 333-346.

## W

- Weidler P. G., Schwinn T., and Gaub H. E. (1996) Vicinal Faces on Synthetic Goethite Observed by Atomic Force Microscopy. *Clay Clay M.* **44**(4), 437-442.
- Westall J. and Hohl H. (1980) A comparison of electrostatic models for the oxide solution interface. *Adv. Colloid Interface Sci.* **12**, 265-294.
- Westall J. C., Jones J. D., Turner G. D., and Zachara J. M. (1995) Models for Association of Metal Ions with Heterogeneous Environmental Sorbents. 1. Complexation of Co(II) by Leonardite Humic Acid as a Function of pH and NaClO<sub>4</sub> Concentration. *Environ. Sci. Technol.* **29**(4), 951-959.
- Wilkins R. G. (1991) *Kinetics and mechanisms of reactions of transition metal complexes*. VCH New York.
- World Health Organisation. (1991) Nickel. In *Environmental Health Criteria*. Vol. 108. Geneva.
- World Health Organisation. (1992) Cadmium-Environmental Aspects. In *Environmental Health Criteria*. Vol. 135. Geneva.
- World Health Organization. (1992) Cadmium. In *Environmental Health Criteria*. Vol. 134. Geneva.
- World Health Organization. (1998) Copper. In *Environmental Health Criteria*. Vol. 200. Geneva.

## X

- Xue H., Janssen S., Prasch A., and Sigg L. (2000) Nickel Speciation and Complexation Kinetics in Freshwater by Ligand-Exchange and DPCSV. *Environ. Sci. Technol.*(submitted).
- Xue H., Oestreich A., Kistler D., and Sigg L. (1996) Free Cupric Ion Concentrations and Cu Complexation in Selected Swiss Lakes and Rivers. *Aquatic Sciences* **58**(1), 69-87.
- Xue H. and Sigg L. (1993) Free Cupric Concentration and Cu(II) Speciation in a Eutrophic Lake. *Limnol. Oceanograph.* **38**(6), 1200-1213.

- Xue H. and Sigg L. (1994) Zinc Speciation in Lake Waters and its Determination by Ligand Exchange with EDTA and Differential Pulse Anodic Stripping Voltammetry. *Analytica Chimica Acta* **284**, 505-515.
- Xue H. and Sigg L. (1998) Cd Speciation and Complexation by Natural Organic Ligands in Freshwater. *Anal. Chim. Acta* **363**, 249-259.
- Xue H. and Sigg L. (1999) Comparison of the Complexation of Cu and Cd by Humic or Fulvic Acids and by Ligands Observed in Lake Waters. *Aquatic Geochem.* **5**, 313-335.
- Xue H. and Sunda W. (1997) Comparison of  $[Cu^{++}]$  Measurements in Lake Water Determined by Ligand-Exchange and Cathodic Stripping Voltammetry and by Ion-Selective Electrode. *Environ. Sci. Technol.* **31**, 1907-1909.
- Xyla A. G., Sulzberger B., Luther G. W., Hering J. G., Van Cappellen P., and Stumm W. (1992) Reductive Dissolution of Manganese (III, IV) (Hydro)oxides by Oxalate: The Effect of pH and Light. *Langmuir* **8**(1), 95-103.

**Y**

- Yost E. C., Tejedor-Tejedor M. I., and Anderson M. A. (1990) In Situ CIR-FTIR Characterization of Salicylate Complexes at the Goethite/Aqueous Solution Interface. *Environ. Sci. Technol.* **24**(6), 822-828.

**Z**

- Zachara J. M., Ainsworth C. C., Cowan C. E., and Resch C. T. (1989) Adsorption of Chromate by Subsurface Soil Horizon. *Soil Sci. Soc. Am. J.* **53**, 418-428.
- Zachara J. M., Girvin D. C., Schmidt R. L., and Resch C. T. (1987) *Environ. Sci. Technol.* **21**, 589.
- Zachara J. M., Resch C. T., and Smith S. C. (1994) Influence of humic substances on Co(II) sorption by a subsurface mineral separate and its mineralogic components. *Geochim. Cosmochim. Acta* **58**(2), 553-566.
- Zobrist J., Müller S. R., Ammann A., Bucheli T. D., Mottier V., Ochs M., Schoenenberger R., Eugster J., and Boller M. (2000) Quality of Roof Runoff for Groundwater Infiltration. *Wat. Res.* **34**(5), 1455-1462.



# *Curriculum Vitae*

13. March 1970      Born in Homburg/Saar (Germany)
- 1976-1982          Primary school in Belair, Luxembourg
- 1982-1991          Lycée Robert-Schuman, Luxembourg
- 1991                  Examen de fin d'études secondaires (section  
mathématiques, option latin)
- 1991-1996          Studies of Chemical Engineering at the Swiss Federal  
Institute of Technology (ETH) Zürich
- 1995                  Practical work at Dupont Nemours, Luxembourg
- 1996                  Diploma in Chemical Engineering  
(Dipl. Chem. Ing. ETH)
- 1996-2000          Ph. D. thesis in environmental chemistry at the Swiss  
Federal Institute for Environmental Science and  
Technology (EAWAG), Dübendorf
- 1996-2000          Teaching assistance in the department of Environmental  
Sciences, ETH Zürich, Aquatic chemistry

Seite Leer /  
Blank leaf

Seite Leer /  
Blank leaf